UNIVERSITÀ DEGLI STUDI DI MILANO

Molecular and Cellular Biology PhD School

Department of Bioscience

XXXII Cycle

PhD Thesis

The MADS-domain SEEDSTICK plays fundamental roles during transmitting tract development and fruit growth in *Arabidopsis thaliana*

Maurizio Di Marzo

Scientific Tutor: prof. Lucia Colombo

PhD director: prof. Martin M. Kater

Academic year: 2018/2019

INDEX

Riassunto

I fattori di trascrizione della famiglia MADS-box e bHLH regolano lo sviluppo del tessuto di trasmissione del pistillo

SEEDSTICK (STK) controlla aspetti diversi della riproduzione in *Arabidopsis*. STK è un fattore di trascrizione MADS-box co-espresso con il fattore di trascrizione bHLH CESTA (CES). È stato dimostrato che CES controlla in modo ridondante con i fattori di risposta ai brassinosteroidi BRASSINOSTEROID ENHANCED EXPRESSION1 (BEE1) e BEE3 lo sviluppo del tessuto di trasmissione dell'apparato riproduttore femminile di Arabidopsis. Attraverso la caratterizzazione del fenotipo del doppio mutante *stk ces-2* abbiamo osservato che STK e CES sono entrambi necessari per lo sviluppo del tessuto di trasmissione. Considerando che CES interagisce con BEE1 e BEE3, abbiamo generato il quadruplo mutante *bee1 bee3 stk ces-2*. Quest'ultimo ha un fenotipo più severo rispetto al doppio mutante *stk ces-2*. Il quadruplo mutante infatti, presenta il tessuto di trasmissione non del tutto differenziato e la mancanza di fusione dei due carpelli, difetti che complessivamente causano una crescita del tubetto pollinico parzialmente compromessa. Per cercare di capire i possibili target del complesso proteico composto da STK-CES-BEE1-BEE3 abbiamo deciso di effettuare un esperimento di trascrittomica per identificare quali geni venissero differenzialmente espressi nel mutante *bee1 bee3 stk ces-2*, rispetto al wild type. Grazie a questo approccio abbiamo identificato geni regolati direttamente o indirettamente dal complesso costituito da STK-CES-BEE1-BEE3 potenzialmente coinvolti nello sviluppo del tessuto di trasmissione. Alcuni di questi geni sono implicati nella sintesi dei componenti della parete cellulare, della matrice extracellulare del tessuto di trasmissione, nel controllo della morte cellulare programmata e probabilmente anche di un segnale legato alla risposta all'ormone auxina. In conclusione, i nostri dati permettono di aggiungere nuovi tasselli alla comprensione dello sviluppo del tessuto di trasmissione grazie all'azione coordinata dei fattori di trascrizione della famiglia MADS-box e bHLH.

ABSTRACT

MADS-box and bHLH transcription factors coordinate transmitting tract development in *Arabidopsis thaliana*

The MADS-box gene *SEEDSTICK* (*STK*) controls several aspects of plant reproduction. *STK* is co-expressed with *CESTA* (*CES*), a basic Helix-Loop-Helix (bHLH) transcription factor-encoding gene. *CES* was reported to control redundantly with the brassinosteroid positive signaling factors BRASSINOSTEROID ENHANCED EXPRESSION1 (BEE1) and BEE3 the transmitting tract development. Through the characterization of the *stk ces-2* double mutant, we observed that STK and CES act together in the regulation of transmitting tract development. Combining the *stk* with *ces-2 bee1 bee3* we have obtained the quadruple mutant showed a clear increase of the unfertilized ovules and septum defects. In the quadruple mutant carpel fusion was compromised, causing the formation of holes at the center of the septum where transmitting tract differentiates. These phenotypes do not allow a proper pollen tube growth in the double mutant *stk ces-2*, and even more in the quadruple mutant *bee1 bee3 stk ces-2* leading to high number of unfertilized ovules. The transcriptome profile of the quadruple mutant *bee1 bee3 stk ces-2* compared to wild type revealed a small subset of misregulated genes, which probably act downstream of the transcription factor described above, mainly involved in cell death, the extracellular matrix of the transmitting tract, cell wall composition and auxin signaling. This specific subset of downstream target genes controlled directly or indirectly by STK-CES-BEE1-BEE3 protein complex, open doors to a new regulatory network controls transmitting tract development. Altogether our data reveal new insights in the regulation of transmitting tract development together by bHLH and MADS-box transcription factors.

Riassunto

SEEDSTICK (STK) controlla la lunghezza del frutto in *Arabidopsis thaliana* regolando la quantità di citochinine e l'attività del gene *FRUITFULL* (*FUL*)

Dopo la fecondazione, l'ovario aumenta di dimensioni grazie a un complesso meccanismo di sviluppo che permetterà di ottenere il frutto. Il frutto della specie modello *A. thaliana* è una siliqua.

Abbiamo dimostrato che le citochinine devono essere degradate per ottenere un corretto allungamento del frutto dopo la fecondazione. L'espressione del gene *CYTOKININ OXIDASE DEHYDROGENASE 7* (*CKX7*), codificante per una proteina capace di degradare le citochinine nel citosol, è regolata direttamente dal fattore di trascrizione MADS-box STK. I due mutanti *ckx7* hanno un fenotipo simile al mutante *stk*, frutti più corti rispetto al wild type. Nel frutto del mutante *stk* abbiamo riscontrato un aumento della quantità di citochinine rispetto al wild type, probabilmente dovuto a una diminuzione dell'attività di CKX7 nel mutante *stk* rispetto al wild type. Infatti, un aumento della degradazione delle citochinine nel citosol grazie all'over-espressione di *CKX7* permette di ottenere un parziale recupero del fenotipo del mutante *stk* per quanto concerne la lunghezza del frutto.

Abbiamo escluso il ruolo di *CKX6* nello sviluppo del frutto. *CKX6* codifica per una proteina capace di degradare le citochinine nell'apoplasto. Il promotore di *CKX6* non è attivo durante lo sviluppo del frutto, e il singolo mutante *ckx6* non presenta fenotipo per quanto concerne la lunghezza del frutto.

Inoltre, abbiamo dimostrato che STK è necessario per regolare l'espressione del gene MADS-box *FUL*. Esso è considerato il gene più importante nello sviluppo del frutto. Il doppio mutante *stk ful*, ha frutti più corti rispetto al wild type, ma anche rispetto ai due singoli mutanti *stk* e *ful*. Il fenotipo additivo suggerisce la possibilità che i due geni agiscano in due pathways diversi in grado di regolare positivamente l'allungamento del frutto. In conclusione, abbiamo proposto un modello che riassume i due diversi pathways di regolazione dello sviluppo del frutto.

ABSTRACT

SEEDSTICK (STK) controls *Arabidopsis thaliana* fruit size by regulating cytokinin levels and *FRUITFULL* (*FUL*)

Upon fertilization, the ovary increases in size and undergoes a complex developmental process to become a fruit. The fruit of *Arabidopsis thaliana* is named silique.

We show that cytokinins (CK), required to define ovary size before fertilization, have to be degraded to obtain the correct fruit growth. The expression of *CYTOKININ OXIDASE DEHYDROGENASE 7* (*CKX7*), which encodes a cytosolic CK degrading enzyme, is directly regulated post-fertilization by the MADS-box transcription factor STK. Similar to *stk*, two *ckx7* mutant alleles possess shorter fruits compared to wild type. Quantification of CKs revealed that *stk* has high CK levels during fruit elongation, which negatively control cell expansion during fruit development, compromising fruit growth. Overexpression of *CKX7* partially complements the *stk* fruit phenotype.

We show that *CKX6* does not regulate fruit elongation process. CKX6 encodes for one of the fourth CK degrading enzymes that acts in the apoplast. The *CKX6* promoter is not active during fruit elongation phases. Moreover, the *ckx6* mutant does not display differences in fruit length when compared to wild type.

Finally, we show that STK is also required for the correct expression of the MADS-box gene *FUL*, which is considered the master regulator of valve elongation in fruit. The double mutant *stk ful* displayed shorter siliques when compared to wild type, but also respect to the two single mutants. The additive phenotype of the double mutant *stk ful* suggests the possibility that the two MADS-box transcription factors act in two parallels pathways that can regulate fruit elongation process. Overall, we provide novel insights into the regulatory pathway that control fruit growth.

AIMS OF THE PROJECTS

I have been focused on the molecular and genetic network controlled by STK regulating later stages of pistil development and early fruit development in Arabidopsis. In particular, the goals of my research were two:

- Study the role of STK in transmitting tract development;
- Study the integrative pathway controlled by STK involved in pistil and fruit size.

During the latest years, a complex model has been described for the development of the transmitting tract tissue. This component is essential for pollen tube growth and permits it to reach the ovules.

To better describe the role of STK in transmitting tract development, that we described for the first time during this year (Herrera-Ubaldo et al., 2019), I used the classical molecular and genetic approach. We focused our attention on the possible link between STK and the bHLH transcription factor CES. The two genes *STK* and *CES*, during fertilization, are co-expressed. *CES* has been described as an important player in the correct transmitting tract development (Crawford and Yanofsky, 2011). Furthermore, considering that *CES* is phylogenetically related to *BEE1* and *BEE3*, and acts with these genes in transmitting tract development, I decided to generate multiple mutant combinations to better understand the interaction between *STK*, *CES* and *BEE*s. I also characterized morphologically the septum thanks to the scanning electron microscope (SEM). Finally, I performed a transcriptome profile of the quadruple mutant *bee1 bee3 stk ces-2*, which is characterized by the most severe phenotype related to the percentage of unfertilized ovules, when compared to wild type. Thanks to this approach I had the opportunity to find new genes involved in the development of the transmitting tract which might influence different aspects of the transmitting tract differentiation, such as genes involving in programmed cell death, extracellular matrix deposition or lipid transport, but also in the auxin signalling.

Regarding the second goal, I focused on the control of fruit final size and length in *A. thaliana* siliques.

I have started by the analysis of the *stk* transcriptome profile published in 2014 by Mizzotti and collaborators. I found as possible target of *STK* genes involved in cytokinin (CK) metabolism and signaling therefore I decided to focus on *CKX7* a gene encoding for an enzyme that

degrades the CK in the cytosol of the cells. In particular, we analysed the expression pattern of *CKX7* in the s*tk* mutant background when compared to wild type using the *pCKX7::GUS* marker-line for qualitative analysis and qRT-PCR to quantify the *CKX7* transcripts. We also performed morphologically characterization of two single T-DNA insertion mutant alleles for *ckx7* related to fruit length. Moreover, I decided to generate new mutant allele for *CKX7* gene thanks to the CRISPR-Cas9 genome editing technology and an over-expression line thanks to CaMV promoter to analyze the fruit length when there is a lack of CKX7 or an overproduction of this enzyme in plants.

Besides, we better characterize the possible role of the CKs in fruit development through a biochemical characterization of the CK profile in the *stk* mutant background compared to wild type before and after fertilization. Thanks to this quantification we discriminated among the different CK types (isopentenyladenine, *trans*-Zeatin, *cis*-Zeatin, dihydrozeatin) to discover which type of cytokinin is involved in fruit elongation process. We confirm that the CKs have a role in fruit elongation pathway acting after double fertilization.

INTRODUCTION

The transmitting tract tissue, function and development

The female reproductive organ of the flower, which is named pistil or gynoecium derived from the fusion of two carpels in *A. thaliana*. The pistil is composed in the apical part by the stigma and the stigma papillae, which are needed to attach the pollen. The stigma is connected to the ovary in which accommodate the ovules by the style. The septum divides into two perfect chambers the ovary. At the centre of the septum, there is the transmitting tract tissue which develops during pistil development and degenerates after fertilization. Pollen tubes must growth through several distinct tissues before reaching ovules, including the style transmitting tract and the septum zone of the transmitting tract (Lord and Russell, 2002; Roeder and Yanofsky, 2006).

The transmitting tract differentiates from the Carpel Margin Meristem (CMM), a meristematic tissue that develops as two internal crests, which fuse when they reach each other in the middle of the young pistil, during its development (Bowman et al., 1999a; Reyes-Olalde et al., 2013). The fusion of the two internal crests occurs at stage 9 of pistil development, and the transmitting tract is fully developed at stage 12, before fertilization (Roeder and Yanofsky, 2006). The cell composing the transmitting tract secrete an extracellular matrix (ECM) that accompanying pollen tube growth. The ECM is a complex mixture of polysaccharides, glycoproteins, and glycolipids that accompanying pollen tube growth (Lennon et al., 1998).

A complex genetic network controls the development of the transmitting tract. The zinc-finger transcription factor, NO TRANSMITTING TRACT (NTT) has a fundamental role during transmitting tract development. In the *ntt* mutant, the programmed cell death (PCD) of the cell composing transmitting tract, which is also influenced by the ECM component secreted by the cells that form the transmitting tract, is severely compromised (Crawford et al., 2007). The absence of cell death and the different matrix of the cell wall in the *ntt* mutant caused a partial failure of the pollen tube growth, with a high percentage of no fertilized ovules from the middle to the lower part of the fruit (Crawford et al., 2007).

NTT acts upstream of three genes necessary for the style and transmitting tract development. The first one is *CESTA* (*CES*), which is also named *HALF FILLED* (*HAF*), a basic helix-loop-helix-type (bHLH) encoding transcription factor, that acts redundantly with two closely related genes *BRASSINOSTEROID ENHANCED EXPRESSION1* (*BEE1*) and *BEE3*. The triple mutant *ces bee1 bee3* shows similar defects in transmitting tract development as Crawford and

collaborators previously found in the *ntt* mutant (Crawford and Yanofsky, 2011). Moreover, ectopic expression of *CES*, through the CaMV35S promoter, increases the diameter of the transmitting tract allowing more pollen tube to pass through it simultaneously (Crawford and Yanofsky, 2011).

Another bHLH-encoding transcription factor gene, which is named *SPATULA* (*SPT*), is necessary to obtain a correct transmitting tract development. Among the different *spt* mutant phenotypes, there is a reduced number of cells composing the CMM meristematic tissue that causes the absence of the septum and consequently of transmitting tract with reduced fertility (Groszmann et al., 2011; Heisler et al., 2001). SPT promotes the development of the medial tissue, in which the two carpels composing the pistil are fused (Groszmann et al., 2011; Heisler et al., 2001). SPT is also able to form heterodimers with HECATE 1 (HEC1), HEC2 and HEC3. The *HEC*s genes encode for bHLH transcription factor. The triple mutant *hec1 hec2 hec3* is complete sterile (Gremski et al., 2007). It is characterized by dramatic defects in the apical portion of the pistil. In fact, there is a complete lack of the stigmatic tissue and it is characterized by an elongated style (Gremski et al., 2007). The triple mutant *hec1 hec2 hec3* also displayed a complete absence of the cells composing transmitting tract (Gremski et al., 2007). The three *HEC* genes work simultaneously in the regulation of pistil structures necessary to obtain the correct fertilization of the ovules (Gremski et al., 2007).

Recently, we demonstrated the role of NTT in link with the MADS-domain transcription factor SEEDSTICK (STK) in transmitting tract differentiation (Herrera-Ubaldo et al., 2019). The two transcription factors work together during transmitting tract development. The *NTT* and *STK* promoters have a similar activity in the medial domain of the pistil during transmitting tract development (Herrera-Ubaldo et al., 2019). In the double mutant *ntt stk* the number of cells composing the CMM is similar respect to wild type (Herrera-Ubaldo et al., 2019). The same number of cell composing the CMM suggests that the abnormal fusion is not related to early stages development but epidermal defects (Herrera-Ubaldo et al., 2019). Despite no differences in the CMM of the double mutant *ntt stk* when compared to wild type, the *ntt stk* fruits are characterized by a partial failure of the septum fusion that appears with holes compared to wild type (Figures I.1-F-G). Moreover, at stage 15, when in the wild type fruit there is the degeneration and a collapse of the cells composing the septum and transmitting tract, in the double mutant *ntt stk* situation the cells do not degenerate (Figures I.1-J-M). In conclusion, the different phenotypes described above, cause a partial failure of pollen tube growth in the *ntt stk* double mutant respect to wild type demonstrated with aniline blue staining (Herrera-Ubaldo et al., 2019), with an increase of pollen tube defects in growth when compared to the single

mutant *ntt*, that has been previously reported also by Crawford and collaborators (Crawford et al., 2007). Indeed, in the *ntt* mutant pollen tube growth was mainly observed in the apical part of the ovary (Figure I.1-O) compared to wild type and *stk* in which the pollen tubes reach the bottom part of the pistil (Figures I.1-N and I.1-P). In the *ntt stk* double mutant, pollen tube growth was more affected and observed only in the upper part of the ovary. In conclusion, the various phenotypes described above of the *ntt stk* double mutant affected dramatically the seed set (Figures I.5-A-E) (Herrera-Ubaldo et al., 2019).

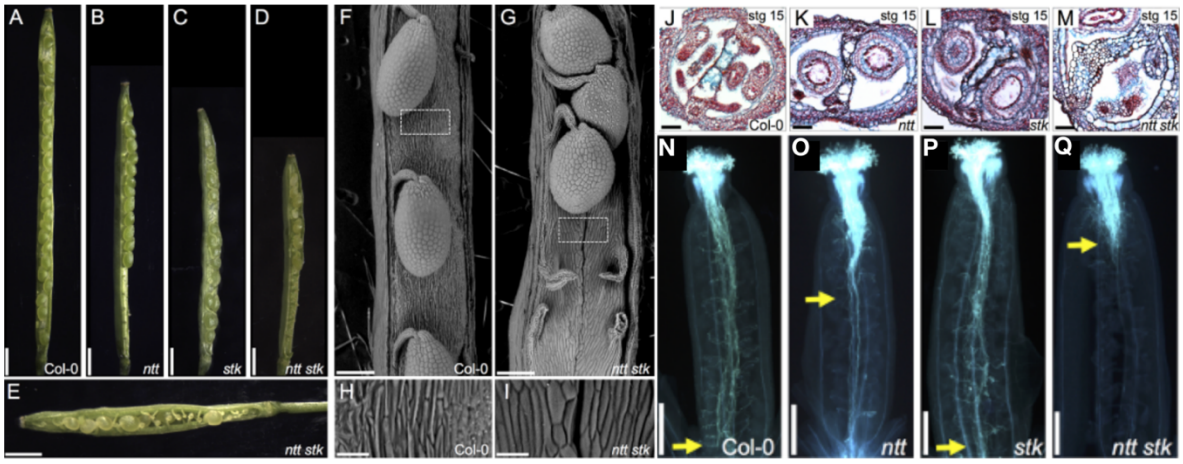

Figure I.1: *ntt* and *stk* mutant phenotypes related to the septum and transmitting tract.
(A-E) Stereomicroscope images of Col-0, *ntt*, *stk* and *ntt stk* siliques; (F,G) SEM pictures of *ntt stk* and Col-0 opened siliques; (J-M) Alcian Blue and Neutral Red stained transverse sections of Col-0, *ntt*, *stk* and *ntt stk* at stage 15 fruits; (N-Q) Aniline Blue staining of Col-0 , *ntt*, *stk* (E) and *ntt stk* (F) pollen tubes in stage 13 of pistil development; Adapted and modified from (Herrera-Ubaldo et al., 2019).

The MADS-box transcription factor SEEDSTICK (STK) plays multiple function in pistil development

The MADS-domain STK was discovered in 2003 by Pinyopich and collaborators. The authors described for the first time the pattern of expression of *STK* in the reproductive organ (Pinyopich et al., 2003). In particular, STK is expressed during pistil development in the ovule primordia, in the ovules, in placenta-derived tissues which are septum and transmitting tract, but also funiculus, nucellus, micropile before fertilization, and also in the outer integument after fertilization (Figure I.2 A-F) (Mizzotti et al., 2014; Pinyopich et al., 2003). STK promoter is in general active in the pistil medial domain, also in the replum during fertilization at stage 13 (Herrera-Ubaldo et al., 2019). The single mutant *stk* has multiple phenotypes. It is characterized by smaller seeds and longer funiculus when compared to wild type (Figure I.2 G-I) (Pinyopich et al., 2003). Moreover, when the single mutation of *stk* is combined with the

double mutant *shatterproof1 shatterproof2* creating the triple mutant *stk shp1 shp2* the ovules become carpelloid like structures (Figure I.2 J, K), causing sterile plants indicating the redundant role of the three MADS-box transcription factor during ovule development (Pinyopich et al., 2003).

Intriguingly, when the valves of *stk* mutant open the seeds don't detach themselves from the siliques (Figure I.2 L) (Balanzà et al., 2016; Pinyopich et al., 2003). This phenotype is caused by an ectopic lignification in the seed abscission zone of the funiculus in the *stk* mutant when compared to wild type (Figure I.2 M, N) (Balanzà et al., 2016). The seed shattering is obtained thanks to a lignification of the secondary cell wall, similar to the lignification that happens in the valve margin to obtain the opening of the two valves. In the valve margin, the MADS-domain transcription factors SHPs act as a positive regulator of *INDEHISCENT* (*IND*), *ALCATRAZ* (*ALC*) and *SPT* (Dinneny et al., 2005; Liljegren et al., 2000; Liljegren et al., 2004). On the contrary, in the abscission zone of the funiculus, to obtain seed shattering, STK acts as a negative regulator of three bHLH transcription factor coding genes *HEC3*, *SPT* and *ALC* (Balanzà et al., 2016).

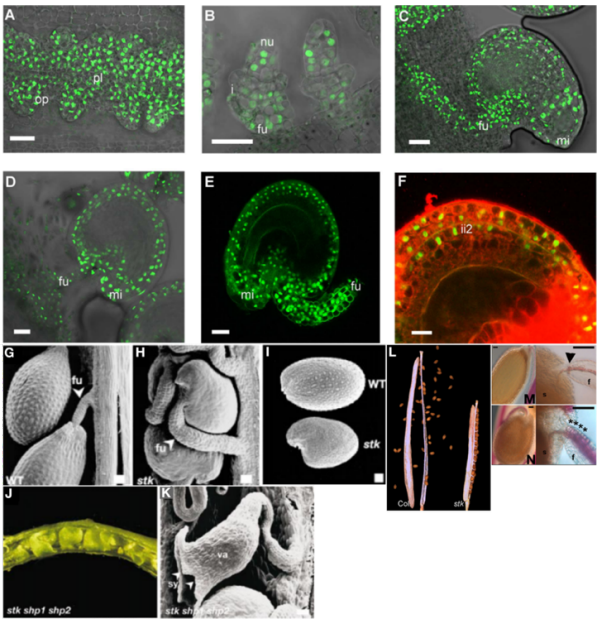

Figure I.2: Expression pattern of *STK* analysed through *STK::STK-GFP*, and *stk* mutant phenotypes. *STK-GFP* nuclear protein detected in placenta (pl) and ovule primorida (op) (A), in nucellus (nu) and in the funiculus (fu) (B), in mature ovule *STK-GFP* signal detected in fu and micropile (mi) (C, D), in the outer integuments and funiculus of developing seeds (E, F); Funiculus and seeds phenotype of the *stk* mutant when compared to wt (G-I); Carpelloid like structures of *stk shp1 shp2* triple mutant (J-K); Seed shattering failure in the *stk* mutant when compare to wt (L); Fluoroglucinol staining of *stk* mutant at stage 17B of the seeds abscission zone (N) when compared to wt (M). Adapted and modified from (Balanzà et al., 2016; Mizzotti et al., 2014; Pinyopich et al., 2003).

Interestingly, the three MADS-box STK, SHP1 and SHP2 that act redundantly during ovule development (Pinyopich et al., 2003), have a clear opposite action in the lignification zones of the fruit. In the valve margin, the SHPs act as positive regulators of lignification (Liljegren et al., 2000), while STK acts as a repressor of lignification in the seed abscission zone of the funiculus (Balanzà et al., 2016).

During the last years, several studies have characterized the roles of STK in plant development. STK is involved in ovule identity, in cell wall metabolism and mechanical properties of the seed coat, in transmitting tract differentiation and seed shattering (Balanzà et al., 2016; Ezquer et al., 2016; Favaro et al., 2003; Herrera-Ubaldo et al., 2019; Mizzotti et al., 2014; Pinyopich et al., 2003).

However, one of the possible roles of *STK* is still unknown. The *stk* mutant plants possess shorter siliques compared to wild type (Herrera-Ubaldo et al., 2019; Pinyopich et al., 2003).

In this project, we try to understand the role of STK in pistil development, in particular in the correct fertilization of the ovules. Moreover, we used as a toll this well-characterized MADS-box transcription factor to understand the role of cytokinins in fruit elongation process.

The Arabidopsis fruit development

The fruit, whose main functions are to protect and disperse the seeds, has contributed to the evolutionary success of the Angiosperms. The dry and dehiscent fruit of the model species *A. thaliana* is named silique. It is obtained upon double fertilization from the female organ which is named pistil. The double fertilization which occurs during the anthesis (stage 13 of pistil development according to Roeder and Yanofsky, 2006) is considered the signal that promotes fruit development. After the double fertilization, the auxin (AUX) biosynthesis is activated in the ovules in which causes an increase of the gibberellin (GA) resulting in an escalation of these hormones inside the ovary, which will develop in a fruit thanks to the coordinating action of AUX and GA in the fruit tissues (Alabadí et al., 2009; Dorcey et al., 2009).

The elongation of the siliques up to the stage 17, when they reach their final size/length (Roeder and Yanofsky, 2006), is triggered by a first phase of cell division, into the tissues composing fruit. These tissues, from the external to the inner part are the exocarp (external tissue), the mesocarp (medial tissue) and the endocarp (internal tissue). The cell division phase is followed

by cell expansion, within particular a longitudinal expansion of the cells which compose the exocarp (Vivian-Smith et al., 2001).

The fruit is divided in a lateral and a medial domain. The lateral domain is composed of the two lateral valves. The valves are separated from the medial domain, which is constituted on the outside, by the replum, thanks to the valve margin tissue which is composed by two cell layers that are the lignified layer close to the valves and the separation layer close to the replum. In the inner part, the septum divides into two perfect chambers the fruit (Figure I.3).

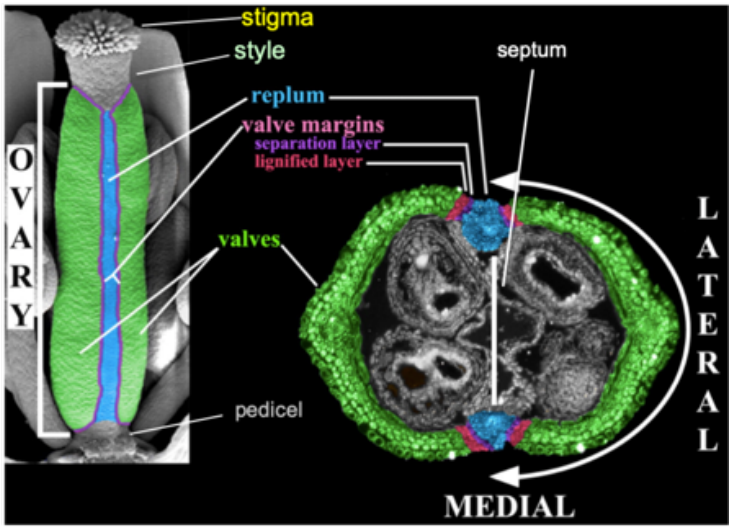

Figure I.3: Representation of the pistil structure at stage 12 (left), cross-section of the silique at stage 16 (right) with the description of the lateral and medial domain, modified and adapted from (Ripoll et al., 2011).

The gene network involved in the fruit structures development

To obtain the development of the various structures composing the siliques in *Arabidopsis* is needed a complex red of pathways connected in a model. The MADS-box transcription factor FRUITFULL (FUL) is defined as the master regulator of valves differentiation (Gu et al., 1998). The valves, in which *FUL* is active, are necessary to protect the ovary in which accommodate the ovules and future seeds. Indeed, the single mutants *ful-1* and *ful-2* are characterized by shorter siliques when compared to wild type (Figure I.4-A). This phenotype is caused by a failure of elongation and differentiation in the cells that formed the valves (Figure I.4-F,G) (Ferrándiz et al., 2000a). *FUL* promotes cell elongation in the lateral domain acting on the inhibition of cell division. However, in the two mutants described above, the cells which compose the replum could elongate, producing the characteristic replum phenotype of *ful-1* and *ful-2* which is named zig-zag (Figure I.4-C,E) (Ferrándiz et al., 2000a).

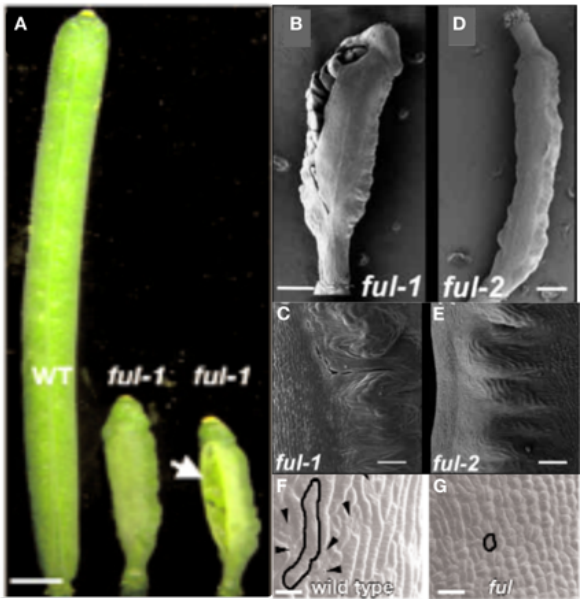

Figure I.4: ***ful-1* and *ful-2* phenotypes in siliques**.
(A) Stereomicroscope pictures of *ful-1* siliques at stage 17 when compared to wt; (B-C; D-E) SEM pictures of *ful-1* and *ful-2* siliques. (F-G) Cell morphology in *ful-1* compared to wt. Modified and adapted from (Ferrándiz et al., 2000a; Roeder and Yanofsky, 2006).

Moreover, FUL is needed for the correct dehiscent phase of the siliques. The dehiscent phase is when the valves open to obtain seed release. This phase depends on the correct differentiation of the valve margin. The valve margin as mentioned before, is composed of two cell layers which are: the lignified layer close to the valves and the separation layer close to the replum. Two MADS-box transcription factor SHP1 and SHP2, which act with a redundant activity, are involved in valve margin differentiation (Liljegren et al., 2000). The two promoters have the same expression pattern, before fertilization and during fruit development, in the valve margin (Flanagan et al., 1996; Savidge et al., 1995). The double mutant *shp1 shp2* is characterized by an indehiscent fruit in which the valves do not open to obtain seed release (Figure I.5-A). The indehiscent phenotype of the double mutant *shp1 shp2* is in particular caused by the absence of valve margin differentiation (Figure I.5-B,C) and by the failure of lignification in the lignified layer (Figure I.5-D,E) (Liljegren et al., 2000). These data confirm the role of the two MADS-box transcription factors in valve margin differentiation and dehiscent phase promoting differentiation and lignification.

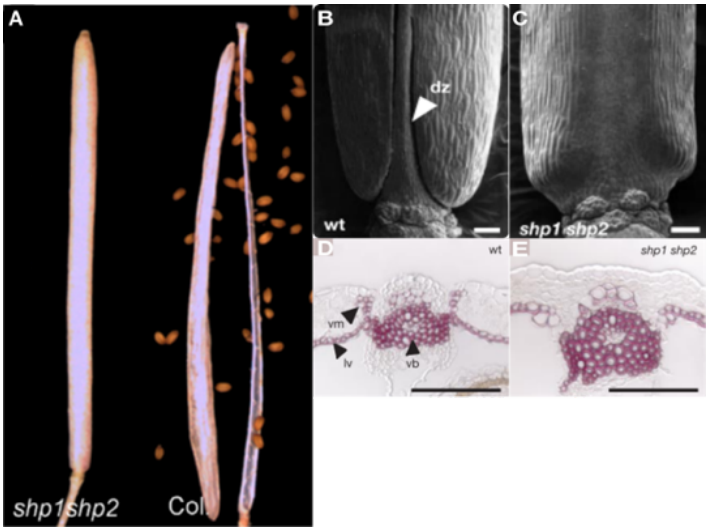

Figure I.5: ***shp1 shp2* double mutant phenotypes**.
(A) indehiscent silique of *shp1 shp2* at dehiscent phase compared to Col-0 wt; (B-C) SEM pictures of wt silique (dz: dehiscent zone) and *shp1 shp2* (B); (D, E) Fluoroglucinol staining of lignin, cross-section of silique at stage 17 of wt and *shp1 shp2* siliques. Modified and adapted from (Balanzà et al., 2016; Liljegren et al., 2000).

Additionally, to differentiate the valve margin, other two transcription factors are needed. These are two bHLH transcription factors IND and ALC. The two transcription factors act downstream of *SHP*s to regulate valve margin development (Liljegren et al., 2000; Liljegren et al., 2004; Rajani and Sundaresan, 2001). The *ind* and *alc* single mutants have both indehiscent fruit. The *alc* mutant phenotype is considered mild respect to *shp1 shp2* indehiscent phenotype because under pressure the fruit will open (Rajani and Sundaresan, 2001). In particular, this phenotype is caused by an ectopic lignification which also happens in the separation layer close to the replum, and not just in the lignified layer close to the valves, as occurs in the wild type siliques (Rajani and Sundaresan, 2001). ALC is required for the differentiation of the separation layer where inhibits the lignification (Rajani and Sundaresan, 2001). In contrast, the single mutant *ind* is characterized by a severe phenotype like *shp1 shp2*, without differentiation of valve margin and lignification of the lignified layer indicates that *IND* can regulate the correct development of the two cell layers composing valve margin (Liljegren et al., 2004). Interestingly, in *ful* mutant *IND* expression pattern changes. It is also detected in the valves, and not confined, as in the wild type, in the valve margin domain (Liljegren et al., 2004). Moreover, the double mutant phenotype *ful-2 ind* partially restores the cell length, but also the fruit length, when compared to the single mutant *ful-2* (Liljegren et al., 2004). These data indicate that in part *ful* phenotype is caused by the presence of the bHLH

transcription factor IND also in the valves, where could cause in *ful* mutant an ectopic accumulation of lignin and a failure of the cell elongation (Liljegren et al., 2004). Furthermore, FUL confines *SHP*s gene expression pattern in the valve margin (Ferrándiz et al., 2000b). In fact, in *ful*, *SHP*s expression is also located in valves. FUL is needed for valve development and for the inhibition of lignification in valve cells through the negative regulation of *SHP*s and *IND* activity and expression, which is confined thanks to the MADS-domain transcription factor FUL in the valve margin layers (Ferrándiz et al., 2000b; Liljegren et al., 2004).

To differentiate the replum in the wild type fruit is necessary the activity of *REPLUMLESS* (*RPL*). This gene encodes for a homeodomain protein. The promoter is active during pistil and fruit development in the replum and the vascular bundle of the medial domain (Roeder et al., 2003). When was identified for the first time, Roeder and collaborators screened three independent mutant alleles, which are *rpl-1, rpl-2* and *rpl-3*. The three mutant alleles have shorter fruits when compared to wild type (Figure I.6-A, D). Moreover, they have a clear reduction in the number of cell layers composing replum. In the *rpl* mutant alleles, the replum becomes narrower when compared to wild type where the replum is composed of eight-layers (Figure I.6-B). The most severe phenotype is related to *rpl-3* mutant in which just one cell layer constitutes the replum (Figure I.6-I) (Roeder et al., 2003).

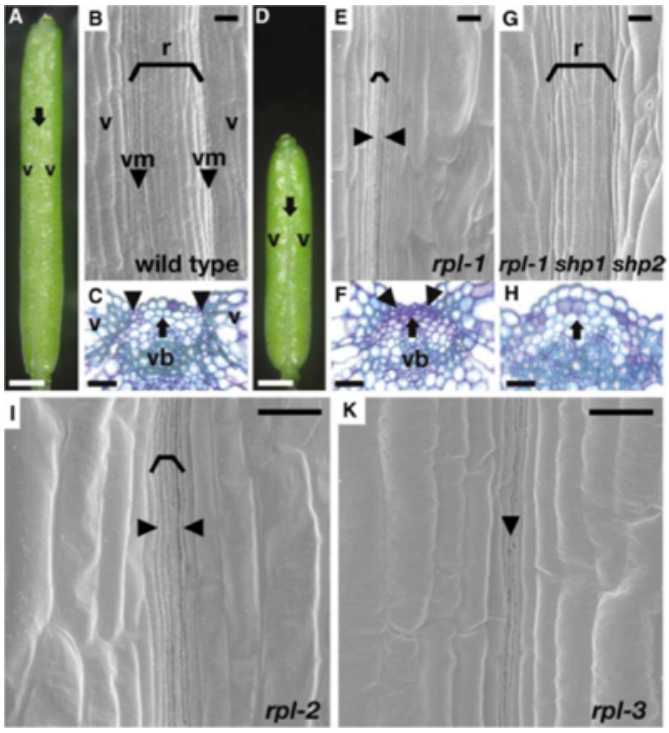

Figure I.6: Phenotypes of the three *rpl* single mutant alleles.
(A-C) wt fruit; (D-F) *rpl-1* fruit; (G-H) *rpl-1 shp1shp2* fruit. (I-K) *rpl-2* and *rpl-3* narrow replum. Adapted and modified from (Roeder et al., 2003).

As in *ful* mutants, also in *rpl* mutants *SHP*s expression pattern domain changes. In this case, it is also located in the replum and not confined in the valve margin, as in the wild type siliques (Roeder et al., 2003). The restore of replum cell layers in the triple mutant *rpl shp1 shp2* (Figure I.6-G) suggests that the failure of replum differentiation in *rpl* mutant alleles is in part caused by the presence of SHPs gene expression in the replum.

In summary, *FUL* is necessary to valve differentiation while *RPL* is needed for replum development, however, the two genes have a similar role in the dehiscent phase. RPL and FUL are necessary to confine the *SHP*s gene expression and activity in the valve margin tissue, to obtain the correct development of the various fruit structure and the dehiscent phase (Ferrándiz et al., 2000b; Roeder et al., 2003).

The floral homeotic gene *APETALA 2* (*AP2*) has multiple roles during fruit development

AP2 is considered a floral organ identity gene (Bowman et al., 1991; Bowman et al., 2007). However, it has multiple roles during plant development such as in flowering time, shoot apical meristem maintenance and seed development (Jofuku et al., 2005; Ohto et al., 2009; Wurschum et al., 2006; Yant et al., 2010). During the last few years has been discovered different roles of *AP2* in fruit development. First of all, *AP2* with *ASYMMETRIC LEAVES1* (*AS1*) acts to prevent replum and valve margin overgrowth, through the negative regulation of *RPL* and *SHP*s genes (Ripoll et al., 2011). The double mutant *ap2 as1* is characterized by an enlarged replum (Ripoll et al., 2011). Moreover, it was described in 2015 by Ripoll and collaborators, the novel role of *AP2* in fruit elongation. Indeed, AUXIN RESPONSE FACTOR 6 (ARF6) and ARF8 interact with FUL, recruit miR172c which is required to down-regulate *AP2* expression. *AP2* expressed in valves negatively regulates cell elongation (Ripoll et al., 2015). Indeed, *AP2* is considered a negative regulator of fruit growth.

Hormone control of fruit development and elongation

Hormones regulate fruit set, development, maturation, senescence and dehiscent phase in *Arabidopsis* siliques. Each step is usually modulated by two or three hormones simultaneously. As mentioned before, a hormonal signal is needed to start fruit growth after double fertilization process. In particular, when fertilization occurs, in the ovules is generated an increase of AUX biosynthesis which causes the stimulation of GA biosynthesis (Alabadí et al., 2009). The fruit growing in relation to the seeds and embryo development. There is an undiscovered signal, that induces valves elongation after fertilization of ovules. Dorcey and collaborators (2009)

described the role of AUX induces GA synthesis in the ovules. However, they discovered that AUX is just present in ovules and not in ovary tissues. They propose GA as the phytohormone that coordinate fruit and seed growth (Dorcey et al., 2009). In particular, GA in the mesocarp (medial tissue composing fruit) induces anticlinal division in the first phase of fruit growth, with a subsequent cell expansion phase, while in the exocarp (most external tissue composing fruit) after a short phase of cell division, the cell increasing length thanks to a longitudinal expansion (Vivian-Smith et al., 2001).

Additional important phytohormone, required for pistil and fruit development are the cytokinins (CKs). The CKs, which are adenine derivates, are plant hormones with several and pivotal roles during all phases of plant development (Werner and Schmülling, 2009). The plants synthetize four different cytokinin-types that are isopentenyl adenine (IP), *trans*-zeatin (*t*Z), *cis*-zeatin (*c*Z) and dehydrozeatin (DHZ) (Mok and Mok, 2001). Exogenous application of cytokinin, in different species, can induce parthenocarpic fruit (Ding et al., 2013) as the application of AUX and GA in Arabidopsis (Vivian-Smith and Koltunow, 1999). However, the action of the CKs with the other two hormones to induce fruit set is still uncharacterized. Moreover, the CKs have a crucial role in placenta development during pistil differentiation (Bartrina et al., 2011; Cucinotta et al., 2016; Reyes-Olalde et al., 2017). Indeed, the *Cytokinin response factor* (*crf*) multiple mutant causes a reduction of ovule number and placenta size (Cucinotta et al., 2016).

Nevertheless, their role in fruit elongation is still poorly understood. It has been shown that CKs are involved in valve margin differentiation (Marsch-Martínez et al., 2012). In the double mutant *shp1 shp2*, the indehiscent fruit phenotype, which is caused by a defect in valve margin differentiation (Liljegren et al., 2000) can be rescued by exogenous CK treatments (Marsch-Martínez et al., 2012). The restore of valve margin in the double mutant *shp1 shp2* treated with exogenous CK suggests a role of these hormones in valve margin differentiation and seed shattering in *Arabidopsis*.

CYTOKININ OXIDASE/DEHYDROGENASE (*CKX*) gene family in *A. thaliana*

The CKX proteins catalyse the irreversible degradation of the cytokinins isopentenyladenine, zeatin and their ribosides transforming them to adenine and the corresponding unsaturated aldehyde (Mok and Mok, 2001). The gene family in *A. thaliana* is composed of seven members (Mok and Mok, 2001). The expression pattern of the genes that encode for CKX proteins change in the vegetative and reproductive phases, consequently, they have different roles in

the regulation of plant development (Werner et al., 2003). Interestingly, the CKX proteins have a clear different cellular localization which reveals their action on different CK pools. Excluding CKX7, which is the only one that acting in the cytosolic compartment of the cell, all the AtCKX proteins have a hydrophobic N-terminal signal peptide that targets them either to vacuoles (CKX1 and CKX3) or to the apoplast (CKX2, CKX4, CKX5, and CKX6) (Frébort et al., 2011; Köllmer et al., 2014; Werner et al., 2003).

The *CKX1* and *CKX2* promoters are in particular active during the reproductive phase, in the shoot apex, where influence the SHOOT APICAL MERISTEM (SAM) size with *CKX3* and *CKX4*. When Werner and collaborators generate the transgenic overexpression of these four genes, the plants were characterized by a reduction in SAM size (Werner et al., 2003). Deficient cytokinin mutants, caused by the over-expression of the genes described above showed smaller SAM when compared to wild type, indicating the role of CK in the regulation of cell proliferation in SAM (Werner et al., 2003).

In contrast, a lack of CK degradation in the double mutant *ckx3 ckx5* causes an increase of pistil size and ovule number, indicating a negative role of the CKs in cell proliferation and expansion in the female organ before fertilization (Bartrina et al., 2011).

One of the less-studied genes of this family is *CKX6*. The promoter of this gene is active in both vegetative and reproductive phases. In particular, it is active in seedling and the funiculus (Carabelli et al., 2007; Werner et al., 2003). The apoplast protein CKX6 has a role in mediating the Shade Avoidance Response (SAS) (Carabelli et al., 2007). Arabidopsis plants carrying a mutated *ckx6* allele lack the block of leaf primordium growth in response to shading (Carabelli et al., 2007).

The *CKX7* is expressed during the vegetative and reproductive phases in *A. thaliana*. It has been demonstrated that the *CKX7* promoter activity, analysed by GUS assay, during vegetative phases is localized in seedlings, in the vasculature of the primary root and shoot organs, vascular cells in the distal tip of the rosette leaf 9 days after germination. During the reproductive phase of plant development, *CKX7* was active in the medial domain of the fruit (replum and transmitting tract), and in the mature embryo sac with the highest activity associated with the egg cell and synergids (Köllmer et al., 2014).

The *CKX7* gene encodes for the unique CKX protein localizes at the cytosolic compartment of the cell where it can degrade a specific CK pool (Köllmer et al., 2014). Schmulling and

collaborators have shown that CKX7 has the lowest similarity with the other members of AtCKX family, although it is the CKX more similar to CKX-like proteins of bacteria and green algae (Schmülling et al., 2003). Recently it was reported that CKX7 is required for proper root growth and xylem differentiation (Köllmer et al., 2014).

RESULTS and DISCUSSION

The MADS-box transcription factor SEEDSTICK is one of the main players involved in the regulation of transmitting tract development

STK and CESTA (CES) guide transmitting tract development

It has been demonstrated the role of *STK* with *NTT* in the regulation of transmitting tract development (Herrera-Ubaldo et al., 2019). Moreover, NTT is a positive regulator of *CES* (also named *HAF*) (Crawford and Yanofsky, 2011). The triple mutant *bee1 bee3 ces* (*haf*) displayed similar phenotypes of the *ntt* mutant, with an important percentage of unfertilized ovules (Crawford and Yanofsky, 2011; Crawford et al., 2007; Herrera-Ubaldo et al., 2019).

The two genes have the same pattern of expression in the pistils before and during fertilization (Figure 1 of the attached manuscript 2 to see *CES* expression profile and for *STK* expression profile see Fig. I.2 A-F). Assumed that the two genes are co-expressed (Mendes et al., 2016) with the same pattern of expression, we suppose that the MADS-box transcription factor STK and the bHLH encoding factor CES can interact to regulate transmitting tract development and ovule fertilization.

First of all, we decided to generate the double mutant *stk ces-2* by crossing the two single mutants. We used the *ces-2* mutant allele that is an uncharacterized knockout mutant (see Figure S1 of the attached manuscript 2 for knockout validation). Moreover, since that SHP1 and SHP2 are closely related MADS-box transcription factor to STK and act redundantly to control ovule identity (Pinyopich et al., 2003), we investigated whether they also could play a role together with CES in the control of transmitting tract development and ovule fertilization. Therefore, the *shp1 shp2* double mutant was crossed with the *ces-2* mutant to obtain *shp1 shp2 ces-2* triple mutant.

We analyzed the percentage of unfertilized ovules in the mutant lines when compared to wild type Col-0 (Figure R.1). The wild type displayed an average of 1% of unfertilized ovules (Figure R.1). The single mutants *stk* and *ces-2* displayed an increase in unfertilized ovules respect to wild type siliques (*stk*=6.2%; *ces-2*= 11.6%) (Figure R.1). However, just *ces-2* is characterized by statistical differences when compared to wild type. In particular, in the two single mutants, the unfertilized ovules are localized at the bottom part of the silique (Figure R.1). This phenotype suggests a partial failure of pollen tube growth in the single mutants and a contribution of the two genes in transmitting tract development. The double mutant *shp1 shp2* had a similar percentage of unfertilized ovules like (7%) as we found in the *stk* mutant (Figure

R.1). However, the unfertilized ovules are located not just in the bottom part of the silique suggest that the *SHP*s are not able to influence transmitting tract development.

When we analyzed the multiple mutant combinations, there was an increase of unfertilized ovules. The *stk ces-2* double mutant displayed the most severe phenotype with an average of 28.1% of unfertilized ovules when compared to wild type (Figure R.1). In particular, the unfertilized ovules are located from the middle to the bottom part of the siliques suggest a defective transmitting tract, as previously described in the double mutant *ntt stk* (Herrera-Ubaldo et al., 2019).

However, not a similar increase of unfertilized ovules, a milder phenotype with respect to *stk ces-2*, was revealed in the triple mutant *shp1 shp2 ces-2* (16.2%) (Figure R.1), suggests that this phenotype it could be an effect of *STK* activity in this triple mutant, in which *STK* is not able to recover all the phenotype. We hypothesize that STK, with CES, play a major role in the control of transmitting tract development and ovule fertilization.

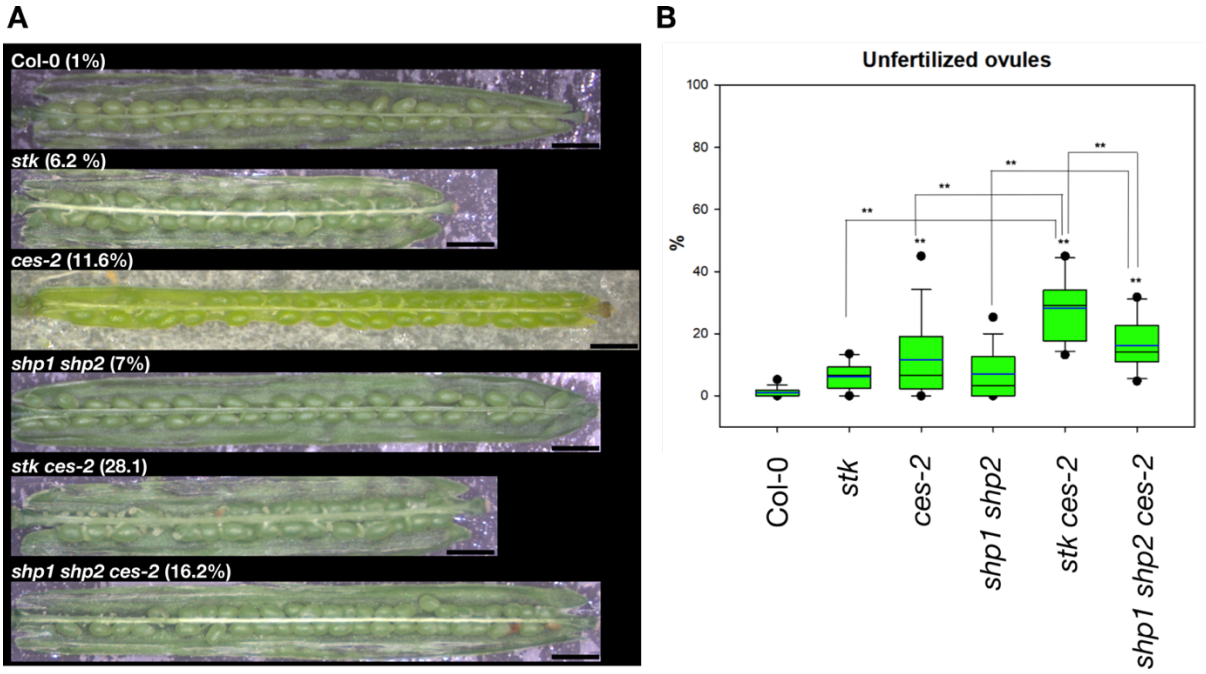

Fig R.1: **Analysis of the unfertilized ovules in multiple mutant combinations.**
(A) Stereomicroscope pictures of opened siliques of *stk*, *ces-2*, *shp1 shp2*, *stk ces-2* and *shp1 shp2 ces-2* compared to Col-0 (wt) Scale bars: 1 mm; (B) Box plot represents the percentage of unfertilized ovules in the single and multiple mutant combinations described above. Statistical analysis was performed using Anova followed by Tukey HSD test (**=p-value <0.01).

STK and CES play a major role in transmitting tract development

As described in literature CES interacts with BEE1 and BEE3 to regulates transmitting tract development (Crawford and Yanofsky, 2011). Moreover, *BEE1* and *BEE3* are closely related

genes of *BEE2* (Friedrichsen et al., 2002). To investigate the contribution of *BEE*s genes with *CES* in transmitting tract development and ovule fertilization we decided to generate by crossing multiple mutant combinations with *ces-2*. We analyzed the unfertilized ovules percentage of the siliques in the double mutant *bee1 bee3*, the triple mutant *bee1 bee2 bee3*, but also in the quadruple mutant *bee1 bee2 bee3 ces-2* (Cifuentes-Esquivel et al., 2013). Besides, to study the possible link between *BEE*s and *STK*, we generated the quadruple mutant *bee1 bee2 bee3 stk.* Finally, we also obtained the quadruple *bee1 bee3 stk ces-2* mutant, and the quintuple mutant *bee1 bee2 bee3 stk ces-2* to confirm that STK and CES play the major role in transmitting tract development (Figure R.2).

The single mutants *bee1* (0.78%) and *bee3* (1.43%) do not display differences in the unfertilized ovules percentage when compared to wild type (0.53%) (Figure R.2). The same results were obtained also for the double mutant *bee1 bee3* (1%) and the triple mutant *bee1 bee2 bee3* (1.78%) that displayed no differences when compared to wild type (Figure R.2). These results suggest that the *BEE*s alone are not able to influence transmitting tract differentiation.

However, when we analyzed the unfertilized ovules in the quadruple mutant combinations *bee1 bee2 bee3 ces-2* (28.79%) and *bee1 bee2 bee3 stk* (9.21%) the percentages increase with statistical differences when compared to wild type (Figure R.2). As we expected, and already described with another mutant allele of *CES* (Crawford and Yanofsky, 2011), the number of unfertilized ovules increases in the quadruple mutant *bee1 bee2 bee3 ces-2* confirmed the redundant action of these genes in transmitting tract. The *bee1 bee2 bee3 stk* mutant is characterized by an increase of unfertilized ovules (9.21%) (Figure R.2) respect to the single mutant *stk* (see Figure R.1), confirms the possibility that also *STK* has genetic relationship to *BEE*s.

The most interestingly phenotypes are obtained from the quadruple mutant *bee1 bee3 stk ces-2* and the quintuple mutant *bee1 bee2 bee3 stk ces-2*. In the *bee1 bee3 stk ces-2* mutant the percentage of unfertilized ovules in average is 46.59%, while in the *bee1 bee2 bee3 stk ces-2* is 43.79% (Figure R.2). The quadruple and quintuple mutants displayed the same percentage of unfertilized ovules that permits to exclude *BEE2* from the pathway that regulates transmitting tract development and consequently the ovule fertilization. Interestingly, the two mutants displayed a clear increase in unfertilized ovules respect to *bee1 bee2 bee3 stk* and *bee1 bee2 bee3 ces-2*, confirmed that the two protein STK and CES have the major role in this pathway.

The different gradation of ovule fertilization phenotypes obtained in the different mutant combinations points to redundancy between the MADS-box, bHLH gene, and the BEEs which also have a dose-dependent effect on the phenotypes. The phenotype was only observed when combining different mutant alleles. This dosage-dependent effect was already described for other MADS-box genes, like FLOWERING LOCUS C (FLC) that acts, in a dosage-dependent manner, as a potent repressor of the floral transition (Bastow et al., 2004; Michaels and Amasino, 2007; Sheldon et al., 2007).

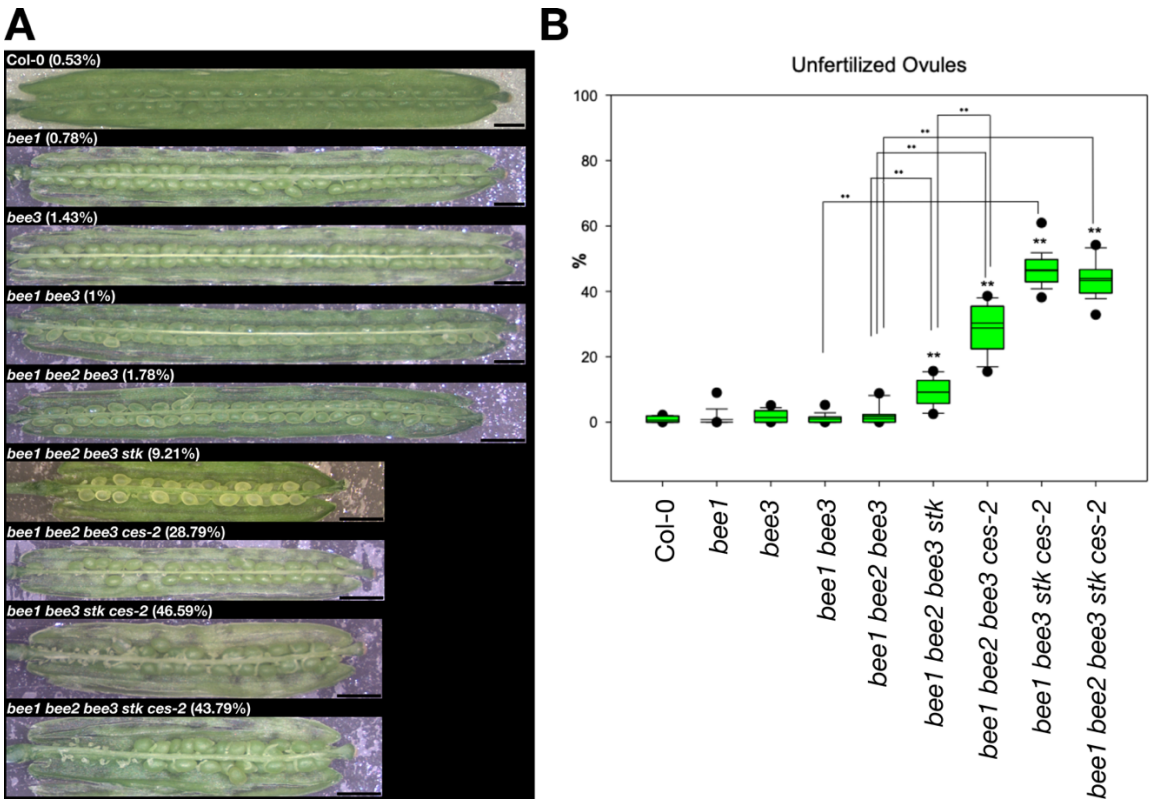

Fig R.2: **Analysis of the unfertilized ovules in multiple mutant combinations.**
(A) Stereomicroscope picture of opened siliques of *bee1*, *bee3*, *bee1 bee3*, *bee1 bee2 bee3*, *bee1 bee2 bee3 stk*, *bee1 bee2 bee3 ces-2*, *bee1 bee3 stk ces-2*, *bee1 bee2 bee3 stk ces-2* compared to Col-0 (wt) Scale bars: 1 mm; (B) Box plot represents the percentage of unfertilized ovules in the single and multiple mutant combinations described above. Statistical analysis was performed using Anova followed by Tukey HSD test (**=p-value <0.01).

The significant number of unfertilized ovules when STK and CES are mutated together, suggests the possibility that the two genes can interact and act together to influence transmitting tract development. Indeed, the two proteins interact with a physical interaction between them in planta analyzed through Bimolecular Fluorescence Complementation (BiFC) (see Figure 5, attached manuscript 2). Moreover, to confirm the protein interaction, we performed the Yeast Two-Hybrid assay. Also, this experiment confirmed the interaction between the MADS-box

transcription factor STK and the bHLH transcription factor CES (see Figure 5, attached manuscript 2).

Y2H and BIFC experiments showed that STK can interact with CES, but not with BEE1 (see Figure 5 and Table S3 attached manuscript 2). These results suggest that CES might bridge the interaction between MADS and BEE proteins. A hypothetical multimeric complex, which is important for correct transmitting tract formation and achievement of fertility, can be formed. Cooperative action of MADS-box and bHLH transcription factors have been previously described in mice. Molkentin and collaborators stated in 1995 that MEF2 factors, a family of MADS-box proteins expressed in muscle cells and other cell types, were not able to activate muscle genes alone, but acting as coregulators of myogenic bHLH proteins (Molkentin et al., 1995). Moreover, the authors show that these two types of transcription factors physically interact and that either factor can interact with the other when one is bound to DNA (Molkentin et al., 1995). Interestingly, the authors present this as a general mechanism for the regulation of transcription in specific cell types (Molkentin et al., 1995). This might also be a mechanism for the combinatorial control of MADS-box (with STK as the main player) and bHLH (CES as the main player) genes of the formation of the transmitting tract tissue in *Arabidopsis*.

RNA sequencing of *bee1 bee3 stk ces-2* to understand new downstream players involving in transmitting tract development

We decided to perform a transcriptome profile of the quadruple mutant *bee1 bee3 stk ces-2* which displayed the most severe phenotype regarding to unfertilized ovules, (see Fig. R.2) when compared to wild type, to deep analyze the regulatory network downstream of STK-CES-BEE1-BEE3 protein complex. The RNA was extracted from inflorescence till stage 12 before fertilization when transmitting tract is fully developed, according to (Reyes-Olalde et al., 2013; Roeder and Yanofsky, 2006). Several genes were mis-regulated in the quadruple mutant when compared to wild type; We have found in total 202 mis-expressed genes in the quadruple mutant when compared to wild type, 31 up-regulated and 171 down-regulated (Table S5 and Table S6 of the attached manuscript 2). Remarkably functional enrichment analyses gene ontology categories such as programmed cell death (PCD), extracellular matrix (ECM) and cell wall biosynthesis components, for the up-regulated genes (Table R.1), while the down-regulated genes were enriched in carbohydrate biosynthesis process (Table R.2).

The most interesting candidates regarding the transmitting tract development are listed in Table R.3.

Table R.1: **Gene Ontology analysis of the genes up-regulated in the quadruple mutant *bee1 bee3 stk ces-2* in comparison with wild type**.

GO_acc	term_type	Term	pvalue	FDR
GO:0050896	P	response to stimulus	2.40E-08	9.20E-06
GO:0010033	P	response to organic substance	2.70E-07	5.10E-05
GO:0042221	P	response to chemical stimulus	2.30E-06	0.00029
GO:0019825	F	oxygen binding	1.80E-06	0.00036
GO:0020037	F	heme binding	4.90E-06	0.00048
GO:0051704	P	multi-organism process	6.20E-06	0.0006
GO:0051707	P	response to other organism	1.10E-05	0.00083
GO:0016798	F	hydrolase activity, acting on glycosyl bonds	1.70E-05	0.0011
GO:0009607	P	response to biotic stimulus	2.00E-05	0.0013
GO:0046906	F	tetrapyrrole binding	3.00E-05	0.0015
GO:0009719	P	response to endogenous stimulus	5.10E-05	0.0028
GO:0005506	F	iron ion binding	7.50E-05	0.003
GO:0003824	F	catalytic activity	0.00011	0.0036
GO:0009725	P	response to hormone stimulus	7.90E-05	0.0038
GO:0005488	F	binding	0.00016	0.0045
GO:0004553	F	hydrolase activity, hydrolyzing O-glycosyl compounds	0.00021	0.0047
GO:0016684	F	oxidoreductase activity, acting on peroxide as acceptor	0.00024	0.0047
GO:0004601	F	peroxidase activity	0.00024	0.0047
GO:0016209	F	antioxidant activity	0.0005	0.009
GO:0009751	P	response to salicylic acid stimulus	0.00024	0.01
GO:0016740	F	transferase activity	0.00066	0.011
GO:0030312	C	external encapsulating structure	0.00037	0.015
GO:0005618	C	cell wall	0.00035	0.015
GO:0009505	C	plant-type cell wall	0.00081	0.022
GO:0016301	F	kinase activity	0.0016	0.024
GO:0009055	F	electron carrier activity	0.0017	0.024
GO:0016491	F	oxidoreductase activity	0.0036	0.048
GO:0008219	P	cell death	0.0015	0.05
GO:0016265	P	death	0.0015	0.05

Column 1: Gene Ontology (GO) term unique identifier; Column 2: Gene Ontology term functional category: P= biological process; F= molecular function; C= cellular component; Column 3: Gene ontology term official name; Column 4: p-value for the enrichment of the GO term in the gene set; Column 5: Benjamin Hochberg adjusted p-value, a significance cut-off of 0.05 is applied.

Table R.2: **Gene Ontology analysis of the genes down-regulated in the quadruple mutant *bee1 bee3 stk ces-2* in comparison with wild type.**

GO_acc	term_type	Term	pvalue	FDR
GO:0019758	P	glycosinolate biosynthetic process	2.20E-14	8.10E-13
GO:0019761	P	glucosinolate biosynthetic process	2.20E-14	8.10E-13
GO:0016144	P	S-glycoside biosynthetic process	2.20E-14	8.10E-13
GO:0019757	P	glycosinolate metabolic process	3.20E-13	5.80E-12
GO:0019760	P	glucosinolate metabolic process	3.20E-13	5.80E-12
GO:0016143	P	S-glycoside metabolic process	3.20E-13	5.80E-12
GO:0016138	P	glycoside biosynthetic process	1.60E-12	2.50E-11
GO:0016137	P	glycoside metabolic process	9.80E-12	1.30E-10
GO:0044272	P	sulfur compound biosynthetic process	1.90E-11	2.30E-10
GO:0044262	P	cellular carbohydrate metabolic process	1.50E-10	1.60E-09
GO:0034637	P	cellular carbohydrate biosynthetic process	3.50E-10	3.50E-09
GO:0006790	P	sulfur metabolic process	1.50E-09	1.40E-08
GO:0016051	P	carbohydrate biosynthetic process	7.00E-09	6.00E-08
GO:0005975	P	carbohydrate metabolic process	7.50E-08	5.90E-07
GO:0019748	P	secondary metabolic process	3.10E-07	2.30E-06
GO:0050896	P	response to stimulus	0.00079	0.0054
GO:0044238	P	primary metabolic process	0.0012	0.008
GO:0009058	P	biosynthetic process	0.0015	0.0094
GO:0009719	P	response to endogenous stimulus	0.0029	0.016
GO:0008152	P	metabolic process	0.003	0.016
GO:0044249	P	cellular biosynthetic process	0.0038	0.02
GO:0010033	P	response to organic substance	0.0076	0.036
GO:0044237	P	cellular metabolic process	0.0075	0.036
GO:0006950	P	response to stress	0.019	0.086
GO:0042221	P	response to chemical stimulus	0.042	0.18
GO:0009987	P	cellular process	0.047	0.2
GO:0044260	P	cellular macromolecule metabolic process	0.57	1
GO:0043170	P	macromolecule metabolic process	0.67	1
GO:0003824	F	catalytic activity	0.0077	0.027
GO:0016740	F	transferase activity	0.0097	0.027
GO:0005488	F	binding	0.93	1
GO:0012505	C	endomembrane system	0.00018	0.0074
GO:0005623	C	cell	0.0021	0.029
GO:0044464	C	cell part	0.0021	0.029
GO:0043229	C	intracellular organelle	0.34	1
GO:0043227	C	membrane-bounded organelle	0.26	1
GO:0043226	C	organelle	0.34	1
GO:0009536	C	plastid	0.14	1
GO:0016020	C	membrane	0.17	1
GO:0005737	C	cytoplasm	0.45	1
GO:0043231	C	intracellular membrane-bounded organelle	0.26	1
GO:0044444	C	cytoplasmic part	0.36	1
GO:0044424	C	intracellular part	0.23	1
GO:0005622	C	intracellular	0.27	1

Column 1: Gene Ontology (GO) term unique identifier; Column 2: Gene Ontology term functional category: P= biological process; F= molecular function; C= cellular component; Column 3: Gene ontology term official name; Column 4: p-value for the enrichment of the GO term in the gene set; Column 5: Benjamin Hochberg adjusted p-value, a significance cut-off of 0.05 is applied.

Table R.3: RNAseq data of the most interestingly genes involving in PCD, ECM, cell wall biosynthesis component and auxin signaling in *bee1 bee3 stk ces-2* when compared to wild type.

Gene code	Gene Name	Fold Change	FDR	Gene function
AT4G14400	*ACD6*	-4.0117	2.33E-05	Cell death
AT1G06080	*ADS1*	-1.0338	2.17E-05	Cell wall and ECM biosynthesis
AT1G35230	*AGP5*	-2.1455	0.0145	Cell death and ECM biosynthesis
AT5G65390	*AGP7*	-1.3013	0.0024	Cell death and ECM biosynthesis
AT5G56540	*AGP14*	-0.7840	0.0473	Cell death and ECM biosynthesis
AT1G72290	*ATWSCP*	-6.5142	1.42E-07	Cell death and pollen tube growth
AT5G09730	*BXL3*	-2.0805	1.71E-06	Cell wall
AT1G75890	GDSL family of serine esterases/lipases	0.8845	0.0038	Cell wall and lipid metabolic process
AT4G28780	GDSL family of serine esterases/lipases	0.6227	0.0393	Cell wall and lipid metabolic process
AT4G16230	GDSL family of serine esterases/lipases	1.0662	0.0127	Cell wall and lipid metabolic process
AT3G26140	Glycosyl hydrolase family 5	-2.7099	3.13E-06	Cell wall and ECM biosynthesis
AT1G53130	*GRI*	-7.9981	4.16E-09	Cell death
AT4G14560	*IAA1*	-0.7727	0.0387	AUX signalling
AT3G23030	*IAA2*	-0.6711	0.0393	AUX signalling
AT4G14550	*IAA14*	-0.9381	0.0265	AUX signalling
AT1G04250	*IAA17*	-1.2215	0.0037	AUX signalling
AT2G38530	*LTP2*	-0.8702	0.0257	Lipid transport, cell death, cuticle biosynthesis
AT1G28710	nucleotide diphospho-sugar transferase protein	-1.2338	0.00008	Cell wall and ECM biosynthesis

AT5G49180	*PME58*	-0.6750	0.0459	Cell wall
AT4G36110	*SAUR9*	-1.2233	0.0447	Auxin response
AT2G21220	*SAUR12*	-0.7960	0.0239	Auxin response

Column 1: gene code; Column 2: Gene name; Column 3: Log Fold change of expression between mutants and wild type plants; Column 4: Benjamini Hochberg adjusted P-value for differential expression. A Significance cut-off of 0.05 is applied; Column 5: gene function.

Among the different genes downregulated in the quadruple mutant respect to wild type, three genes were previously described as direct targets of STK (Herrera-Ubaldo et al., 2019). The first one is *AT3G26140* (glycosyl hydrolase, family 5, subfamily 11) expressed in CMM during pistil development, which encodes a glycosyl hydrolase (GH5_11). The GH5 enzymes are all mannan endo-beta-1,4-mannosidases involving in cell wall remodelling process (Aspeborg et al., 2012). The second one is *AT1G28710* (nucleotide diphospho-sugar transferase protein) which encodes for an enzyme involving in polysaccharides biosynthesis (Lombard et al., 2014), that are fundamental components of the ECM. The third one is *DELTA 9 DESATURASE1* (*ADS1*) *AT1G06080*, encoding for a fatty acid desaturase involved in lipid biosynthesis, expressed in flowers (Fukuchi-Mizutani et al., 1998; Heilmann et al., 2004; Yao et al., 2003) (Table R.3). These three genes resulted down-regulated in RNAseq data, were used for the RNAseq validation through qRT-PCR (Figure R.3).

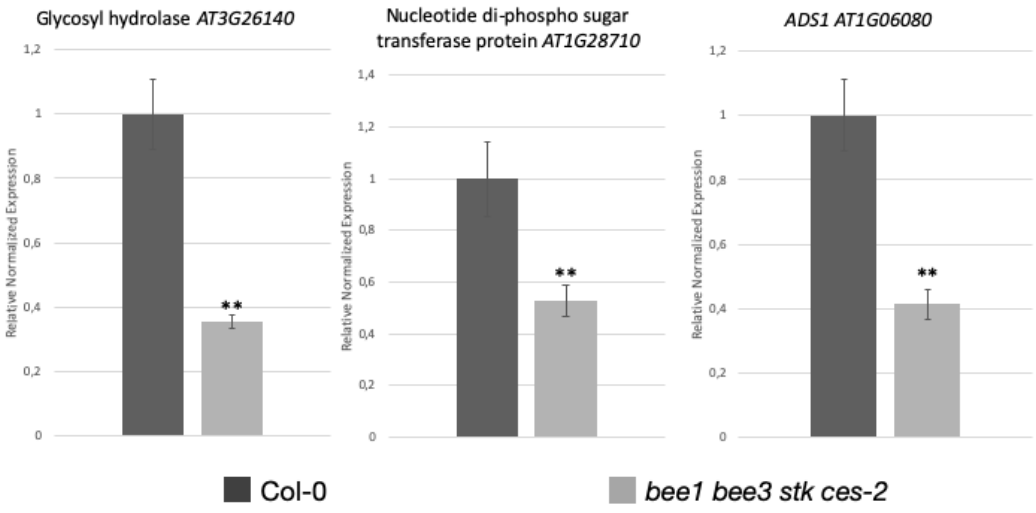

Fig R.3: **qRT-PCR to validate RNAseq data.**
The genes selected to validate are: *AT3G26140*; *AT1G28710* and *AT1G06080*. Student's *t*-test was used to analyze statistical differences in gene expression between the mutant and wild type backgrounds (** = p<0.01). Normalized with *ACTIN* and *UBIQUITIN*.

Different genes described in the regulation of cell death are downregulated in the quadruple mutant when compared to wild type (Table R.3). One of the most important is *GRIM REAPER* (*GRI*, *AT1G53130*) that encodes for a small protein with an extracellular localization that positively regulates cell death (Wrzaczek et al., 2009; Wrzaczek et al., 2015) (Table R.3). Moreover, it is also downregulated *ACCELERATED CELL DEATH 6* (*ACD6*, *AT4G14400*) another positive regulator of cell death (Rate et al., 2007) (Table R.3). Three genes encoding for the Arabinogalactan proteins (AGPs) are downregulated, these are *ARABINOGALACTAN PROTEIN 5* (*AGP5*, *AT1G35230*), *AGP7* (*AT5G65390*) and *AGP14* (*AT5G56540*) (Table R.3). The AGPs proteins are structurally complex plasma membrane and cell wall proteoglycans that are implicated in diverse developmental processes, including plant sexual reproduction (Coimbra et al., 2007; Coimbra et al., 2009; Lennon et al., 1998). Besides, these protein can regulate cell death in Arabidopsis cell culture (Gao and Showalter, 1999; Guan and Nothnagel, 2004).

Cell death and tissue degeneration are required for pollen tube growth in the transmitting tract of *Arabidopsis* (Crawford et al., 2007). The phenotype described for combined *ces* and *bee* mutants showed that they fail to form the ECM and to accomplish the PCD within the transmitting tract (Crawford and Yanofsky, 2011; Poppenberger et al., 2011). Interestingly, STK has already shown to control PCD in transmitting tract with NTT (Herrera-Ubaldo et al., 2019) but also in the receptive synergid cell through regulation of its direct target genes, *VERDANDI (VDD)* and *VALKYRIA (VAL)*, two Reproductive Meristem (REM) transcription factors (Matias-Hernandez et. al 2010; Mendes et al., 2016).

One of the most interestingly candidate that could be downstream of MADS-bHLH protein complex is *WATER-SOLUBLE CHLOROPHYLL PROTEIN 1* (*ATWSCP*, *AT1G72290*) (Table R.3). It encodes for a Kunitz-type protease inhibitor localized preferentially in the transmitting and septum, which is involved in ECM and PCD but also in the exit of pollen tube from the septum to reach the ovules during fertilization phase (Bektas et al., 2012; Boex-Fontvieille et al., 2015). *ATWSCP* is expressed in the septum and transmitting tract during its development, and after fertilization, the protein is localized in the medial domain of the silique (Bektas et al., 2012; Boex-Fontvieille et al., 2015).

Probably, the PCD in the quadruple mutant is totally or in part compromised, caused by the downregulation of different genes involved in cell death.

The most interesting candidates involved in cell wall biosynthesis process are *BETA-XYLOSIDASE 3* (*BXL3*, *AT5G09730*), that encodes for an enzyme involved in arabinan and

xylan catabolic process (Minic et al., 2006), and *PECTIN METHYLESTERASE 58* (*PME58*, *AT5G49180*), which encodes for a pectin methylesterases contributes to cell wall modification (Turbant et al., 2016) which resulted down-regulated in the quadruple mutant respect to wild type (Table R.3).

Among the up-regulated genes, there are three genes of the GDSL family of serine esterases/lipases, *AT1G75890*, *AT4G28780* and *AT4G16230* (Table R.3). These genes coding for enzymes involved in the acetylxylan esterase activity that is important for the degradation of the cell wall in association with xylanases, cellulases, and mannanases (Akoh et al., 2004).

Modification of cell wall components and ECM during transmitting tract development is essential to obtain a correct pollen tube growth and to permit them to reach the ovules and fertilize it (Crawford and Yanofsky, 2008; Crawford et al., 2007; Herrera-Ubaldo and de Folter, 2018). It is also clear from our RNAseq analysis that, as for PCD, in the quadruple mutant the cell wall biosynthesis and remodeling process is altered.

Interestingly, in the quadruple mutant respect to wild type, also the auxin signaling pathway is altered. The auxin plays a role in the specification and formation of the tissues along the pistil axis (Larsson et al., 2013a; Robert et al., 2015). However, the role of auxin signaling in transmitting tract development is not fully clear. ARF6 and ARF8 regulate *CES* expression in the medial domain of the pistil during transmitting tract development (Crawford and Yanofsky, 2011). The double mutant *arf6 arf8* displayed reduced alcian blue staining, that detects acid polysaccharides, the major component of the ECM (Crawford and Yanofsky, 2011).

In our RNAseq dataset we found that different genes encoding for Aux/IAAs proteins, *INDOLE-3-ACETIC ACID INDUCIBLE 1* (*IAA1*) (*AT4G14560*), *IAA2* (*AT3G23030*), *IAA14* (*AT4G14550*) and *IAA17* (*AT1G04250*) were downregulated (Table R.3). The Aux/IAA proteins are the early auxin response proteins and participate in auxin signaling through interacting, as repressors, with ARF proteins (Lavy and Estelle, 2016). Also, the *SMALL AUXIN UPREGULATED RNA 9* (*SAUR9*) and *SAUR12* resulted downregulated (Table R.3). The SAURs are small transcripts induced by auxin, especially localized in elongated tissue (Knauss et al., 2003; McClure and Guilfoyle, 1987). *SAUR9* and *SAUR12* are part of the same clade, the *SAUR10*-clade (van Mourik et al., 2017).

Aux/IAAs protein and SAURs could be activated in the presence of brassinosteroid. Evidence of crosstalk between auxin and brassinosteroid are already described, depending on cell and organ types (Nakamura et al., 2006). Moreover, *SAUR9* expression is induced by a combination of auxin and brassinosteroid treatment (van Mourik et al., 2017). Probably the STK-CES-

BEE1-BEE3 complex is able to regulate the auxin-brassinosteroid crosstalk in transmitting tract tissue. However, it is unclear the role of this crosstalk in the regulation of transmitting tract development. Future analyses are needed to understand how this crosstalk contributes to the differentiation of transmitting tract and in the correct ovule fertilization.

STK and CES guide carpel fusion and transmitting tract development

When we discovered that the male part of the flowers, was not compromised in the mutant *stk ces-2* and *shp1 shp2 ces-2* thanks to the backcross (see Supplemental Figure 2 of attached manuscript 2), we decided to perform a detailed analysis of the septum morphology of the mutant displayed the most severe phenotype related to the percentage of unfertilized ovules (Figure R.4). To understand if the two genes are able to influence carpel fusion during pistil development, we analyzed the septum morphology by Scanning Electronic Microscope (SEM) at stage 17 of the fruit in single mutants *stk* and *ces-2*, in the double mutant *stk ces-2*, in the quadruple mutants *bee1 bee2 bee3 stk*, *bee1 bee2 bee3 ces-2*, *bee1 bee3 stk ces-2* and in the quintuple mutant *bee1 bee2 bee3 stk ces-2*, in order to see if this component is damaged, or the cells appear different in the mutants when compared to wild type. Single mutants *stk* and *ces-2* presented a similar septum when compared to wild type, while the double mutant *stk ces-2* disclosed a defect in septum morphology (Figure R.4). The double mutant *stk ces-2* is characterized by a partial failure of the septum fusion, in the central portion of the septum in conjunction with the medium portion of the ovary (Figure R.4). The quadruple mutant combinations *bee1 bee2 bee3 stk* and *bee1 bee2 bee3 ces-2* did not display defects in septum morphology when compared to wild type (Figure R.4). However, the damage of the septum appears stronger in the quadruple mutant *bee1 bee3 stk ces-2* and in the quintuple mutant *bee1 bee2 bee3 stk ces-2* where a hole in the central portion of the septum was seen in conjunction with the medium portion of the ovary (Figure R.4).

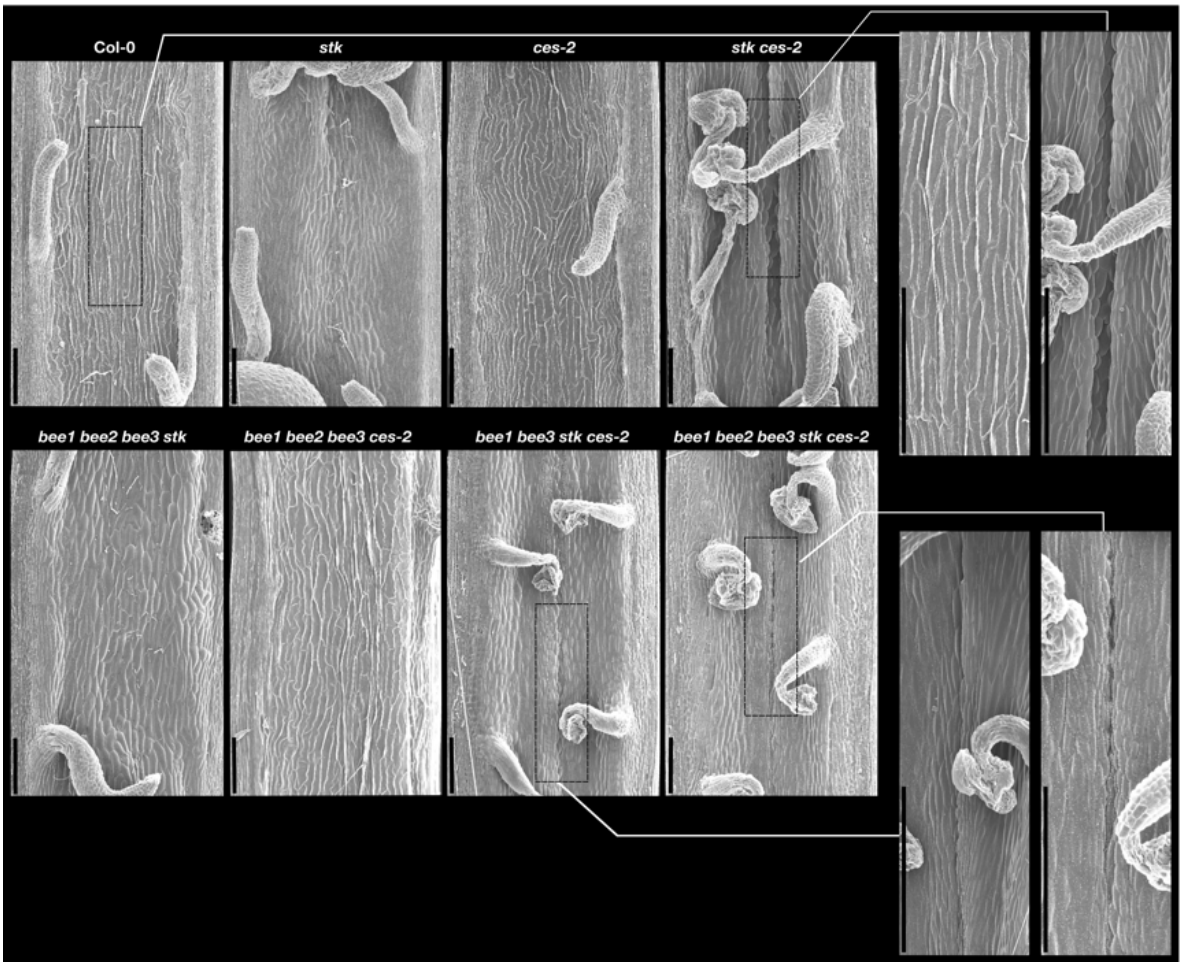

Fig R.4: **Analysis of the septum morphology.**
SEM pictures of the septum at stage 17 in the single mutants *stk* and *ces-2*, in the double mutant *stk ces-2*, in the quadruple mutants *bee1 bee2 bee3 stk*, *bee1 bee2 bee3 ces-2*, *bee1 bee3 stk ces-2* and in the quintuple mutant *bee1 bee2 bee3 stk ces-2*; Scale bars: 100µm.

To confirm that the defects in the septum fusion, described in *stk ces-2*, *bee1 bee3 stk ces-2* and *bee1 bee2 bee3 stk ces-2* respect to wild type, cause a defective growth of the pollen tube through the transmitting tract ovary tissue, 36 hours after the pistils were hand-pollinated aniline blue staining was performed to observe pollen tube growth (see Figure 4B attached manuscript 2). Pollen tube growth is affected in the mutant combinations when compared to wild type, probably caused by a failure of transmitting tract differentiation at the center of the septum.

The failure of carpel fusion, that we find in the double mutant *stk ces-2*, in the quadruple mutant *bee1 bee3 stk ces-2* and in the quintuple mutant *bee1 bee2 bee3 stk ces-2*, was previously described also in the double mutant *ntt stk*, where in concomitancy with the middle portion of

the ovary, there is a failure of organ fusion with a septum that has a hole (Herrera-Ubaldo et al., 2019).

The failure of carpel fusion could be explained by mis-regulation of the genes involved in cuticle formation. The cuticle is a lipidic alteration of the cell wall (Yeats and Rose, 2013). The alteration in cuticle biosynthesis, deposition and wax component transports could cause organ fusion defects in plants, but in particular in flowers and pistils (Nawrath, 2006; Panikashvili et al., 2010; Sieber et al., 2007). In the quadruple mutant RNAseq dataset there is an interesting candidate to explain this phenotype. This is *LIPID TRANSFER PROTEIN 2* (*LTP2, AT2G38530*) which is downregulated in *bee1 bee3 stk ces-2* mutant when compared to wild type (Table R.3). *LTP2* gene encodes for a lipid transfer protein necessary for the movement of hydrophobic wax components through the hydrophilic cell wall matrix to reach and form the cuticle (Kunst and Samuels, 2003). LTP2 also mediates cell wall loosening in vitro (Nieuwland et al., 2005). Interestingly, in the same gene family of *LTP2*, the *LTP5* gene, expressed in transmitting tract, which did not show significantly altered expression in the quadruple mutant according to our analysis, that codes for lipid transport protein that has been previously identified to be involved in pollen tube guidance to reach the ovules through the transmitting tract (Chae et al., 2009; Kunst and Samuels, 2003). We think that also *LTP2* is involved in the correct fertilization of the ovules influencing not just the pollen tube growth but also the correct fusion of the two carpels that permits to form the septum, and the transmitting tract.

Moreover, in the quadruple mutant, we found overexpression of three genes encoding for GDSL esterase/lipase involving in lipid catabolism (Table R.3). Overexpression of *CUTICLE DESTRUCTING FACTOR 1* (*CDEF1*), causes abnormal organ fusion in leaf, stem and flowers (Takahashi et al., 2010). This gene coding for a protein which is considered a cutinase (Takahashi et al., 2010). Probably, as in the *CDEF1* overexpression, the excess of cutinase caused by the overexpression of the three genes coding for the GDSL esterase/lipase in the quadruple mutant respect to wild type causes abnormal organ fusion, with defective septum and transmitting tract formation.

In summary, the data presented here suggest that a MADS-box-bHLH protein complex mastered by the physical interaction of STK-CES, plays a role in the regulation of different genes involved in the PCD, ECM and cell wall biosynthesis pathways and by that controlling correct carpel fusion and transmitting tract development to guarantee efficient ovule fertilization (Figure R.5).

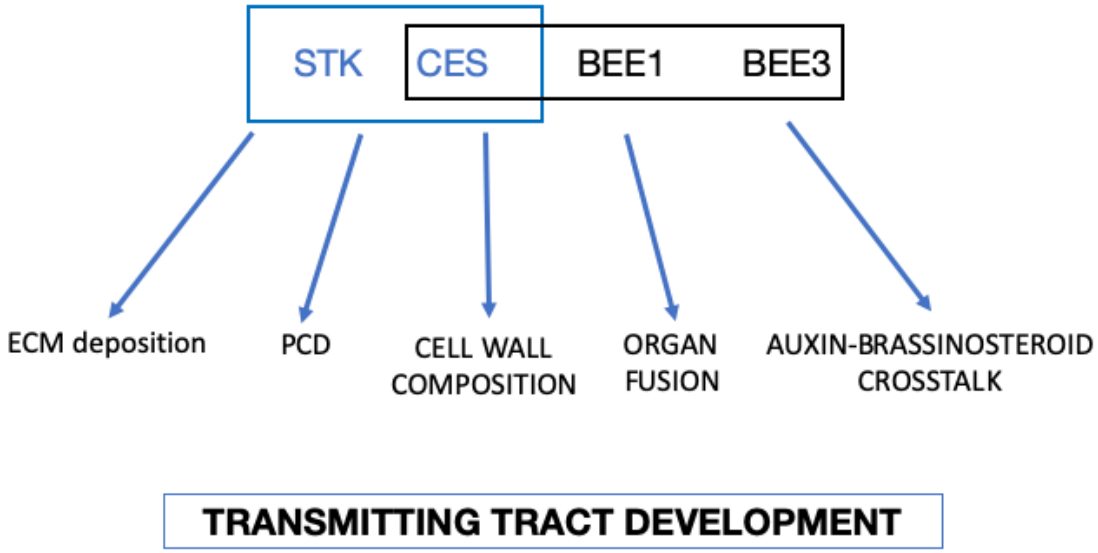

Figure R.5: Proposed model of transmitting development.

SEEDSTICK plays a major role to integrate cytokinins and *FRUITFULL* pathways to guide the fruit elongation process

The MADS-box transcription factor STK has a role in the fruit elongation process

The *stk* mutant is characterized by shorter siliques when compared to wild type (Herrera-Ubaldo et al., 2019; Pinyopich et al., 2003). We analyzed the fruit length of the mutant at stage 17, when the fruit reaches their maximum elongation. As shown in Figure R.6 C, D, the *stk* (*n*=60) mutant displays shorter fruits when compared to Col-0 wild type (*n*=60) (*stk*: mean = 8.84 mm; Col-0: mean =13.82 mm). Interestingly, the pistils of the *stk* (*n*=40) mutant at stage 13 (Figure R.6 A, B), during anthesis, has no differences in length when compared to wild type pistil (*n*=40) (*stk*: mean = 2.03 mm; Col-0: mean = 2.11). These data show that STK plays a positive role in the fruit elongation process, acting after the fertilization, because the mutant doesn't display any differences when compared to wild type when siliques start their elongation at stage 13, during the anthesis.

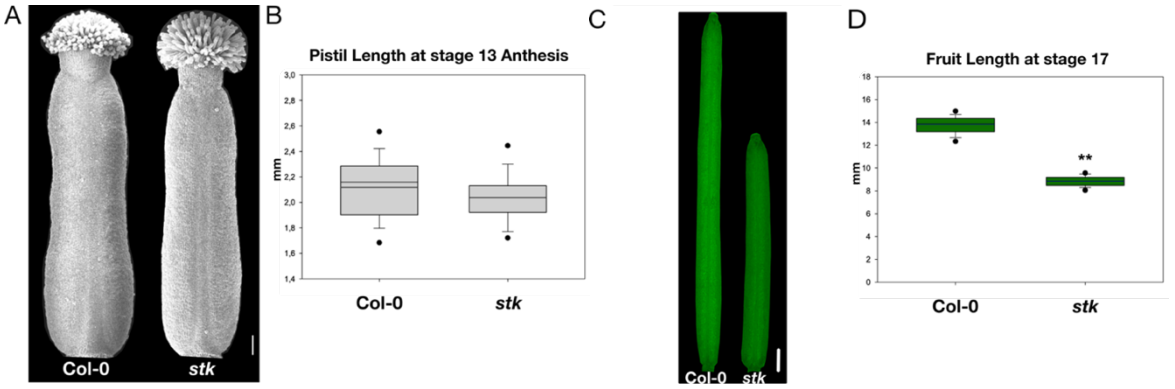

Figure R.6: Morphological characterization of *stk* pistil and fruit.
(A) SEM microscopy imaging of *stk* and Col-0 (wt) pistils at stage 13, scale bar: 100 µm; (B) Box plot represents the *stk* and Col-0 pistil length at stage 13. (C) Stereomicroscope images of *stk* and Col-0 siliques at stage 17, scale bar: 1mm; (D) Box plot represents *stk* and Col-0 siliques length at stage 17. Statistical analysis was performed using Student's *t*-test (** p- value <0.01).

TCSn::GFP marker-line reveals an altered cytokinin signaling in *stk* mutant during fruit elongation

Beforehand a transcriptome profile was performed from the *stk* mutant compared to wild type, using inflorescence and siliques until 5 DAP (Day After Pollination) (Mizzotti et al., 2014). The re-analysis of this dataset showed that several genes involved in the CK signaling and metabolism are mis-regulated (Table R.4). Genes involved in CK signalling, *HPT*

PHOSPHOTRANSMITTER 4 (*AHP4*) and *RESPONSE REGULATOR 11* (*ARR 11*) (Heyl and Schmülling, 2003), were up-regulated in the *stk* mutant (Table R.4). *LONELY GUY 1* (*LOG1*) and *ADENINE PHOSPHORIBOSYL TRANSFERASE* (*APT3*), which are involved in CK biosynthesis (Kuroha et al., 2009; Sakakibara, 2006) resulted upregulated (only *APT3* with statistical significance) (Table R.4). On the other hand, different members of *AtCKX* family, that catalyse the irreversible CK degradation (Mok and Mok, 2001), were downregulated (Table R.4). These data suggest an involvement of STK in controlling CK signaling and metabolism.

Table R.4: RNAseq. data of *stk* inflorescence till 5 DAP (Day After Pollination) when compared to wild type, re-analysed from Mizzotti et al., 2014, of the genes involved in CK signaling and metabolism.

Gene Model	Gene name	wt Expression	*stk* Expression	Fold change	p-value
AT3G16360	*AHP4*	0.207824	0.278461	1.52997	0.843
AT1G67710	*ARR11*	0.446185	0.559622	1.40844	0.828
AT2G28305	*LOG1*	15.8494	20.64877	1.29527	0.374
AT4G22570	*APT3*	109.4094	139.4019	1.35752	0.007
AT2G19500	*CKX2*	7.275059	6.84739	-1.06583	0.764
AT5G56970	*CKX3*	5.385108	3.614738	-1.49073	0.365
AT4G29740	*CKX4*	0.173474	0.039869	-2.75965	0.7433
AT1G75450	*CKX5*	6.545108	5.416359	-1.22376	0.554
AT3G63440	*CKX6*	3.59656	2.498509	-1.40803	0.509
AT5G21482	*CKX7*	12.82886	9.913211	-1.32271	0.281

Column 1: Gene locus detail according to TAIR; Column 2: Gene name according to TAIR; Column 3: Gene expression in the wild type background which value are expressed in log Counts Per Million (CPM); Column 4: Gene expression in the *stk* background which value are expressed in log Counts Per Million (CPM); Column 5: Fold change of expression between mutant and wild type backgrounds; Column 6: p-value for differential expression.

To better characterize this aspect and to analyse the CK signaling, we decided to perform the analysis of the Two Component signaling Sensor new::green fluorescent protein (*TCSn::GFP*) marker line in *stk* pistil, before fertilization (stage12), during fertilization at anthesis which is

the latest pistil developmental stage (stage 13), and after fertilization, during fruit elongation, from stages 14 to 17 (Figure R.7). The promoter *TCSn::GFP* is activated in response to CK stimulus (Zurcher et al., 2013). In particular it is an evolved monitoring system from the previous one which is named *TCS::GFP*, with the same mechanism. The TCS reflects the activity of the type-B ARABIDOPSIS RESPONSE REGULATOR (ARR) which positively induces the transcriptional activity of the CK response genes. Zurcher and collaborators have been improved this system through a modification of the TCS sequence. They changed the nonessential nucleotides which broke the monotony of the repetitive TCS sequence and they extend the binding ARRs type-B motifs to increase the sensitivity of the TCSn respect to the old TCS system (Zurcher et al., 2013).

In wild type background, in pistils before fertilization at stage 12, the GFP signal is localized in the medial domain, in the replum, style and stigma (Figure R.7-A). A similar pattern of GFP expression was detected in the *stk* mutant at stage 12 (Figure R.7-G). At stage 13, during fertilization, we found an increase of GFP signal in the replum and style of *stk* mutant (Figure R.7-H) respect to wild type (Figure R.7-B). During fruit elongation, CK signaling decreased in the medial domain of wild type fruit. In particular, at stage 14 a weak GFP signal is still detected in the replum (Figure R.7-C), while at stage 15 no GFP signal is found (Figure R.7-D). Then, at stage 16 a weak GFP signal is revealed in the valve margin (Figure R.7-E), while in the last stage of fruit elongation, stage 17-B, no GFP signal is found (Figure R.7-F). On the contrary, at stage 14 in *stk* the *TCSn::GFP* reporter protein was detected in both replum and style (Figure R.7-I), a residual GFP signal was also detected in the replum at stage 15 (Figure R.7-J) and in the valve margin at stage 16 (Figure R.7-K), while at stage 17-B no GFP signal was detected (Figure R.7-L).

In conclusion before fertilization, no differences were found in TCS-GFP signal in the *stk* mutant compared to wild type. After fertilization, in wild type, CK signalling decreases, in concomitancy with the beginning of fruit elongation, but the CK signal re-emerges at stage 16 in the valve margin, to permit the correct differentiation of the dehiscent zone (Marsch-Martínez et al., 2012). In *stk*, CK signaling seems to be still detectable at least until stage 16, demonstrating the global perturbation of CK signaling in the *stk* mutant during fruit elongation process.

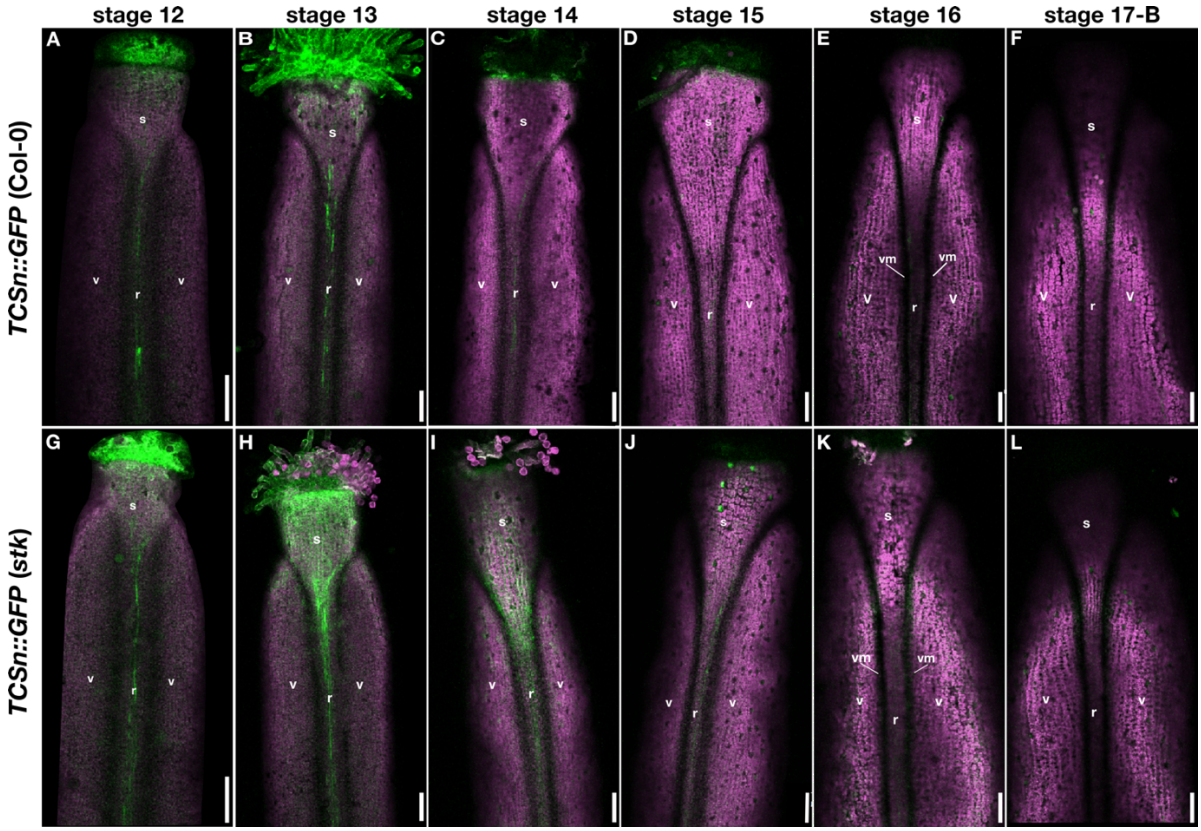

Figure R.7: Comparative in vivo cytokinin signalling visualization in fruits, through *TCSn::GFP* marker-line confocal analysis in *stk* compared to Col-0 (wt), at stage 13 (anthesis) and during fruit elongation process from stage.

(A-F) *TCSn::GFP* pictures in Col-0 background, (G-L) *TCSn::GFP* pictures in *stk* background. r: replum; s: style; v: valve; vm: valve margin. *TCSn::GFP* signal is depicted in green, and autofluorescence of plastids is depicted in magenta. Scale bars: 100 µm.

CKX7 is a direct target of STK

Among the genes that are deregulated in *stk* respect to the wild type (Table R.4) (Mizzotti et al., 2014) involved in CK metabolism we have focused our attention on *CKX7*, which is involved in CK degradation (Mok and Mok, 2001). CKX7 protein is the only one among the CKX that acts in the cytosol (Köllmer et al., 2014). This protein has a role in the regulation of xylem and procambium differentiation in roots and stem (Köllmer et al., 2014).

First of all, we analyzed the promoter activity and localization in the *stk* mutant, from stage 13, during fertilization, and fruit growth stages (from stage 14 to stage 16) when compared to wild type. We used in this analysis the marker-line p*CKX7::GUS* (Mendes et al., 2016) (Figure R.8-A). In the wild type background, the GUS activity which reflects the *CKX7* promoter localization was revealed in particular the vascular tissues of the replum (vascular bundle) and in the lateral vascular tissue of the valves (Figure R.8-A). In the *stk* mutant, the GUS activity was completely absent both fertilization and during fruit elongation phases (Figure R.8-A). Then, we analyzed the *CKX7* expression in wild type and *stk* in fruits (from stage 14 to 17) by Real-Time qPCR (Figure R.8-B). We confirmed that the *CKX7* expression was reduced in the *stk* mutant when compared to wild type (Figure R.8 B). These results suggest that STK could play a role in the control of CK degradation by the transcriptional regulation of *CKX7*. To determine whether STK, could directly regulate *CKX7*, we performed a ChIP (Chromatin Immunoprecipitation) using GFP antibodies, with chromatin extracted from the *stk* siliques of plants expressing *STK::STK-GFP* (Mizzotti et al., 2014). We analysed the *CKX7* promoter sequence for the presence of MADS domain CArG-box binding sites (Egea-Cortines et al., 1999). We found eight possible CArG-boxes. The ChIP assay showed significant enrichment for binding to the regions spanning CArG-box 4 and CArG-box 5 in the *CKX7* promoter in *STK::ST-:GFP* when compared to wild type control (Figure R.8-C). The ChIP assay confirmed that STK directly binds *CKX7* promoter and that the increased level of CK signaling, observed in *stk* fruit medial tissues during fruit elongation (Figure R.8), might be caused by a local downregulation of *CKX7*, which is critical for CK degradation in the fruit tissues. We also suppose that the amount of CK could be critical for fruit elongation process.

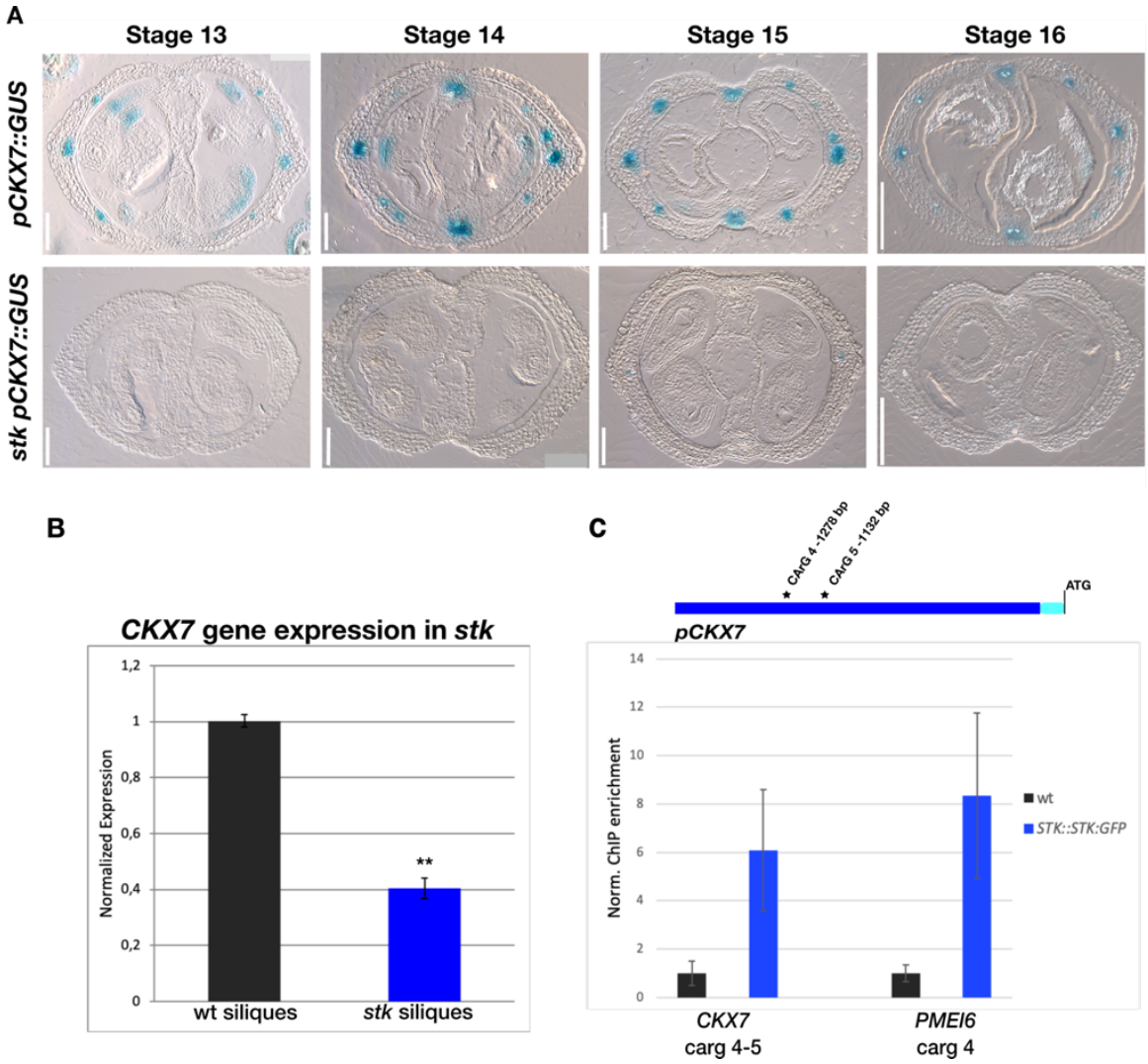

Figure R.8: *CKX7* promoter activity and STK directly binds *CKX7* promoter.
(A) Cross sections of *pCKX7::GUS* marker-line from stage 13 to stage 16 in *stk* mutant when compared to Col-0; Scale bars: 100 µm; (B) Real-Time qPCR to analyze *CKX7* gene expression in *stk* mutant siliques when compared to Col-0, statistical analysis was performed using Student's *t*-test (** p-value <0.01). Normalized with *ACTIN* and *UBIQUITIN*; (C) Scheme of the *CKX7* promoter with position of CARG boxes. ChIP Representative experiment between *STK::STK:GFP* and Col-0. Error bars represent the standard deviation of three technical replicate. Fold enrichment was calculated against the signal in the Col-0. *PECTIN METHYLESTERASE INHIBITOR 6* (*PMEI6*) carg 4 was used as a positive control. Normalized with *ACTIN2/7*.

stk mutant has more *trans*-Zeatin-types CK during fruit elongation phases

The downregulation of *CKX7* expression in *stk* during fruit growth suggest us the possibility that in the mutant during fruit elongation could be a higher amount of CK respect to the wild type, caused by a reduction of CKX7 degradation in the cytosol of the fruit tissues. To confirm this hypothesis, we performed a metabolic analysis to analyze the CK profile in the *stk* mutant when compared to the wild type. In particular, we performed this analysis with inflorescence

before fertilization (pre-anthesis) and siliques from stage 14 to stage 17 of fruit elongation process (post-anthesis). We decided also to analyze the amount of CKs before fertilization (pre-anthesis) to corroborate that STK and the CKs act after fertilization and not before it, to guide fruit elongation. We have found a higher amount of trans-zeatin-type CKs (*t*Z) in *stk* fruits respect to wild type during fruit elongation process, while before fertilization in general, we found the same amount of *t*Z in the *stk* mutant when compared to wild type (Table R.5-A). In *stk* we detected a higher level of *t*ZR (trans-zeatin Riboside) and *t*ZRMP (trans-zeatin Riboside Monophosphate), that are direct precursors of *t*Z (Spíchal, 2012). The O-glucosides, which are the CK reversible inactivated forms, *t*ZOG (trans-zeatin O-Glucoside) and *t*ZROG (trans-zeatin Ribosides O-Glucosides), were more abundant in the *stk* mutant during fruit elongation, but in lower fraction respect to the riboside precursors (Table R.5-A). The irreversible inactivate forms (trans-zeatin-7-Glucosides, tZ7G; trans-zeatin-9-Glucoside, tZ9G) were detected in the same amount in *stk* when compared with wt before and after fertilization (Table R.5-A). Interestingly, the dihydrozeatin (DHZ), a reduced form of *t*Z (Mok and Mok, 2001), was also increased in *stk*, during fruit elongation phases, when compared with wild type (Table R.5-B).

These results confirmed that the global perturbation of CK metabolism in the *stk* leads to higher concentration of active CKs during fruit elongation process, while before fertilization, the same amount detected in the *stk* mutant respect to wild type of the *t*Z but also of the DHZ, suggest us that STK regulate fruit elongation process after fertilization, in relation to CKs. Moreover, the increased amount of the reversible inactive forms suggests that in *stk* new active CKs might be obtained rapidly through the enzymatic conversion of the reversible inactive *t*Z-type CKs. We can conclude that the CKs cytosolic pool, must be composed by tZ-types-CK and in a little fraction by DHZ, have to degrade to obtain the correct fruit elongation process in *A. thaliana* siliques.

We propose that CKX7 is needed to degrade the CKs cytosolic pool which is preferentially composed by *t*Z. This conclusion is also supported by Köllmer and collaborators that reported a significative reduction of *t*ZR and *t*ZRMP when *CKX7* is overexpressed in seedlings (Köllmer et al., 2014). The increased quantity of DHZ might not be caused directly by a lack of CKX7 action in the cytosol, because CKX proteins are not able to degrade this type of CK (Mok and Mok, 2001). It is possible that the increased amount of *t*Z causes an increase in their conversion in DHZ.

Table R.5: *trans*-Zeatin-type cytokinin (*tZ*) and dihydrozeatin (DHZ) profiles in *stk* when compared to Col-0 (wt) before anthesis, and after anthesis during fruit elongation process.

A

Genotype	Total tZ pre anthesis pmol/g	Total tZ post anthesis pmol/g	±SD pre	±SD post
Col-0	3.00	7.93	0.61	0.44
stk	3.23	**10.42**	0.58	**1.26**
	tZ pre anthesis pmol/g	tZ post anthesis pmol/g	±SD pre	±SD post
Col-0	0.58	1.00	0.07	0.23
stk	0.47	1.04	0.05	0.20
	tZR pre anthesis pmol/g	tZR types post anthesis pmol/g	±SD pre	±SD post
Col-0	0.14	0.31	0.04	0.04
stk	0.16	**0.44**	0.04	**0.05**
	tZRMP pre anthesis pmol/g	tZRMP post anthesis pmol/g	±SD pre	±SD post
Col-0	1.46	5.81	0.42	0.18
stk	1.67	**7.91**	0.49	**1.26**
	tZOG pre anthesis pmol/g	tZOG post anthesis pmol/g	±SD pre	±SD post
Col-0	0.29	0.39	0.03	0.04
stk	0.34	**0.57**	0.03	**0.08**
	tZROG pre anthesis pmol/g	tZROG post anthesis pmol/g	±SD pre	±SD post
Col-0	0.058	0.16	0.014	0.01
stk	0.068	**0.21**	0.011	**0.02**
	tZ7G pre anthesis pmol/g	tZ7G post anthesis pmol/g	±SD pre	±SD post
Col-0	0.38	0.21	0.04	0.02
stk	0.41	0.20	0.02	0.03
	tZ9G pre anthesis pmol/g	tZ9G post anthesis pmol/g	±SD pre	±SD post
Col-0	0.10	0.053	0.01	0.007
stk	0.11	0.058	0.01	0.007

B

Genotype	Total DHZ types pre anthesis pmol/g	Total DHZ types post anthesis pmol/g	±SD pre	±SD post
Col-0	0.49	0.47	0.08	0.03
stk	0.55	0.44	0.08	0.06
	DHZ pre anthesis pmol/g	DHZ post anthesis pmol/g	±SD pre	±SD post
Col-0	0.006	0.017	0.001	0.001
stk	0.007	**0.021**	0.001	**0.002**
	DHZR pre anthesis pmol/g	DHZR post anthesis pmol/g	±SD pre	±SD post
Col-0	0.013	0.020	0.003	0.001
stk	0.015	0.020	0.002	0.004
	DHZRMP pre anthesis pmol/g	DHZRMP post anthesis pmol/g	±SD pre	±SD post
Col-0	0.072	0.10	0.014	0.01
stk	0.069	0.10	0.016	0.02
	DHZOG pre anthesis pmol/g	DHZOG post anthesis pmol/g	±SD pre	±SD post
Col-0	0.053	0.068	0.005	0.003
stk	0.058	0.070	0.005	0.010
	DHZ7G pre anthesis pmol/g	DHZ7G post anthesis pmol/g	±SD pre	±SD post
Col-0	0.26	0.19	0.05	0.02
stk	0.30	0.16	0.04	0.03
	DHZ9G pre anthesis pmol/g	DHZ9G post anthesis pmol/g	±SD pre	±SD post
Col-0	0.006	0.005	0.001	0.000
stk	0.010	0.005	0.002	0.001

Data shown are pmol/g fresh weight; means ± S.D. (n=4), pre anthesis data (inflorescence) and post anthesis data (siliques from stage 14 to stage 17). (A) Total *trans*-zeatin types (Total *tZ*); *trans*-zeatin (*tZ*); *trans*-zeatin riboside (*tZR*); *trans*-zeatin riboside-5′-monophosphate (*tZRMP*); *trans*-zeatin *O*-glucoside (*tZOG*); *trans*-zeatin riboside-*O*-glucoside (*tZROG*); *trans*-zeatin-7-glucosides (*tZ7G*); *trans*-zeatin-9-glucoside (*tZ9G*). (B) DHZ, dihydrozeatin; DHZR, dihydrozeatin riboside; (DHZRMP) dihydrozeatin riboside-5′-monophosphate; DHZOG, dihydrozeatin *O*-glucosides; DHZROG, dihydrozeatin riboside-*O*-glucoside; DHZ7G dihydrozeatin 7-glucoside; DHZ9G, dihydrozeatin 9-glucoside. The p-value was calculated through Student's *t*-test ($p<0.05$= *; $p<0.01$ **).

CKX7 regulates fruit elongation process

After discovered that STK directly controls *CKX7* and that this gene is active during fruit elongation process, we decided to analyze the fruit length phenotype of two different T-DNA mutant alleles for *ckx7* (Figure R.9). Depending on the insertion site and the nature of T-DNA insertion, it leads several defects, such us knockout, knockdown, knockon. The first one is the SALK_082784, characterized by a T-DNA insertion in the last intron while the second one, the SAIL_515_A07, is characterized by a T-DNA insertion in the second intron of the *CKX7* gene. The first mutant allele *ckx7* SALK_082784 displayed no differences in fruit length when compared to wild type (Figure R.9 A-D). Probably, the T-DNA insertion not generates a knockout mutant because it is present in the last intron, but further analyses are needed. The second one, the *ckx7* SAIL_515_A07, displayed shorter fruit when compared to wild type (Figure R.9 A-D). We also confirmed that the *ckx7* SAIL_515_A07 is a knockout mutant through a qRT-PCR (Figure R.9-E). Actually, no *CKX7* transcripts have been revealed by qPCR in the mutant respect to wild type (Figure R.9-E).

To validate that the phenotype observed in the knockout mutant for *ckx7* SAIL_515_A07 is due to a mutation in the *CKX7* gene, we decided to generate a new mutant allele for *ckx7*

through the CRISPR-Cas9 genome editing technology. We used a single-guide RNA (sgRNA) approaches (see materials and methods for sequences details and constructs). The sgRNA guides the Cas9 proteins to a specific genomic target region. Recognition and cleavage occur via complementarity of a 20-nucleotide (nt) sequence within the sgRNA to the genomic target, i.e, the on-target, upstream of a protospacer adjacent motif (PAM) at its 3' end (Doench et al., 2014). We generated, thanks to this technology, a third mutant allele (called *ckx7* T) carried a T insertion in the first exon, position 254 (see Figure M.3). This insertion causes a frameshift in the FAD-binding domain and the formation of a premature stop codon after 129 aa (see Figure M.3), creating a truncated protein with no enzymatic activity (Bae et al., 2008). The *ckx7* T displayed shorter fruit when compared to wild type (Figure R.9-F-H).

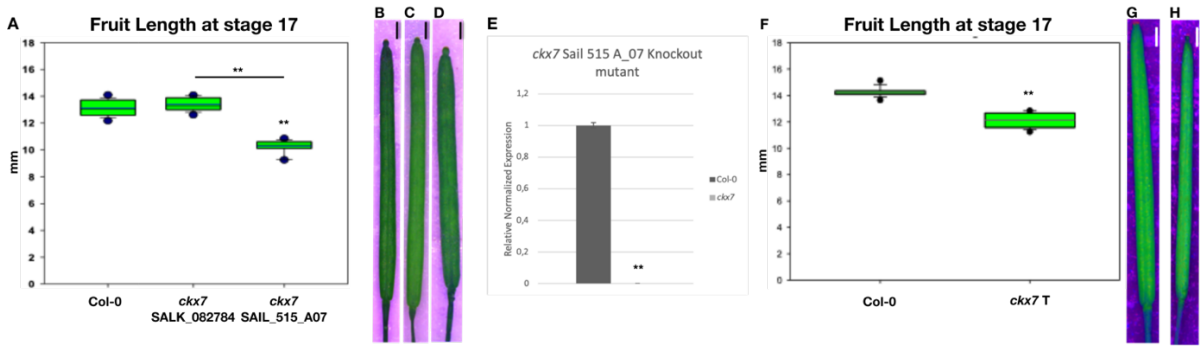

Figure R.9: *ckx7* mutants fruit length phenotype at stage 17.
(A) Box plot represents *ckx7* mutant alleles and Col-0 siliques length at stage 17, Statistical analysis was performed using Anova followed by Tukey HSD test. (**, p-value <0.01); (B-D) Stereomicroscope images of siliques at stage 17, (B) Col-0, (C) *ckx7* SALK_082784, (D) *ckx7* SAIL_515_A07; Scale bars: 1mm; (E) qRT-PCR of *ckx7* SAIL_515_A07, knockout mutant allele, Normalized with *ACTIN* and *UBIQUITIN*; Statistical analysis was performed using Student's *t*-test (** p-value <0.01); (F) Box plot represents *ckx7* T CRISPR Cas9 line and Col-0 siliques length at stage 17; (G-H) Stereomicroscope images of siliques at stage 17 (G) Col-0 and (H) *ckx7* T, scale bars: 1mm. Statistical analysis was performed using Student's *t*-test (** p-value <0.01)

Additionally, we generated plants overexpressing *CKX7* thanks to the constitutive 35S Cauliflower Mosaic Virus (CaMV) promoter. The *35S::CKX7* plants possess longer fruit when compared to wild type (Figure R.10 A-B). It is exactly the opposite phenotype of the two mutant alleles previously described. We tested the *CKX7* transcript levels in the *35S::CKX7* plants. The number of transcripts increased in the *35S::CKX7* plants respect to wild type (Figure R.10 C).

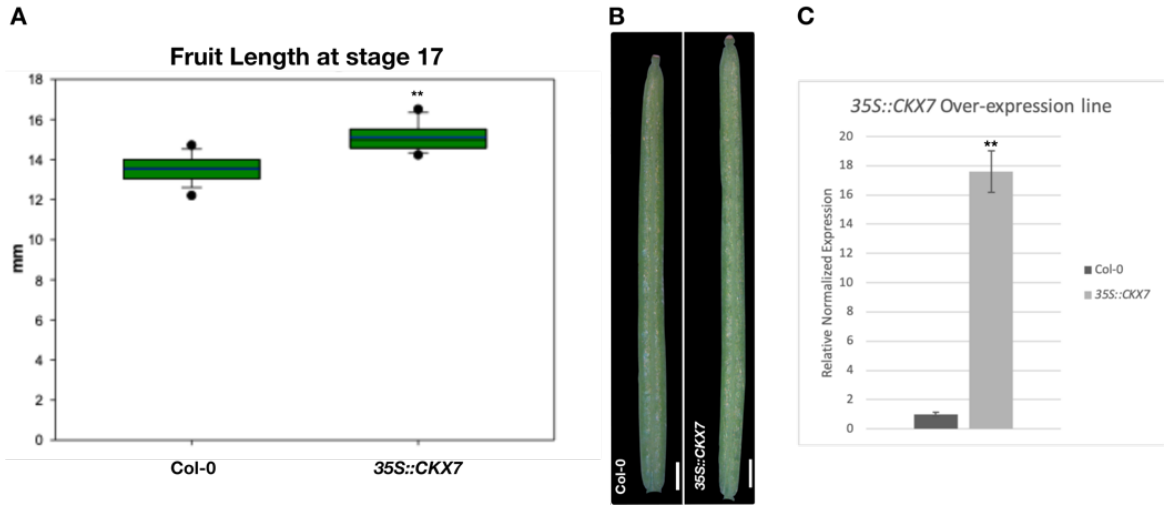

Figure R.10: *35S::CKX7* fruit length phenotype at stage 17.
(A) Box plot represents *35S::CKX7* and Col-0 siliques length at stage 17, Statistical analysis was performed using Student's *t*-test (** p-value <0.01); (B) Stereomicroscope images of Col-0 and *35S::CKX7* siliques at stage 17; Scale bars: 1mm; (C) Real Time qPCR of *35S::CKX7* plants to analyze transcript levels and confirm overexpression line, normalized with *ACTIN* and *UBIQUITIN*; Statistical analysis was performed using Student's *t*-test (** p-value <0.01).

Finally, we analyzed the pistil length at stage 13 of the *ckx7* SAIL_515_A07, *ckx7* T and *35S::CKX7* when compared to wild type (Figure R.11) to corroborate that also *CKX7*, as *STK*, has a role in fruit elongation, acting after fertilization. The two mutants and the overexpression line displayed pistils with the same length compared to wild type, at stage 13, when fertilization occurs (Figure R.11).

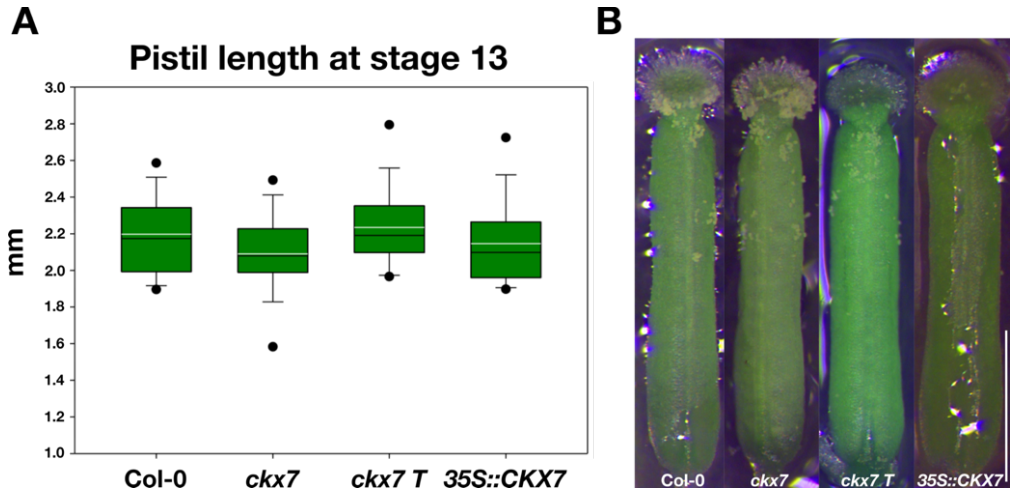

Figure R.11: *CKX7* acts after fertilization to influence fruit elongation process.
(A) Box plot represents *ckx7*, *ckx7* T and *35S::CKX7* compared to Col-0 pistils ; (B) Stereomicroscope images of ckx7, ckx7 T and *35S::CKX7* pistils when compared to wild type at stage 13; Scale bar: 1mm.

In summary, when there is a lack of CKX7 activity with an absence of cytokinin degradation in the cytosol, as we showed in the two mutant alleles (*ckx7* SAIL_515_A07 and *ckx7* T), there is a partial failure of fruit elongation with shorter fruits when compared to wild type, while when there is an increase of CKX7 activity, with a subsequent increase of cytokinin degradation in the cytosol, as we showed in the overexpression line situation, there is an increase of fruit elongation respect to wild type.

Lately, the role of CKX proteins in fruit elongation has been suggested on the base of expression analysis in other species like *Brassica Napus*. Liu and collaborators, through an expression analysis of the different *BnCKX* genes from vegetative to reproductive phases, found that one of the orthologs of *AtCKX7*, *BnCKX7-1* which is preferentially expressed in leaves and siliques, is more expressed in the *B. Napus* cultivar with longer siliques respect to the cultivar characterized by shorter siliques (Liu et al., 2018; Song et al., 2015). Taking into account our results in Arabidopsis, it seems that the role of CKs and *CKX7* in fruit growth is maintained at least among the Brassicaceae.

CK cytosolic pool influences cell elongation in fruit

CK are plant hormones involved in different aspects of plant development such as cell division, cell differentiation but also cell expansion/elongation during vegetative and reproductive phases (Bartrina et al., 2011; Cucinotta et al., 2016; Reyes-Olalde et al., 2017; Street et al., 2016). To understand which is the role of CK during fruit growth, we analyzed the cell shape of *stk*, *ckx7*, *ckx7* T and *35S::CKX7* when compared to wild type at stage 17 (Figure R.12). In particular, we analysed the valve cells because is demonstrated that the increase in fruit size is due to elongation of epidermal cells (Vivian-Smith et al., 2001). To analyse cell shape, we used the feulgen staining, which permits to mark the polysaccharides component of the cell wall (Braselton et al., 1996).

The total number of cells seems to be the same in the mutants and overexpression lines when compared to wild type, while the cell length was different between the genotypes analyzed (Figure R.12). The *stk* mutant (Figure R.12-B) showed a decrease in the average of the cell length when compared with wild type (Figure R.12-A) (*stk*=155.11; Col-0=237.33 µm, Figure R.12-F). A similar decrease of the cell length was found in the two *ckx7* mutant alleles (Figure R.12-C and R.12-D) (*ckx7*=185.38; *ckx7* T=206.82, Figure R.12-F), while the *35S::CKX7* (Figure R.12-E) had longer cell when compared to wild type (*35::CKX7*=281.26, Figure R.12-F).

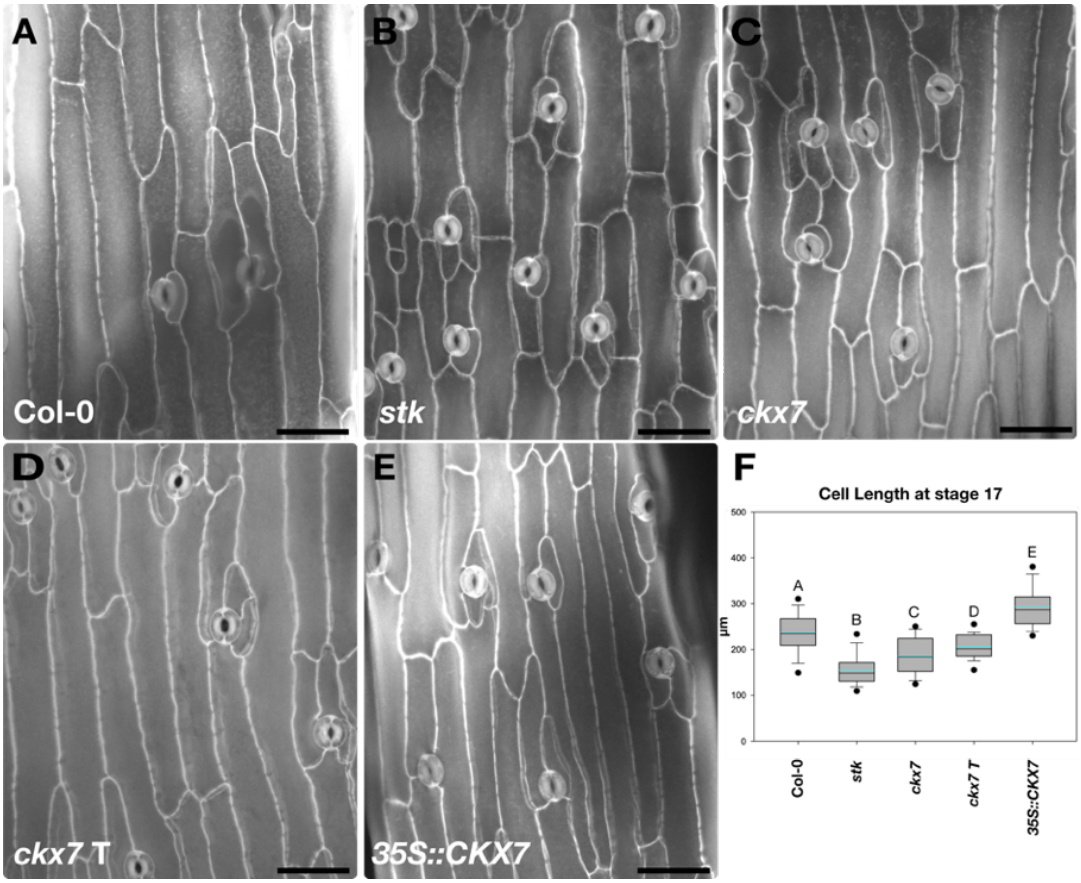

Figure R.12: CK cytosolic pool regulates cell elongation in fruit.
Confocal images of valve cells at stage 17 of fruit development. (A) Col-0 valve cells, (B) *stk* valve cells, (C) *ckx7* valve cells, (D) *ckx7* T valve cells, (E) *35S::CKX7* valve cells, (F) Box plots represents cell length values of the genotypes described above. Statistical analysis was performed using Anova followed by Tukey HSD test. Different letters indicate statistically different groups (p-value <0.01).

In conclusion in *stk*, *ckx7* and *ckx7 T* mutants, where the partial absence of CKX7 as in *stk*, or a complete lack of CKX7 activity like in the single mutants *ckx7* causes an increase of the CK cytosolic pool, the cells of the valve were shorter compared to wild type. On the contrary, in the *35S::CKX7* line the cells were longer. These data suggest that the CKs cytosolic pool plays an important role in the regulation of cell elongation and consequently in the regulation of fruit growth. We propose that *t*Z-types-CK have to be degraded to obtain a correct cell elongation during fruit growth.

In the primary root, it was demonstrated that CKs, through the stimulation of type-B ARRs, activate auxin influx carrier AUX1 to modulate auxin movement and inhibits cell elongation (Street et al., 2016). Our results propose that CKs cytosolic pool could be able to influence cell elongation in fruit. Thus, it could possible that CKs act as a repressor of cell elongation in fruit, as in root. In particular, the CKs cytosolic pool, which is preferentially composed by *t*Z, could

be involved in this repression activity. Interestingly, they act in fruit with opposite role respect to the action in pistils. The importance of the CKs in the control of placenta size and number of ovules before fertilization has been shown. Indeed, the reduction of the CK transcriptional response, during pistil development, in the triple mutant *crf2/3/6* causes a reduction of the pistil size with a decrease of the total number of ovules (Cucinotta et al., 2016). As well, the reduced pistil size and ovule number have been shown in CK signaling mutants (Reyes-Olalde et al., 2017). The positive role of CKs in pistil elongation, is also confirmed by the double mutant *ckx3 ckx5*, in which the pistil becomes longer when compared to wild type, thanks to an increase of CKs amount caused by a lack of the CKX proteins, with a consequent increase of CK transcriptional response (Bartrina et al., 2011). In the pistil, before fertilization CKs promote cell division and elongation, and regulate the number of ovule primordia.

To allow the pistil to elongate, cell proliferation has to exceed cell differentiation. This process is positively regulated by CKs in pistils before fertilization and negatively after fertilization in fruit.

STK and CKX7 act in the same pathway to guide the fruit elongation process

To confirm that STK acts upstream to *CKX7* we decided to generate, by crossing the two single mutants, the double mutant *stk ckx7* (SAIL_515_A07) in which we analyzed the fruit length phenotype at stage 17 compared to the single mutants and the wild type control (Figure R.13 A-B). The double mutant *stk ckx7* displayed shorter fruit when compared both to wild type and the single mutant *ckx7*. However, it displayed the same fruit length when compared to the single mutant *stk*, without statistical differences (Figure R.13 A-B). This result confirms that STK acts upstream to *CKX7* in the fruit elongation pathway. Moreover, we had to confirm the hypothesis that the two genes act in the same pathway to control fruit elongation. To do that, we transformed *stk* mutant plants with the *35S::CKX7* construct, previously described (see Figure R.10). The idea is that if the *stk* phenotype regarding the fruit length is caused by a down-regulation of *CKX7* with a consequent decrease of CK degradation in the cytosol, an ectopic *CKX7* expression in *stk* could rescue the fruit length phenotype. We obtained five independent transformed plants (*stk* x *35S::CKX7*), with a partial rescue of *stk* mutant phenotype when compared to *stk* single mutant (Figure R.13 C-D). However, the five transformed plant lines displayed shorter fruit when compared to wild type but also when compared to the *35S::CKX7* fruits (Figure R.13 C-D).

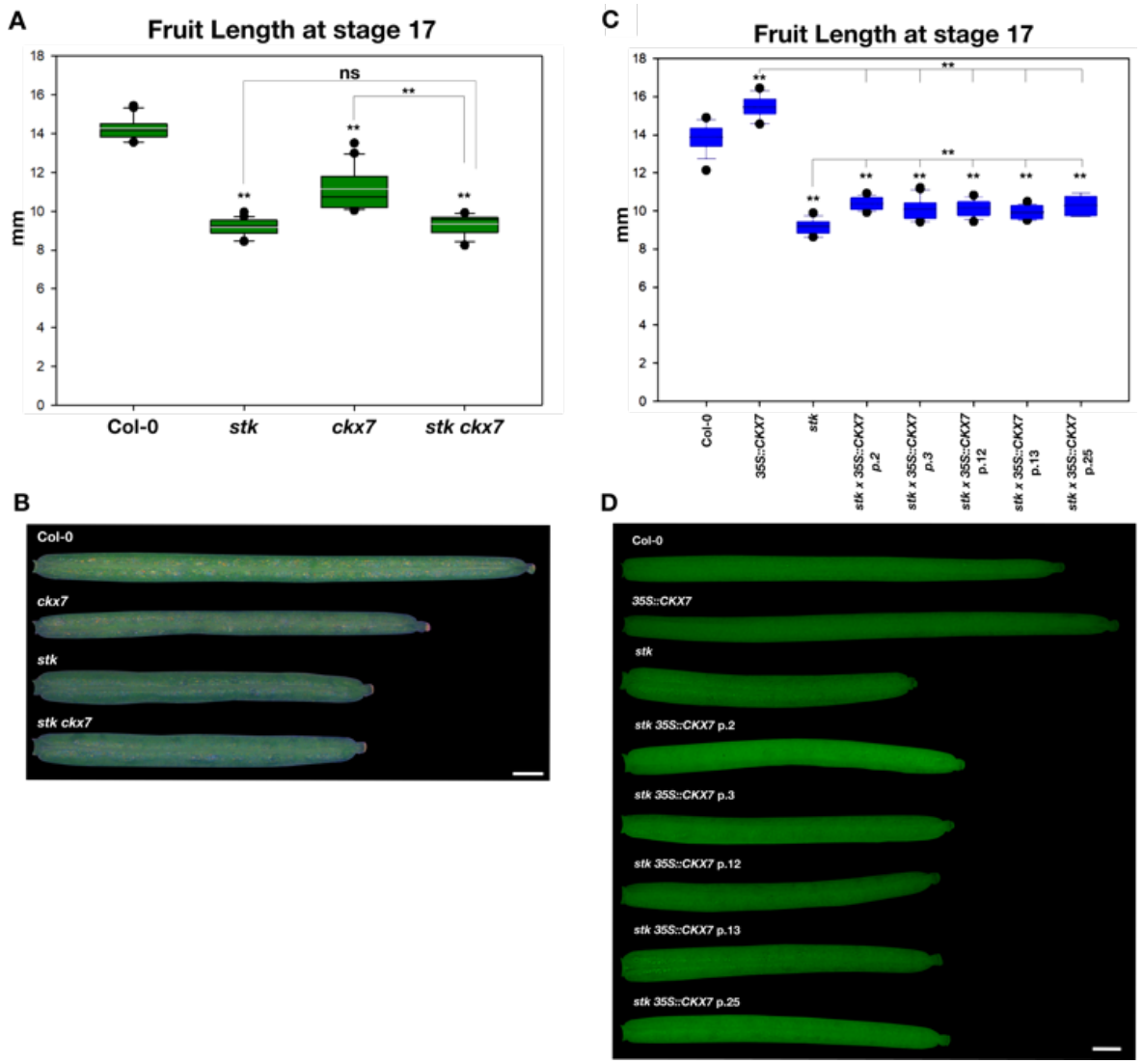

Figure R.13: STK and CKX7 act in the same pathway, with STK upstream to *CKX7*, to guide fruit elongation.
(A) The box plot represents fruit length at stage 17 of *stk* (mean = 9.18 mm, *n* = 20), *ckx7* (mean = 11.14 mm, *n* = 20), *stk ckx7* (mean = 9.35 mm, *n* = 20) compared to Col-0 (mean = 14.65 mm, *n* = 20); (B) Stereomicroscope images of *stk*, *ckx7*, *stk ckx7* and Col-0 siliques at stage 17-B. Scale bar = 1 mm; (C) The box plots represents a rescue experiment of *stk x 35S::CKX7* plants (plant 2 mean = 10.40 mm; p 3 mean = 10.30 mm; p 12 mean = 10.15 mm; p 13 mean = 9.95 mm; plant 25 mean = 10.31 mm; *n* = 15), *stk* (mean = 9.19 mm, *n* = 15) and *35S::CKX7* (mean = 15.46 mm, *n* = 15) compared to Col-0 (mean = 13.88 mm, *n*=15); (D) Stereomicroscope images of *stk* x *35S::CKX7*, *35S::CKX7*, *stk* and Col-0 siliques at stage 17; Scale bar = 1 mm. Statistical analyses were performed using Anova followed by Tukey HSD test. (**, p-value <0.01; ns: not significant).

The partial rescue confirms that *STK* and *CKX7* work in the same pathway to influence fruit elongation, but it could be possible that STK acts in more than one pathway or regulates directly or indirectly more than one gene to guide fruit growth.

CKX6 does not have a role in the fruit elongation process

CKX6 protein is one of the seven members of the cytokinin oxidase enzymes in *A. thaliana.* The CKX6 enzyme acts in the apoplast (Werner et al., 2003). As mentioned before in *stk* RNAseq was found more than one *CKX* gene deregulated (Mizzotti et al., 2014). One of them is *CKX6* (Table R.4). To investigate the possible role of this gene concerning to STK in fruit development, we analyzed the *CKX6* promoter activity in *stk* mutant when compared to wild type, through *pCKX6::GUS* construct (Figure R.14 A-I). In the wild type background *CKX6* promoter is in particular active during pistil development (Figure R.14 A-C), while during silique elongation phases no GUS activity was detected (Figure R.14 D). Similarly, in *stk* mutant, the GUS activity represented the *CKX6* promoter, was found during pistil development, without any differences when compared to wild type (Figure R.14 E-G). Also, in *stk* mutant the GUS activity was not detected during fruit elongation phases (Figure R.14 H, I). Moreover, we analyzed the fruit length of the *ckx6* T -DNA insertion line (Bartrina et al., 2011). The *ckx6* mutant displayed the same fruit length at stage 17, without any statistical differences, when compared to wild type (*ckx6*: mean = 13.21 mm, *n*=20; Col-0: mean =13.13 mm, *n*=20) (Figure R.14 J, K). In summary, STK is not able to influence *CKX6* promoter activity, that is not present during fruit elongation phases. Moreover, the mutant does not present differences when compared to wild type. These data suggest that *CKX6* does not have any role in fruit elongation process.

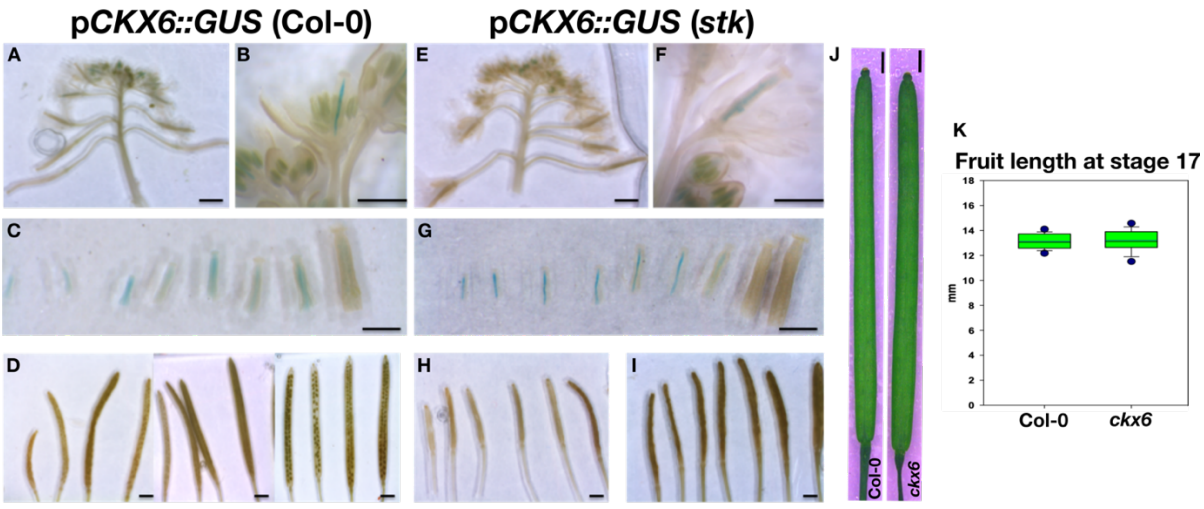

Figure R.14: Analysis of the *CKX6* promoter activity and *ckx6* mutant fruit length.
(A-D) Stereomicroscope images of *pCKX6::GUS* in Col-0 (wt), (E-F) Stereomicroscope images of *pCKX6::GUS* in *stk* mutant, scale bars: 1mm; (J) Stereomicroscope images of *ckx6* and Col-0 siliques at stage 17, scale bars: 1mm; (K) Box plot represents *ckx6* and Col-0 siliques length at stage 17. Statistical analysis was performed using Student's *t*-test (** p-value <0.01).

To confirm that CKX6 does not performed any function in fruit elongation and that CKX7 is the only player acting in this process, we decided to generate the double mutant *ckx6 ckx7*. We transformed the single mutant *ckx6* plants using the CRISPR-Cas9 construct, that we used to generate the single mutant *ckx7 T* (Figure R.9). We obtained two different insertional double mutants, one with a G insertion and one with an A insertion in the *CKX7* gene, but in the same position of the insertion that we found in the *ckx7 T* mutant (Figure M.3). The two double mutants displayed shorter fruit when compared to both single mutant *ckx6* and the wild type (Figure R.15). The double mutant displayed the same phenotype of the single mutant *ckx7 T* (Figure R.9).

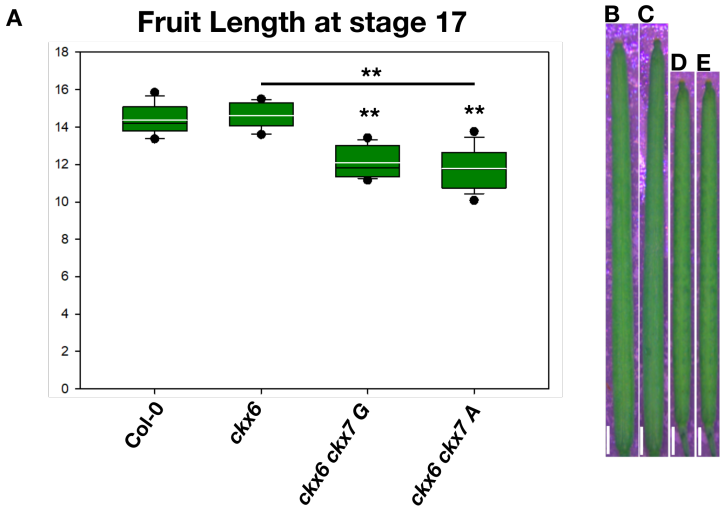

Figure R.15: *ckx6 ckx7* double mutant fruit length.
(A) Box plot represents *ckx6*, *ckx6 ckx7* G, *ckx6 ckx7* A and Col-0 siliques length at stage 17 (B) Stereomicroscope images of *ckx6*, *ckx6 ckx7* G, *ckx6 ckx7* A and Col-0 siliques at stage 17. Scale bars: 1mm. Statistical analysis was performed using Anova followed by Tukey HSD test (**, p-value <0.01).

This experiment confirms that *CKX7* is the only one player involved in fruit elongation, because the double mutant *ckx6 ckx7* possess the same fruit length of the single mutants *ckx7 T*, confirmed the major role of the cytosolic CKX in the regulation of fruit growth.

STK can influence *FUL* pathways in fruit valves

The partial complementation of *stk* mutant through the ectopic overexpression of *CKX7* (Figure R.8), suggests us that STK could act in more than one pathway to influence fruit elongation process.

The most important gene for valves elongation in the *Arabidopsis thaliana* siliques is *FUL* (Ferrándiz et al., 2000a; Gu et al., 1998). We decided to analyse the *FUL* promoter activity

through the *pFUL::GUS* construct, and the FUL protein localization through the *gFUL:GFP* marker-line in *stk* mutant during fruit elongation phases. The *FUL* promoter activity, revealed by GUS assay, was less intense in *stk* mutant when compared to wild type, in particular in the valves of the *stk* mutant siliques during fruit developmental stages (Figures R.16 A-D).

To analyse FUL protein localization, we decided to perform cross-sections of pistil and fruit to obtain a better analysis of protein localization in the two backgrounds from stage 13 (during fertilization) up to stage 16 of fruit elongation process (Figures R.16 E-L). The *gFUL:GFP* fusion protein is localized in the valves and replum upon fertilization at stage 13. During fruit elongation process from stage 14 to stage 16, FUL-GFP is less expressed respect to the stage 13 in the wild type background (Figures R.16 E-H). In *stk* mutant, FUL-GFP expression is reduced respect to wild type starting from stage 13 and completely starting from stage 15 (Figures R.16 I-L). These data suggest us the possibility that STK regulates the correct activity of *FUL* during fruit growth.

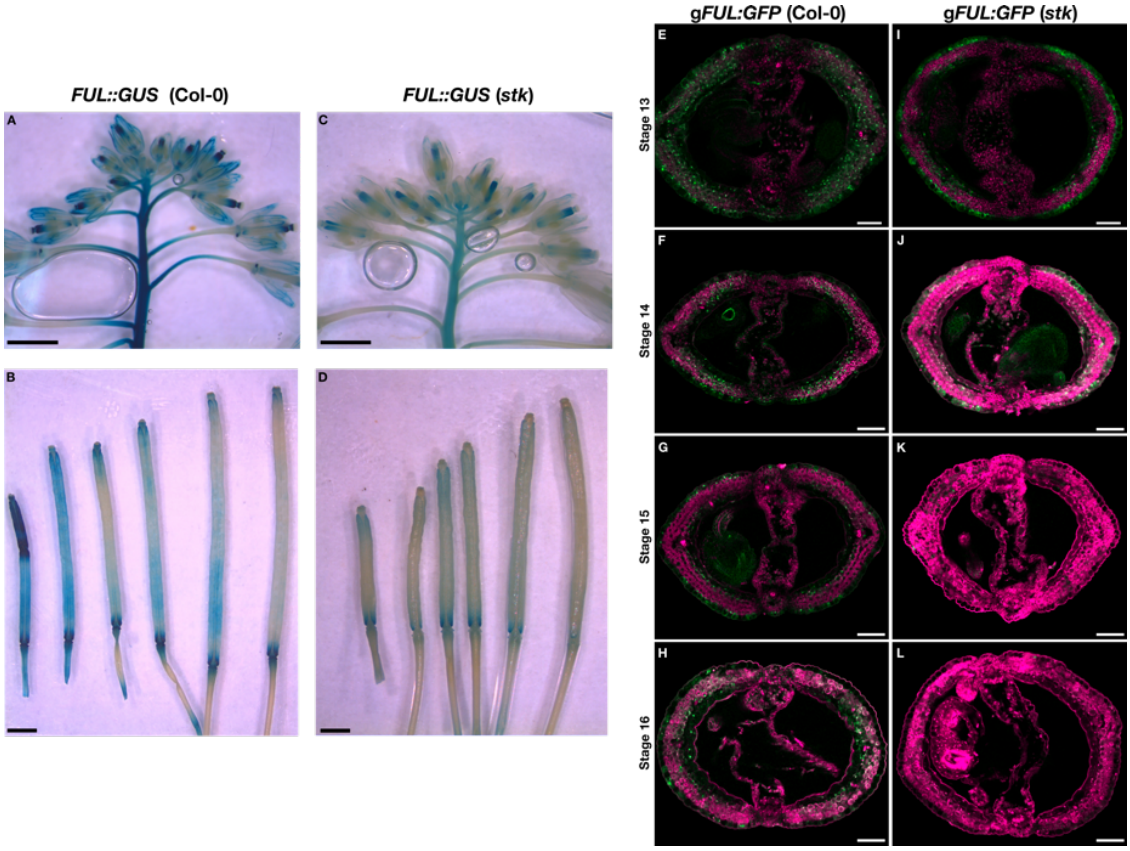

Figure R.16: *STK* could regulate FUL activity in valves during fruit elongation.
FUL promoter activity analyzed through *FUL::GUS* construct. (A-B) *FUL::GUS* in Col-0, (C-D) *FUL::GUS* in *stk*; Scale bars:1mm; Confocal images of *gFUL:GFP* in *stk* compared to Col-0 (wt) from stage 13 during anthesis to stage 16 of fruit development; (E-H) g*FUL:GFP* in Col-0, (I-L) *gFUL:GFP* in *stk*; FUL-GFP signal is depicted in green, and autofluorescence of plastids is depicted in magenta. Scale bars 50 µm.

To better characterize the relationship between the two MADS-box transcription factor we decided to generate the double mutant *stk ful-2* by crossing the single mutant plants. The *stk ful-2* plants possess shorter fruit when compared to wild type (Figure R.17). Interestingly, the fruits of the double mutant are shorter when compared to both single mutants *stk* and *ful-2* (Figure R.17). The double mutant displayed an additive phenotype which suggests that the two MADS-domain transcription factors act in two different pathways to influence fruit elongation process. However, STK is needed for the correct *FUL* expression pattern in fruit, with an indirect regulation of it.

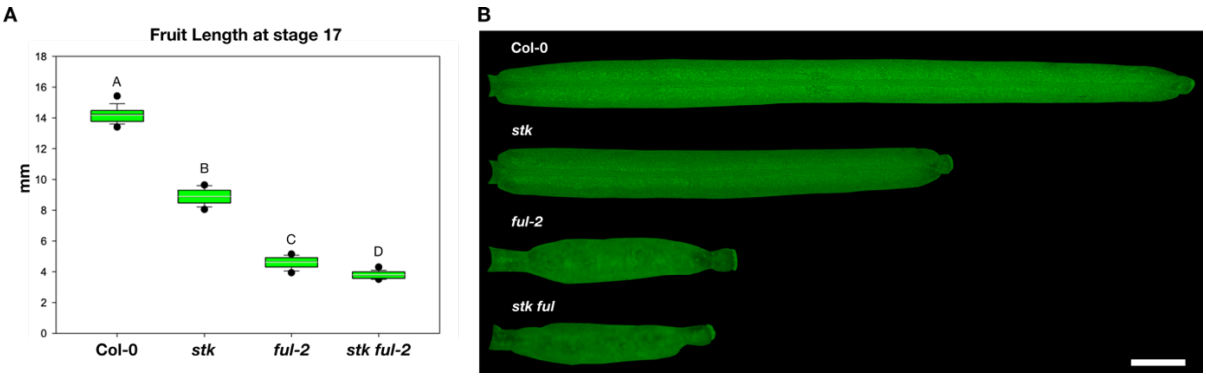

Figure R.17: STK and FUL acting in two different pathways to regulate fruit elongation process. (A) Box plot represents the fruit length values of *stk*, *ful-2*, *stk ful* compared to Col-0 at stage 17; (B) Stereomicroscope images of *stk*, *ful-2*, *stk ful* siliques at stage 17 compared to Col-0; Scale bar:1mm; Statistical analysis was performed using Anova followed by Tukey HSD test. Different letters indicate statistically different groups (p-value <0.01).

Finally, to confirm that the FUL pathways are in part compromised in *stk*, causing a partial failure of fruit elongation, we decided to analyse the transcript levels of *MIR172*c and *IND* in the *stk* siliques when compared to wild type (Figure R.18). Indeed, it has been reported that FUL regulates siliques elongation by the regulation of *MIR172*c required to repress *AP2*, a negative regulator of fruit growth (Ripoll et al., 2015). Moreover, FUL is also necessary to confine *IND* action in the valve margin (Liljegren et al., 2004). In fact, it has been known that *IND* expression in *ful* mutant valves, causes ectopic lignification, and is considered to be responsible for the lack of cell elongation in the *ful* mutant valves (Liljegren et al., 2004).
The *MIR172*c transcript levels are less in *stk* when compared to wild type, probably caused by the downregulation of FUL which is necessary to activate miR172 valve margin gene (Figure R.18-A). The *IND* gene is upregulated in *stk* compared to wild type, probably also in this case

a direct consequence of *FUL* down-regulation, because FUL is a negative regulator of *IND* expression (Figure R. R.18-B).

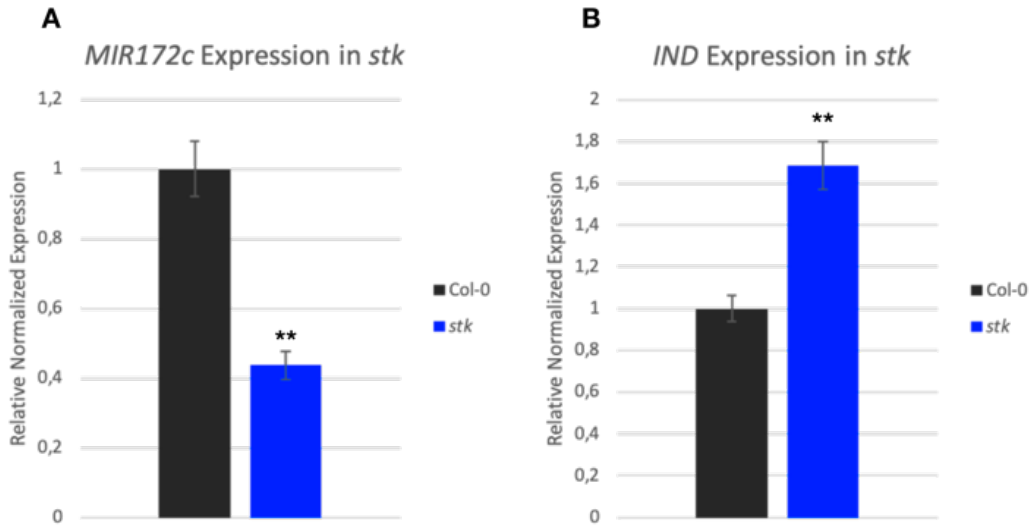

Figure R.18: in *stk* mutant *MIR172C* and *IND* are mis-regulated.
(A) qRT-PCR on *stk* siliques when compared to wt, to analyse *MIR172c* gene expression; (B) Real Time qPCR on *stk* siliques when compared to wt, to analyse *IND* gene expression. Statistical analysis was performed using Student's *t*-test (** p-value <0.01).

These evidences also connect the two MADS-box in the regulation of fruit elongation process. In the two mutants *stk* and *ful*, part of the phenotype related to fruit elongation is caused by an increase in CK signaling. In fact, as in the *stk* mutant, also in the *ful* mutant, there is an increase of CK signaling when compared to wild type (Marsch-Martínez et al., 2012), analyzed through *TCS::GFP*. However, in *stk* the increased GFP signal was revealed in the replum (Figure R.7), where *STK* is expressed, while in the *ful* mutant the increased GFP signal was revealed in the valves, where *FUL* is preferentially expressed (Marsch-Martínez et al., 2012).
These data suggest that STK could impact on a pathway independent from the *STK-CKX7* described above. Indeed, it could influence FUL-MIR172 and FUL-IND pathways that control valve elongation. Overall, taking into account the data presented here we propose a major role for STK in the integration of two pathways in which CKs, in general, and *tZ* levels, in particular, are critical to controlling fruit size (Figure R.19).

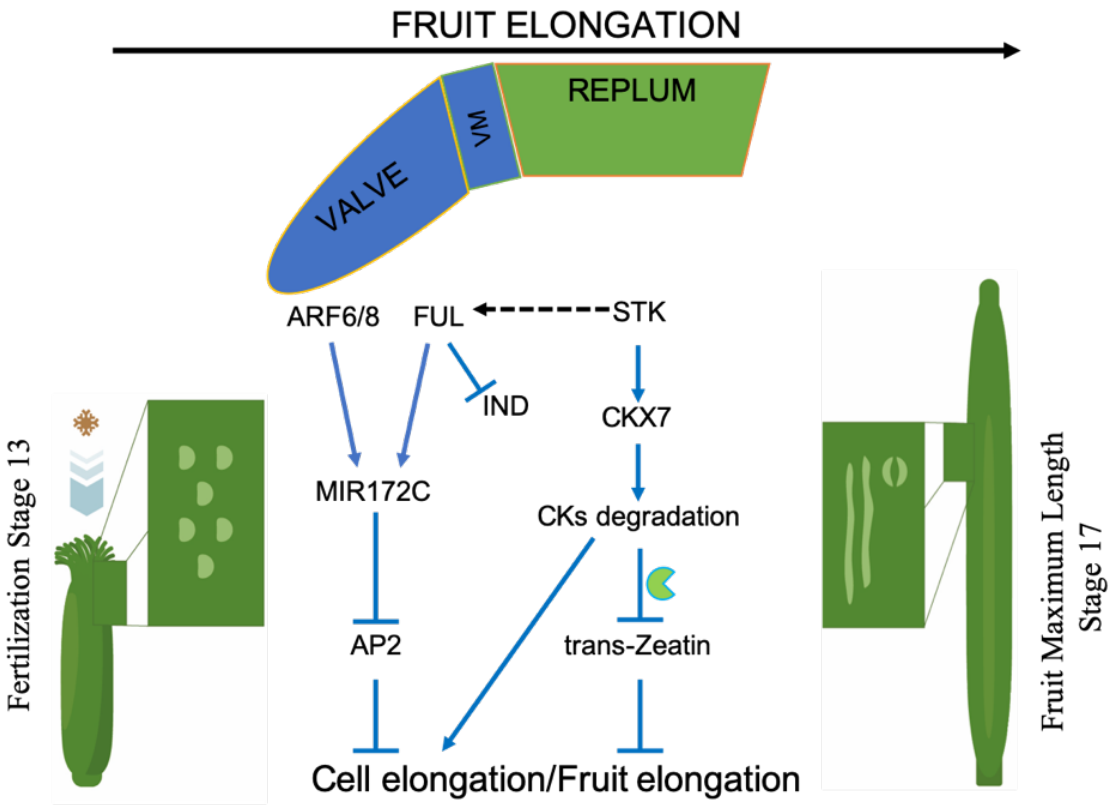

Figure R.19: Molecular and genetic pathway regulating fruit elongation process.

CONCLUSIONS

The pistil has critically importance to facilitate the fertilization process contributing to the evolutionary success of the Angiosperm.

Upon double fertilization, the pistil is transformed into fruit that plays a pivotal role in seed protection and dispersal. In dehiscent fruit, as the silique of Arabidopsis, the seeds have to detach themselves from the siliques to permit to the plant species to colonize new areas. This process is essential for the life of sessile organisms like plants.

With my work, I have contributed to new insights in the molecular mechanism controlling pistil development and in particular, transmitting tract differentiation and silique elongation process.

We demonstrated that the STK MADS-domain transcription factor might be the most important player in the control of transmitting tract development. The MADS-box transcription factors usually form homodimer or heterodimer with other MADS-box family members. However, they might interact also with other types of factors. We demonstrated that STK interacts with NTT to regulate genes involved in ECM and cell wall components pathways required for a proper transmitting tract differentiation. Furthermore, STK also plays a role in the downstream pathway of NTT. STK interacts with the bHLH transcription factor CES and regulates not just the ECM and cell wall components biosynthesis but also the fusion of the two carpels during pistil development, to obtain the correct formation of the transmitting tract. Moreover, we have also suggested a role of auxin-brassinosteroid crosstalk that, regulating by STK-CES-BEE1-BEE3 complex, seems to be involved in the regulation of transmitting tract development. The transcriptome profile analyses that we have performed and analyzed is opening new insight in the network controlling pollen-pistil interaction and fertilization process.

Hormones are also central in the regulation of fruit growth as in past different research groups demonstrated for example for auxin but also gibberellins. Thanks to the analysis of STK role in fruit elongation process, we revealed for the first time the importance of the cytokinins in the correct elongation of the fruit. In particular, we demonstrated the importance of the correct degradation of the *trans*-zeatin-type-cytokinins. STK directly regulates *CKX7* which is necessary to degrade these hormones in the cytosolic compartment of the cells composing fruit to permit the correct elongation of the cells composing it. For the first time, the CKs are linked to cell elongation, because usually this type of hormones is linked with the correct cell cycle and number of cells. Furthermore, thanks to our silique project, we connect the STK-CKX7

pathway to FUL-IND and FUL-MIR172 pathways. In conclusion, we propose a complex genetic model to permit the correct elongation of the cell composing fruit, and consequently influences the correct fruit growth and the final fruit length in *A. thaliana*. It could be a piece of important evidence that might be used to improve crop species to get bigger fruit.

MATERIALS and METHODS

Plant lines used during PhD project

Arabidopsis thaliana plants were germinated in soil in long day condition (16 hours light, 8 hours dark) at 22° C. All the lines used in the PhD project are in Columbia-0 (Col-0) ecotype. The *stk*-2 and *shp1 shp2* mutant was provided by M. Yanofsky (Pinyopich et al., 2003). The *ces-2* mutant was obtained from NASC (SAIL_674_A01 lines). The T-DNA insertion mutants for *ckx7* and *ckx6* were obtained from the Nottingham Arabidopsis Stock Centre (NASC), SAIL_515_A07 line (*ckx7*, see Figure R.9 for knockout validation), SALK_082784 (*ckx7*), and SALK_070071 (*ckx6-2*) (http://arabidopsis.info). The *ful-2* mutant was provided by C. Ferrándiz (Ferrándiz et al., 2000a). The *stk ckx7* (SAIL_515_A07) and *stk ful* and *stk ces-2* plants were obtained by crossing the single mutants. The *bee1 bee2 bee3* triple and *bee1 bee2 bee3 ces-2* quadruple mutants were provided by J. Chory and J. Martinez, respectively (Cifuentes-Esquivel et al., 2013). The *shp1 shp2 ces-2*, *bee1 bee2 bee3 stk*, *bee1 bee3 stk ces-2* and the *bee1 bee2 bee3 stk ces-2* lines were obtained by crossing.

The transgenic line *TCSn::GFP* was provided by B. Muller (Zurcher et al., 2013). The transgenic lines g*FUL:GFP* was provided by S. de Folter (de Folter et al., 2007) and *pFUL::GUS* was provided by C. Ferrándiz (Gu et al., 1998). The *pSTK::STK-GFP* was previously generated in the laboratory (Mizzotti et al., 2014). The transgenic line *pCKX7::GUS* was provided by Nadine Baumann and Rita Groß-Hardt (Mendes et al., 2016). The transgenic line *pCKX6::GUS* was provided by Isabel Bartrina (Bartrina et al., 2011). The *stk TCSn::GFP*, *stk* g*FUL:GFP*, *stk pFUL::GUS* and *stk pCKX7::GUS* and *stk pCKX6::GUS* plants were obtained by crossing.

CRISPR Cas9 genome editing technology with single gRNA construct

The cloning of the construct was realized following the protocol published by F.Fauser (Fauser et al., 2014). The protospacer sequence was selected with the aid of the CRISPR-P 2.0 software.

Gene *CKX7*	Primer name	Primer sequence
At5g21482	Atp_6702	attg**TGTCGATATGAGTACCACGG**
	Atp_6703	aaac**CCGTGGTACTCATATCGACA**

The underline sequences allow the directional cloning of the protospacer in the pEn-Chimera entry vector. The protospacers were cloned in the entry vector with the following protocol:

2 µL of each oligo (50 µM) were diluted in 46 µL of ddH2O and incubated at 95°C for 5’ in order to allow annealing.

The pEn-Chimera entry vector was digested with the following procedure:

pEn-Chimera	10 µL
10X CUTSMART NEB Buffer	2 µL
BbsI Enzyme 5000 U/mL	1 µL
ddH2O	To a final volume of 20 µL

The reaction was incubated for 1h at 37°C

The ligation reaction was performed as following:

Digested pEn-Chimera	2 µL
Annealed Oligo	3 µL
T4 Ligase 3U/mL	1 µL
T4 DNA Ligase Buffer 10X	1 µL
ddH2O	Up to a final volume of 20 µL

5 µL of the ligation reaction were transformed in *E. coli* electrocompetent cells. Transformed cells were plated on solid LB containing Amp and incubated O/N at 37°C.

Positive colonies were checked by PCR, using as primers the forward oligo and a primer designed on the pEn-Chimera plasmid.

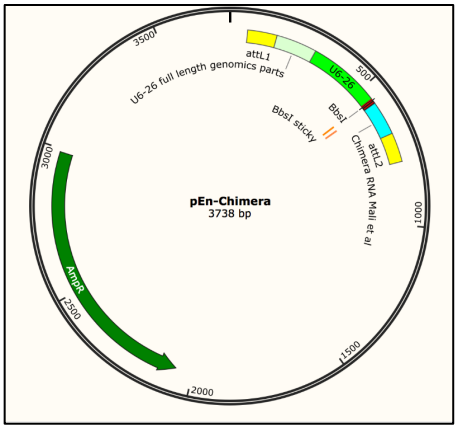

Figure M.1: Schematic map of pEn-Chimera Entry Vector

Plasmid was then extracted from the positive colonies using the procedure described before.

The gRNA was cloned into the destination vector (pDeCas9) using the Gateway technology. The reaction was performed as following:

Entry vector	2 µL
pDe-Cas9	3 µL
TE Buffer	4 µL
LR Clonase II	1 µL

The reaction was incubated at room temperature for 2h.

After the incubation time, the Proteinase K Treatment was performed (1 µL of Proteinase K 2 µg/µL was added at each sample, following a 10' incubation at 37°C).

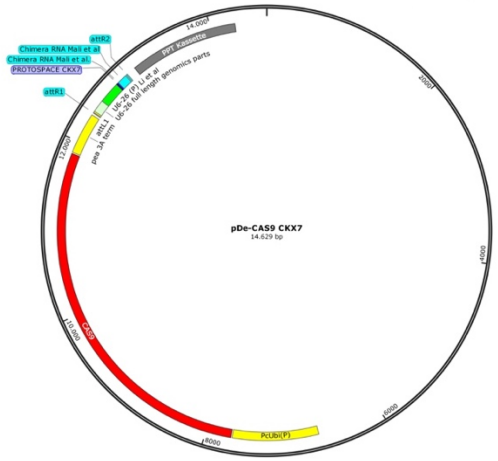

Figure M.2: Schematic map of pDe-Cas9 destination vector

Plasmid was then transformed in *E. coli* competent cells. Transformed cells were plated on solid LB plates containing streptomycin. The positive colonies were checked by PCR. Plasmid from positive colonies was extracted and sent to sequence.

The protospacer generated has this sequence: TGTCGATATGAGTACCACGG.

When the positive colonies were selected, we transformed Col-0 and *ckx6* plants through *Agrobacterium tumefaciens* using floral DIP method (Clough and Bent, 1998). To find the single insertion generated by the CRISPR-Cas9 construct, we used the Fw primer Atp_6702 to sequence. Finally, we analysed plants with single insertion without Cas9, in T3, T4 and T5 generation in order to obtain three independent biological replicates.

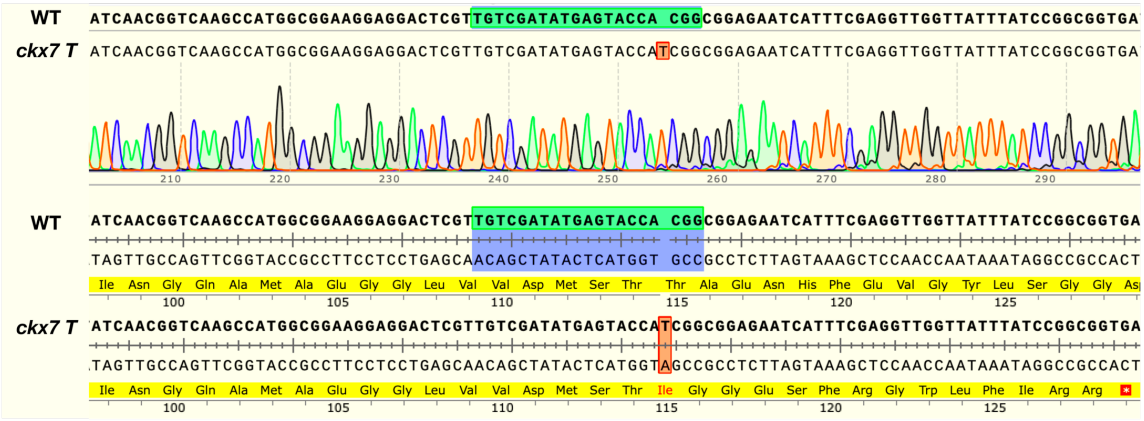

Figure M.3: Example of a *ckx7* mutant sequence generated through the CRISPR Cas9 technique. Single mutant *ckx7* T sequence with a single insertion of a T, and the amino acid sequence of the inactive protein. In green the protospacer sequence, in red the T insertion.

Binary construct and Arabidopsis transformation

For ectopic *CKX7* expression in wild type and *stk* plants, the *CKX7* cDNA was cloned under the control of a 35S promoter of Cauliflower mosaic virus (CaMV) (NOB2252). The *CKX7* cDNA was amplified by PCR by high-fidelity Phusion DNA polymerase (Thermo Fisher Scientific) using primers Atp_4677 and Atp_4678 (see Table S.2 attached manuscript 3). The PCR product was then recombined into the pDONR207 vector (BP Gateway reaction) and sequenced. The PCR product cloned into the DONOR vector was then recombined into the pB2GW7 binary vector under control of the CaMV 35S promoter (LR Gateway reaction) according to the manufacturer's instructions (Thermo Fisher Scientific). Positive colonies (NOB 2252) were isolated on LB agar plates containing spectinomycin (100 mg/L) and sequenced. Binary vectors were used to transform *Agrobacterium tumefaciens* (NOB 2329) and Arabidopsis plants were transformed using the floral dip method described by Clough and Bent (1998). The primers used for cloning and genotyping are listed in Table S.2 of the attached manuscript 3. See Figure R.10 for overexpression validation.

Mutant genotyping

DNA extraction from leaves was performed using Tris HCl 200 mM, NaCl 250 mM, EDTA 25 mM and SDS 0,5% extraction buffer and subsequently followed by DNA pellet precipitation using 2-propanol. The DNA obtained from mutants and over-expression line has been used for PCR-based genotyping. All the primers used in this study are listed in Table S.9 (Attached manuscript 2) and Table S.2 (Attached manuscript 3).

PCR purification to sequence

After PCR-based genotyping to obtain a PCR product in which the amplicon could has the insertion created through the CRISPR Cas9 technique, at the PCR product (15 µL) was add 185 µL of deionised water to obtain a final volume of 200 µL. Then, we add 500 µL of EtOH 70% and 20 µL of NaAc (5M). The final product precipitate for 1 hour and 30 minutes at -20°. After the precipitation step, the product centrifugate (13,200 x *g*) for 15 minutes and washing with EtOH 70%. The purification product could elute in 30 µL of deionised water and then send for sequencing.

Phenotypical characterization of the mutants used in the research projects

The percentage of unfertilized ovules per fruit in *stk*, *ces-2*, *bee1*, *bee3*, *stk ces-2*, *shp1 shp2*, *bee1 bee3*, *bee1 bee2 bee3*, *shp1 shp2 ces-2*, *bee1 bee2 bee3 ces-2*, *bee1 bee2 bee3 stk*, *bee1 bee3 stk ces-2* and *bee1 bee2 bee3 stk ces-2* compared to wt Col-0, was determined by opening at least 20 mature siliques for each genotype by dissection under a stereomicroscope, counting the number of unfertilized ovules and the total number of developed seeds per silique under a stereomicroscope.

The statistical analyses were made using Student's *t*-test ($p<0.05$=*; $p<0.01$=**) and ANOVA test followed by Tukey HSD test ($p<0.05$=*; $p<0.01$=**). All the experiments were repeated four times.

For morphologically characterization of pistils and siliques length analysis, the pistils at stage 13 (*stk*, *ckx7*, *ckx7* T, *35S::CKX7*, and Col-0) and the siliques at stage 17 of each genotype (*stk*, *ckx7*, *ckx7* T, *35S::CKX7*, *stk ckx7*, *stk* x *35S::CKX7*, *ful-2*, *stk ful-2* and Col-0) were collected in the greenhouse from the plants. Pictures were taken using a stereomicroscope. The pistil and fruit length measures were obtained using Fiji software (Schindelin et al., 2012). For each genotype, 20 siliques or pistils were analysed in each biological replicate. All the experiments were repeated three times. The statistical significance of the differences in pistils and fruit length was analyzed using Student's *t*-test ($p<0.05$=*; $p<0.01$=**) and ANOVA test followed by Tukey HSD test ($p<0.05$=*; $p<0.01$=**).

Quantification of endogenous cytokinins before and after fertilization

Quantification of CK metabolites was performed as previously described in (Svačinová et al., 2012). Approximately 0.2 g of inflorescence until stage 12 and silique from stage 14 to 17 was harvested for each genotype. Samples (20 mg FW) were extracted in 1.0 mL modified Bieleski

buffer (60% MeOH, 10% HCOOH and 30% H_2O) together with a cocktail of stable isotope-labelled internal standards (0.25 pmol CK bases, ribosides, *N*-glucosides, and 0.5 pmol CK *O*-glucosides and nucleotides were added per sample). The extracts were purified using multi-StageTips (containing C18/SDB-RPSS/Cation-SR layers), the eluates were then evaporated to dryness in a vacuum and stored at -20°C. Cytokinin levels were determined using ultra-high performance liquid chromatography-electrospray tandem mass spectrometry (UHPLC-MS/MS) using stable isotope-labelled internal standards as a reference. Four independent biological replicates were harvested for each genotype. Statistical analysis was performed using the Student's *t*-test (* $p < 0.05$; ** $p < 0.01$).

Chromatin Immunoprecipitation (ChIP) assay

The *CKX7* promoter region was analysed to identify potential CArG boxes. The ChIP experiment was performed as previously described in (Ezquer et al., 2016). One gram of silique material from stage 14 to stage 16 was used for chromatin extraction from *STK::STK*:*GFP* (Mizzotti et al., 2014) and Col-0 wild type plants. For immunoprecipitation, we used 1.5 µL anti-GFP polyclonal antibody for each sample (Clontech 632460). Enrichment of the target regions was calculated by qPCR (iTaq Universal SYBR Green Supermix, Bio-Rad) using a Bio-Rad iCycler iQ optical system. The relative enrichment of the targets obtained from *STK::STK*:*GFP* silique were compared with the enrichment obtained from wild type. *ACTIN* 2/7 was used for normalization as previously described (Matias-Hernandez et al., 2010). To establish the efficiency of the chromatin immunoprecipitation, we used the fourth CArG box of *PMEI6* as a positive control (Ezquer et al., 2016). Three independent ChIP experiments were performed. The primers used are listed in Table S.2 (Attached manuscript 3).

qRT-PCR to analyse gene expression

Total RNA was extracted from siliques from stage 14 to stage 16 using LiCl protocol (Verwoerd et al., 1989) to analyse *CKX7*, *IND* and *MIR172C* gene expression in *stk* when compared to wt. The RNA for the validation of *ckx7* SAIL515_A07 (knockout mutant) and the *35S::CKX7* line (over-expression), was extracted from inflorescence and siliques up to stage 17 using LiCl protocol (Verwoerd et al., 1989). The cDNA was obtained using an IMProm-II™ Reverse Transcription System (Promega). Fold enrichments were detected using a SYBER Green assay (Bio-Rad, http://www.bio-rad.com). Real-Time PCR test was performed in three biological replicates using a Bio-Rad iCycler iQ optical system. The relative transcript

enrichment was calculated against two housekeeping genes (*UBIQUITIN* and *ACTIN*). Statistical differences were analysed through the Student's *t*-test (* $p < 0.05$; ** $p < 0.01$). The primers used for qRT-PCR are listed in Table S.2 (Attached manuscript 3).

RNA sequencing and qRT-PCR for validation

Total RNA was extracted from three biological replicates (1 gr) from both wild-type and *bee1 bee3 stk ces-2* mutant inflorescences till stage 12 before fertilization, using the Macherey Nagel 'Nucleospin RNA Plant' according to the manufacturer's instructions. RNA concentrations and integrity were determined using Qubit Fluorometer and the Qubit™ RNA XR Assay Kit (ThermoFisher Scientific). Sequencing libraries were prepared using the NEBNext Ultra II Directional RNA library Prep Kit for illumina (NEB) according to the manufacture's instruction and sequenced on HiSeq Illumina platform. Reads were mapped on the reference *Arabidopsis thaliana* transcriptome (TAIR, version 10) using the bowtie2 program (Langmead Ben and Steven, 2012). Estimation of gene expression levels was performed using RSEM (Li and Dewey, 2011). Identification of differentially expressed genes was performed by the quasi-likelihood F-test as implemented by edgeR (Robinson et al., 2009). To validate the data obtained from RNAseq. experiment, we extracted total RNA from wild type *bee1 bee3 stk ces-2* mutant inflorescences till stage 12 before fertilization and cDNA was obtained as previously described in the section "qRT-PCR to analyse gene expression". The primers used for qRT-PCR of RNAseq validation are listed in Table S.9 of the attached manuscript 2.

GUS assay

For GUS histochemical detection of the *pFUL::GUS* and *pCKX6::GUS* in Col-0 and *stk* backgrounds, inflorescences and siliques up to stage 17 were treated for 15 min in 90% ice-cold acetone and then washed for 5 min with washing buffer (25 mM sodium phosphate, 5 mM ferrocyanide, 5 mM ferricyanide, and 1% Triton X-100) and incubated 16 h at 37 °C with staining buffer (washing buffer+1 mM X-Gluc). Following staining, plant material was fixed, cleared in chloral hydrate, and mounted to take pictures with stereomicroscope. For GUS histochemical detection of the *pCKX7::GUS* in Col-0 and *stk* backgrounds the procedure was previously described in Herrera-Ubaldo et al., 2019.

Scanning Electron Microscope (SEM) pictures

Biological samples (pistils at stage 13 and siliques at stage 17) were collected and fixed overnight at 4°C in FAE solution (10 mL formaldehyde 37%, 50 mL absolute ethanol, 5 mL glacial acetic acid, 35 mL deionized water). Fixed tissues were washed with water and post-fixed with aqueous 2% osmium tetroxide for 2 hours at room temperature. Tissues were rinsed several times in deionized water and dehydrated in a graded series of ethanol for 15 min per rinse. This step was followed by critical point drying with liquid CO_2 and sputter-coating with gold in a Nanotech sputter coater. Specimens were analyzed using a LEO 1430 Scanning Electron Microscope.

Confocal analysis of the marker-lines used in the research projects

The marker-line analysis of *TCSn::GFP* and g*FUL:GFP* in *stk* and Col-0 backgrounds was performed using the protocol described before by Reyes-Olalde et al., 2015 and confocal fluorescent images were captured using a confocal laser scanning inverted microscope LSM 510 META (Carl Zeiss, Germany).

Feulgen staining for siliques

The reagents were made as previously described by Braselton et al., 1996 with slight modifications. We used 20 different siliques, for each genotype (*stk*, *ckx7*, *ckx7* T and *35S::CKX7* when compared to wt) analysed, at stage 17 for cell length analysis. The samples were seen with argon ion laser at 488nm excitation and emissions were detected between 515 and 600 nm. To take pictures we used the Nikon A1 laser scanning confocal. The statistical analysis was made using ANOVA test followed by Tukey HSD test ($p<0.05$=*; $p<0.01$=**).

BIBLIOGRAPHY

Akoh, C. C., Lee, G. C., Liaw, Y. C., Huang, T. H. and Shaw, J. F. (2004). GDSL family of serine esterases/lipases. *Prog. Lipid Res.* **43**, 534–552.

Alabadí, D., Blázquez, M. A., Carbonell, J., Ferrándiz, C. and Pérez-Amador, M. A. (2009). Instructive roles for hormones in plant development. *Int. J. Dev. Biol.* **53**, 1597–1608.

Alonso-Blanco, C., Blankestijn-de Vries, H., Hanhart, C. J. and Koornneef, M. (1999). Natural allelic variation at seed size loci in relation to other life history traits of Arabidopsis thaliana. *Proc. Natl. Acad. Sci.* **96**, 4710–4717.

Alonso, J. M. and Stepanova, A. N. (2003). T-DNA Mutagenesis in Arabidopsis BT - Plant Functional Genomics. In *Plant Molecular Biology* (ed. Grotewold, E.), pp. 177–187. Totowa, NJ: Humana Press.

Alvarez-buylla, E. R., Benítez, M., Corvera-poiré, A., Cador, C., Folter, S. De, Buen, A. G. De, Garay-arroyo, A., García-ponce, B., Jaimes-miranda, F., Rigoberto, V., et al. (2010). Flower Development. 1–57.

Alvarez, J. and Smyth, D. R. (1999). CRABS CLAW and SPATULA, two Arabidopsis genes that control carpel development in parallel with AGAMOUS. *Development* **126**, 2377–2386.

Alvarez, J. and Smyth, D. R. (2002a). CRABS CLAW and SPATULA genes regulate growth and pattern formation during gynoecium development in Arabidopsis thaliana. *Int. J. Plant Sci.* **163**, 17–41.

Alvarez, J. and Smyth, D. R. (2002b). CRABS CLAW and SPATULA Genes Regulate Growth and Pattern Formation during Gynoecium Development in Arabidopsis thaliana. *Int. J. Plant Sci.* **163**, 17–41.

Angenent, G. C. and Colombo, L. (1996). Molecular control of ovule development. *Trends Plant Sci.* **1**, 228–232.

Aoki, K., Ogata, Y. and Shibata, D. (2007). Approaches for extracting practical information from gene co-expression networks in plant biology. *Plant Cell Physiol.* **48**, 381–390.

Aspeborg, H., Coutinho, P. M., Wang, Y., Brumer, H. and Henrissat, B. (2012). Evolution, substrate specificity and subfamily classification of glycoside hydrolase family 5 (GH5). *BMC Evol. Biol.* **12**, 186.

Azhakanandam, S., Nole-Wilson, S., Bao, F. and Franks, R. G. (2008). SEUSS and AINTEGUMENTA mediate patterning and ovule initiation during gynoecium medial domain development. *Plant Physiol.* **146**, 1165–1181.

Bae, E., Bingman, C. A., Bitto, E., Aceti, D. J. and Phillips Jr., G. N. (2008). Crystal structure of Arabidopsis thaliana cytokinin dehydrogenase. *Proteins Struct. Funct. Bioinforma.* **70**, 303–306.

Balanzá, V., Navarrete, M., Trigueros, M. and Ferrándiz, C. (2006). Patterning the female side of Arabidopsis: the importance of hormones. *J. Exp. Bot.* **57**, 3457–69.

Balanzà, V., Roig-Villanova, I., Di Marzo, M., Masiero, S. and Colombo, L. (2016). Seed abscission and fruit dehiscence required for seed dispersal rely on similar genetic networks. *Development* **143**, 3372–3381.

Bartrina, I., Otto, E., Strnad, M., Werner, T. and Schmülling, T. (2011). Cytokinin Regulates the Activity of Reproductive Meristems, Flower Organ Size, Ovule Formation, and Thus Seed Yield in *Arabidopsis thaliana*. *Plant Cell* **23**, 69–80.

Bastow, R., Mylne, J. S., Lister, C., Lippman, Z., Martienssen, R. A. and Dean, C. (2004). Vernalization requires epigenetic silencing of FLC by histone methylation. *Nature* **427**, 164–167.

Bektas, I., Fellenberg, C. and Paulsen, H. (2012). Water-soluble chlorophyll protein (WSCP) of Arabidopsis is expressed in the gynoecium and developing silique. *Planta* **236**, 251–259.

Bencivenga, S., Colombo, L. and Masiero, S. (2011). Cross talk between the sporophyte and the megagametophyte during ovule development. *Sex. Plant Reprod.* **24**, 113–121.

Bencivenga, S., Simonini, S., Benková, E. and Colombo, L. (2012). The transcription factors BEL1 and SPL are required for cytokinin and auxin signaling during ovule development in Arabidopsis. *Plant Cell* **24**, 2886–2897.

Benková, E., Michniewicz, M., Sauer, M., Teichmann, T., Seifertová, D., Jürgens, G. and Friml, J. (2003). Local, efflux-dependent auxin gradients as a common module for plant organ formation. *Cell* **115**, 591–602.

Bennett, S. R. M., Alvarez, J., Bossinger, G. and Smyth, D. R. (1995). Morphogenesis in pinoid mutants of Arabidopsis thaliana. *Plant J.* **8**, 505–520.

Boex-Fontvieille, E., Rustgi, S., von Wettstein, D., Reinbothe, S. and Reinbothe, C. (2015). Water-soluble chlorophyll protein is involved in herbivore resistance

activation during greening of Arabidopsis thaliana. *J. Exp. Bot.* **66**, 6119–6135.

Bowman, J. L., Smyth, D. R. and Meyerowitz, E. M. (1991). Genetic interactions among floral homeotic genes of Arabidopsis. *Development* **112**, 1–20.

Bowman, J. L., Baum, S. F., Eshed, Y., Putterill, J. and Alvarez, J. (1999a). Molecular Genetics of Gynoecium Development in Arabidopsis. In (ed. Pedersen, R. A.) and Schatten, G. P.), pp. 155–205. Academic Press.

Bowman, J. L., Baum, S. F., Eshed, Y., Putterill, J. and Alvarez, J. (1999b). Molecular genetics of gynoecium development in Arabidopsis. *Curr. Top. Dev. Biol.* **45**, 155–205.

Bowman, J. L., Smyth, D. R. and Meyerowitz, E. M. (2007). Genes Directing Flower Development in Arabidopsis. *Plant Cell* **1**, 37.

Braatz, J., Harloff, H. J., Mascher, M., Stein, N., Himmelbach, A. and Jung, C. (2017). CRISPR-Cas9 targeted mutagenesis leads to simultaneous modification of different homoeologous gene copies in polyploid oilseed rape (Brassica napus). *Plant Physiol.* **174**, 935–942.

Braselton, J. P., Wilkinson, M. J. and Clulow, S. A. (1996). Feulgen Staining of Intact Plant Tissues for Confocal Microscopy. *Biotech. Histochem.* **71**, 84–87.

Broadhvest, J., Baker, S. C. and Gasser, C. S. (2000). SHORT INTEGUMENTS 2 promotes growth during Arabidopsis reproductive development. *Genetics* **155**, 899–907.

Carabelli, M., M., P., G., S., A., C., M., S., G., M., I., R., Carabelli, M., Possenti, M., Sessa, G., et al. (2007). Canopy shade causes a rapid and transient arrest in leaf development through auxin-induced cytokinin oxidase activity. *Genes Dev.* **21**, 1863–1868.

Carbonell-Bejerano, P., Urbez, C., Granell, A., Carbonell, J. and Perez-Amador, M. A. (2011). Ethylene is involved in pistil fate by modulating the onset of ovule senescence and the GA-mediated fruit set in Arabidopsis. *BMC Plant Biol.* **11**, 84.

Chae, K., Kieslich, C. A., Morikis, D., Kim, S.-C. and Lord, E. M. (2009). A Gain-of-Function Mutation of Arabidopsis Lipid Transfer Protein 5 Disturbs Pollen Tube Tip Growth and Fertilization . *Plant Cell* **21**, 3902–3914.

Cheng, Y., Dai, X. and Zhao, Y. (2006). Auxin biosynthesis by the YUCCA flavin monooxygenases controls the formation of floral organs and vascular tissues in Arabidopsis. *Genes Dev* **20**, 1790–1799.

Cifuentes-Esquivel, N., Bou-Torrent, J., Galstyan, A., Gallemí, M., Sessa, G., Salla Martret, M., Roig-Villanova, I., Ruberti, I. and Martínez-García, J. F. (2013). The bHLH proteins BEE and BIM positively modulate the shade avoidance syndrome in Arabidopsis seedlings. *Plant J.* **75**, 989–1002.

Clough, S. J. and Bent, A. F. (1998). Floral dip: A simplified method for Agrobacterium-mediated transformation of Arabidopsis thaliana. *Plant J.* **16**, 735–743.

Coimbra, S., Almeida, J., Junqueira, V., Costa, M. L. and Pereira, L. G. (2007). Arabinogalactan proteins as molecular markers in Arabidopsis thaliana sexual reproduction. *J. Exp. Bot.* **58**, 4027–4035.

Coimbra, S., Costa, M., Jones, B., Mendes, M. A. and Pereira, L. G. (2009). Pollen grain development is compromised in Arabidopsis agp6 agp11 null mutants. *J. Exp. Bot.* **60**, 3133–3142.

Colombo, L., Battaglia, R. and Kater, M. M. (2008). Arabidopsis ovule development and its evolutionary conservation. *Trends Plant Sci.* **13**, 444–50.

Crawford, B. C. W. and Yanofsky, M. F. (2008). The Formation and Function of the Female Reproductive Tract in Flowering Plants. *Curr. Biol.* **18**, 972–978.

Crawford, B. C. W. and Yanofsky, M. F. (2011). HALF FILLED promotes reproductive tract development and fertilization efficiency in Arabidopsis thaliana. *Development* **138**, 2999–3009.

Crawford, B. C. W., Ditta, G. and Yanofsky, M. F. (2007). The NTT Gene Is Required for Transmitting-Tract Development in Carpels of Arabidopsis thaliana. *Curr. Biol.* **17**, 1101–1108.

Cucinotta, M., Colombo, L. and Roig-villanova, I. (2014). Ovule development , a new model for lateral organ formation. **5**, 1–12.

Cucinotta, M., Manrique, S., Guazzotti, A., Quadrelli, N. E., Mendes, M. A., Benkova, E. and Colombo, L. (2016). Cytokinin response factors integrate auxin and cytokinin pathways for female reproductive organ development. *Development* **143**, 4419–4424.

Cucinotta, M., Manrique, S., Cuesta, C., Benkova, E., Novak, O. and Colombo, L. (2018). CUP-SHAPED COTYLEDON1 (CUC1) and CUC2 regulate cytokinin homeostasis to determine ovule number in Arabidopsis. *J. Exp. Bot.* **69**, 5169–5176.

Davies, P. J. (2004). *Plant Hormones: biosynthesis, signal, transduction, action!*

Kluwer Academic Publishers. Dordrecht, The Netherlands.

de Folter, S. and Angenent, G. C. (2006). trans meets cis in MADS science. *Trends Plant Sci.* **11**, 224–231.

De Folter, S., Urbanus, S. L., Van Zuijlen, L. G. C., Kaufmann, K. and Angenent, G. C. (2007). Tagging of MADS domain proteins for chromatin immunoprecipitation. *BMC Plant Biol.* **7**, 1–11.

Ding, J., Chen, B., Xia, X., Mao, W., Shi, K., Zhou, Y. and Yu, J. (2013). Cytokinin-Induced Parthenocarpic Fruit Development in Tomato Is Partly Dependent on Enhanced Gibberellin and Auxin Biosynthesis. *PLoS One* **8**, 1–11.

Dinneny, J. R., Weigel, D. and Yanofsky, M. F. (2005). A genetic framework for fruit patterning in Arabidopsis thaliana. *Development* **132**, 4687–4696.

Doench, J. G., Hartenian, E., Graham, D. B., Tothova, Z., Hegde, M., Smith, I., Sullender, M., Ebert, B. L., Xavier, R. J. and Root, D. E. (2014). Rational design of highly active sgRNAs for CRISPR-Cas9-mediated gene inactivation. *Nat. Biotechnol.* **32**, 1262–1267.

Dorcey, E., Urbez, C., Blázquez, M. A., Carbonell, J. and Perez-Amador, M. A. (2009). Fertilization-dependent auxin response in ovules triggers fruit development through the modulation of gibberellin metabolism in Arabidopsis. *Plant J.* **58**, 318–332.

Dreni, L., Pilatone, A., Yun, D., Erreni, S., Pajoro, A., Caporali, E., Zhang, D. and Kater, M. M. (2011). Functional Analysis of All AGAMOUS Subfamily Members in Rice Reveals Their Roles in Reproductive Organ Identity Determination and Meristem Determinacy. *Plant Cell* **23**, 2850–2863.

Drews, G. N. and Koltunow, A. M. . (2011). The Female Gametophyte. *Arab. B.* **9**, e0155.

Duszynska, D., McKeown, P. C., Juenger, T. E., Pietraszewska-Bogiel, A., Geelen, D. and Spillane, C. (2013). Gamete fertility and ovule number variation in selfed reciprocal F1 hybrid triploid plants are heritable and display epigenetic parent-of-origin effects. *New Phytol.* **198**, 71–81.

Egea-Cortines, M., Saedler, H. and Sommer, H. (1999). Ternary complex formation between the MADS-box proteins SQUAMOSA, DEFICIENS and GLOBOSA is involved in the control of floral architecture in Antirrhinum majus. *EMBO J.* **18**, 5370–5379.

Elliott, R. C., Betzner, A. S., Huttner, E., Oakes, M. P., Tucker, W. Q. J.,

Gerentes, D., Perez, P. and Smyth, D. R. (1996). AINTEGUMENTA, an APETALA2-like gene of arabidopsis with pleiotropic roles in ovule development and floral organ growth. *Plant Cell* **8**, 155–168.

Endress, P. K. (2011). Angiosperm ovules: diversity, development, evolution. *Ann. Bot.* **107**, 1465–89.

Endress, P. K. and Igersheim, A. (2000). Gynoecium Structure and Evolution in Basal Angiosperms. *Int. J. Plant Sci.* **161**, S211–S213.

Ezquer, I., Mizzotti, C., Nguema-Ona, E., Gotté, M., Beauzamy, L., Viana, V. E., Dubrulle, N., Costa de Oliveira, A., Caporali, E., Koroney, A.-S., et al. (2016). The Developmental Regulator SEEDSTICK Controls Structural and Mechanical Properties of the Arabidopsis Seed Coat. *Plant Cell* **28**, 2478–2492.

Fauser, F., Schiml, S. and Puchta, H. (2014). Both CRISPR/Cas-based nucleases and nickases can be used efficiently for genome engineering in Arabidopsis thaliana. *Plant J.* **79**, 348–359.

Favaro, R., Pinyopich, A., Battaglia, R., Kooiker, M., Borghi, L., Ditta, G., Yanofsky, M. F., Kater, M. M. and Colombo, L. (2003). MADS-box protein complexes control carpel and ovule development in Arabidopsis. *Plant Cell* **15**, 2603–2611.

Ferrándiz, C., Pelaez, S. and Yanofsky, M. F. (1999). Control of Carpel and Fruit Development. *Annu. Rev. Biochem* 321–354.

Ferrándiz, C., Gu, Q., Martienssen, R. and Yanofsky, M. F. (2000a). Redundant regulation of meristem identity and plant architecture by FRUITFULL, APETALA1 and CAULIFLOWER. *Development* **127**, 725–34.

Ferrándiz, C., Liljegren, S. J. and Yanofsky, M. F. (2000b). Negative regulation of the SHATTERPROOF genes by FRUITFULL during Arabidopsis fruit development. *Science (80-.).* **289**, 436–438.

Flanagan, C. A., Hu, Y. and Ma, H. (1996). Specific expression of the AGL1 MADS-box gene suggests regulatory functions in Arabidopsis gynoecium and ovule development. *Plant J.* **10**, 343–353.

Frébort, I., Kowalska, M., Hluska, T., Frébortová, J. and Galuszka, P. (2011). Evolution of cytokinin biosynthesis and degradation. *J. Exp. Bot.* **62**, 2431–2452.

Friedrichsen, D. M., Nemhauser, J., Muramitsu, T., Maloof, J. N., Alonso, J., Ecker, J. R., Furuya, M. and Chory, J. (2002). Three redundant brassinosteroid early response genes encode putative bHLH transcription

factors required for normal growth. *Genetics* **162**, 1445–1456.

Friml, J., Yang, X., Michniewicz, M., Weijers, D., Quint, A., Tietz, O., Benjamins, R., Ouwerkerk, P. B. F., Ljung, K., Sandberg, G., et al. (2004). A PINOID-Dependent Binary Switch in Apical-Basal PIN Polar Targeting Directs Auxin Efflux. *Sci.* **306**, 862–865.

Fukuchi-Mizutani, M., Tasaka, Y., Tanaka, Y., Ashikari, T., Kusumi, T. and Murata, N. (1998). Characterization of Δ9 acyl-lipid desaturase homologues from Arabidopsis thaliana. *Plant Cell Physiol.* **39**, 247–253.

Galbiati, F., Sinha Roy, D., Simonini, S., Cucinotta, M., Ceccato, L., Cuesta, C., Simaskova, M., Benková, E., Kamiuchi, Y., Aida, M., et al. (2013). An integrative model of the control of ovule primordia formation. *Plant J.* **76**, 446–55.

Galuszka, P., Popelková, H., Werner, T., Frébortová, J., Pospíšilová, H., Mik, V., Köllmer, I., Schmülling, T. and Frébort, I. (2007). Biochemical characterization of cytokinin oxidases/dehydrogenases from Arabidopsis thaliana expressed in Nicotiana tabacum L. *J. Plant Growth Regul.* **26**, 255–267.

Gane, A. M., Clarke, A. E. and Bacic, A. (1995). Localisation and expression of arabinogalactan-proteins in the ovaries of Nicotiana alata Link and Otto. *Sex. Plant Reprod.* **8**, 278–282.

Gao, M. and Showalter, A. M. (1999). Yariv reagent treatment induces programmed cell death in Arabidopsis cell cultures and implicates arabinogalactan protein involvement. *Plant J.* **19**, 321–331.

Gasser, C. S. and Skinner, D. J. (2019). Development and evolution of the unique ovules of flowering plants.pp. 373–399.

Gasser, C. S., Broadhvest, J. and Hauser, B. A. (1998). GENETIC ANALYSIS OF OVULE DEVELOPMENT. *Annu. Rev. Plant Physiol. Plant Mol. Biol.* **49**, 1–24.

Girin, T., Paicu, T., Stephenson, P., Fuentes, S., Körner, E., O'Brien, M., Sorefan, K., Wood, T. A., Balanzá, V., Ferrándiz, C., et al. (2011). INDEHISCENT and SPATULA interact to specify carpel and valve margin tissue and thus promote seed dispersal in Arabidopsis. *Plant Cell* **23**, 3641–3653.

Gomez, M. D., Urbez, C., Perez-Amador, M. a and Carbonell, J. (2011). Characterization of constricted fruit (ctf) mutant uncovers a role for AtMYB117/LOF1 in ovule and fruit development in Arabidopsis thaliana. *PLoS One* **6**, e18760.

Gomez, M. D., Barro-Trastoy, D., Escoms, E., Saura-Sańchez, M., Sańchez, I., Briones-Moreno, A., Vera-Sirera, F., Carrera, E., Ripoll, J. J., Yanofsky, M. F., et al. (2018). Gibberellins negatively modulate ovule number in plants. *Dev.* **145**, dev163865.

Gómez, M. D., Fuster-Almunia, C., Ocaña-Cuesta, J., Alonso, J. M. and Pérez-Amador, M. A. (2019). RGL2 controls flower development, ovule number and fertility in Arabidopsis. *Plant Sci.* **281**, 82–92.

Gonçalves, B., Hasson, A., Belcram, K., Cortizo, M., Morin, H., Nikovics, K., Vialette-Guiraud, A., Takeda, S., Aida, M., Laufs, P., et al. (2015). A conserved role for CUP-SHAPED COTYLEDON genes during ovule development. *Plant J.* **83**, 732–742.

Govaerts, R. (2001). How many species of seed plants are there? *Taxon* **50**, 1085–1090.

Gremski, K., Ditta, G. and Yanofsky, M. F. (2007). The HECATE genes regulate female reproductive tract development in Arabidopsis thaliana. *Development* **134**, 3593–3601.

Grini, P. E., Thorstensen, T., Alm, V., Vizcay-Barrena, G., Windju, S. S., Jørstad, T. S., Wilson, Z. A. and Aalen, R. B. (2009). The ASH1 HOMOLOG 2 (ASHH2) histone H3 methyltransferase is required for ovule and anther development in Arabidopsis. *PLoS One* **4**,.

Gross, T., Broholm, S. and Becker, A. (2018). CRABS CLAW acts as a bifunctional transcription factor in flower development. *Front. Plant Sci.* **9**, 1–13.

Grossniklaus, U. and Schneitz, K. (1998). The molecular and genetic basis of ovule and megagametophyte development. *Semin. Cell Dev. Biol.* **9**, 227–238.

Groszmann, M., Paicu, T., Alvarez, J. P., Swain, S. M. and Smyth, D. R. (2011). SPATULA and ALCATRAZ, are partially redundant, functionally diverging bHLH genes required for Arabidopsis gynoecium and fruit development. *Plant J.* **68**, 816–829.

Gu, Q., Ferrándiz, C., Yanofsky, M. F. and Martienssen, R. (1998). The FRUITFULL MADS-box gene mediates cell differentiation during Arabidopsis fruit development. *Development* **125**, 1509–1517.

Guan, Y. and Nothnagel, E. A. (2004). Binding of Arabinogalactan Proteins by Yariv Phenylglycoside Triggers Wound-Like Responses in Arabidopsis Cell Cultures. *Plant Physiol.* **135**, 1346–1366.

Hedden, P. and Sponsel, V. (2015). A Century of Gibberellin Research. *J. Plant Growth Regul.* **34**, 740–760.

Heilmann, I., Pidkowich, M. S., Girke, T. and Shanklin, J. (2004). Switching desaturase enzyme specificity by alternate subcellular targeting. *Proc. Natl. Acad. Sci.* **101**, 10266–10271.

Heisler, M. G. B., Atkinson, A., Bylstra, Y. H., Walsh, R. and Smyth, D. R. (2001). SPATULA, a gene that controls development of carpel margin tissues in Arabidopsis, encodes a bHLH protein. *Development* **128**, 1089–98.

Herrera-Ubaldo, H. and de Folter, S. (2018). Exploring Cell Wall Composition and Modifications During the Development of the Gynoecium Medial Domain in Arabidopsis. *Front. Plant Sci.* **9**, 1–11.

Herrera-Ubaldo, H., Lozano-Sotomayor, P., Ezquer, I., Di Marzo, M., Chávez Montes, R. A., Gómez-Felipe, A., Pablo-Villa, J., Diaz-Ramirez, D., Ballester, P., Ferrándiz, C., et al. (2019). New roles of NO TRANSMITTING TRACT and SEEDSTICK during medial domain development in Arabidopsis fruits . *Development* **146**, dev172395.

Heyl, A. and Schmülling, T. (2003). Cytokinin signal perception and transduction. *Curr. Opin. Plant Biol.* **6**, 480–488.

Higuchi, M., Pischke, M. S., Mähönen, A. P., Miyawaki, K., Hashimoto, Y., Seki, M., Kobayashi, M., Shinozaki, K., Kato, T., Tabata, S., et al. (2004). In planta functions of the Arabidopsis cytokinin receptor family. *Proc. Natl. Acad. Sci. U. S. A.* **101**, 8821–8826.

Hill, T. A., Broadhvest, J., Kuzoff, R. K. and Gasser, C. S. (2006). Arabidopsis SHORT INTEGUMENTS 2 Is a Mitochondrial DAR GTPase. *Genetics* **174**, 707–718.

Hoggart, R. M. and Clarke, A. E. (1984). Arabinogalactans are common components of angiosperm styles. *Phytochemistry* **23**, 1571–1573.

Hu, Xie and Chua (2003). The Arabidopsis Auxin-Inducible Gene ARGOS Controls Lateral Organ Size. *Plant Cell* **15**, 1951–1961.

Huang, H. Y., Jiang, W. B., Hu, Y. W., Wu, P., Zhu, J. Y., Liang, W. Q., Wang, Z. Y. and Lin, W. H. (2013). BR signal influences arabidopsis ovule and seed number through regulating related genes expression by BZR1. *Mol. Plant* **6**, 456–469.

Iglesias, F. M. and Cerdán, P. D. (2016). Maintaining Epigenetic Inheritance During

DNA Replication in Plants. *Front. Plant Sci.* **7**,.

Ishida, T., Aida, M., Takada, S. and Tasaka, M. (2000a). Involvement of CUP-SHAPED COTYLEDON genes in gynoecium and ovule development in Arabidopsis thaliana. *Plant Cell Physiol.* **41**, 60–67.

Ishida, T., Aida, M., Takada, S. and Tasaka, M. (2000b). Involvement of CUP-SHAPED COTYLEDON genes in gynoecium and ovule development in Arabidopsis thaliana. *Plant Cell Physiol.* **41**, 60–7.

Ishida, T., Fukuda, H., Nagawa, S., Ueda, N., Sakakibara, H., Sugimoto, K., Kuroha, T., Kojima, M. and Tokunaga, H. (2009). Functional Analyses of LONELY GUY Cytokinin-Activating Enzymes Reveal the Importance of the Direct Activation Pathway in Arabidopsis. *Plant Cell* **21**, 3152–3169.

Jofuku, K. D., Omidyar, P. K., Gee, Z. and Okamuro, J. K. (2005). Control of seed mass and seed yield by the floral homeotic gene APETALA2. *Proc. Natl. Acad. Sci.* **102**, 3117–3122.

Kant, S., Burch, D., Badenhorst, P., Palanisamy, R., Mason, J. and Spangenberg, G. (2015). Regulated Expression of a cytokinin biosynthesis gene IPT delays leaf senescence and improves yield under rainfed and irrigated conditions in canola (Brassica napus L.). *PLoS One* **10**, 1–18.

Klucher, K. M., Chow, H., Reiser, L. and Fischer, R. L. (1996). The AINTEGUMENTA gene of Arabidopsis required for ovule and female gametophyte development is related to the floral homeotic gene APETALA2. *Plant Cell* **8**, 137–153.

Knauss, S., Rohrmeier, T. and Lehle, L. (2003). The auxin-induced maize gene ZmSAUR2 encodes a short-lived nuclear protein expressed in elongating tissues. *J. Biol. Chem.* **278**, 23936–23943.

Köllmer, I., Novák, O., Strnad, M., Schmülling, T. and Werner, T. (2014). Overexpression of the cytosolic cytokinin oxidase/dehydrogenase (CKX7) from Arabidopsis causes specific changes in root growth and xylem differentiation. *Plant J.* **78**, 359–371.

Kowalska, M., Galuszka, P., Frébortová, J., Šebela, M., Béres, T., Hluska, T., Šmehilová, M., Bilyeu, K. D. and Frébort, I. (2010). Vacuolar and cytosolic cytokinin dehydrogenases of Arabidopsis thaliana: Heterologous expression, purification and properties. *Phytochemistry* **71**, 1970–1978.

Krizek, B. A. (2009). AINTEGUMENTA and AINTEGUMENTA-LIKE6 act

redundantly to regulate arabidopsis floral growth and patterning. *Plant Physiol.* **150**, 1916–1929.

Kunst, L. and Samuels, A. L. (2003). Biosynthesis and secretion of plant cuticular wax. *Prog. Lipid Res.* **42**, 51–80.

Langmead Ben and Steven, S. (2012). Fast gapped-read alignment with Bowtie 2. *Nat. Methods* **9**, 357–359.

Larsson, E., Franks, R. G. and Sundberg, E. (2013a). Auxin and the arabidopsis thaliana gynoecium. *J. Exp. Bot.* **64**, 2619–2627.

Larsson, E., Franks, R. G. and Sundberg, E. (2013b). Auxin and the Arabidopsis thaliana gynoecium. *J. Exp. Bot.* **64**, 2619–27.

Laufs, P., Peaucelle, A., Morin, H. and Traas, J. (2004). MicroRNA regulation of the CUC genes is required for boundary size control in Arabidopsis meristems. *Development* **131**, 4311–22.

Lavy, M. and Estelle, M. (2016). Mechanisms of auxin signaling. *Development* **143**, 3226–3229.

Lennon, K. A., Stéphane, R., Peter, H. K. and Lord, E. M. (1998). The structure of the transmitting tissue of Arabidopsis thaliana (L.) and the path of pollen tube growth. *Sex. Plant Reprod.* 49–59.

Li, B. and Dewey, C. N. (2011). RSEM: Accurate transcript quantification from RNA-seq data with or without a reference genome. *BMC, Bionformatics* **12**, 41–74.

Liljegren, S. J., Ditta, G. S., Eshed, Y., Savidge, B., Bowman, J. L. and Yanofsky, M. F. (2000). SHATTERPROOF MADS-box genes control seed dispersal in Arabidopsis. *Nature* **404**, 766–770.

Liljegren, S. J., Roeder, A. H. K., Kempin, S. a., Gremski, K., Østergaard, L., Guimil, S., Reyes, D. K. and Yanofsky, M. F. (2004). Control of fruit patterning in Arabidopsis by INDEHISCENT. *Cell* **116**, 843–853.

Liu, Z., Franks, R. G. and Klink, V. P. (2000). Regulation of gynoecium marginal tissue formation by LEUNIG and AINTEGUMENTA. *Plant Cell* **12**, 1879–1891.

Liu, H., Ding, Y., Zhou, Y., Jin, W., Xie, K. and Chen, L. L. (2017). CRISPR-P 2.0: An Improved CRISPR-Cas9 Tool for Genome Editing in Plants. *Mol. Plant* **10**, 530–532.

Liu, P., Zhang, C., Ma, J. Q., Zhang, L. Y., Yang, B., Tang, X. Y., Huang, L., Zhou, X. T., Lu, K. and Li, J. N. (2018). Genome-wide identification and expression profiling of cytokinin oxidase/dehydrogenase (CKX) genes reveal

likely roles in pod development and stress responses in oilseed rape (brassica napus L.). *Genes (Basel).* **9**, 168.

Lombard, V., Golaconda Ramulu, H., Drula, E., Coutinho, P. M. and Henrissat, B. (2014). The carbohydrate-active enzymes database (CAZy) in 2013. *Nucleic Acids Res.* **42**, 490–495.

Lord, E. M. and Russell, S. D. (2002). The Mechanisms of Pollination and Fertilization in Plants. *Annu. Rev. Cell Dev. Biol.* **18**, 81–105.

Mallory, A. C., Reinhart, B. J., Jones-Rhoades, M. W., Tang, G., Zamore, P. D., Barton, M. K. and Bartel, D. P. (2004). MicroRNA control of PHABULOSA in leaf development: importance of pairing to the microRNA 5′ region. *EMBO J.* **23**, 3356–3364.

Mantegazza, O., Gregis, V., Mendes, M. A., Morandini, P., Alves-Ferreira, M., Patreze, C. M., Nardeli, S. M., Kater, M. M. and Colombo, L. (2014). Analysis of the arabidopsis REM gene family predicts functions during flower development. *Ann. Bot.* **114**, 1507–1515.

Marhavý, P., Bielach, A., Abas, L., Abuzeineh, A., Duclercq, J., Tanaka, H., Pařezová, M., Petrášek, J., Friml, J., Kleine-Vehn, J., et al. (2011). Cytokinin Modulates Endocytic Trafficking of PIN1 Auxin Efflux Carrier to Control Plant Organogenesis. *Dev. Cell* **21**, 796–804.

Marsch-Martínez, N. and de Folter, S. (2016). Hormonal control of the development of the gynoecium. *Curr. Opin. Plant Biol.* **29**, 104–114.

Marsch-Martínez, N., Ramos-Cruz, D., Irepan Reyes-Olalde, J., Lozano-Sotomayor, P., Zúñiga-Mayo, V. M. and De Folter, S. (2012). The role of cytokinin during Arabidopsis gynoecia and fruit morphogenesis and patterning. *Plant J.* **72**, 222–234.

Masiero, S., Palme, K., Roig-Villanova, I., Sinha Roy, D., Colombo, L., Ditengou, F. A., Bencivenga, S., Simon, R. and Ceccato, L. (2013). Maternal Control of PIN1 Is Required for Female Gametophyte Development in Arabidopsis. *PLoS One* **8**, e66148.

Matias-Hernandez, L., Battaglia, R., Galbiati, F., Rubes, M., Eichenberger, C., Grossniklaus, U., Kater, M. M. and Colombo, L. (2010). *VERDANDI* Is a Direct Target of the MADS Domain Ovule Identity Complex and Affects Embryo Sac Differentiation in *Arabidopsis*. *Plant Cell* **22**, 1702–1715.

McClure, B. A. and Guilfoyle, T. (1987). Characterization of a class of small auxin-

inducible soybean polyadenylated RNAs. *Plant Mol. Biol.* **9**, 611–623.

Mendes, M. A., Guerra, R. F., Castelnovo, B., Silva-Velazquez, Y., Morandini, P., Manrique, S., Baumann, N., Groß-Hardt, R., Dickinson, H. and Colombo, L. (2016). Live and let die: a REM complex promotes fertilization through synergid cell death in *Arabidopsis*. *Development* **143**, 2780–2790.

Michaels, S. D. and Amasino, R. M. (2007). FLOWERING LOCUS C Encodes a Novel MADS Domain Protein That Acts as a Repressor of Flowering. *Plant Cell* **11**, 949.

Minic, Z., Do, C. T., Rihouey, C., Morin, H., Lerouge, P. and Jouanin, L. (2006). Purification, functional characterization, cloning, and identification of mutants of a seed-specific arabinan hydrolase in Arabidopsis. *J. Exp. Bot.* **57**, 2339–2351.

Mizukami, Y. and Fischer, R. L. (2000). Plant organ size control: AINTEGUMENTA regulates growth and cell numbers during organogenesis. *Proc. Natl. Acad. Sci. U. S. A.* **97**, 942–947.

Mizzotti, C., Mendes, M. A., Caporali, E., Schnittger, A., Kater, M. M., Battaglia, R. and Colombo, L. (2012). The MADS box genes SEEDSTICK and ARABIDOPSIS Bsister play a maternal role in fertilization and seed development. *Plant J.* **70**, 409–420.

Mizzotti, C., Ezquer, I., Paolo, D., Rueda-Romero, P., Guerra, R. F., Battaglia, R., Rogachev, I., Aharoni, A., Kater, M. M., Caporali, E., et al. (2014). SEEDSTICK is a Master Regulator of Development and Metabolism in the Arabidopsis Seed Coat. *PLoS Genet.* **10**, e1004856.

Mizzotti, C., Rotasperti, L., Moretto, M., Tadini, L., Resentini, F., Galliani, B. M., Galbiati, M., Engelen, K., Pesaresi, P. and Masiero, S. (2018). Time-course transcriptome analysis of arabidopsis siliques discloses genes essential for fruit development and maturation. *Plant Physiol.* **178**, 1249–1268.

Mok, D. W. S. and Mok, M. C. (2001). CYTOKININ METABOLISM AND ACTION. *Annu. Rev. Plant Physiol. Plant Mol. Bio* **52**, 89–118.

Molkentin, J. D., Black, B. L., Martin, J. F. and Olson, E. N. (1995). Cooperative activation of muscle gene expression by MEF2 and myogenic bHLH proteins. *Cell* **83**, 1125–1136.

Moubayidin, L. and Østergaard, L. (2014). Dynamic control of auxin distribution imposes a bilateral-to-radial symmetry switch during gynoecium development. *Curr. Biol.* **24**, 2743–2748.

Nahar, M. A. U., Ishida, T., Smyth, D. R., Tasaka, M. and Aida, M. (2012). Interactions of CUP-SHAPED COTYLEDON and SPATULA genes control carpel margin development in arabidopsis thaliana. *Plant Cell Physiol.* **53**, 1134–1143.

Nakamura, A., Nakajima, N., Goda, H., Shimada, Y., Hayashi, K. I., Nozaki, H., Asami, T., Yoshida, S. and Fujioka, S. (2006). Arabidopsis Aux/IAA genes are involved in brassinosteroid-mediated growth responses in a manner dependent on organ type. *Plant J.* **45**, 193–205.

Nawrath, C. (2006). Unraveling the complex network of cuticular structure and function. *Curr. Opin. Plant Biol.* **9**, 281–287.

Nemhauser, J. L., Feldman, L. J. and Zambryski, P. C. (2000). Auxin and ETTIN in Arabidopsis gynoecium morphogenesis. *Development* **127**, 3877–3888.

Nieuwland, J., Feron, R., Huisman, B. A. H., Fasolino, A., Hilbers, C. W., Derksen, J. and Mariani, C. (2005). Lipid Transfer Proteins Enhance Cell Wall Extension in Tobacco. *Plant Cell* **17**, 2009–2019.

Nole-Wilson, S., Rueschhoff, E. E., Bhatti, H. and Franks, R. G. (2010a). Synergistic disruptions in seuss cyp85A2 double mutants reveal a role for brassinolide synthesis during gynoecium and ovule development. *BMC Plant Biol.* **10**, 198.

Nole-Wilson, S., Azhakanandam, S. and Franks, R. G. (2010b). Polar auxin transport together with aintegumenta and revoluta coordinate early Arabidopsis gynoecium development. *Dev. Biol.* **346**, 181–95.

Nomura, T., Kushiro, T., Yokota, T., Kamiya, Y., Bishop, G. J. and Yamaguchi, S. (2005). The last reaction producing brassinolide is catalyzed by cytochrome P-450s, CYP85A3 in tomato and CYP85A2 in Arabidopsis. *J. Biol. Chem.* **280**, 17873–17879.

Novák, O., Hauserová, E., Amakorová, P., Doležal, K. and Strnad, M. (2008). Cytokinin profiling in plant tissues using ultra-performance liquid chromatography-electrospray tandem mass spectrometry. *Phytochemistry* **69**, 2214–2224.

Ohto, M. aki, Floyd, S. K., Fischer, R. L., Goldberg, R. B. and Harada, J. J. (2009). Effects of APETALA2 on embryo, endosperm, and seed coat development determine seed size in Arabidopsis. *Sex. Plant Reprod.* **22**, 277–289.

Okada, K., Ueda, J., Komaki, M. K., Bell, C. J. and Shimura, Y. (1991). Requirement of the Auxin Polar Transport System in Early Stages of Arabidopsis Floral Bud Formation. *Plant Cell Online* **3**, 677–684.

Pagnussat, G. C. (2005). Genetic and molecular identification of genes required for female gametophyte development and function in Arabidopsis. *Development* **132**, 603–614.

Panikashvili, D., Shi, J. X., Bocobza, S., Franke, R. B., Schreiber, L. and Aharoni, A. (2010). The arabidopsis DSO/ABCG11 transporter affects cutin metabolism in reproductive organs and suberin in roots. *Mol. Plant* **3**, 563–575.

Pinto, S. C., Mendes, M. A., Coimbra, S. and Tucker, M. R. (2019). Revisiting the Female Germline and Its Expanding Toolbox. *Trends Plant Sci.* **24**, 455–467.

Pinyopich, A., Ditta, G. S., Savidge, B., Liljegren, S. J., Baumann, E., Wisman, E. and Yanofsky, M. F. (2003). Assessing the redundancy of MADS-box genes during carpel and ovule development. *Nature* **424**, 85–8.

Poppenberger, B., Rozhon, W., Khan, M., Husar, S., Adam, G., Luschnig, C., Fujioka, S. and Sieberer, T. (2011). CESTA, a positive regulator of brassinosteroid biosynthesis. *EMBO J.* **30**, 1149–1161.

Rate, D. N., Cuenca, J. V., Bowman, G. R., Guttman, D. S. and Greenberg, J. T. (2007). The Gain-of-Function Arabidopsis acd6 Mutant Reveals Novel Regulation and Function of the Salicylic Acid Signaling Pathway in Controlling Cell Death, Defenses, and Cell Growth. *Plant Cell* **11**, 1695.

Reiser, L. and Fischer, R. L. (1993). The Ovule and the Embryo Sac. *Plant Cell* **5**, 1291–1301.

Reyes-Olalde, J. I. and de Folter, S. (2019). Control of stem cell activity in the carpel margin meristem (CMM) in Arabidopsis. *Plant Reprod.* **32**, 123–136.

Reyes-Olalde, J. I., Zuñiga-Mayo, V. M., Chávez Montes, R. A., Marsch-Martínez, N. and de Folter, S. (2013). Inside the gynoecium: At the carpel margin. *Trends Plant Sci.* **18**, 644–655.

Reyes-Olalde, J. I., Marsch-Martínez, N. and de Folter, S. (2015). Imaging early stages of the female reproductive structure of arabidopsis by confocal laser scanning microscopy. *Dev. Dyn.* **244**, 1286–1290.

Reyes-Olalde, J. I., Montes, A. C., Lozano-sotomayor, P., Herrera-ubaldo, H., Ezquer, I., Ballester, P., Jose, J., Paolo, D., Heyl, A., Colombo, L., et al. (2017). *The bHLH transcription factor SPATULA enables cytokinin signaling ,*

and both activate auxin biosynthesis and transport genes at the medial domain of the gynoecium.

Ripoll, J. J., Roeder, A. H. K., Ditta, G. S. and Yanofsky, M. F. (2011). A novel role for the floral homeotic gene APETALA2 during Arabidopsis fruit development. *Development* **138**, 5167–5176.

Ripoll, J. J., Bailey, L. J., Mai, Q.-A., Wu, S. L., Hon, C. T., Chapman, E. J., Ditta, G. S., Estelle, M. and Yanofsky, M. F. (2015). microRNA regulation of fruit growth. *Nat. Plants* **1**, 15036.

Rizza, A. and Jones, A. M. (2019). The makings of a gradient: spatiotemporal distribution of gibberellins in plant development. *Curr. Opin. Plant Biol.* **47**, 9–15.

Robert, H. S., Crhak Khaitova, L., Mroue, S. and Benková, E. (2015). The importance of localized auxin production for morphogenesis of reproductive organs and embryos in Arabidopsis. *J. Exp. Bot.* **66**, 5029–5042.

Robinson, M. D., McCarthy, D. J. and Smyth, G. K. (2009). edgeR: A Bioconductor package for differential expression analysis of digital gene expression data. *Bioinformatics* **26**, 139–140.

Roeder, A. H. K. and Yanofsky, M. F. (2006). *Fruit Development in Arabidopsis*.

Roeder, A. H. K., Ferrándiz, C. and Yanofsky, M. F. (2003). The Role of the REPLUMLESS Homeodomain Protein in Patterning the Arabidopsis Fruit. *Curr. Biol.* **13**, 1630–1635.

Romanov, G. A., Lomin, S. N. and Schmülling, T. (2006). Biochemical characteristics and ligand-binding properties of Arabidopsis cytokinin receptor AHK3 compared to CRE1/AHK4 as revealed by a direct binding assay. *J. Exp. Bot.* **57**, 4051–4058.

Ruzicka, K., Simásková, M., Duclercq, J., Petrásek, J., Zazímalová, E., Simon, S., Friml, J., Van Montagu, M. C. E. and Benková, E. (2009). Cytokinin regulates root meristem activity via modulation of the polar auxin transport. *Proc. Natl. Acad. Sci. U. S. A.* **106**, 4284–4289.

Sakakibara, H. (2006). CYTOKININS: Activity, Biosynthesis, and Translocation. *Annu. Rev. Plant Biol.* **57**, 431–449.

Sarojam Rajani and Venkatesan Sundaresan (2001). The Arabidopsis myc / bHLH gene ALCATRAZ enables cell separation in fruit dehiscence Sarojam Rajani * † and Venkatesan Sundaresan * ‡. *Curr. Biol.* **1**, 1914–1922.

Savidge, B., Rounsley, S. D. and Yanofsky, M. F. (1995). Temporal Relationship

between the Transcription of Two Arabidopsis MADS Box Genes and the Floral Organ Identity Genes. *Plant Cell* **7**, 721.

Schaller, G. E., Bishopp, A. and Kieber, J. J. (2015). The Yin-Yang of Hormones: Cytokinin and Auxin Interactions in Plant Development. *Plant Cell Online* **27**, 44–63.

Schindelin, J., Arganda-Carreras, I., Frise, E., Kaynig, V., Longair, M., Pietzsch, T., Preibisch, S., Rueden, C., Saalfeld, S., Schmid, B., et al. (2012). Fiji: An open-source platform for biological-image analysis. *Nat. Methods* **9**, 676–682.

Schlereth, A., Moller, B., Liu, W., Kientz, M., Flipse, J., Rademacher, E. H., Schmid, M., Jurgens, G. and Weijers, D. (2010). MONOPTEROS controls embryonic root initiation by regulating a mobile transcription factor. *Nature* **464**, 913–916.

Schmülling, T., Werner, T., Riefler, M., Krupková, E., Bartrina, I. and Manns (2003). Structure and function of cytokinin oxidase/dehydrogenase genes of maize, rice, Arabidopsis and other species. *J. Plant Res.* 241–252.

Schneitz, K., Hulskamp, M. and Pruitt, R. E. (1995). Wild-type ovule development in Arabidopsis thaliana: a light microscope study of cleared whole-mount tissue. *Plant J.* **7**, 731–749.

Schneitz, K., Baker, S. C., Gasser, C. S. and Redweik, A. (1998). Pattern formation and growth during floral organogenesis: HUELLENLOS and AINTEGUMENTA are required for the formation of the proximal region of the ovule primordium in Arabidopsis thaliana. *Development* **125**, 2555–63.

Schuster, C., Gaillochet, C. and Lohmann, J. U. (2015). Arabidopsis HECATE genes function in phytohormone control during gynoecium development. *Dev.* **142**, 3343–3350.

Sessions, A., Nemhauser, J. L., McColl, A., Roe, J. L., Feldmann, K. A. and Zambryski, P. C. (1997). ETTIN patterns the Arabidopsis floral meristem and reproductive organs. *Development* **124**, 4481–4491.

Shah, S., Karunarathna, N. L., Jung, C. and Emrani, N. (2018). An APETALA1 ortholog affects plant architecture and seed yield component in oilseed rape (Brassica napus L.). *BMC Plant Biol.* **18**, 1–12.

Sheldon, C. C., Burn, J. E., Perez, P. P., Metzger, J., Edwards, J. A., Peacock, W. J. and Dennis, E. S. (2007). The FLF MADS Box Gene: A Repressor of Flowering in Arabidopsis Regulated by Vernalization and Methylation. *Plant Cell*

11, 445.

Shi, D.-Q. and Yang, W.-C. (2011). Ovule development in Arabidopsis: progress and challenge. *Curr. Opin. Plant Biol.* **14**, 74–80.

Shirley, N. J., Aubert, M. K., Wilkinson, L. G., Bird, D. C., Lora, J., Yang, X. and Tucker, M. R. (2019). Translating auxin responses into ovules, seeds and yield: Insight from Arabidopsis and the cereals. *J. Integr. Plant Biol.* **61**, 310–336.

Sieber, P., Schorderet, M., Ryser, U., Buchala, A., Kolattukudy, P., Metraux, J.-P. and Nawrath, C. (2007). Transgenic Arabidopsis Plants Expressing a Fungal Cutinase Show Alterations in the Structure and Properties of the Cuticle and Postgenital Organ Fusions. *Plant Cell* **12**, 721.

Šimášková, M., O'Brien, J. A., Khan, M., Van Noorden, G., Ötvös, K., Vieten, A., De Clercq, I., Van Haperen, J. M. A., Cuesta, C., Hoyerová, K., et al. (2015). Cytokinin response factors regulate PIN-FORMED auxin transporters. *Nat. Commun.* **6**, 8717.

Skinner, D. J., Baker, S. C., Meister, R. J., Broadhvest, J., Schneitz, K. and Gasser, C. S. (2001). The Arabidopsis HUELLENLOS gene, which is essential for normal ovule development, encodes a mitochondrial ribosomal protein. *Plant Cell* **13**, 2719–30.

Skinner, D. J., Hill, T. A. and Gasser, C. S. (2004). Regulation of Ovule Development. **16**, 32–46.

Smyth, D. R., Bowman, J. L. and Meyerowitz, E. M. (1990). Early flower development in Arabidopsis. *Plant Cell* **2**, 755–767.

Snowdon, Rod, Lühs, Wilfried, Friedt, W. (2007). Genome Mapping and Molecular Breeding in Plants - Oilseeds. **6**, 54–56.

Sohlberg, J. J., Myrenås, M., Kuusk, S., Lagercrantz, U., Kowalczyk, M., Sandberg, G. and Sundberg, E. (2006). STY1 regulates auxin homeostasis and affects apical-basal patterning of the Arabidopsis gynoecium. *Plant J.* **47**, 112–23.

Song, J., Jiang, L. and Jameson, P. E. (2015). Expression patterns of Brassica napus genes implicate IPT, CKX, sucrose transporter, cell wall invertase, and amino acid permease gene family members in leaf, flower, silique, and seed development. *J. Exp. Bot.* **66**, 5067–5082.

Spíchal, L. (2012). Cytokinins - recent news and views of evolutionally old molecules. *Funct. Plant Biol.* **39**, 267.

Stinchcombe, J. R., Weinig, C., Ungerer, M., Olsen, K. M., Mays, C., Halldorsdottir, S. S., Purugganan, M. D. and Schmitt, J. (2004). A latitudinal cline in flowering time in Arabidopsis thaliana modulated by the flowering time gene FRIGIDA. *Proc. Natl. Acad. Sci. U. S. A.* **101**, 4712–7.

Stolz, A., Riefler, M., Lomin, S. N., Achazi, K., Romanov, G. A. and Schmülling, T. (2011). The specificity of cytokinin signalling in Arabidopsis thaliana is mediated by differing ligand affinities and expression profiles of the receptors. *Plant J.* **67**, 157–168.

Street, I. H., Mathews, D. E., Yamburkenko, M. V., Sorooshzadeh, A., John, R. T., Swarup, R., Bennett, M. J., Kieber, J. J. and Schaller, G. E. (2016). Cytokinin acts through the auxin influx carrier AUX1 to regulate cell elongation in the root. *Development* **143**, 3982–3993.

Sun, Y., Fan, X.-Y., Cao, D.-M., Tang, W., He, K., Zhu, J.-Y., He, J.-X., Bai, M.-Y., Zhu, S., Oh, E., et al. (2010). Integration of Brassinosteroid Signal Transduction with the Transcription Network for Plant Growth Regulation in Arabidopsis. *Dev. Cell* **19**, 765–777.

Svačinová, J., Novák, O., Plačková, L., Lenobel, R., Holík, J., Strnad, M. and Doležal, K. (2012). A new approach for cytokinin isolation from Arabidopsis tissues using miniaturized purification: pipette tip solid-phase extraction. *Plant Methods* **8**, 1–14.

Takahashi, K., Shimada, T., Kondo, M., Tamai, A., Mori, M., Nishimura, M. and Hara-Nishimura, I. (2010). Ectopic expression of an esterase, which is a candidate for the unidentified plant cutinase, causes cuticular defects in arabidopsis thaliana. *Plant Cell Physiol.* **51**, 123–131.

Tan, M., Li, G., Qi, S., Liu, X., Chen, X., Ma, J., Zhang, D. and Han, M. (2018). Identification and expression analysis of the IPT and CKX gene families during axillary bud outgrowth in apple (Malus domestica Borkh.). *Gene* **651**, 106–117.

Theo C.Verwoerd, Ben M.M.Dekker and Andre Hoekema (1989). A small scale procedure for the rapid isolation of plant RNAs. *Nucleic Acid Res.* **17**, 2362.

Tung, C.-W., Dwyer, K. G., Nasrallah, M. E. and Nasrallah, J. B. (2005). Genome-Wide Identification of Genes Expressed in Arabidopsis Pistils Specifically along the Path of Pollen Tube Growth. *Plant Physiol.* **138**, 977–989.

Turbant, A., Fournet, F., Lequart, M., Zabijak, L., Pageau, K., Bouton, S. and Van Wuytswinkel, O. (2016). PME58 plays a role in pectin distribution during

seed coat mucilage extrusion through homogalacturonan modification. *J. Exp. Bot.* **67**, 2177–2190.

van Mourik, H., van Dijk, A. D. J., Stortenbeker, N., Angenent, G. C. and Bemer, M. (2017). Divergent regulation of Arabidopsis SAUR genes: A focus on the SAUR10-clade. *BMC Plant Biol.* **17**, 1–14.

Vanstraelen, M. and Benková, E. (2012). Hormonal interactions in the regulation of plant development. *Annu. Rev. Cell Dev. Biol.* **28**, 463–87.

Vivian-Smith, A. and Koltunow, A. M. (1999). Genetic analysis of growth-regulator-induced parthenocarpy in Arabidopsis. *Plant Physiol.* **121**, 437–51.

Vivian-Smith, A., Luo, M., Chaudhury, A. and Koltunow, A. (2001). Fruit development is actively restricted in the absence of fertilization in Arabidopsis. *Development* **128**, 2321–31.

Webb, M. C. and Williams, E. G. (1988). The Pollen Tube Pathway in the Pistil of Lycopersicon peruvianum. *Ann. Bot.* **61**, 415–423.

Werner, T. and Schmülling, T. (2009). Cytokinin action in plant development. *Curr. Opin. Plant Biol.* **12**, 527–538.

Werner, T., Motyka, V., Laucou, V., Smets, R., Van Onckelen, H. and Schmülling, T. (2003). Cytokinin-Deficient Transgenic Arabidopsis Plants Show Multiple Developmental Alterations Indicating Opposite Functions of Cytokinins in the Regulation of Shoot and Root Meristem Activity. *Plant Cell Online* **15**, 2532–2550.

Wetzstein, H. Y., Yi, W., Porter, J. A. and Ravid, N. (2013). Flower Position and Size Impact Ovule Number per Flower, Fruitset, and Fruit Size in Pomegranate. *J. Am. Soc. Hortic. Sci.* **138**, 159–166.

Willis, K.J. Royal Botanic Gardens, K. (2017). State of the World's Plants 2017. Report.

Wrzaczek, M., Brosche, M., Kollist, H. and Kangasjarvi, J. (2009). Arabidopsis GRI is involved in the regulation of cell death induced by extracellular ROS. *Proc. Natl. Acad. Sci.* **106**, 5412–5417.

Wrzaczek, M., Vainonen, J. P., Stael, S., Tsiatsiani, L., Help-Rinta-Rahko, H., Gauthier, A., Kaufholdt, D., Bollhoner, B., Lamminmaki, A., Staes, A., et al. (2015). GRIM REAPER peptide binds to receptor kinase PRK5 to trigger cell death in Arabidopsis. *EMBO J.* **34**, 55–66.

Wurschum, T., Groß-hardt, R. and Laux, T. (2006). APETALA2 Regulates the

Stem Cell Niche in the Arabidopsis Shoot Meristem, Supplemental Date2.pdf. **18**, 295–307.

Wynn, A. N., Seaman, A. A., Jones, A. L. and Franks, R. G. (2014). Novel functional roles for PERIANTHIA and SEUSS during floral organ identity specification, floral meristem termination, and gynoecial development. *Front. Plant Sci.* **5**,.

Xu, L., Zhao, Z., Dong, A., Soubigou-Taconnat, L., Renou, J.-P., Steinmetz, A. and Shen, W.-H. (2008). Di- and Tri- but Not Monomethylation on Histone H3 Lysine 36 Marks Active Transcription of Genes Involved in Flowering Time Regulation and Other Processes in Arabidopsis thaliana. *Mol. Cell. Biol.* **28**, 1348–1360.

Yang, Y., Wang, Y., Zhan, J., Shi, J., Wang, X., Liu, G. and Wang, H. (2017). Genetic and Cytological Analyses of the Natural Variation of file:///Users/mauriziodimarzo/Downloads/2007_Bookmatter_Oilseeds.pdfSeed Number per Pod in Rapeseed (Brassica napus L.). *Front. Plant Sci.* **8**, 1890.

Yant, L., Mathieu, J., Dinh, T. T., Ott, F., Lanz, C., Wollmann, H., Chen, X. and Schmid, M. (2010). Orchestration of the Floral Transition and Floral Development in Arabidopsis by the Bifunctional Transcription Factor APETALA2. *Plant Cell Online* **22**, 2156–2170.

Yao, K., Bacchetto, R. G., Lockhart, K. M., Friesen, L. J., Potts, D. A., Covello, P. S. and Taylor, D. C. (2003). Expression of the Arabidopsis ADS1 gene in Brassica juncea results in a decreased level of total saturated fatty acids. *Plant Biotechnol. J.* **1**, 221–229.

Yeats, T. H. and Rose, J. K. C. (2013). The Formation and Function of Plant Cuticles. *Plant Physiol.* **163**, 5–20.

Yuan, J. and Kessler, S. A. (2019). A genome-wide association study reveals a novel regulator of ovule number and fertility in Arabidopsis thaliana. *PLOS Genet.* **15**, e1007934.

Zuñiga-Mayo, V. M., Baños-Bayardo, C. R., Díaz-Ramírez, D., Marsch-Martínez, N. and De Folter, S. (2018). Conserved and novel responses to cytokinin treatments during flower and fruit development in Brassica napus and Arabidopsis thaliana. *Sci. Rep.* **8**, 1–10.

Zúñiga-Mayo, V. M., Gómez-Felipe, A., Herrera-Ubaldo, H. and De Folter, S. (2019). Gynoecium development: Networks in Arabidopsis and beyond. *J. Exp.*

Bot. **70**, 1447–1460.

Zurcher, E., Tavor-Deslex, D., Lituiev, D., Enkerli, K., Tarr, P. T. and Muller, B. (2013). A Robust and Sensitive Synthetic Sensor to Monitor the Transcriptional Output of the Cytokinin Signaling Network in Planta. *Plant Physiol.* **161**, 1066–1075.

APPENDIX

In the research article, where I am coauthor, which title is "New role of NO TRANSMITTING TRACT and SEEDSTICK during medial domain development in *Arabidopsis* fruits" published in 2019 by the Company of Biologists Ltd *Development*, my contribute was in particular related to the characterization of non-fertilized ovules, total number of seeds and silique length analysis of the single mutants *stk* and *ntt* and the double mutant *ntt stk* when compared to wild type fruits (see Fig.3 A, B and G, H of attached manuscript 1). I also analysed the phenotypes of the single insertional mutant line of the gene At3g26140 (glycosyl hydrolase) which results are described in the Figure S5 of attached manuscript 1. Moreover, I have done the ChIP-qPCR assay to test the region used by the two transcription factors STK and NTT to bind the gene targets that play roles in transmitting tract development, using the marker-lines *pSTK::STK-GFP* and *gNTT-n2YPET*. Finally, I contributed to the writing of the manuscript.

© 2019. Published by The Company of Biologists Ltd | Development (2019) 146, dev172395. doi:10.1242/dev.172395

RESEARCH ARTICLE

New roles of NO TRANSMITTING TRACT and SEEDSTICK during medial domain development in *Arabidopsis* fruits

Humberto Herrera-Ubaldo[1], Paulina Lozano-Sotomayor[1,*], Ignacio Ezquer[2], Maurizio Di Marzo[2], Ricardo Aarón Chávez Montes[1], Andrea Gómez-Felipe[1], Jeanneth Pablo-Villa[1], David Diaz-Ramirez[3], Patricia Ballester[4], Cristina Ferrándiz[4], Martin Sagasser[5], Lucia Colombo[2], Nayelli Marsch-Martínez[3] and Stefan de Folter[1,‡]

ABSTRACT

The gynoecium, the female reproductive part of the flower, is key for plant sexual reproduction. During its development, inner tissues such as the septum and the transmitting tract tissue, important for pollen germination and guidance, are formed. In *Arabidopsis*, several transcription factors are known to be involved in the development of these tissues. One of them is NO TRANSMITTING TRACT (NTT), essential for transmitting tract formation. We found that the NTT protein can interact with several gynoecium-related transcription factors, including several MADS-box proteins, such as SEEDSTICK (STK), known to specify ovule identity. Evidence suggests that NTT and STK control enzyme and transporter-encoding genes involved in cell wall polysaccharide and lipid distribution in gynoecial medial domain cells. The results indicate that the simultaneous loss of NTT and STK activity affects polysaccharide and lipid deposition and septum fusion, and delays entry of septum cells to their normal degradation program. Furthermore, we identified *KAWAK*, a direct target of NTT and STK, which is required for the correct formation of fruits in *Arabidopsis*. These findings position NTT and STK as important factors in determining reproductive competence.

KEY WORDS: NO TRANSMITTING TRACT, SEEDSTICK, Fruit, Gynoecium, Medial domain, Septum, Cell wall, Lipids, Polysaccharide, KAWAK

INTRODUCTION

A large part of our food comes from floral parts, fruits and seeds. Therefore, a deep understanding of the regulatory networks guiding the developmental processes of these structures and tissues is important. Flowering species mostly give rise to the pistil, or so-called gynoecium, in the center of the flower. The gynoecium, from a biological point of view, is essential for plant reproduction. In general, at the apical end it has a stigma to facilitate pollen capture and germination, and the stigma is connected via the style to the ovary where the ovules will be formed. The transmitting tract facilitates pollen tube growth through the style and the ovary, and, upon fertilization inside each ovule, seed development starts. The gynoecium is now called a fruit, which increases rapidly in size owing to hormones produced by the seeds (Roeder and Yanofsky, 2006; Alvarez-Buylla et al., 2010; Ferrándiz et al., 2010; Sotelo-Silveira et al., 2013; Marsch-Martínez and de Folter, 2016).

In *Arabidopsis*, the correct formation of the medial domain in the gynoecium is a key process for female reproductive competence and seed formation. This domain includes placental tissues and ovules, and the structures that capture the pollen grains and guide pollen tubes to reach the ovules and, therefore, facilitate fertilization. These structures and tissues, including stigma, style, septum and transmitting tract, are also known as the marginal tissues (Fig. 1A). These tissues arise from the carpel margin meristem (CMM) (Bowman et al., 1999; Alvarez and Smyth, 2002; Nole-Wilson et al., 2010; Wynn et al., 2011; Reyes-Olalde et al., 2013), a meristematic tissue that emerges as two internal ridges (termed medial ridges) in the young gynoecium (Fig. 1A), which fuse together when they reach each other in the middle of the gynoecium, thereby forming the septum. This postgenital fusion occurs at stage 9 of gynoecium development (Bowman et al., 1999; Roeder and Yanofsky, 2006). Ovule primordia can be seen at stage 9 (Bowman et al., 1999; Roeder and Yanofsky, 2006; Reyes-Olalde et al., 2013). At stage 11, the gynoecium fully closes and the stigma is then fully developed. During stage 12, the style and the transmitting tract differentiate, and at stage 13 the gynoecium is fully mature (Smyth et al., 1990; Bowman et al., 1999; Roeder and Yanofsky, 2006; Reyes-Olalde et al., 2013).

Over 80 genes have been identified as regulators of medial domain development, mainly participating at stages 9 to 11 (Reyes-Olalde et al., 2013). For instance, in the case of the postgenital fusion of the medial ridges, the basic helix-loop-helix (bHLH) gene *SPATULA* (*SPT*) has been found to be an important player (Alvarez and Smyth, 1999, 2002; Heisler et al., 2001; Reyes-Olalde et al., 2017). The formation of the stigma and style is controlled by *NGATHA* (*NGA*), *STYLISH* (*STY*) and *HECATE* (*HEC*) genes (Gremski et al., 2007; Alvarez et al., 2009; Trigueros et al., 2009). *SEEDSTICK* (*STK*) directs ovule specification, funiculus development, and seed abscission (Favaro et al., 2003; Pinyopich et al., 2003; Balanzà et al., 2016). Fertilization is a key process for sexual reproduction, and an important point in this process is that the pollen tubes can reach the ovules. The synergid cells, in the embryo sac inside the ovule, produce signals to attract the pollen tube (Mizuta and Higashiyama, 2018). For pollen tubes

[1]Unidad de Genómica Avanzada (LANGEBIO), Centro de Investigación y de Estudios Avanzados del Instituto Politécnico Nacional (CINVESTAV-IPN), Irapuato 36824, Guanajuato, México. [2]Dipartimento di Bioscienze, Università degli Studi di Milano, Milan 20133, Italy. [3]Departamento de Biotecnología y Bioquímica, Unidad Irapuato, CINVESTAV-IPN, Irapuato 36824, Guanajuato, México. [4]Instituto de Biología Molecular y Celular de Plantas, CSIC-UPV Universidad Politécnica de Valencia, 46022, Spain. [5]Bielefeld University, Faculty of Biology, Chair of Genetics and Genomics of Plants, Bielefeld 33615, Germany.
*Present address: Departamento de Química, División de Ciencias Naturales y Exactas, Universidad de Guanajuato, Guanajuato, México.

‡Author for correspondence (stefan.defolter@cinvestav.mx)

H.H., 0000-0002-5408-4022; P.L., 0000-0002-3933-0002; I.E., 0000-0003-1886-0095; M.D., 0000-0001-9045-8370; J.P., 0000-0003-3134-5901; N.M., 0000-0001-9522-0062; S.d.F., 0000-0003-4363-7274

Received 2 October 2018; Accepted 3 December 2018

Development (2019) 146, dev172395. doi:10.1242/dev.172395

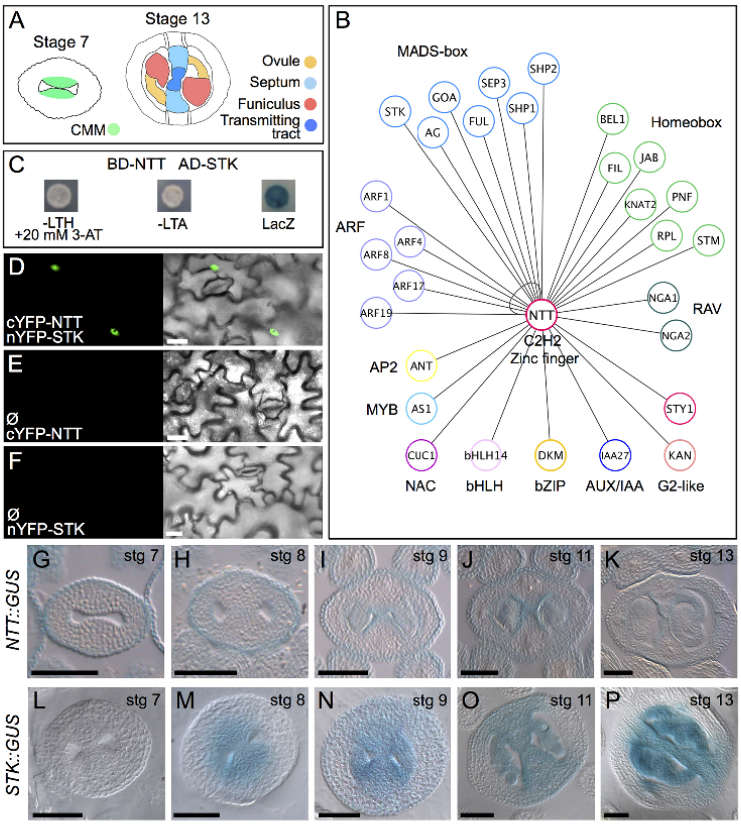

Fig. 1. NTT and STK physically interact and are co-expressed in the gynoecium medial domain. (A) Schematic of the medial domain in stage 7 and 13 gynoecium; the CMM gives rise to all medial tissues present at stage 13: septum, transmitting tract, funiculus and ovules. (B) NTT protein interactions (lines represent interactions) based on a Y2H assay. (C) Y2H assay of the NTT-STK combination for the three reporter genes, showing positive results. (D-F) BiFC assay in tobacco leaves for *STK-NTT* (D) and negative controls with empty vectors (E,F). (G-P) *NTT::GUS* (G-K) and *STK::GUS* (L-P) in transverse gynoecia sections at different stages. Scale bars: 20 µm in D-F; 50 µm in G-P.

to reach the ovules, cell wall modifications have to take place (Crawford and Yanofsky, 2008; Dresselhaus and Franklin-Tong, 2013). On the female side, these modifications take place when the transmitting tract forms. Cells in this tissue produce an extracellular matrix (ECM) containing glycoproteins, glycolipids and polysaccharides that facilitates pollen tube growth (Lennon et al., 1998; Crawford and Yanofsky, 2008). A genetic pathway controlling transmitting tract formation includes the three redundant bHLH *HEC* transcription factors (Gremski et al., 2007), the *HALF FILLED* (*HAF*) gene (also known as *CESTA*, *CES*), which acts redundantly with the closely related *BRASSINOSTEROID ENHANCED EXPRESSION 1* (*BEE1*) and *BEE3* genes (Crawford and Yanofsky, 2011), and the zinc-finger transcription factor *NO TRANSMITTING TRACT* (*NTT*), which controls this process in the ovary but not in the style (Crawford and Yanofsky, 2011). All these genes contribute to ECM production and programmed cell death (Crawford et al., 2007; Crawford and Yanofsky, 2011). Furthermore, other genes expressed in the style and transmitting tract encode enzymes that modify cell walls (Dresselhaus and Franklin-Tong, 2013), e.g. beta-1,3-glucanases (Delp and Palva, 1999). On the male side, growing pollen tubes secrete cell wall-degrading enzymes that help pollen tubes on their way through the pistil (Mollet et al., 2013; Hepler et al., 2013), e.g. the pectin methylesterase *VANGUARD1* (*VGD1*) (Jiang et al., 2005).

The NTT transcription factor, besides its role in transmitting tract formation, is also important for root meristem development (Crawford et al., 2015), and during fruit development NTT is involved in valve margin formation (Chung et al., 2013) and replum development (Marsch-Martínez et al., 2014). In the latter report, we detected protein-protein interactions between NTT and other fruit-related transcription factors, including some MADS-box proteins such as SHATTERPROOF1 (SHP1) and SHP2.

The MADS-box transcription factor STK has been well-characterized in ovule and funiculus development, and is involved in ovule identity determination together with SHP1 and SHP2 (Colombo et al., 1995; Favaro et al., 2003; Pinyopich et al., 2003). Furthermore, it has been shown that STK participates in seed development by controlling secondary metabolism (Mizzotti et al., 2012, 2014), cell wall properties (Ezquer et al., 2016) and seed abscission (Balanzà et al., 2016). Here, we report NTT protein interaction with STK and describe novel roles for NTT and STK during medial domain development, further demonstrating that they are important for the reproductive competence of *Arabidopsis* plants. Our results indicate that NTT and STK are involved in the control of early events of gynoecium development, such as septum fusion, septum cell integrity, impact fertilization efficiency and seed-set, and affect senescence after fertilization. They control genes involved in carbohydrate metabolism and lipid distribution in septum cell walls.

Development (2019) 146, dev172395. doi:10.1242/dev.172395

RESULTS

The NTT and STK proteins interact

We recently reported that the transcription factor NO TRANSMITTING TRACT (NTT) promotes replum development, and that it interacts in the yeast two-hybrid (Y2H) system with proteins related to fruit development such as FRUITFULL (FUL), REPLUMLESS (RPL), SHP1, SHP2 and SHOOT MERISTEMLESS (STM) (Marsch-Martínez et al., 2014). We expanded this interaction survey with a uni-directional Y2H screen (see Materials and Methods) and found that NTT was able to interact with an additional 24 transcription factors (Fig. 1B; Table S1), suggesting that NTT fulfils various roles by forming part of different protein complexes. Of particular interest is the fact that NTT interacted with all MADS-box proteins tested.

In this work, we focused on the interaction of NTT with the MADS-box protein SEEDSTICK (STK), which is known to provide the D-function for ovule identity (Favaro et al., 2003; Pinyopich et al., 2003). In the Y2H assay, the combination NTT-STK activated all three reporter genes (*HIS3*, *ADE* and *lacZ*), indicating that these proteins are able to interact (Fig. 1C).

To confirm this Y2H result, a bimolecular fluorescence complementation assay (BiFC; Fig. 1D-F) was performed. For this, NTT was fused to the cYFP and STK fused to nYFP region, and fluorescence from the reconstituted YFP was detected in leaf cells (Fig. 1D), indicating that the two proteins interact *in planta*, confirming the Y2H result. Fluorescence was observed in the nucleus, in agreement with the expected localization of transcription factors.

NTT and *STK* are co-expressed during gynoecium development

The Y2H and BiFC assays suggested that NTT and STK could be interacting during gynoecia development in *Arabidopsis*, as both participate in this process. In order to visualize those regions where these proteins could be acting together, we analyzed transverse thin sections of stage 7 to stage 13 gynoecia of the reporter lines *NTT::GUS* and *STK::GUS* (Kooiker et al., 2005).

Activity of the *NTT* promoter was detected from stage 9 to 13 gynoecia in the medial domain (Fig. 1I-K), as reported before (Crawford et al., 2007; Chung et al., 2013; Marsch-Martínez et al., 2014). The activity of the *STK* promoter was visible in the medial domain from stage 8 till stage 13 gynoecia (Fig. 1M-P). Blue staining was observed in the medial domain in ovule primordia and later in ovules and the septum (Fig. 1N-P), in agreement with previous reports (Kooiker et al., 2005; Losa et al., 2010). In summary, based on the two promoter activity analyses, *NTT* and *STK* are co-expressed during gynoecium development, specifically in medial domain tissues. These results support the possibility of the formation of a dimer or higher-order complex containing NTT and STK in these tissues.

Constitutive expression of *NTT* together with *STK* affects flower development

We showed that NTT can physically interact with STK, and that the genes are co-expressed in the medial domain of the gynoecium. Subsequently, we wanted to explore the biological relevance of this putative NTT-STK protein dimer or complex during *Arabidopsis* flower development. The first approach we took was to generate double constitutive expression plants, assuming that this would increase the accumulation of the NTT-STK protein complex in the plant. For this, we crossed a *35S::NTT* line (Marsch-Martínez et al., 2014) with a *35S::STK* line (Favaro et al., 2003) and we analyzed the F1 generation. Fertility is affected in the single *35S::NTT* line, although this line is still able to produce some seeds (Marsch-Martínez et al., 2014). The *35S::STK* line flowers early with respect to wild type and develops small flowers with reduced fertility (Favaro et al., 2003). Interestingly, in double constitutive *35S::NTT 35S::STK* plants, reproductive development was severely affected (Fig. S1), and the phenotypic alterations were stronger with respect to those observed in the single constitutive expression lines. In general, plants were very small, and when the first flowers reached around floral stage 10, an arrest of floral development was observed and flowers began to senesce. The formed flowers were male and female sterile and, as a consequence, we never observed fruit development, in contrast to the two single constitutive expression lines (Fig. S1). These results show that increased levels of the possible NTT-STK complex can severely affect flower development, suggesting that they may work together in the plant.

The *ntt stk* double mutant is affected in gynoecium medial domain development

To understand better the biological role of the NTT-STK interaction, and to unravel new putative roles for these transcription factors, we generated an *ntt stk* double mutant. Fruits of the double mutant presented some phenotypes that were a combination of those observed in the single mutants, such as smaller fruits, fewer seeds, no transmitting tract, larger funiculi, irregular seed spacing, lack of seed abscission and reduced seed size (Fig. 2A-D; Fig. 3A,B,G,H) (Pinyopich et al., 2003; Crawford et al., 2007). Interestingly, new phenotypes were observed in the *ntt stk* double mutant, all related to septum development. First, septum fusion defects were observed in 16% of the fruits (n=360), a phenotype never observed in either single mutant (*ntt* n=106, *stk* n=121), nor in wild-type fruits (n=49) (Fig. 2A-E). These septum fusion defects were observed as holes (up to three holes) in the septum of a fruit. In the most severe cases, the septum fusion defects could be seen along 60% of the length of the fruit (Fig. 2E). Furthermore, alteration in septum fusion was also observed at stage 14 as a longitudinal division line (furrow) in the middle of the septum, which corresponds to the place where the two septum primordia meet and normally fuse during wild-type gynoecium development (Fig. 2F,G). This latter phenotype was observed in most of the *ntt stk* fruits.

A second phenotype observed was related to the aspect of septum cells. When the septum of stage 14 fruits was inspected using scanning electron microscopy (SEM), septum cell integrity in *ntt stk* fruits appeared to be preserved (Fig. 2G,I). In contrast, septum cells in wild-type fruits at the same stage presented signs of degeneration and collapse (Fig. 2F,H).

As septum development continues, at stage 15, generalized degradation and holes can be observed in the medial domain of wild-type, *ntt* and *stk* single mutant fruits (Fig. 2J-L). Strikingly, in the *ntt stk* double mutant no cell degradation in this region was observed (Fig. 2M). This lack of septum cell degradation was still visible at late stages of fruit development: at stages 17-18 the integrity of septum cells was still maintained (Fig. 2N,O). Also, the imperfect septum fusion was still visible (Fig. 2O), which probably corresponds to the division line observed in Fig. 2G.

The third phenotype that we noticed was the alteration in septum thickness. In wild-type, *ntt*, and *stk* single mutant gynoecia at anthesis (stage 13), septum thickness is around six to seven cells (n=5). At this stage, septa from *ntt stk* double mutant gynoecia presented no difference in the number of cells. Note, however, that pollen tube growth is affected in *ntt stk* gynoecia, as discussed in the next paragraph (Fig. S2). However, at stage 17-18, septa thickness in

Development (2019) 146, dev172395. doi:10.1242/dev.172395

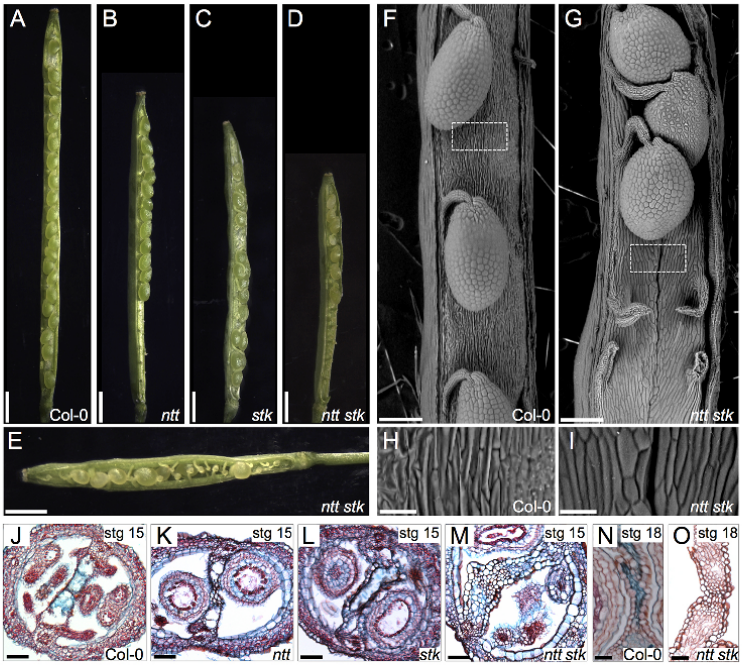

Fig. 2. The *ntt stk* double mutant is affected in gynoecium medial domain development. (A-E) Images of Col-0 (A), *ntt* (B), *stk* (C) and *ntt stk* (D,E) fruits, showing affected seed-set and septum development. (F-I) Scanning electron microscopy images of Col-0 (F,H), and *ntt stk* (G,I) fruits and septum. H and I are magnifications of the boxed areas in F and G, respectively. (J-O) Alcian Blue- and Neutral Red-stained transverse sections of Col-0 (J), *ntt* (K), *stk* (L) and *ntt stk* (M) stage 15 fruits, and Col-0 (N) and *ntt stk* (O) stage 17 septa. Scale bars: 1 mm in A-E; 200 µm in F,G; 50 µm in H-M; 25 µm in N,O.

ntt stk fruits increased to ten cells (Fig. 2O). In summary, these results suggest that the simultaneous loss of NTT and STK activity leads to altered septum fusion and delays entry of septum cells to their normal degradation program.

Pollen tube growth and seed-set are affected in the *ntt stk* double mutant

The observed septum defects in the *ntt stk* double mutant could account for the reduced seed-set and fruit length (Fig. 3). Reduction in seed-set and fruit length has previously been observed for the *ntt* single mutant (Crawford et al., 2007). For the *stk* single mutant, a reduction in fruit length has been reported (Pinyopich et al., 2003) as well as a slight reduction in seed-set (Mizzotti et al., 2012). The transmitting tract differentiates at stage 12 and it is functional at the mature gynoecium stage when anthesis occurs (stage 13). In the *ntt* mutant, no transmitting tract is formed (Fig. 2K) and seed-set is only observed in the apical part of the fruit, owing to reduced pollen tube growth (Crawford et al., 2007). In the *stk* mutant, Alcian Blue staining of gynoecia suggests that transmitting tract formation is not affected, and the pattern of seed-distribution is similar to wild type (Fig. 2C,L; Fig. S2).

We tested whether the absence of transmitting tract and the absence of dead cells in the septum caused by the *ntt stk* double mutation could further affect pollen tube growth through the ovary. Therefore, we monitored pollen tube movement in *ntt stk* gynoecia using Aniline Blue staining. As expected, we observed pollen tubes that reached the ovules along the wild-type and *stk* ovaries (Fig. 3C,E). By contrast, as reported before, in the *ntt* mutant, pollen tube growth was mainly observed in the apical part of the ovary (40-50% of total ovary length; Fig. 3D). In the *ntt stk* double mutant, pollen tube growth was further affected, and observed only in the upper 20% of total ovary length (Fig. 3F).

Our results suggest that NTT and STK together impact cell degradation in the septum and, as a consequence, affect the transmitting tract, fertilization efficiency and final seed-set.

A co-expression network links *NTT* and *STK* to their putative transcriptional targets

To gain further insight into the biological processes controlled by NTT and STK, we generated an ARACNE-based co-expression network of flowers for both transcription factors (see Materials and Methods). Connections in this network indicate transcriptional correlation between genes. Three gene groups could be identified: those connected to *NTT*, those connected to *STK*, and those genes connected to both *NTT* and *STK*. The complete list of genes in the network is presented in Table S2 and illustrated in Fig. S7. We focused on the third group (genes connected to both *NTT* and *STK*), which we called the core network (Fig. 4A). Interestingly, in the core network two transcription factors belonging to the REPRODUCTIVE MERISTEM (REM) family are present, *REM11* and *REM13*, which are known to be expressed in the developing gynoecium, specifically in the CMM and ovules (Wynn et al., 2011; Mendes et al., 2016), and the transcription factor *HAF*, known to be involved in transmitting tract development (Crawford and Yanofsky, 2011). Recently, *REM11* (also known as *VALKYRIE*) already has been shown to be a direct target of STK (Mendes et al., 2016), providing evidence that supports this co-expression network. Furthermore, in the core network four enzyme and transporter-encoding genes are present: *AT1G28710* (a nucleotide-diphospho-sugar transferase family gene), *AT3G26140* (a family 5, subfamily 11 glycosyl hydrolase), *AT3G21090* (ABC transporter G family member 15, *ABCG15*) and *AT1G06080* (delta-9 acyl-lipid desaturase 1, *ADS1*), related to polysaccharide metabolism or membrane lipid transport and synthesis (Kang et al., 2011; Li-Beisson et al., 2013).

Development (2019) 146, dev172395. doi:10.1242/dev.172395

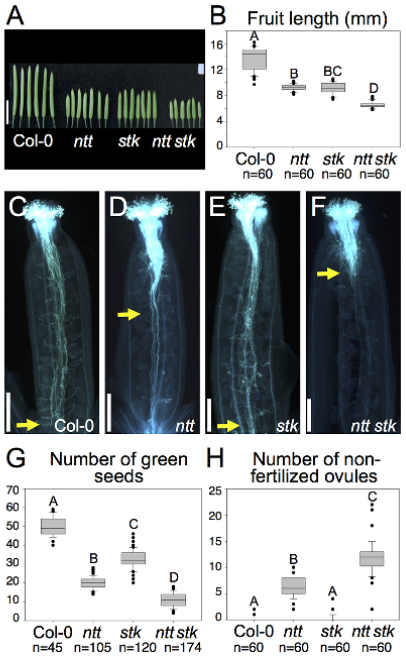

Fig. 3. Seed-set is affected in the *ntt stk* double mutant. (A,B) Overview of Col-0, *ntt*, *stk* and *ntt stk* fruits and length analysis (B). (C-F) Aniline Blue staining of Col-0 (C), *ntt* (D), *stk* (E) and *ntt stk* (F) pollen tubes in stage 13 gynoecia. Pollen tubes are visible as cyan filamentous structures. Yellow arrows indicate the location up to where pollen tube growth is observed. (G,H) Green seed number (G) and non-fertilized ovules (H) in Col-0, *ntt*, *stk* and *ntt stk* fruits. Boxes indicate first quartile (Q1), median, third quartile (Q3); whiskers indicate minimum and maximum; dots represent outliers. Statistical analyses were performed using an ANOVA followed by Tukey HSD tests. Letters indicate statistically different groups (P<0.01). Scale bars: 0.5 cm in A; 200 µm in C-F.

In co-expression networks, the connection between two nodes may indicate a possible direct regulation when transcription factors are involved (Serin et al., 2016; van Dam et al., 2017). NTT and STK are both transcription factors, so they might directly regulate the expression of the core genes. A consensus binding site for NTT is not known, so we used the DNA-binding site predictor for C2H2 zinc finger proteins (Persikov and Singh, 2013). For MADS-box proteins the consensus binding site is well-known and is called the CArG-box (de Folter and Angenent, 2006). We analyzed whether putative binding sites for NTT and STK were present in promoter or intron sequences of the core network genes. Interestingly, the regulatory regions of all core network genes have putative binding sites (Fig. 4B).

NTT and STK are regulators of cell wall and lipid metabolism genes

To confirm experimentally the putative transcriptional regulation of the core network genes by NTT and STK, and to understand better the biochemical processes through which NTT and STK exert their effect in the tissues, we obtained experimental evidence for their regulation of the genes coding for enzymes and a transporter involved in cell wall polysaccharide and lipid metabolism (Fig. 4). Interestingly, recently it has been shown that STK is involved in cell

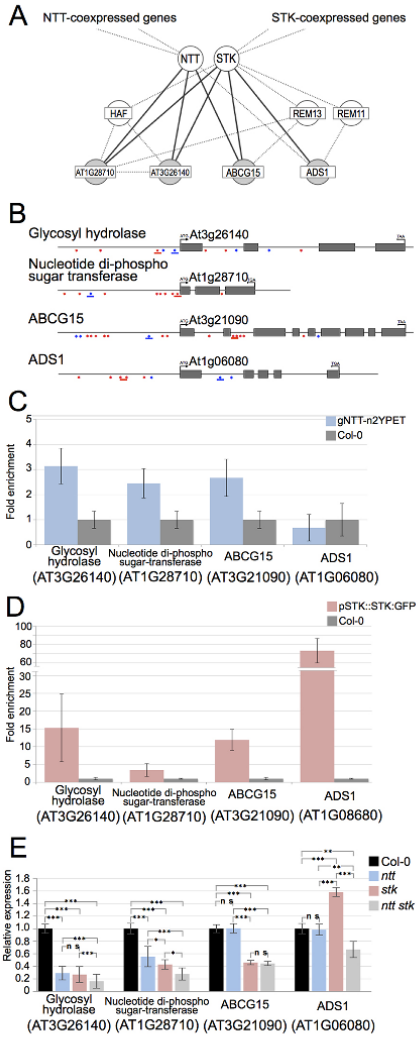

Fig. 4. *NTT* and *STK* are co-expressed with cell wall and lipid metabolism enzyme and transporter-encoding genes. (A) *NTT-STK* core co-expression network. Nodes represent genes and edges represent co-expression. White nodes are transcription factors and gray nodes represent enzyme- and transporter-encoding genes. Dotted lines represent co-expression and solid lines represent possible direct regulation based on ChIP experiments. (B) Schematic of the four enzyme- and transporter-encoding genes present in the core network; arrows indicate the translation start site; gray boxes represent exons; red asterisks indicate CArG-boxes and blue diamonds indicate predicted NTT-binding sites (TCWNAGS); lines under the asterisks/diamonds indicate regions selected for ChIP enrichment tests. (C) ChIP-qPCR results of regulatory regions (blue lines in B) using a *gNTT-n2YPET* line versus wild type. (D) ChIP-qPCR results of CArG-box-containing regulatory regions (red lines in B) using a *STK::STK:GFP* line versus wild type. A representative experiment is shown. Error bars represent the s.d. of three technical replicates. (E) qRT-PCR results of the enzyme-coding genes present in the core network in Col-0, *ntt*, *stk* and *ntt stk* gynoecia. Error bars represent the s.d. of three biological replicates. Statistical analyses were performed using a Tukey test: *P<0.05, **P<0.01, ***P<0.001. n.s., not significant.

Development (2019) 146, dev172395. doi:10.1242/dev.172395

wall architecture of the seed (Ezquer et al., 2016). First, we performed chromatin immunoprecipitation (ChIP) assays using an anti-GFP antibody on wild-type, *STK::STK:GFP* and *gNTT-n2YPET* inflorescence tissue, followed by qPCR analysis (Fig. 4C,D). Compared with wild type, ChIP-qPCR results from the *STK::STK:GFP* line showed a significant enrichment of promoter/intron regions for all four genes tested (Fig. 4D). ChIP-qPCR results from the *gNTT-n2YPET* line showed a significant enrichment of promoter regions for three genes (Fig. 4C). No enrichment was observed for *ADS1*, although we cannot exclude the possibility of NTT binding to other sites.

We then reasoned that if NTT and/or STK are transcriptional regulators of the genes present in the core network their expression should be altered in the *ntt*, *stk* and *ntt stk* mutant backgrounds. We analyzed the expression of the four enzyme- and transporter-encoding genes present in the core co-expression network using qRT-PCR (Fig. 4E). The expression of all four genes was reduced in the *ntt stk* double mutant gynoecia, compared with the wild-type sample (Fig. 4B). The *AT3G26140* and *AT1G28710* genes presented a roughly similar reduction in expression levels in the single and double mutants, which suggests that these genes could be under the control of an NTT- and STK-containing protein complex, such that single disruption of *NTT* or *STK* is enough to impact the regulatory effect of the complex. Note that we could still detect some expression in the double mutant, suggesting they are regulated by more genes. On the other hand, we could not detect a difference in expression level of *ABCG15* and *ADS1* in whole inflorescence tissue tested in the *ntt* single mutant background. Furthermore, *ADS1* expression was slightly increased in the *stk* single mutant. Nevertheless, ChIP and expression analyses support a role for NTT and STK as regulators of the genes present in the core co-expression network.

One of the genes present in the core network, *AT3G26140*, encodes a glycosyl hydrolase (GH5_11). The GH5 *Arabidopsis* enzymes that have been biochemically characterized are all mannan endo-beta-1,4-mannosidases (mannanase; E.C. 3.2.1.78), which are involved in cell wall remodeling. Although no biochemical evidence is available for GH5_11 enzymes (Aspeborg et al., 2012), it is possible that *AT3G26140* could also encode a mannanase involved in septum development, in particular the deposition or remodeling of the transmitting tract polysaccharide matrix. We therefore decided to explore further the role of *AT3G26140* in developing gynoecia. For this, we performed *in situ* hybridization for *AT3G26140* in wild-type, *ntt*, *stk* and *ntt stk* genetic backgrounds (Fig. 5A-H; Fig. S4). In wild-type gynoecia, signal was detected from early developmental stages in the CMM, in septa, funiculi and ovules (Fig. 5A,E). In the *ntt* and *stk* single mutants, comparable expression patterns were observed (Fig. 5B,C, F,G), although this is not reflected by the qRT-PCR results on whole inflorescence tissue, suggesting that there is tissue-dependent regulation. However, and in accordance to the qRT-PCR results, in the *ntt stk* double mutant only a weak signal was detected

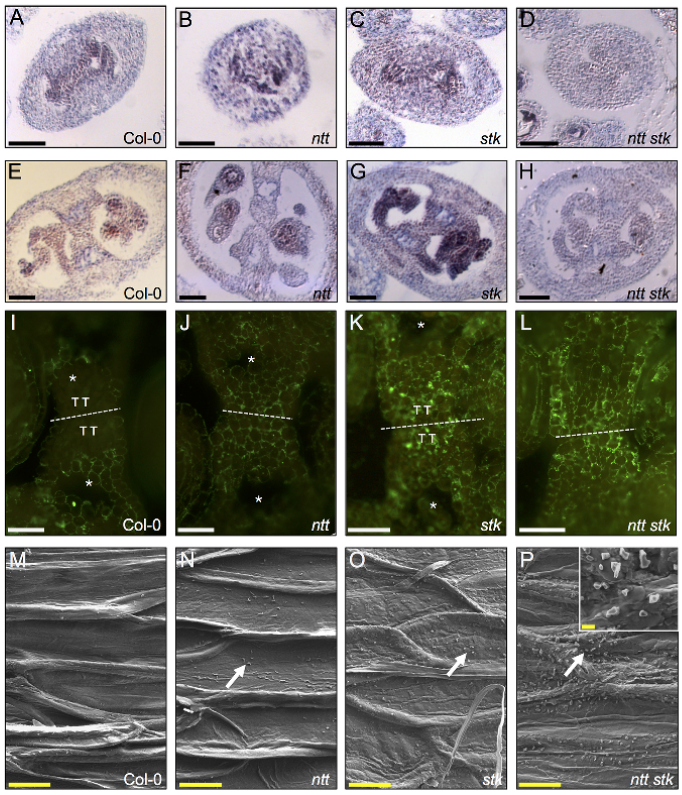

Fig. 5. NTT and STK control polysaccharide distribution and lipid metabolism in septum cells. (A-H) *In situ* hybridization of *AT3G26140* mRNA in Col-0 (A,E), *ntt* (B,F), *stk* (C,G) and *ntt stk* (D,H) in stage 8-9 (A-D) and stage 12 (E-H) gynoecia. (I-L) Immunolabeling of mannan polysaccharides in Col-0 (I), *ntt* (J), *stk* (K) and *ntt stk* (L) septa of stage 12 gynoecia; the septum fusion zone is indicated with a white dashed line; TT indicates the transmitting tract (only present in wild type and *stk*); asterisks indicate cell degradation zones. (M-P) SEM images showing wax deposition on the septum epidermis of mature fruits of Col-0 (M), *ntt* (N), *stk* (O) and *ntt stk* (P); the inset in P shows a 10,000× magnification of wax granules; arrows indicate wax deposition. Scale bars: 50 µm in A-H; 20 µm in I-L; 10 µm in M-P; 1 µm in P, inset.

Development (2019) 146, dev172395. doi:10.1242/dev.172395

(Fig. 5D,H). This indicates that *AT3G26140* is regulated by NTT and STK and suggests that this enzyme participates in cell wall metabolism in the cells of medial domain tissues.

Mannan and lipid deposition are altered in *ntt stk* septum cells

We observed a low *AT3G26140* mRNA signal by *in situ* hybridization in gynoecia of the *ntt stk* double mutant (Fig. 5), and we wondered if this could be translated into an altered mannan content in septum cell walls. We analyzed mannan polysaccharides distribution in septum cells during gynoecium development by immunofluorescence using the LM21 antibody, which recognizes mannan, glucomannan and galactomannan polysaccharides (Marcus et al., 2010). Significant labeling was detected in septum cell walls, but almost no signal was detected in cells of the transmitting tract of wild-type gynoecia (Fig. 5I). In the *ntt* mutant, which lacks transmitting tract tissue, a low but detectable mannan signal was present throughout the septum, as expected (Fig. 5J). Surprisingly, in the *stk* single mutant signal was detected in the septum, but also in the transmitting tract tissue, suggesting that transmitting tract cells in the *stk* mutant have an altered cell wall polysaccharide composition (Fig. 5K). In the *ntt stk* double mutant, which as in the *ntt* mutant also lacks transmitting tract tissue, a continuous signal was observed throughout the gynoecium (Fig. 5L). These results suggest that NTT and STK are both necessary for the correct expression of the putative mannanase-encoding gene *AT3G26140* in the medial domain.

The presence of lipid-related genes in the core co-expression network also prompted us to look for possible lipid deposition defects in *ntt stk* septum cells. Using SEM we observed the presence of wax granules on the septum epidermis cells of mature (stage 19-20) fruits (Fig. 5M-P). These wax granules were scarce on wild-type septum cells, but clearly visible in the *ntt* or *stk* single mutants (Fig. 5N,O, arrows). In the *ntt stk* double mutant a larger number of wax granules was observed (Fig. 5P).

Mutations in *ABCG15* (*KAWAK*) severely affect gynoecium development

In order to study the individual contribution of the enzyme and transporter-encoding genes to the *ntt stk* phenotype, we analyzed T-DNA insertion lines for two NTT-STK target genes (Fig. 4). For the putative mannanase-encoding gene *AT3G26140*, a statistically significant reduction in seed-set and fruit length was detected (Fig. S5). The mild phenotype could be explained by functional redundancy among cell wall regulators.

For *ABCG15*, we obtained two mutant alleles that showed dramatic and pleiotropic phenotypes, probably related to altered meristematic activity (Fig. 6; Fig. S6). We named this transporter KAWAK (KWK), which comes from Mayan mythology. It is the name of one of the 20 months of the Mayan calendar, and it means 'storm' and also 'monster with two heads'. In these *kwk* mutant plants, shoot apical meristem (SAM) maintenance was reduced or even absent (Fig. 6A; Fig. S6). The loss of the apical dominance caused growth of secondary shoots. Defects were also observed in inflorescence and floral meristems, causing altered floral bud positioning and number, and alterations in floral organ arrangement (Fig. 6; Fig. S6). Furthermore, we observed floral organ fusion defects, unfused carpels and septa, ectopic formation of ovules and

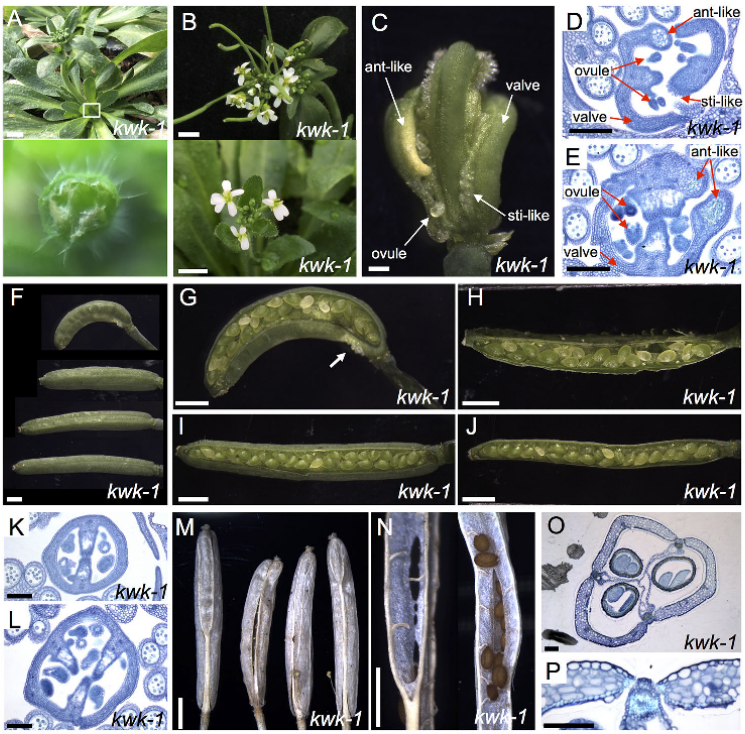

Fig. 6. The *kwk* mutant is affected in meristematic activity and reproduction. (A) Defects in SAM maintenance can lead to meristem arrest and loss of apical dominance (lower panel is a magnification of the boxed area in A). (B) Inflorescences with abnormal phyllotaxis and flowers with defects in organ number. (C) Gynoecium with fusion defects and growth abnormalities. (D,E) Transverse sections of Toluidine Blue-stained gynoecia; anther-like (ant-like) or stigma-like (sti-like) tissues are visible. (F) Overview of the shape of *kwk-1* fruits. (G-J) Internal view of fruits showing defects in seed formation and septum fusion. (K,L) Transverse sections of fruits with two or three valves. (M,N) External (M) and internal (N) views of mature fruits. (O) Transverse section of a mature fruit with three valves. (P) Toluidine Blue staining reveals that fruit lignification and dehiscence is normal in *kwk-1*. Scale bars: 5 mm in A,B; 200 µm in C; 100 µm in D,E,K,L,O,P; 2 mm in F-J,M,N.

Development (2019) 146, dev172395. doi:10.1242/dev.172395

stigmatic tissue or repla. Fruits developed from less-affected gynoecia presented alterations in carpel number, and all fruits had alterations in seed formation and seed arrangement, the latter probably due to funiculi alterations (Fig. 6F-P; Fig. S6). These results highlight the importance of ABCG15 (KAWAK) during *Arabidopsis* development, making it an interesting target of NTT and STK to study further in future work.

DISCUSSION

Multiple roles have been reported for the NTT transcription factor during gynoecium development, including transmitting tract formation (Crawford et al., 2007), replum development (Marsch-Martínez et al., 2014) and valve margin specification (Chung et al., 2013). We identified that NTT interacts with a large number of transcription factors belonging to different families, suggesting that NTT participates in many protein complexes during development, possibly performing different, as yet unknown, functions.

In this work, we focused on the interaction with STK, a MADS-box protein that determines ovule identity, correct funiculus development, seed abscission (Pinyopich et al., 2003; Balanzà et al., 2016) and regulation of seed development (Mizzotti et al., 2014; Ezquer et al., 2016). MADS-box transcription factors are able to interact with each other and form functional protein complexes that guide flower development (Honma and Goto, 2001; de Folter et al., 2005; Immink et al., 2009). For STK, protein-interaction partners important for ovule and seed development, such as AG, SEPALLATA3 (SEP3) and ARABIDOPSIS B SISTER (ABS), have been reported (de Folter et al., 2005; Kaufmann et al., 2005; de Folter et al., 2006; Mizzotti et al., 2012). In general, MADS-box proteins interact with MADS family members, and few interactions with members of other transcription factor families have been described to date (Smaczniak et al., 2012; Bemer et al., 2017). Interestingly, we found that NTT, a zinc finger transcription factor, interacts with various MADS-box proteins such as AG, SHP1, SHP2 and STK, which are all paralogs (Marsch-Martínez et al., 2014; this work). Based on the data presented in this work, we suggest that NTT and STK can work cooperatively during gynoecial medial domain development in *Arabidopsis*.

Co-expression network to identify target genes

One of the current challenges in understanding the regulation of flower development is the identification of transcriptional targets of key transcription factors (Wellmer et al., 2014). In order to identify possible target genes of NTT and STK, we generated an ARACNE-based co-expression network, which uses microarray expression data and infers putative transcriptional interactions (Margolin et al., 2006a) (Fig. 4A). Networks inferred using this method are a useful tool in the understanding of biological processes (Yu et al., 2011; Chávez Montes et al., 2014; González-Morales et al., 2016).

Interestingly, by searching in the current literature, we found that many of the inferred interactions in the *NTT-STK* co-expression network are supported by several reports, indicating that these interactions are biologically relevant. There are examples of functional interactions between *STK* and *SHP2* (Pinyopich et al., 2003; Brambilla et al., 2007) and, in some cases, of direct transcriptional regulation, for instance STK to *VERDANDI* (Matias-Hernandez et al., 2010), *BANYULS* (Mizzotti et al., 2014), and *REM11* (Mendes et al., 2016). These genes are present in the *NTT-STK* co-expression network (Table S1). For NTT, a transcriptional relationship with *HAF* has been reported (Crawford and Yanofsky, 2011), which is also connected in the network to *STK*. Besides *HAF*, *REM11* and *REM13* are also connected to *NTT* and *STK* in the network, and they are expressed in young gynoecia in the CMM (Wynn et al., 2011; Mantegazza et al., 2014), which supports a role for *NTT* and *STK* in early gynoecium development. Beyond transcription factors, four enzyme and transporter-encoding genes are co-expressed with *NTT* and *STK* (Fig. 4). These enzymes and transporter could provide clues about the biochemical processes regulated by NTT and STK.

ChIP experiments indicated binding of STK to CArG-box-containing regions in the promoters/introns of all four genes, and binding of NTT to putative C2H2 zinc finger protein-binding sites of at least three genes, suggesting that they could be direct STK/NTT targets. Moreover, qRT-PCR experiments showed reduced expression of all four enzyme-encoding genes in the *ntt stk* double mutant; however, this was not the case for all of the single mutants, possibly due to redundancy. But, in general, the results suggest that these enzyme- and transporter-encoding genes are targeted by NTT and/or STK (Fig. 4).

The first enzyme (AT3G26140) we found belongs to the GH5 family for which (1-4)-beta-mannan endohydrolase and cellulase activities have been identified for some members (Aspeborg et al., 2012). The second enzyme is a nucleotide-diphospho-sugar transferase (AT1G28710), a glycosyltransferase involved in the synthesis of polysaccharides. Based on the CAZy database, it belongs to the GT77 family for which α-xylosyltransferase (EC 2.4.2.39), α-1,3-galactosyltransferase (EC 2.4.1.37) and arabinosyltransferase (EC 2.4.2.-) activities have been reported (Lombard et al., 2014). The third enzyme, ADS1 (AT1G06080), has been characterized as a functional fatty acid desaturase (Yao et al., 2003; Heilmann et al., 2004) and is expressed in flowers (Fukuchi-Mizutani et al., 1998). Heterologous expression of this enzyme in *Brassica juncea* generated decreased levels of total saturated fatty acid in seeds and altered the normal fatty acid profile (Yao et al., 2003). The last gene is ABCG15 (AT3G21090), an ATP-binding cassette (ABC) transporter, which we named KAWAK (KWK; discussed below). Members of this ABCG group are required for lipid deposition and cutin formation (Kang et al., 2011). ABCG15 is phylogenetically close to ABCG12 (also known as CER5), which is required for wax transport to the cuticle (Pighin et al., 2004), and it is also close to ABCG13, which is involved in the transport of cuticular lipids in flowers (Panikashvili et al., 2011), and to ABCG11 (also known as DSO), which is involved in cuticular lipid export (Bird et al., 2007; Luo et al., 2007; Panikashvili et al., 2007; Ukitsu et al., 2007).

So, the four genes found are related to cell wall polysaccharide metabolism or membrane lipid synthesis and transport. Our findings suggest that these two processes are altered in septum cells of the *ntt stk* mutant. We have recently shown that global changes in cell wall composition take place during gynoecium development (Herrera-Ubaldo and de Folter, 2018), for instance mannan polysaccharide content decreases when the gynoecium matures. Here, mannan polysaccharide content in mutant and wild-type gynoecia was analyzed; an evident alteration in mannan accumulation was observed in the medial region of the single and double mutants, suggesting that the reduction in expression of the mannanase gene *AT3G26140* observed by *in situ* hybridization and qRT-PCR could be related to the increase in mannan accumulation. Reduced fertility is to be expected when this enzyme is affected, which we did indeed observe in a T-DNA insertional mutant for *AT3G26140* (Fig. S5). The subtle reduction in fertility observed is probably due to the involvement of other redundant proteins or additional enzymes. This was recently shown for silique dehiscence zone formation, where various cell wall-modifying enzymes participate, such as

Development (2019) 146, dev172395. doi:10.1242/dev.172395

ARABIDOPSIS DEHISCENCE ZONE POLYGARACTURONASE 1 (ADPG1), ADPG2, CELLULASE 6 (CEL6) and MANNANASE 7 (MAN7) (Ogawa et al., 2009; He et al., 2018). On the other hand, the altered wax deposition in septum cells is a sign of altered lipid metabolism or transport. Alterations in these processes could explain the phenotypes observed in the *ntt stk* double mutant.

Septum fusion and cuticle formation

Defects in septum fusion were observed in the *ntt stk* double mutant. However, these defects are different to those observed in, for example, the *spt* mutant, which has a reduced cell number in the CMM and reduced growth of the septa primordia (Alvarez and Smyth, 1999, 2002; Heisler et al., 2001). Cell number in the CMM in the *ntt stk* mutant is similar to that observed in wild type, and septa primordia grow normally and encounter each other to form the septum. This suggests that the observed fusion abnormalities (Fig. 2) are not related to defects in early growth, but might be related to epidermal defects, such as altered cuticle, which is a specialized lipidic modification of the cell wall (Yeats and Rose, 2013). Cuticle seems to be involved in cell-to-cell communication (Tanaka and Machida, 2007), and alterations in cuticle formation cause organ fusion defects (Nawrath, 2006).

The correct formation and composition of the cuticle is important for flower development, as it promotes carpel fusions and prevents ectopic or organ fusions (Lolle and Cheung, 1993; Panikashvili et al., 2010). Mutants such as *fiddlehead* and *hothead* have floral organ fusion defects caused by altered cuticle formation (Lolle et al., 1998; Yephremov et al., 1999; Pruitt et al., 2000; Krolikowski et al., 2003). Interestingly, a mutation in the epidermis-expressed ABCG11 transporter (related to ABCG15) affects organ fusion due to altered epicuticular wax on the surface of organs (Luo et al., 2007; Panikashvili et al., 2010). We also observed altered wax deposition on the septum surface of the *ntt stk* double mutant, which could be related to its septum fusion defects. Furthermore, the expression of *ABCG15* was clearly reduced in the double mutant and regulatory regions of *ABCG15* were enriched in ChIP assays for STK and NTT (Fig. 4). Interestingly, we identified *kwk* mutants that showed dramatic phenotypes in meristem development and during reproductive development. Alterations in the ABCG15 transporter function could lead to impaired lipid export and altered cuticle formation. It could also affect membrane structure or block the correct position of membrane proteins. The *kwk* mutant might be helpful in understanding the role of plant surface lipids and epidermis development, and the role of the epidermis in developmental processes (e.g. Delude et al., 2016; Verger et al., 2018).

Cell integrity and senescence

Modifications of the cell wall and cell death are important processes during the formation of the transmitting tract and its ECM that allow for pollen tube growth through the ovary, and therefore directly affect fertilization efficiency and seed-set (Crawford et al., 2007; Crawford and Yanofsky, 2008). The *ntt* mutant lacks a transmitting tract, as indicated by the lack of acidic polysaccharide staining. However, cell degradation does take place in the septum, observed as irregular-shaped, degraded cells and empty spaces (Crawford et al., 2007; Fig. 2). These tissues appear normal in the *stk* mutant. The *ntt stk* double mutant, however, lacks cell degradation in the septum. Moreover, the double mutation produces a clear increase in severity of pollen tube growth through the gynoecium. Whereas pollen tube growth is reduced in the single *ntt* mutant, and does not appear to be affected in the *stk* mutant, it is severely reduced in the *ntt stk* double mutant.

Part of the altered cell degradation phenotype could be related to the observed lack of mannanase expression in the medial domain of young *ntt stk* gynoecia. Furthermore, the nucleotide-diphospho-sugar transferase might be involved in the synthesis of any of the polysaccharides, glycoproteins or glycolipids of the ECM, suggested to provide nutrients and adhesion for correct pollen tube growth (Crawford and Yanofsky, 2008).

Taken together, the data presented indicate that NTT and STK have clear roles in septum fusion and the modification of cell walls, affecting fertilization efficiency and seed-set.

Another important process for which cell wall modifications play a role is during fruit ripening, which is followed by senescence (Gapper et al., 2013; Gómez et al., 2014). Our work also hints that senescence is induced by *NTT* and *STK* (Fig. S1). Note that we observed already some induced senescence and cell death by *NTT* alone, and this could be due to interactions with other proteins, possibly with other related MADS-box proteins (Fig. S3). Though arguably a bit preliminary, this suggests that NTT, enhanced by STK, can promote senescence and induce cell death and, thereby, might regulate fruit maturation. Research in tomato has demonstrated that MADS-box proteins control fruit ripening (Karlova et al., 2014). *RIPENING INHIBITOR* (*RIN*), a homolog of the *Arabidopsis* SEP genes (Vrebalov et al., 2002), regulates the expression of genes involved in cell wall modifications, such as polygaracturonase and B-galactosidase, in addition to proteins controlling shelf life (A-expansin) and fruit softening (B-mannanase) (Fujisawa et al., 2011). The latter is dramatically downregulated in fruit ripening-defective tomato plants (Fujisawa et al., 2014; Shima et al., 2014). Other MADS-box genes involved in tomato fruit ripening are homologs of the *AG* clade (Itkin et al., 2009; Vrebalov et al., 2009; Pan et al., 2010) and *FUL* homologs (Bemer et al., 2012). In addition, some zinc finger proteins are also involved in fruit ripening, such as SlZFP2 (Rohrmann et al., 2011; Weng et al., 2015) and MaC2H2-1/2 (Han et al., 2016).

In summary, we found that NTT and STK control genes coding for enzymes and transporters involved in synthesis and degradation of cell wall polysaccharides, and synthesis and transport of fatty acids. It would be particularly interesting to know whether homologous genes could perform similar activities in other fruits, especially those important for food and industry.

MATERIALS AND METHODS

Plant material and growth

Arabidopsis thaliana plants were germinated in soil (3:1:1, peat moss: perlite:vermiculite) in a growth chamber under long-day conditions (16 h light, 22°C; 8 h dark, 20°C) for 10 days and transferred to standard greenhouse conditions (22-27°C, natural light). The following mutants and lines were used in this work: the transposon insertion line *ntt-3* is the NASC line N104422 (SM_3.16705) in Col (Tissier et al., 1999); *stk-2* (Pinyopich et al., 2003); *STK::GUS* (Kooiker et al., 2005); *35S::STK* (Favaro et al., 2003); *35S::NTT* (Marsch-Martínez et al., 2014); *gNTT-n2YPET* (Crawford et al., 2015); *kwk-1* is the line GT_5_99063 in L*er* (T-DNA in the third exon); *kwk-2* is SALKseq_125172 in Col-0 (T-DNA in the third exon); insertion line for *AT3G26140* is SALK_128093 (T-DNA in the third intron); *Nicotiana benthamiana* and *Nicotiana tabacum* were used for cell death assays and BiFC, respectively.

NTT::GUS construct

For the *NTT* promoter::GUS fusion, a 1216 bp DNA sequence upstream of the predicted translation start was amplified by PCR from genomic Col-0 DNA, using Pwo DNA polymerase (Roche) and primers S314 and S318 (Table S3). The PCR product was cloned in front of the GUS ORF of the binary vector pANGUS [a derivative of pPAM (GenBank AY027531) described by Stracke et al., 2007] using the restriction endonucleases

Development (2019) 146, dev172395. doi:10.1242/dev.172395

ARABIDOPSIS DEHISCENCE ZONE POLYGARACTURONASE 1 (ADPG1), ADPG2, CELLULASE 6 (CEL6) and MANNANASE 7 (MAN7) (Ogawa et al., 2009; He et al., 2018). On the other hand, the altered wax deposition in septum cells is a sign of altered lipid metabolism or transport. Alterations in these processes could explain the phenotypes observed in the *ntt stk* double mutant.

Septum fusion and cuticle formation

Defects in septum fusion were observed in the *ntt stk* double mutant. However, these defects are different to those observed in, for example, the *spt* mutant, which has a reduced cell number in the CMM and reduced growth of the septa primordia (Alvarez and Smyth, 1999, 2002; Heisler et al., 2001). Cell number in the CMM in the *ntt stk* mutant is similar to that observed in wild type, and septa primordia grow normally and encounter each other to form the septum. This suggests that the observed fusion abnormalities (Fig. 2) are not related to defects in early growth, but might be related to epidermal defects, such as altered cuticle, which is a specialized lipidic modification of the cell wall (Yeats and Rose, 2013). Cuticle seems to be involved in cell-to-cell communication (Tanaka and Machida, 2007), and alterations in cuticle formation cause organ fusion defects (Nawrath, 2006).

The correct formation and composition of the cuticle is important for flower development, as it promotes carpel fusions and prevents ectopic or organ fusions (Lolle and Cheung, 1993; Panikashvili et al., 2010). Mutants such as *fiddlehead* and *hothead* have floral organ fusion defects caused by altered cuticle formation (Lolle et al., 1998; Yephremov et al., 1999; Pruitt et al., 2000; Krolikowski et al., 2003). Interestingly, a mutation in the epidermis-expressed ABCG11 transporter (related to ABCG15) affects organ fusion due to altered epicuticular wax on the surface of organs (Luo et al., 2007; Panikashvili et al., 2010). We also observed altered wax deposition on the septum surface of the *ntt stk* double mutant, which could be related to its septum fusion defects. Furthermore, the expression of *ABCG15* was clearly reduced in the double mutant and regulatory regions of *ABCG15* were enriched in ChIP assays for STK and NTT (Fig. 4). Interestingly, we identified *kwk* mutants that showed dramatic phenotypes in meristem development and during reproductive development. Alterations in the ABCG15 transporter function could lead to impaired lipid export and altered cuticle formation. It could also affect membrane structure or block the correct position of membrane proteins. The *kwk* mutant might be helpful in understanding the role of plant surface lipids and epidermis development, and the role of the epidermis in developmental processes (e.g. Delude et al., 2016; Verger et al., 2018).

Cell integrity and senescence

Modifications of the cell wall and cell death are important processes during the formation of the transmitting tract and its ECM that allow for pollen tube growth through the ovary, and therefore directly affect fertilization efficiency and seed-set (Crawford et al., 2007; Crawford and Yanofsky, 2008). The *ntt* mutant lacks a transmitting tract, as indicated by the lack of acidic polysaccharide staining. However, cell degradation does take place in the septum, observed as irregular-shaped, degraded cells and empty spaces (Crawford et al., 2007; Fig. 2). These tissues appear normal in the *stk* mutant. The *ntt stk* double mutant, however, lacks cell degradation in the septum. Moreover, the double mutation produces a clear increase in severity of pollen tube growth through the gynoecium. Whereas pollen tube growth is reduced in the single *ntt* mutant, and does not appear to be affected in the *stk* mutant, it is severely reduced in the *ntt stk* double mutant.

Part of the altered cell degradation phenotype could be related to the observed lack of mannanase expression in the medial domain of young *ntt stk* gynoecia. Furthermore, the nucleotide-diphospho-sugar transferase might be involved in the synthesis of any of the polysaccharides, glycoproteins or glycolipids of the ECM, suggested to provide nutrients and adhesion for correct pollen tube growth (Crawford and Yanofsky, 2008).

Taken together, the data presented indicate that NTT and STK have clear roles in septum fusion and the modification of cell walls, affecting fertilization efficiency and seed-set.

Another important process for which cell wall modifications play a role is during fruit ripening, which is followed by senescence (Gapper et al., 2013; Gómez et al., 2014). Our work also hints that senescence is induced by *NTT* and *STK* (Fig. S1). Note that we observed already some induced senescence and cell death by *NTT* alone, and this could be due to interactions with other proteins, possibly with other related MADS-box proteins (Fig. S3). Though arguably a bit preliminary, this suggests that NTT, enhanced by STK, can promote senescence and induce cell death and, thereby, might regulate fruit maturation. Research in tomato has demonstrated that MADS-box proteins control fruit ripening (Karlova et al., 2014). *RIPENING INHIBITOR* (*RIN*), a homolog of the *Arabidopsis* SEP genes (Vrebalov et al., 2002), regulates the expression of genes involved in cell wall modifications, such as polygaracturonase and B-galactosidase, in addition to proteins controlling shelf life (A-expansin) and fruit softening (B-mannanase) (Fujisawa et al., 2011). The latter is dramatically downregulated in fruit ripening-defective tomato plants (Fujisawa et al., 2014; Shima et al., 2014). Other MADS-box genes involved in tomato fruit ripening are homologs of the *AG* clade (Itkin et al., 2009; Vrebalov et al., 2009; Pan et al., 2010) and *FUL* homologs (Bemer et al., 2012). In addition, some zinc finger proteins are also involved in fruit ripening, such as SlZFP2 (Rohrmann et al., 2011; Weng et al., 2015) and MaC2H2-1/2 (Han et al., 2016).

In summary, we found that NTT and STK control genes coding for enzymes and transporters involved in synthesis and degradation of cell wall polysaccharides, and synthesis and transport of fatty acids. It would be particularly interesting to know whether homologous genes could perform similar activities in other fruits, especially those important for food and industry.

MATERIALS AND METHODS

Plant material and growth

Arabidopsis thaliana plants were germinated in soil (3:1:1, peat moss: perlite:vermiculite) in a growth chamber under long-day conditions (16 h light, 22°C; 8 h dark, 20°C) for 10 days and transferred to standard greenhouse conditions (22-27°C, natural light). The following mutants and lines were used in this work: the transposon insertion line *ntt-3* is the NASC line N104422 (SM_3.16705) in Col (Tissier et al., 1999); *stk-2* (Pinyopich et al., 2003); *STK::GUS* (Kooiker et al., 2005); *35S::STK* (Favaro et al., 2003); *35S::NTT* (Marsch-Martínez et al., 2014); *gNTT-n2YPET* (Crawford et al., 2015); *kwk-1* is the line GT_5_99063 in L*er* (T-DNA in the third exon); *kwk-2* is SALKseq_125172 in Col-0 (T-DNA in the third exon); insertion line for *AT3G26140* is SALK_128093 (T-DNA in the third intron); *Nicotiana benthamiana* and *Nicotiana tabacum* were used for cell death assays and BiFC, respectively.

NTT::GUS construct

For the *NTT* promoter::GUS fusion, a 1216 bp DNA sequence upstream of the predicted translation start was amplified by PCR from genomic Col-0 DNA, using Pwo DNA polymerase (Roche) and primers S314 and S318 (Table S3). The PCR product was cloned in front of the GUS ORF of the binary vector pANGUS [a derivative of pPAM (GenBank AY027531) described by Stracke et al., 2007] using the restriction endonucleases

Development (2019) 146, dev172395. doi:10.1242/dev.172395

*Cla*I and *Nco*I. *A. thaliana* Col-0 was transformed by floral dip (Clough and Bent, 1998).

Y2H assay

Y2H assays were performed using the GAL4 system (pDEST22 and pDEST32; Invitrogen) as previously described (de Folter et al., 2005; de Folter and Immink, 2011). NTT-BD cloning and yeast autoactivation test was previously described (Marsch-Martínez et al., 2014). The STK-AD clone was derived from recombining the *STK* Gateway ENTRY clone from the EU-REGIA project (Paz-Ares and The REGIA Consortium, 2002) with the pDEST22 vector (Castrillo et al., 2011). We used the yeast strain PJ69-4 mating type A and α (James et al., 1996). The uni-directional Y2H screen with 45 selected AD clones has been described before (Zúñiga-Mayo et al., 2012; Marsch-Martínez et al., 2014; Lozano-Sotomayor et al., 2016), but, in short, it contains selected transcription factors from the EU-REGIA project (Paz-Ares and The REGIA Consortium, 2002) that are known to be involved in flower and gynoecium development, and meristem activity (Table S1). Interaction assays were performed on SD-GLUC medium lacking Leu, Trp and Ade, and on medium lacking Leu, Trp and His, supplemented with 20 mM 3-AT. Protein-protein interactions were scored after 5 days of growth at 25°C. Positive results (yeast growth) were confirmed by a *lacZ* assay.

BiFC assay

In planta protein interaction assays were performed as previously described (Marsch-Martínez et al., 2014). The cDNA of *STK* was cloned in pDONR201 (Invitrogen) by the REGIA Consortium (Paz-Ares and The REGIA Consortium, 2002). This clone was recombined with pYFN43 (Belda-Palazón et al., 2012) using an LR Gateway-based reaction to generate N-terminal fusions with the N-terminal part of YFP. NTT entry clone was also recombined with pYFC43 (Belda-Palazón et al., 2012) to generate an N-terminal fusion with the C-terminal part of the YFP protein. The constructs were individually introduced in to *Agrobacterium tumefaciens* GV2260 and cultured on LB supplemented with 100 µg/ml kanamycin and 25 µg/ml rifampicin. Overnight cultures of *Agrobacterium* (O.D.: 1.2-1.6) were collected and re-suspended in a similar volume of infiltration medium (10 mM $MgCl_2$, 10 mM MES pH 5.6, 200 µM acetosyringone), the O.D. was adjusted to 1.0, and the re-suspension was incubated at 25°C during 3 h with weak shaking. Before co-infiltration, *Agrobacterium* containing pYFC43-NTT was mixed with a similar volume of *Agrobacterium* with pYFN43-STK. This mixture was introduced in the abaxial air space of young *Nicotiana tabacum* leaves using a needle-less syringe. YFP fluorescence restoration was assayed 2 days after infiltration using an inverted LSM 510 META confocal laser scanning microscope (Carl Zeiss). YFP was excited using the 488 nm line of an argon laser and emission was filtered using a BP 500-550 nm filter.

Histology and microscopy analyses

For thin tissue section analysis, inflorescences and stage 15, 17-18 fruits of Col-0, *ntt-3*, *stk-2*, and *ntt stk* were collected (according to Smyth et al., 1990), tissue was fixed in FAE solution (3.7% formaldehyde, 5% glacial acetic acid and 50% ethanol) with vacuum (15 min, 4°C) and incubated for 60 min at room temperature. The material was rinsed with 70% ethanol and incubated overnight at 4°C in 70% ethanol, followed by dehydration in a series of ethanol dilutions (70%, 85%, 95% and 100% ethanol) for 60 min each. Inflorescences and stage 17-18 fruits were embedded in Technovit 7100 (Heraeus Kulzer) according to the manufacturer's instructions. Stage 15 fruits were embedded in Paraplast (Sigma-Aldrich) as previously described (Zúñiga-Mayo et al., 2012). Sections (12-15 µm) were obtained on a rotary microtome (Reichert-Jung 2040; Leica). Tissue sections were stained with a solution of 0.5% Alcian Blue and counterstained with 0.5% Neutral Red as previously described (Zúñiga-Mayo et al., 2012), or with Toluidine Blue as previously described (Herrera-Ubaldo and de Folter, 2018). *NTT::GUS* and *STK::GUS* inflorescences were collected and stained as previously described (Marsch-Martínez et al., 2014). The GUS-stained inflorescences were fixed, dehydrated as described above and embedded in Technovit 7100; 12-15 µm sections were analyzed. Pictures were taken using a DM6000B microscope (Leica).

For septum epidermis cell observations, fresh fruit samples were dissected and visualized in an EVO 40 scanning electron microscope (Carl Zeiss), using the VPSE G3 detector, with a 15-20 kV beam and at 50 Pa pressure.

Pollen tube growth within the pistil was monitored with Aniline Blue staining. Pistils were collected 24 h after pollination, and tissue fixation and softening were performed as previously described (Jiang et al., 2005). Pistils were washed with distilled water three times and stained with aniline blue solution (0.01% Aniline Blue in 150 mM K_2HPO_4 buffer, pH 11) for 4 h in the dark. Pistils were observed and imaged with a DM6000B fluorescence microscope under UV light (Leica).

Gene co-expression analysis

A flower co-expression matrix was obtained from microarray data using the ARACNE algorithm (Margolin et al., 2006a,b). Sample data relationship files for ATH1-121501 microarray experiments were downloaded in August 2016 from the ArrayExpress website (http://www.ebi.ac.uk/arrayexpress/; accession numbers E-GEOD-15555, E-GEOD-16056, E-GEOD-2473, E-GEOD-27281, E-GEOD-2848, E-GEOD-30492, E-GEOD-3056, E-GEOD-32193, E-GEOD-40998, E-GEOD-42403, E-GEOD-42841, E-GEOD-46050, E-GEOD-52067, E-GEOD-5526, E-GEOD-55431, E-GEOD-55799, E-GEOD-5632, E-GEOD-66419, E-MEXP-1246, E-MEXP-1592, E-MEXP-1920, E-MEXP-3293, E-MEXP-849 and E-TABM-17) and manually curated to identify 24 experiments that contained 106 high-quality microarray hybridizations for wild-type flower samples. The corresponding CEL files were manually curated and processed as previously described (Chávez Montes et al., 2014; González-Morales et al., 2016), with a single modification: custom CDF version 20 files (http://brainarray.mbni.med.umich.edu/Brainarray/Database/CustomCDF/genomic_curated_CDF.asp; Dai et al., 2005) were used for gcrma normalization. The output of the ARACNE algorithm, which is a mutual information-ranked list of pairs of interactors (i.e. of co-expressed genes), was used to identify genes (both transcription factors and non-transcription factors) co-expressed with *NTT* and *STK*.

ChIP and qPCR

Genomic regions located between the flanking genes in the co-expression network core were analyzed bioinformatically to identify putative CArG-box regions and predicted NTT-binding sites (Persikov and Singh, 2014). ChIP assays were performed as previously described (Ezquer et al., 2016). One gram of unfertilized flowers from Col-0, *STK::STK:GFP* (Mizzotti et al., 2014) and *gNTT-n2YPET* (Crawford et al., 2015) plants were collected. For the immunoprecipitation, we used 2 µl anti-GFP polyclonal antibody per sample (Clontech 632460 for ChIP with STK; Roche 11814460001 for ChIP with NTT). Enrichment of the target regions was calculated by qPCR (iQ_SYBR Green Supermix, Bio-Rad) using a Bio-Rad iCycler iQ optical system. The relative enrichment of the listed targets obtained from *STK*::*STK:GFP* and *pNTT-n2YPET* unfertilized flowers were compared with the enrichment obtained from Col-0 wild-type unfertilized flowers. *ACTIN 7* was used for normalization as previously described (Matias-Hernandez et al., 2010). Primers used for ChIP analysis are listed in Table S3.

qRT-PCR analysis

For the qRT-PCR analysis, gynoecia from stage 7 to 12 were collected under a stereomicroscope (Stemi 2000, Zeiss). Three biological replicates were sampled for each genotype (Col wt, *ntt*, *stk*, *ntt stk*), each containing around 40 gynoecia. Total RNA was extracted using the Quick-RNA MicroPrep Kit (Zymo Research). The samples were treated with DNase I, included in the kit. Reverse transcription and amplification were performed using the KAPA SYBR FAST One-Step qRT-PCR Kit (Kapa Biosystems). The qPCR was performed on a StepOne thermocycler (Applied Biosystems). Target gene expression levels were normalized to *ACTIN 2*. Data were analyzed using the $2^{-\Delta\Delta Ct}$ method (Livak and Schmittgen, 2001). Primers used are listed in Table S3.

In situ hybridization

Inflorescences from Col-0, *ntt*, *stk* and *ntt stk* plants were collected, fixed and embedded in Paraplast as previously described (Sotelo-Silveira et al.,

2013). A DNA fragment corresponding to nucleotides 1176-1368 of the *AT3G26140* coding sequence was amplified using the At3g26140_probe primers (Table S3) and cloned into pGEM-T easy vector (Promega). The sense and antisense RNA probes were synthesized by an *in vitro* transcription reaction using SP6 and T7 polymerase (Invitrogen), respectively. Digoxigenin-labeled RNA probes for detection and hybridization were prepared as previously described (Ambrose et al., 2000).

Mannan immunolabeling

Col-0, *ntt*, *stk* and *ntt stk* inflorescences were fixed overnight at 4°C in 3% paraformaldehyde, 1×PBS 1% pH 7.0. Samples were dehydrated in a series of ethanol dilutions (70%, 85%, 95% and 100% ethanol) and embedded in Technovit 7100 (Heraeus Kulzer) according to the manufacturer's recommendations. Thin sections (14-18 µm) were obtained on a rotary microtome (Reichert-Jung 2040, Leica). Sections were treated with 1 M KOH for 60 min to unmask the manna epitopes (Marcus et al., 2010). Sections were washed three times with wash buffer (2% BSA, 1% PBS pH 7.0) at room temperature before incubation with the LM21 anti-mannan monoclonal antibody (PlantProbes; Marcus et al., 2010) diluted 1:500 in wash buffer for 16 h at 25°C; as described previously (Herrera-Ubaldo and de Folter, 2018). Samples were washed three times with wash buffer and incubated for 4 h at 25°C with the secondary antibody DyLight 488-conjugated goat anti-rat IgM mu chain (ab98368, Abcam) diluted 1:1000 in wash buffer. Samples were washed twice with wash buffer and mounted in 50% glycerol. Photographs of immunolabeled samples were taken using a DM6000B microscope under UV light (Leica).

Nicotiana leaf cell death assay

Three-week-old *Nicotiana benthamiana* leaves were infiltrated with *Agrobacterium* cells containing vectors for the transient expression of NTT (pC1300intB-35SnosEX, AY560325; Kuijt et al., 2004; Marsch-Martínez et al., 2014) or GFP (pMOG800; Knoester et al., 1998) in infiltration medium (10 mM $MgCl_2$, 10 mM MES pH 5.6, 200 µM acetosyringone). Three different *Agrobacterium* concentrations were used (OD600: 0.2, 0.4 and 0.8). Cell death was monitored with a modified version of the Trypan Blue (TB) staining protocol (Mauch-Mani and Slusarenko, 1994). The TB solution contains: lactic acid:phenol:glycerol: distilled water (1:1:1:1) and Trypan Blue (T-0776, Sigma-Aldrich) in a final concentration of 0.25 mg/ml. Before staining, the TB solution was diluted in 2 volumes of 100% ethanol.

Leaf sections (2 cm diameter) were collected 1, 2 and 3 days after infiltration, boiled in diluted TB solution for 1 min. Samples were de-stained in chloral hydrate solution (8:1:2 w/v/v chloral hydrate:glycerol:water) during 1 h at 65°C, followed by overnight incubation in chloral hydrate solution at 50°C with shaking. The samples were washed with 70% ethanol, mounted in 50% glycerol. Brightfield images were acquired using an Eclipse E-600 microscope with a Digital Sight (DS-Ri1) (Nikon Instruments).

Acknowledgements

We thank lab members and other colleagues for discussions regarding this work. We also thank Karla L. González-Aguilera and Vincent E. Cerbantez-Bueno for lab logistics and technical support. We thank Brian Crawford for *gNTT-n2YPET* seeds and the ABRC and NASC for insertion lines.

Competing interests

The authors declare no competing or financial interests.

Author contributions

Conceptualization: H.H.-U., N.M.-M., S.d.F.; Methodology: H.H.-U., I.E., M.D.M., R.A.C.M., A.G.-F., P.B., M.S.; Validation: H.H.-U.; Formal analysis: H.H.-U.; Investigation: H.H.-U., P.L.-S., I.E., M.D.M., R.A.C.M., A.G.-F., J.P.-V., D.D.-R., P.B., M.S.; Writing - original draft: H.H.-U., S.d.F.; Writing - review & editing: C.F., L.C., N.M.-M., S.d.F.; Supervision: C.F., L.C., N.M.-M., S.d.F.; Project administration: S.d.F.; Funding acquisition: S.d.F.

Funding

This work was supported by the Mexican National Council of Science and Technology (Consejo Nacional de Ciencia y Tecnología, CONACyT; PhD fellowships 243380, 219883 and 254467 to H.H.-U., P.L.-S. and D.D.-R., respectively; grants CB-2012-177739, FC-2015-2/1061 and INFR-2015-253504 to S.d.F., and CB-2015-255069 to N.M.-M.). S.d.F., L.C. and C.F. acknowledge the support of the European Union H2020 Marie Skłodowska-Curie Actions RISE-2015 project ExpoSEED (grant 691109). I.E. acknowledges the International European Fellowship-METMADS project (FP7 People: Marie-Curie Actions; 302606) and the Università degli Studi di Milano (RTD-A; 2016).

Data availability

Sequence and data from the genes studied in this article can be found in the Arabidopsis Genome Initiative database under the following accession numbers: *NTT*, AT3G57670; *STK*, AT4G09960; manannase (glycosyl hydrolase), AT3G26140; nucleotide di-phospho sugar transferase, AT1G28710; *ABCG15*, AT3G21090; *ADS1*, AT1G06080; *REM11*, AT5G60140; *REM13*, AT3G46770; *HAF*, AT1G25330; *ACTIN 7*, AT5G09810; *ACTIN 8*, AT1G49240.

Supplementary information

Supplementary information available online at
http://dev.biologists.org/lookup/doi/10.1242/dev.172395.supplemental

References

Alvarez, J. and Smyth, D. R. (1999). CRABS CLAW and SPATULA, two Arabidopsis genes that control carpel development in parallel with AGAMOUS. *Development* **126**, 2377-2386.

Alvarez, J. and Smyth, D. R. (2002). Crabs claw and Spatula genes regulate growth and pattern formation during gynoecium development in Arabidopsis thaliana. *Int. J. Plant Sci.* **163**, 17-41.

Alvarez, J. P., Goldshmidt, A., Efroni, I., Bowman, J. L. and Eshed, Y. (2009). The NGATHA distal organ development genes are essential for style specification in Arabidopsis. *Plant Cell* **21**, 1373-1393.

Alvarez-Buylla, E. R., Benitez, M., Corvera-Poire, A., Chaos Cador, A., de Folter, S., Gamboa de Buen, A., Garay-Arroyo, A., Garcia-Ponce, B., Jaimes-Miranda, F., Perez-Ruiz, R. V. et al. (2010). Flower development. *Arabidopsis Book* **8**, e0127.

Ambrose, B. A., Lerner, D. R., Ciceri, P., Padilla, C. M., Yanofsky, M. F. and Schmidt, R. J. (2000). Molecular and genetic analyses of the silky1 gene reveal conservation in floral organ specification between eudicots and monocots. *Mol. Cell* **5**, 569-579.

Aspeborg, H., Coutinho, P. M., Wang, Y., Brumer, H., III and Henrissat, B. (2012). Evolution, substrate specificity and subfamily classification of glycoside hydrolase family 5 (GH5). *BMC Evol. Biol.* **12**, 186.

Balanzà, V., Roig-Villanova, I., Di Marzo, M., Masiero, S. and Colombo, L. (2016). Seed abscission and fruit dehiscence required for seed dispersal rely on similar genetic networks. *Development* **143**, 3372-3381.

Belda-Palazón, B., Ruiz, L., Martí, E., Tárraga, S., Tiburcio, A. F., Culiáñez, F., Farràs, R., Carrasco, P. and Ferrando, A. (2012). Aminopropyltransferases involved in polyamine biosynthesis localize preferentially in the nucleus of plant cells. *PLoS ONE* **7**, e46907.

Bemer, M., Karlova, R., Ballester, A. R., Tikunov, Y. M., Bovy, A. G., Wolters-Arts, M., Rossetto, P. B., Angenent, G. C. and de Maagd, R. A. (2012). The tomato FRUITFULL homologs TDR4/FUL1 and MBP7/FUL2 regulate ethylene-independent aspects of fruit ripening. *Plant Cell* **24**, 4437-4451.

Bemer, M., van Dijk, A. D. J., Immink, R. G. H. and Angenent, G. C. (2017). Cross-family transcription factor interactions: an additional layer of gene regulation. *Trends Plant Sci.* **22**, 66-80.

Bird, D., Beisson, F., Brigham, A., Shin, J., Greer, S., Jetter, R., Kunst, L., Wu, X., Yephremov, A. and Samuels, L. (2007). Characterization of Arabidopsis ABCG11/WBC11, an ATP binding cassette (ABC) transporter that is required for cuticular lipid secretion. *Plant J.* **52**, 485-498.

Bowman, J. L., Baum, S. F., Eshed, Y., Putterill, J. and Alvarez, J. (1999). Molecular genetics of gynoecium development in Arabidopsis. *Curr. Top. Dev. Biol.* **45**, 155-205.

Brambilla, V., Battaglia, R., Colombo, M., Masiero, S., Bencivenga, S., Kater, M. M. and Colombo, L. (2007). Genetic and molecular interactions between BELL1 and MADS box factors support ovule development in Arabidopsis. *Plant Cell* **19**, 2544-2556.

Castrillo, G., Turck, F., Leveugle, M., Lecharny, A., Carbonero, P., Coupland, G., Paz-Ares, J. and Oñate-Sánchez, L. (2011). Speeding cis-trans regulation discovery by phylogenomic analyses coupled with screenings of an arrayed library of Arabidopsis transcription factors. *PLoS ONE* **6**, e21524.

Chávez Montes, R. A., Coello, G., González-Aguilera, K. L., Marsch-Martínez, N., de Folter, S. and Alvarez-Buylla, E. R. (2014). ARACNe-based inference, using curated microarray data, of Arabidopsis thaliana root transcriptional regulatory networks. *BMC Plant Biol.* **14**, 97.

Chung, K. S., Lee, J. H., Lee, J. S. and Ahn, J. H. (2013). Fruit indehiscence caused by enhanced expression of NO TRANSMITTING TRACT in Arabidopsis thaliana. *Mol. Cells* **35**, 519-525.

Clough, S. J. and Bent, A. F. (1998). Floral dip: a simplified method for *Agrobacterium*-mediated transformation of *Arabidopsis thaliana*. *Plant J.* **16**, 735-743.
Colombo, L., Franken, J., Koetje, E., van Went, J., Dons, H. J., Angenent, G. C. and van Tunen, A. J. (1995). The petunia MADS box gene FBP11 determines ovule identity. *Plant Cell* **7**, 1859-1868.
Crawford, B. C. W. and Yanofsky, M. F. (2008). The formation and function of the female reproductive tract in flowering plants. *Curr. Biol.* **18**, R972-R978.
Crawford, B. C. W. and Yanofsky, M. F. (2011). HALF FILLED promotes reproductive tract development and fertilization efficiency in Arabidopsis thaliana. *Development* **138**, 2999-3009.
Crawford, B. C. W., Ditta, G. and Yanofsky, M. F. (2007). The NTT gene is required for transmitting-tract development in carpels of Arabidopsis thaliana. *Curr. Biol.* **17**, 1101-1108.
Crawford, B. C. W., Sewell, J., Golembeski, G., Roshan, C., Long, J. A. and Yanofsky, M. F. (2015). Genetic control of distal stem cell fate within root and embryonic meristems. *Science* **347**, 655-659.
Dai, M., Wang, P., Boyd, A. D., Kostov, G., Athey, B., Jones, E. G., Bunney, W. E., Myers, R. M., Speed, T. P., Akil, H. et al. (2005). Evolving gene/transcript definitions significantly alter the interpretation of GeneChip data. *Nucleic Acids Res.* **33**, e175.
de Folter, S. and Angenent, G. C. (2006). trans meets cis in MADS science. *Trends Plant Sci.* **11**, 224-231.
de Folter, S. and Immink, R. G. H. (2011). Yeast protein-protein interaction assays and screens. *Methods Mol. Biol.* **754**, 145-165.
de Folter, S., Immink, R. G., Kieffer, M., Parenicova, L., Henz, S. R., Weigel, D., Busscher, M., Kooiker, M., Colombo, L., Kater, M. M. et al. (2005). Comprehensive interaction map of the Arabidopsis MADS box transcription factors. *Plant Cell* **17**, 1424-1433.
de Folter, S., Shchennikova, A. V., Franken, J., Busscher, M., Baskar, R., Grossniklaus, U., Angenent, G. C. and Immink, R. G. H. (2006). A Bsister MADS-box gene involved in ovule and seed development in petunia and Arabidopsis. *Plant J.* **47**, 934-946.
Delp, G. and Palva, E. T. (1999). A novel flower-specific Arabidopsis gene related to both pathogen-induced and developmentally regulated plant beta-1,3-glucanase genes. *Plant Mol. Biol.* **39**, 565-575.
Delude, C., Moussu, S., Joubès, J., Ingram, G. and Domergue, F. (2016). Plant surface lipids and epidermis development. *Subcell. Biochem.* **86**, 287-313.
Dresselhaus, T. and Franklin-Tong, N. (2013). Male-female crosstalk during pollen germination, tube growth and guidance, and double fertilization. *Mol. Plant* **6**, 1018-1036.
Ezquer, I., Mizzotti, C., Nguema-Ona, E., Gotté, M., Beauzamy, L., Viana, V. E., Dubrulle, N., Costa de Oliveira, A., Caporali, E., Koroney, A.-S. et al. (2016). The developmental regulator SEEDSTICK controls structural and mechanical properties of the arabidopsis seed coat. *Plant Cell* **28**, 2478-2492.
Favaro, R., Pinyopich, A., Battaglia, R., Kooiker, M., Borghi, L., Ditta, G., Yanofsky, M. F., Kater, M. M. and Colombo, L. (2003). MADS-box protein complexes control carpel and ovule development in Arabidopsis. *Plant Cell* **15**, 2603-2611.
Ferrándiz, C., Fourquin, C., Prunet, N., Scutt, C. P., Sundberg, E., Trehin, C. and Vialette-Guiraud, A. C. M. (2010). Carpel development. *Adv. Bot. Res.* **55**, 1-73.
Fujisawa, M., Nakano, T. and Ito, Y. (2011). Identification of potential target genes for the tomato fruit-ripening regulator RIN by chromatin immunoprecipitation. *BMC Plant Biol.* **11**, 26.
Fujisawa, M., Shima, Y., Nakagawa, H., Kitagawa, M., Kimbara, J., Nakano, T., Kasumi, T. and Ito, Y. (2014). Transcriptional regulation of fruit ripening by tomato FRUITFULL homologs and associated MADS box proteins. *Plant Cell* **26**, 89-101.
Fukuchi-Mizutani, M., Tasaka, Y., Tanaka, Y., Ashikari, T., Kusumi, T. and Murata, N. (1998). Characterization of delta 9 acyl-lipid desaturase homologues from *Arabidopsis thaliana*. *Plant Cell Physiol.* **39**, 247-253.
Gapper, N. E., McQuinn, R. P. and Giovannoni, J. J. (2013). Molecular and genetic regulation of fruit ripening. *Plant Mol. Biol.* **82**, 575-591.
Gómez, M. D., Vera-Sirera, F. and Pérez-Amador, M. A. (2014). Molecular programme of senescence in dry and fleshy fruits. *J. Exp. Bot.* **65**, 4515-4526.
González-Morales, S. I., Chávez-Montes, R. A., Hayano-Kanashiro, C., Alejo-Jacuinde, G., Rico-Cambron, T. Y., de Folter, S. and Herrera-Estrella, L. (2016). Regulatory network analysis reveals novel regulators of seed desiccation tolerance in Arabidopsis thaliana. *Proc. Natl. Acad. Sci. USA* **113**, E5232-E5241.
Gremski, K., Ditta, G. and Yanofsky, M. F. (2007). The HECATE genes regulate female reproductive tract development in Arabidopsis thaliana. *Development* **134**, 3593-3601.
Han, Y.-C., Fu, C.-C., Kuang, J.-F., Chen, J.-Y. and Lu, W.-J. (2016). Two banana fruit ripening-related C2H2 zinc finger proteins are transcriptional repressors of ethylene biosynthetic genes. *Postharvest Biol. Technol.* **116**, 8-15.
He, H., Bai, M., Tong, P., Hu, Y., Yang, M. and Wu, H. (2018). CELLULASE6 and MANNANASE7 affect cell differentiation and silique dehiscence. *Plant Physiol.* **176**, 2186-2201.
Heilmann, I., Pidkowich, M. S., Girke, T. and Shanklin, J. (2004). Switching desaturase enzyme specificity by alternate subcellular targeting. *Proc. Natl. Acad. Sci. USA* **101**, 10266-10271.
Heisler, M. G., Atkinson, A., Bylstra, Y. H., Walsh, R. and Smyth, D. R. (2001). SPATULA, a gene that controls development of carpel margin tissues in Arabidopsis, encodes a bHLH protein. *Development* **128**, 1089-1098.
Hepler, P. K., Rounds, C. M. and Winship, L. J. (2013). Control of cell wall extensibility during pollen tube growth. *Mol. Plant* **6**, 998-1017.
Herrera-Ubaldo, H. and de Folter, S. (2018). Exploring cell wall composition and modifications during the development of the gynoecium medial domain in Arabidopsis. *Frontier. Plant Sci.* **9**, 454.
Honma, T. and Goto, K. (2001). Complexes of MADS-box proteins are sufficient to convert leaves into floral organs. *Nature* **409**, 525-529.
Immink, R. G. H., Tonaco, I. A. N., de Folter, S., Shchennikova, A., van Dijk, A. D. J., Busscher-Lange, J., Borst, J. W. and Angenent, G. C. (2009). SEPALLATA3: the 'glue' for MADS box transcription factor complex formation. *Genome Biol.* **10**, R24.
Itkin, M., Seybold, H., Breitel, D., Rogachev, I., Meir, S. and Aharoni, A. (2009). TOMATO AGAMOUS-LIKE 1 is a component of the fruit ripening regulatory network. *Plant J.* **60**, 1081-1095.
James, P., Halladay, J. and Craig, E. A. (1996). Genomic libraries and a host strain designed for highly efficient two-hybrid selection in yeast. *Genetics* **144**, 1425-1436.
Jiang, L., Yang, S. L., Xie, L. F., Puah, C. S., Zhang, X. Q., Yang, W. C., Sundaresan, V. and Ye, D. (2005). VANGUARD1 encodes a pectin methylesterase that enhances pollen tube growth in the Arabidopsis style and transmitting tract. *Plant Cell* **17**, 584-596.
Kang, J., Park, J., Choi, H., Burla, B., Kretzschmar, T., Lee, Y. and Martinoia, E. (2011). Plant ABC Transporters. *Arabidopsis Book* **9**, e0153.
Karlova, R., Chapman, N., David, K., Angenent, G. C., Seymour, G. B. and de Maagd, R. A. (2014). Transcriptional control of fleshy fruit development and ripening. *J. Exp. Bot.* **65**, 4527-4541.
Kaufmann, K., Anfang, N., Saedler, H. and Theissen, G. (2005). Mutant analysis, protein-protein interactions and subcellular localization of the Arabidopsis B sister (ABS) protein. *Mol. Genet. Genomics* **274**, 103-118.
Knoester, M., van Loon, L. C., van den Heuvel, J., Hennig, J., Bol, J. F. and Linthorst, H. J. M. (1998). Ethylene-insensitive tobacco lacks nonhost resistance against soil-borne fungi. *Proc. Natl. Acad. Sci. USA* **95**, 1933-1937.
Kooiker, M., Airoldi, C. A., Losa, A., Manzotti, P. S., Finzi, L., Kater, M. M. and Colombo, L. (2005). BASIC PENTACYSTEINE1, a GA binding protein that induces conformational changes in the regulatory region of the homeotic Arabidopsis gene SEEDSTICK. *Plant Cell* **17**, 722-729.
Krolikowski, K. A., Victor, J. L., Wagler, T. N., Lolle, S. J. and Pruitt, R. E. (2003). Isolation and characterization of the Arabidopsis organ fusion gene HOTHEAD. *Plant J.* **35**, 501-511.
Kuijt, S. J. H., Lamers, G. E. M., Rueb, S., Scarpella, E., Ouwerkerk, P. B. F., Spaink, H. P. and Meijer, A. H. (2004). Different subcellular localization and trafficking properties of KNOX class 1 homeodomain proteins from rice. *Plant Mol. Biol.* **55**, 781-796.
Lennon, K. A., Roy, S. E., Hepler, P. K. and Lord, E. M. (1998). The structure of the transmitting tissue of Arabidopsis thaliana (L.) and the path of pollen tube growth. *Sex. Plant Reprod.* **11**, 49-59.
Li-Beisson, Y., Shorrosh, B., Beisson, F., Andersson, M. X., Arondel, V., Bates, P. D., Baud, S., Bird, D., Debono, A., Durrett, T. P. et al. (2013). Acyl-lipid metabolism. *Arabidopsis Book* **11**, e0161.
Livak, K. J. and Schmittgen, T. D. (2001). Analysis of relative gene expression data using real-time quantitative PCR and the 2(−Delta Delta C(T)) Method. *Methods* **25**, 402-408.
Lolle, S. J. and Cheung, A. Y. (1993). Promiscuous germination and growth of wildtype pollen from Arabidopsis and related species on the shoot of the Arabidopsis mutant, fiddlehead. *Dev. Biol.* **155**, 250-258.
Lolle, S. J., Hsu, W. and Pruitt, R. E. (1998). Genetic analysis of organ fusion in Arabidopsis thaliana. *Genetics* **149**, 607-619.
Lombard, V., Golaconda Ramulu, H., Drula, E., Coutinho, P. M. and Henrissat, B. (2014). The carbohydrate-active enzymes database (CAZy) in 2013. *Nucleic Acids Res.* **42**, D490-D495.
Losa, A., Colombo, M., Brambilla, V. and Colombo, L. (2010). Genetic interaction between AINTEGUMENTA (ANT) and the ovule identity genes SEEDSTICK (STK), SHATTERPROOF1 (SHP1) and SHATTERPROOF2 (SHP2). *Sex. Plant Reprod.* **23**, 115-121.
Lozano-Sotomayor, P., Chávez Montes, R. A., Silvestre-Vañó, M., Herrera-Ubaldo, H., Greco, R., Pablo-Villa, J., Galliani, B. M., Diaz-Ramirez, D., Weemen, M., Boutilier, K. et al. (2016). Altered expression of the bZIP transcription factor DRINK ME affects growth and reproductive development in *Arabidopsis thaliana*. *Plant J.* **88**, 437-451.
Luo, B., Xue, X.-Y., Hu, W.-L., Wang, L.-J. and Chen, X.-Y. (2007). An ABC transporter gene of Arabidopsis thaliana, AtWBC11, is involved in cuticle development and prevention of organ fusion. *Plant Cell Physiol.* **48**, 1790-1802.
Mantegazza, O., Gregis, V., Mendes, M. A., Morandini, P., Alves-Ferreira, M., Patreze, C. M., Nardeli, S. M., Kater, M. M. and Colombo, L. (2014). Analysis of the Arabidopsis REM gene family predicts functions during flower development. *Ann. Bot.* **114**, 1507-1515.
Marcus, S. E., Blake, A. W., Benians, T. A. S., Lee, K. J. D., Poyser, C., Donaldson, L., Leroux, O., Rogowski, A., Petersen, H. L., Boraston, A. et al.

(2010). Restricted access of proteins to mannan polysaccharides in intact plant cell walls. *Plant J.* **64**, 191-203.
Margolin, A. A., Nemenman, I., Basso, K., Wiggins, C., Stolovitzky, G., Dalla Favera, R. and Califano, A. (2006a). ARACNE: an algorithm for the reconstruction of gene regulatory networks in a mammalian cellular context. *BMC Bioinformatics* **7** Suppl. 1, S7.
Margolin, A. A., Wang, K., Lim, W. K., Kustagi, M., Nemenman, I. and Califano, A. (2006b). Reverse engineering cellular networks. *Nat. Protoc.* **1**, 662-671.
Marsch-Martínez, N. and de Folter, S. (2016). Hormonal control of the development of the gynoecium. *Curr. Opin. Plant Biol.* **29**, 104-114.
Marsch-Martínez, N., Zúñiga-Mayo, V. M., Herrera-Ubaldo, H., Ouwerkerk, P. B. F., Pablo-Villa, J., Lozano-Sotomayor, P., Greco, R., Ballester, P., Balanzà, V., Kuijt, S. J. H. et al. (2014). The NTT transcription factor promotes replum development in Arabidopsis fruits. *Plant J.* **80**, 69-81.
Matias-Hernandez, L., Battaglia, R., Galbiati, F., Rubes, M., Eichenberger, C., Grossniklaus, U., Kater, M. M. and Colombo, L. (2010). VERDANDI is a direct target of the MADS domain ovule identity complex and affects embryo sac differentiation in Arabidopsis. *Plant Cell* **22**, 1702-1715.
Mauch-Mani, B. and Slusarenko, A. J. (1994). Systemic acquired resistance in Arabidopsis Thaliana induced by a predisposing infection with a pathogenic isolate of fusarium oxysporum. *Mol. Plant-Microbe Interact.* **7**, 378-383.
Mendes, M. A., Guerra, R. F., Castelnovo, B., Silva-Velazquez, Y., Morandini, P., Manrique, S., Baumann, N., Gross-Hardt, R., Dickinson, H. and Colombo, L. (2016). Live and let die: a REM complex promotes fertilization through synergid cell death in Arabidopsis. *Development* **143**, 2780-2790.
Mizuta, Y. and Higashiyama, T. (2018). Chemical signaling for pollen tube guidance at a glance. *J. Cell Sci.* **131**, jcs208447.
Mizzotti, C., Mendes, M. A., Caporali, E., Schnittger, A., Kater, M. M., Battaglia, R. and Colombo, L. (2012). The MADS box genes SEEDSTICK and ARABIDOPSIS Bsister play a maternal role in fertilization and seed development. *Plant J.* **70**, 409-420.
Mizzotti, C., Ezquer, I., Paolo, D., Rueda-Romero, P., Guerra, R. F., Battaglia, R., Rogachev, I., Aharoni, A., Kater, M. M., Caporali, E. et al. (2014). SEEDSTICK is a master regulator of development and metabolism in the arabidopsis seed coat. *PLoS Genet.* **10**, e1004856.
Mollet, J.-C., Leroux, C., Dardelle, F. and Lehner, A. (2013). Cell wall composition, biosynthesis and remodeling during pollen tube growth. *Plants (Basel)* **2**, 107-147.
Nawrath, C. (2006). Unraveling the complex network of cuticular structure and function. *Curr. Opin. Plant Biol.* **9**, 281-287.
Nole-Wilson, S., Azhakanandam, S. and Franks, R. G. (2010). Polar auxin transport together with aintegumenta and revoluta coordinate early Arabidopsis gynoecium development. *Dev. Biol.* **346**, 181-195.
Ogawa, M., Kay, P., Wilson, S. and Swain, S. M. (2009). ARABIDOPSIS DEHISCENCE ZONE POLYGALACTURONASE1 (ADPG1), ADPG2, and QUARTET2 are Polygalacturonases required for cell separation during reproductive development in Arabidopsis. *Plant Cell* **21**, 216-233.
Pan, I. L., McQuinn, R., Giovannoni, J. J. and Irish, V. F. (2010). Functional diversification of AGAMOUS lineage genes in regulating tomato flower and fruit development. *J. Exp. Bot.* **61**, 1795-1806.
Panikashvili, D., Savaldi-Goldstein, S., Mandel, T., Yifhar, T., Franke, R. B., Hofer, R., Schreiber, L., Chory, J. and Aharoni, A. (2007). The Arabidopsis DESPERADO/AtWBC11 transporter is required for cutin and wax secretion. *Plant Physiol.* **145**, 1345-1360.
Panikashvili, D., Shi, J. X., Bocobza, S., Franke, R. B., Schreiber, L. and Aharoni, A. (2010). The arabidopsis DSO/ABCG11 transporter affects cutin metabolism in reproductive organs and suberin in roots. *Mol. Plant* **3**, 563-575.
Panikashvili, D., Shi, J. X., Schreiber, L. and Aharoni, A. (2011). The Arabidopsis ABCG13 transporter is required for flower cuticle secretion and patterning of the petal epidermis. *New Phytol.* **190**, 113-124.
Paz-Ares, J. and The REGIA Consortium. (2002). REGIA, an EU project on functional genomics of transcription factors from Arabidopsis thaliana. *Comp. Funct. Genomics* **3**, 102-108.
Persikov, A. V. and Singh, M. (2014). De novo prediction of DNA-binding specificities for Cys2His2 zinc finger proteins. *Nucleic Acids Res.* **42**, 97-108.
Pighin, J. A., Zheng, H. Q., Balakshin, L. J., Goodman, I. P., Western, T. L., Jetter, R., Kunst, L. and Samuels, A. L. (2004). Plant cuticular lipid export requires an ABC transporter. *Science* **306**, 702-704.
Pinyopich, A., Ditta, G. S., Savidge, B., Liljegren, S. J., Baumann, E., Wisman, E. and Yanofsky, M. F. (2003). Assessing the redundancy of MADS-box genes during carpel and ovule development. *Nature* **424**, 85-88.
Pruitt, R. E., Vielle-Calzada, J.-P., Ploense, S. E., Grossniklaus, U. and Lolle, S. J. (2000). FIDDLEHEAD, a gene required to suppress epidermal cell interactions in Arabidopsis, encodes a putative lipid biosynthetic enzyme. *Proc. Natl. Acad. Sci. USA* **97**, 1311-1316.
Reyes-Olalde, J. I., Zuñiga-Mayo, V. M., Chávez Montes, R. A., Marsch-Martínez, N. and de Folter, S. (2013). Inside the gynoecium: at the carpel margin. *Trends Plant Sci.* **18**, 644-655.
Reyes-Olalde, J. I., Zúñiga-Mayo, V. M., Serwatowska, J., Montes, R. A. C., Lozano-Sotomayor, P., Herrera-Ubaldo, H., Gonzalez-Aguilera, K. L., Ballester, P., Ripoll, J. J., Ezquer, I. et al. (2017). The bHLH transcription factor SPATULA enables cytokinin signaling, and both activate auxin biosynthesis and transport genes at the medial domain of the gynoecium. *PLoS Genet.* **13**, e1006726.
Roeder, A. H. K. and Yanofsky, M. F. (2006). Fruit development in Arabidopsis. *Arabidopsis Book* **4**, e0075.
Rohrmann, J., Tohge, T., Alba, R., Osorio, S., Caldana, C., McQuinn, R., Arvidsson, S., van der Merwe, M. J., Riaño-Pachón, D. M., Mueller-Roeber, B. et al. (2011). Combined transcription factor profiling, microarray analysis and metabolite profiling reveals the transcriptional control of metabolic shifts occurring during tomato fruit development. *Plant J.* **68**, 999-1013.
Serin, E. A. R., Nijveen, H., Hilhorst, H. W. M. and Ligterink, W. (2016). Learning from co-expression networks: possibilities and challenges. *Front. Plant Sci.* **7**, 444.
Shima, Y., Fujisawa, M., Kitagawa, M., Nakano, T., Kimbara, J., Nakamura, N., Shiina, T., Sugiyama, J., Nakamura, T., Kasumi, T. et al. (2014). Tomato FRUITFULL homologs regulate fruit ripening via ethylene biosynthesis. *Biosci. Biotechnol. Biochem.* **78**, 231-237.
Smaczniak, C., Immink, R. G. H., Muino, J. M., Blanvillain, R., Busscher, M., Busscher-Lange, J., Dinh, Q. D., Liu, S., Westphal, A. H., Boeren, S. et al. (2012). Characterization of MADS-domain transcription factor complexes in Arabidopsis flower development. *Proc. Natl. Acad. Sci. USA* **109**, 1560-1565.
Smyth, D. R., Bowman, J. L. and Meyerowitz, E. M. (1990). Early flower development in Arabidopsis. *Plant Cell* **2**, 755-767.
Sotelo-Silveira, M., Cucinotta, M., Chauvin, A.-L., Chavez Montes, R. A., Colombo, L., Marsch-Martinez, N. and de Folter, S. (2013). Cytochrome P450 CYP78A9 is involved in Arabidopsis reproductive development. *Plant Physiol.* **162**, 779-799.
Stracke, R., Ishihara, H., Huep, G., Barsch, A., Mehrtens, F., Niehaus, K. and Weisshaar, B. (2007). Differential regulation of closely related R2R3-MYB transcription factors controls flavonol accumulation in different parts of the Arabidopsis thaliana seedling. *Plant J.* **50**, 660-677.
Tanaka, H. and Machida, Y. (2007). *The Cuticle and Cellular Interactions Annual Plant Reviews Volume 23: Biology of the Plant Cuticle*. Blackwell Publishing Ltd.
Tissier, A. F., Marillonnet, S., Klimyuk, V., Patel, K., Torres, M. A., Murphy, G. and Jones, J. D. (1999). Multiple independent defective suppressor-mutator transposon insertions in Arabidopsis: a tool for functional genomics. *Plant Cell* **11**, 1841-1852.
Trigueros, M., Navarrete-Gomez, M., Sato, S., Christensen, S. K., Pelaz, S., Weigel, D., Yanofsky, M. F. and Ferrandiz, C. (2009). The NGATHA genes direct style development in the Arabidopsis gynoecium. *Plant Cell* **21**, 1394-1409.
Ukitsu, H., Kuromori, T., Toyooka, K., Goto, Y., Matsuoka, K., Sakuradani, E., Shimizu, S., Kamiya, A., Imura, Y., Yuguchi, M. et al. (2007). Cytological and biochemical analysis of COF1, an Arabidopsis mutant of an ABC transporter gene. *Plant Cell Physiol.* **48**, 1524-1533.
van Dam, S., Vosa, U., van der Graaf, A., Franke, L. and de Magalhaes, J. P. (2017). Gene co-expression analysis for functional classification and gene-disease predictions. *Brief. Bioinform.* **19**, 575-592.
Verger, S., Long, Y., Boudaoud, A. and Hamant, O. (2018). A tension-adhesion feedback loop in plant epidermis. *eLife* **7**, e34460.
Vrebalov, J., Ruezinsky, D., Padmanabhan, V., White, R., Medrano, D., Drake, R., Schuch, W. and Giovannoni, J. (2002). A MADS-box gene necessary for fruit ripening at the tomato ripening-inhibitor (rin). locus. *Science* **296**, 343-346.
Vrebalov, J., Pan, I. L., Arroyo, A. J. M., McQuinn, R., Chung, M., Poole, M., Rose, J., Seymour, G., Grandillo, S., Giovannoni, J. et al. (2009). Fleshy fruit expansion and ripening are regulated by the Tomato SHATTERPROOF gene TAGL1. *Plant Cell* **21**, 3041-3062.
Wellmer, F., Bowman, J. L., Davies, B., Ferrándiz, C., Fletcher, J. C., Franks, R. G., Graciet, E., Gregis, V., Ito, T., Jack, T. P. et al. (2014). Flower development: open questions and future directions. In *Flower Development: Methods and Protocols* (ed. J. L. Riechmann and F. Wellmer), pp. 103-124. New York, NY: Springer New York.
Weng, L., Zhao, F., Li, R., Xu, C., Chen, K. and Xiao, H. (2015). The zinc finger transcription factor SlZFP2 negatively regulates abscisic acid biosynthesis and fruit ripening in tomato. *Plant Physiol.* **167**, 931-949.
Wynn, A. N., Rueschhoff, E. E. and Franks, R. G. (2011). Transcriptomic characterization of a synergistic genetic interaction during carpel margin meristem development in Arabidopsis thaliana. *PLoS ONE* **6**, e26231.
Yao, K., Bacchetto, R. G., Lockhart, K. M., Friesen, L. J., Potts, D. A., Covello, P. S. and Taylor, D. C. (2003). Expression of the Arabidopsis ADS1 gene in Brassica juncea results in a decreased level of total saturated fatty acids. *Plant Biotechnol. J.* **1**, 221-229.
Yeats, T. H. and Rose, J. K. C. (2013). The formation and function of plant cuticles. *Plant Physiol.* **163**, 5-20.
Yephremov, A., Wisman, E., Huijser, P., Huijser, C., Wellesen, K. and Saedler, H. (1999). Characterization of the FIDDLEHEAD gene of Arabidopsis reveals a link between adhesion response and cell differentiation in the epidermis. *Plant Cell* **11**, 2187-2201.

Yu, X., Li, L., Zola, J., Aluru, M., Ye, H., Foudree, A., Guo, H., Anderson, S., Aluru, S., Liu, P. et al. (2011). A brassinosteroid transcriptional network revealed by genome-wide identification of BESI target genes in Arabidopsis thaliana. *Plant J.* **65**, 634-646.

Zúñiga-Mayo, V. M., Marsch-Martínez, N. and de Folter, S. (2012). JAIBA, a class-II HD-ZIP transcription factor involved in the regulation of meristematic activity, and important for correct gynoecium and fruit development in Arabidopsis. *Plant J.* **71**, 314-326.

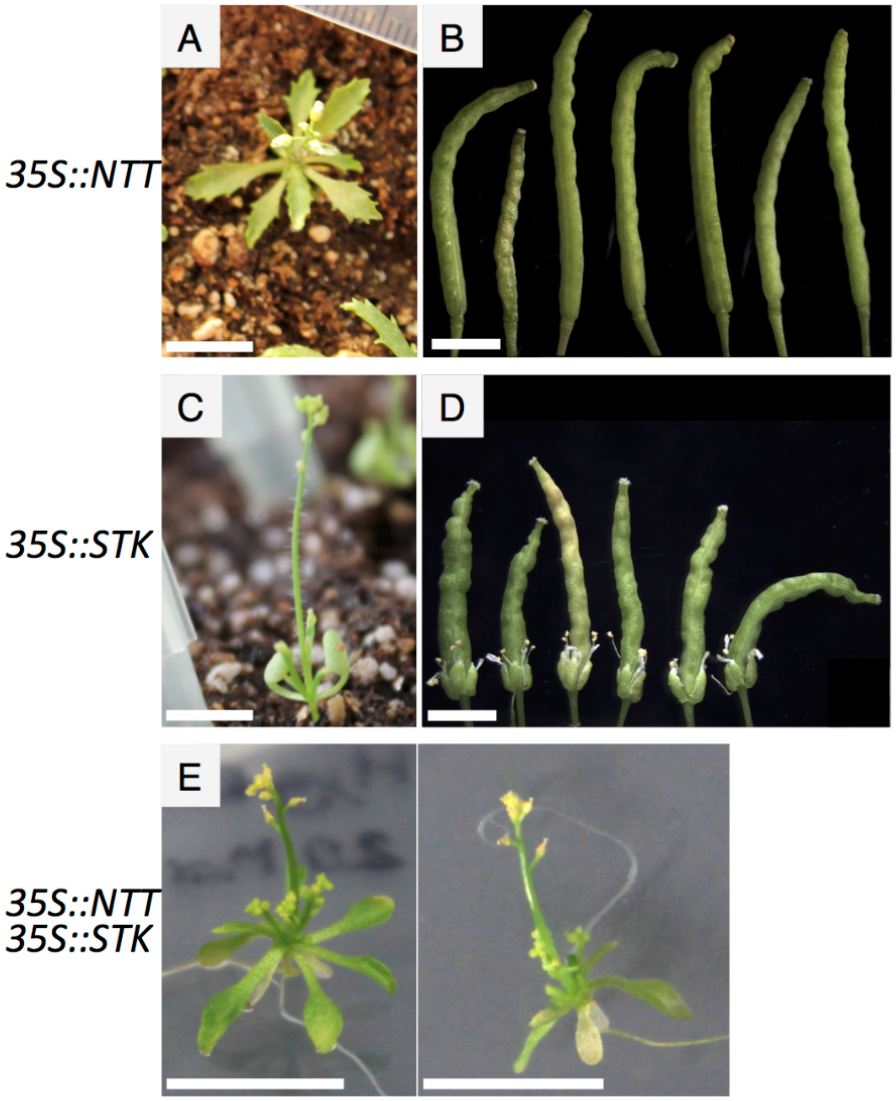

Figure S1. Phenotype of *NTT* and *STK* overexpression lines. Early flowering plants of *35S::NTT* (A) or *35S::STK* (C) overexpression lines. Fruits of the *35S::NTT* (B) and *35S::STK* (D) overexpression lines. E, Plants of the *35S::NTT 35S::STK* double overexpression line, which do not produce fruits. Scale bars = 1 cm in A, C and E; 0.2 cm in B and D.

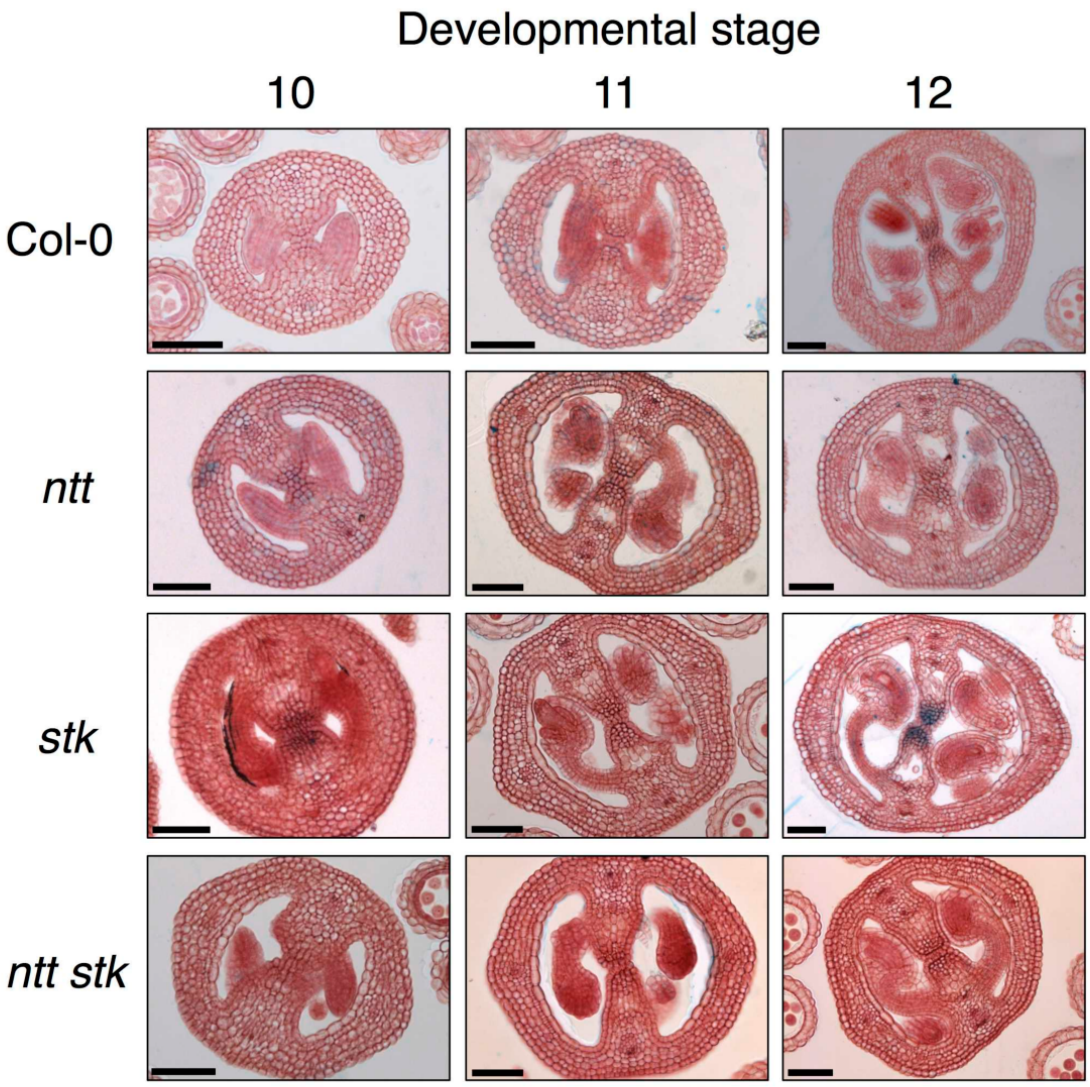

Figure S2. Transverse sections of stage 10–12 gynoecia of Col-0, *ntt*, *stk* and *ntt stk* double mutant. Scale bars = 50 μm.

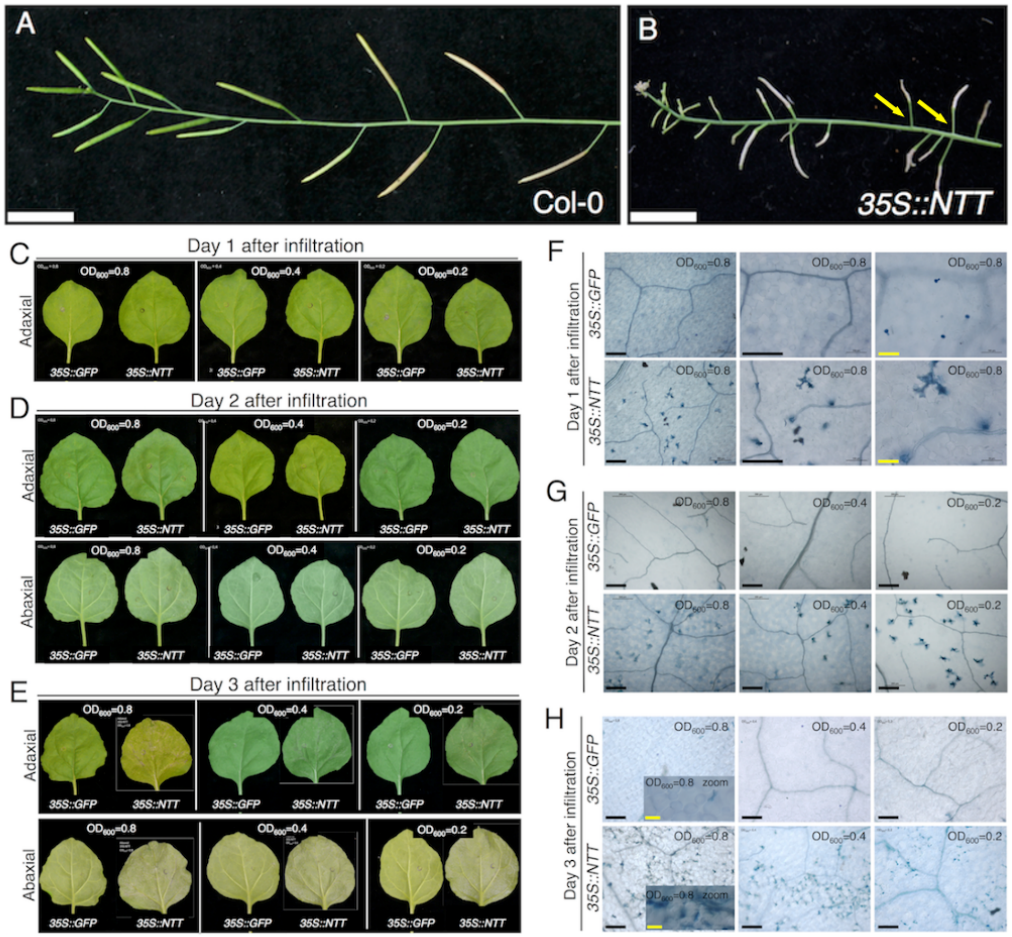

Figure S3. NTT accelerates senescence and promotes cell death. A-B, Fruit senescence in Col-0 (A) and *35S::NTT*; no senescence is observed in pedicels (yellow arrows) (B). C-H, NTT can trigger transcriptional responses leading to cell death. Analysis of cell death caused by *NTT* or *GFP* transient expression in Nicotiana leaves. *GFP* expression was used as a negative control (note: no leaf damage was observed when *STK* alone was infiltrated in the BiFC experiment, while *NTT* alone or together *NTT* and *STK* it was observed). Overview of Nicotiana leaves 1 day (C), 2 days (D) and 3 days (E) after agro-infiltration. Detection of dead cells using the trypan blue staining in Nicotiana leaves 1 day (F), 2 days (G) and 3 days (H) after agro-infiltration. Bars represent 1 cm in A,B; in F-H, black bars represent 200 μm and yellow bars 50 μm.

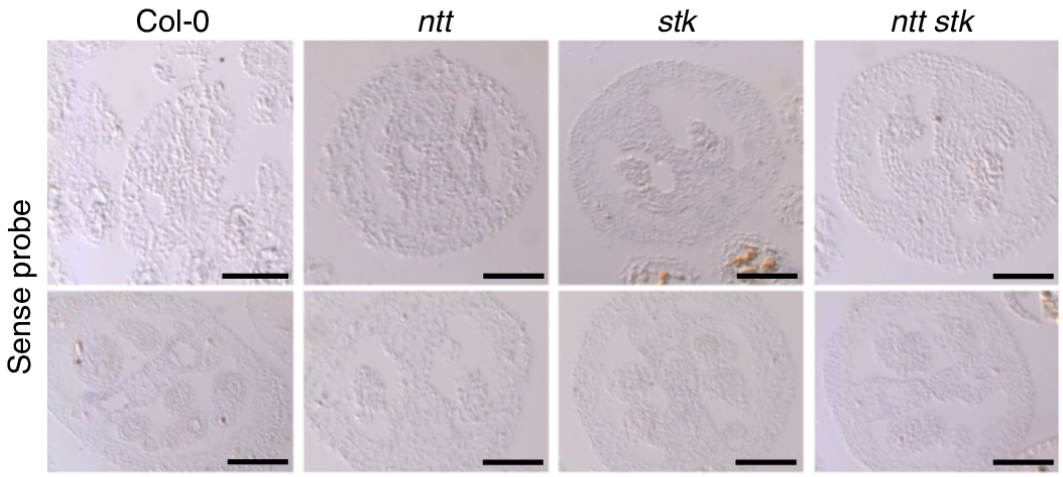

Figure S4: Sense probe controls for the *In situ* hybridization detection of *AT3G26140* (Glycosyl Hydrolase) in the gynoecium. The four genetic backgrounds are shown. Scale bars = 50 μm.

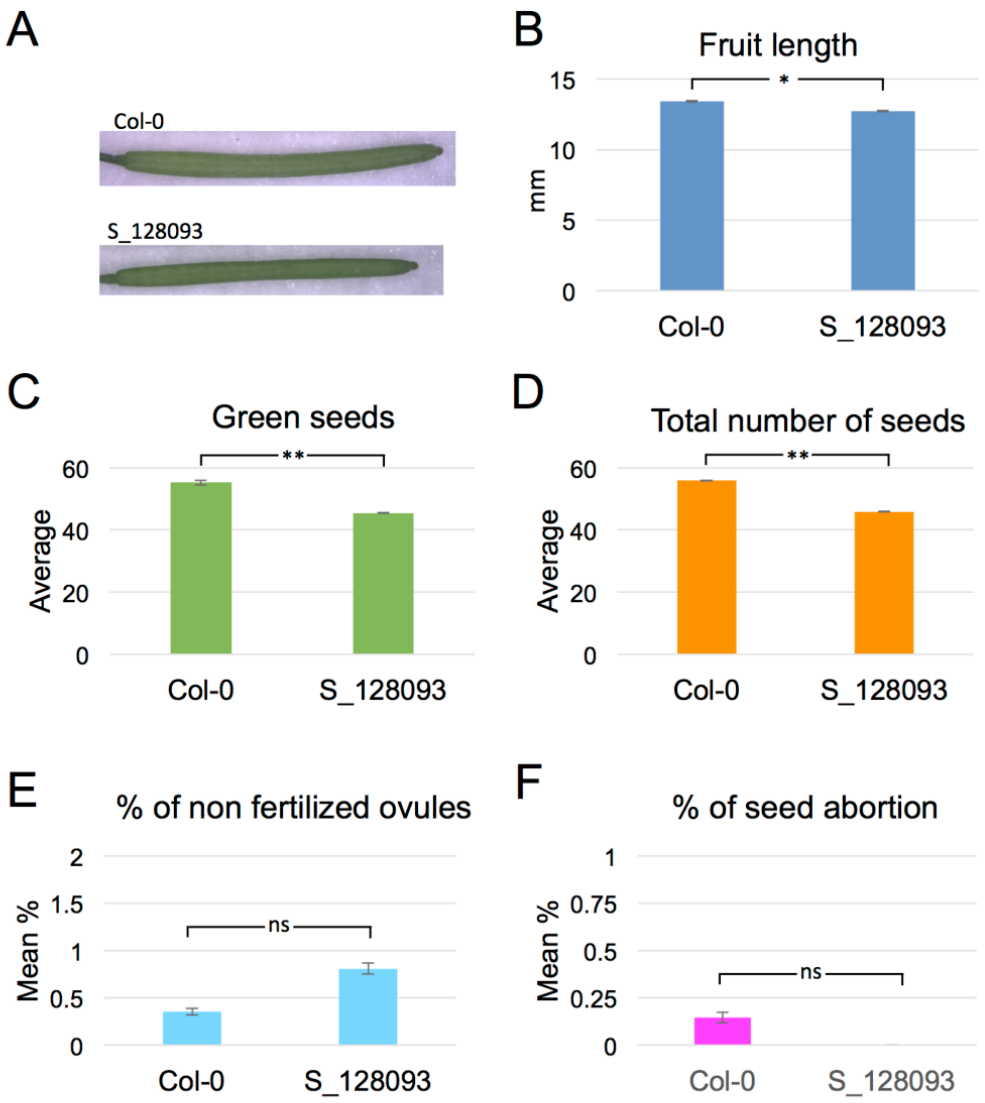

Figure S5. Analysis of At3g26140 (glycosyl hydrolase) insertional line. A, Overview of fruits of Col-0 and S_128093 line. Analysis of fruit length (B), number of green seeds (C), total number of seeds (D), % of non fertilized ovules (E) and seed abortion (F). Statistical analyses were performed using a T-test, $p < 0.01$ (*) or < 0.001 (**).

Development: doi:10.1242/dev.172395: Supplementary information

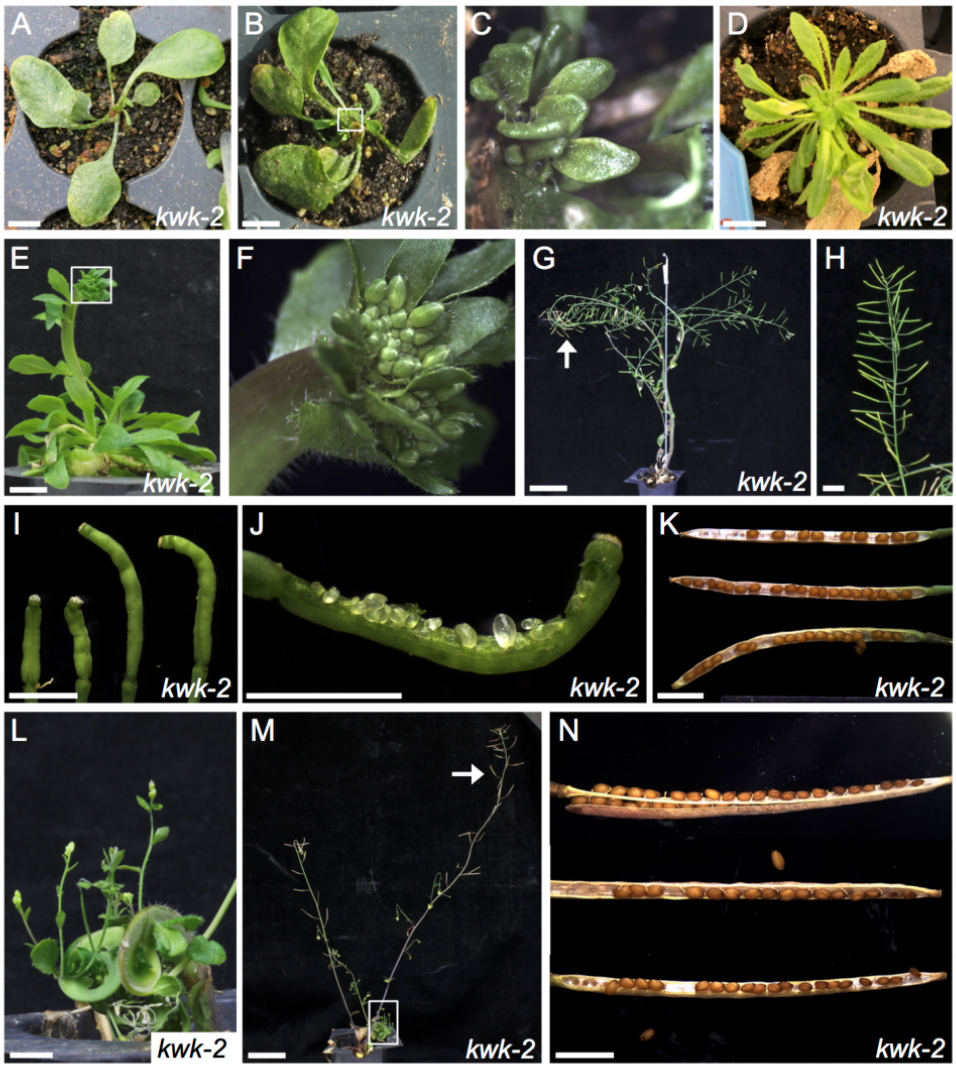

Figure S6. *kwk/abcg15* mutant phenotype in the Col-0 background.

A-N, Examples of *kwk-2* mutant plants severely affected in development. Young plant (A) affected in SAM development, producing few leaves (B), lateral growth is observed in older plant (D), C is a close-up of boxed region in B. E-F, The main inflorescence is affected producing abnormal fruits (I) with severe defects in ovule development (J). Secondary inflorescences seem to grow normally (G). H, a close-up of shoot marked in G with an arrow, the seed-set and development of these fruits (K) is similar to WT, but phyllotaxis is affected. L,M, Another plant with similar phenotypes, main shoot is severely affected (L is a close-up of boxed region in M). Secondary shoots (arrow in M) produce normal fruits (N). Scale bars = 1 cm in A-E and H; 5 cm in G and M; and 2 mm in I-K and N.

Figure S7. ARACNe-based coexpression network.

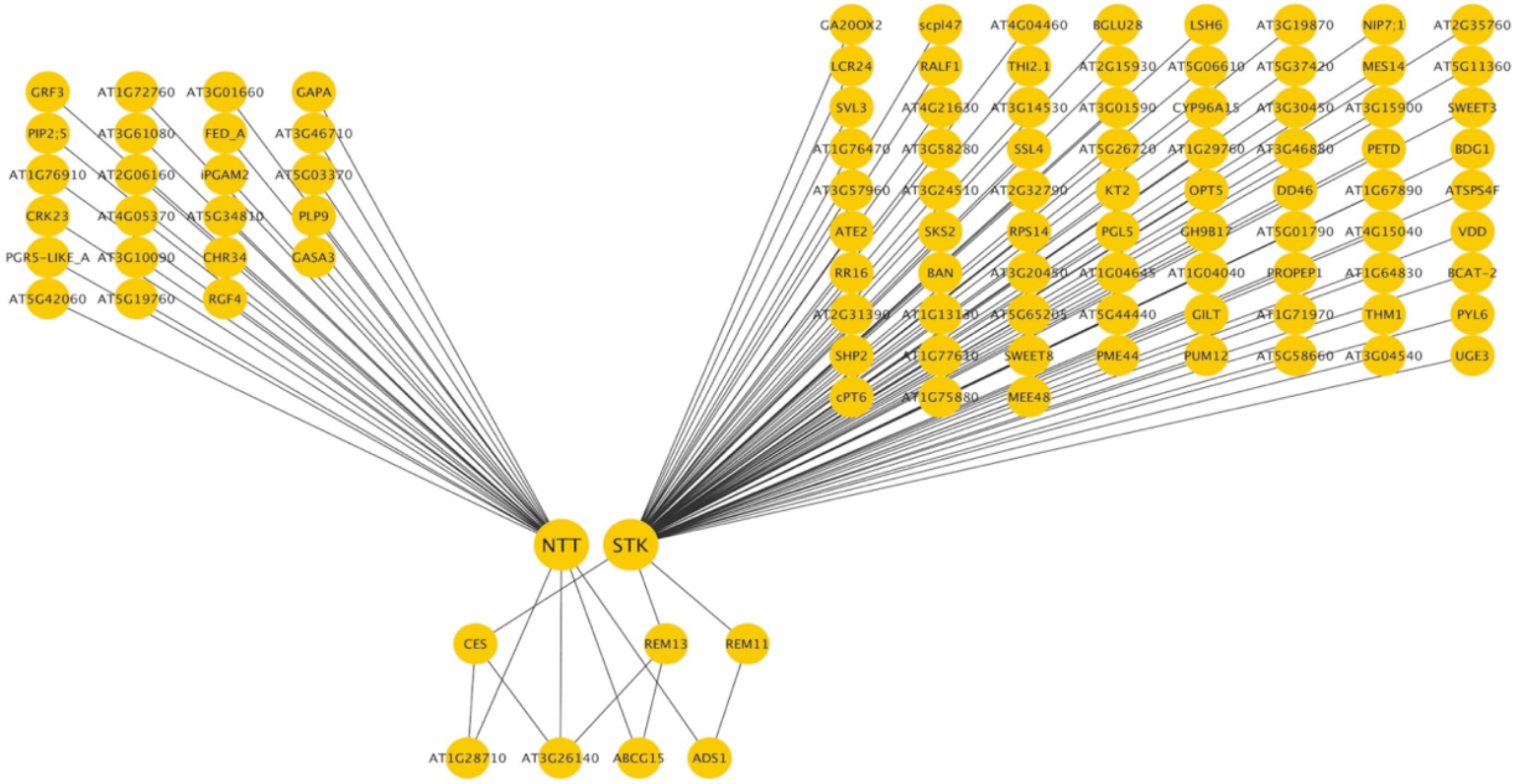

Table S1. Results of tested interactions in the Y2H assays.

The + simbol indicates yeast growth and blue intensity in LacZ assays.
- indicates no growth or no staining.

BD clone (AG ID)	BD clone (alias)	AD clone (AG ID)	AD clone (alias)	Selection medium 1 SD-ADE	Selection medium 1 LacZ	Selection medium 2 SD-HIS	Selection medium 2 LacZ
AT3G57670	NTT	AT1G77850	ARF17	+ + +	+ + +	+ + +	+ + +
AT3G57670	NTT	AT4G29080	IAA27	+ + +	+ + +	+ + +	+ + +
AT3G57670	NTT	AT3G57670	NTT	+ + +	+ + +	+ + +	+ + +
AT3G57670	NTT	AT4G00870	bHLH14	+ + +	+ + +	+ + +	+
AT3G57670	NTT	AT4G18960	AG	+ + +	-	+ + +	+ + +
AT3G57670	NTT	AT1G31140	GOA	+ + +	-	+ + +	+ + +
AT3G57670	NTT	AT4G09960	STK	+ + +	-	+ + +	+ + +
AT3G57670	NTT	AT4G37750	ANT	+	+	+ + +	+ + +
AT3G57670	NTT	AT2G37630	AS1	+	+	+ + +	+ + +
AT3G57670	NTT	AT2G21230	DKM	+	+	+ + +	+ + +
AT3G57670	NTT	AT1G19220	ARF19	+ + +	+ + +	-	-
AT3G57670	NTT	AT5G37020	ARF8	-	-	+ + +	+ + +
AT3G57670	NTT	AT4G17460	JAB	+ + +	+ + +	-	-
AT3G57670	NTT	AT1G70510	KNAT2	+ + +	+ + +	-	-
AT3G57670	NTT	AT2G46870	NGA1	+ + +	+ + +	-	-
AT3G57670	NTT	AT1G24260	SEP3	-	-	+ + +	+ + +
AT3G57670	NTT	AT2G27990	PNF	-	-	+ + +	+
AT3G57670	NTT	AT1G59750	ARF1	-	-	+ + +	+
AT3G57670	NTT	AT5G41410	BEL1	-	-	+ + +	+
AT3G57670	NTT	AT3G61970	NGA2	-	-	+	+
AT3G57670	NTT	AT2G45190	FIL	+ + +	+	-	-
AT3G57670	NTT	AT5G60450	ARF4	+	+	-	-
AT3G57670	NTT	AT3G15170	CUC1	+	+	-	-
AT3G57670	NTT	AT5G16560	KAN	+	+	-	-
AT3G57670	NTT	AT3G51060	STY1	+	+	-	-
AT3G57670	NTT	AT3G50330	HEC2	+	-	-	-
AT3G57670	NTT	AT3G61830	ARF18	-	-	-	-
AT3G57670	NTT	AT1G69180	CRC	-	-	-	-
AT3G57670	NTT	AT5G53950	CUC2	-	-	-	-
AT3G57670	NTT	AT2G33860	ETT	-	-	-	-
AT3G57670	NTT	AT5G67060	HEC1	-	-	-	-
AT3G57670	NTT	AT1G23380	KNAT6	-	-	-	-
AT3G57670	NTT	AT1G01030	NGA3	-	-	-	-
AT3G57670	NTT	AT1G68640	PAN	-	-	-	-
AT3G57670	NTT	AT2G34710	PHB	-	-	-	-
AT3G57670	NTT	AT3G54220	SCR1	-	-	-	-
AT3G57670	NTT	AT4G36260	STY2	-	-	-	-
AT3G57670	NTT	AT2G17950	WUS	-	-	-	-
* AT3G57670	NTT	AT4G08150	BP	-	-	-	-
* AT3G57670	NTT	AT5G02030	RPL	+	-	+ + +	+
* AT3G57670	NTT	AT1G62360	STM	+ + +	+ + +	-	-
* AT3G57670	NTT	AT5G60910	FUL	+ + +	-	+ + +	+ + +
* AT3G57670	NTT	AT3G58780	SHP1	+ + +	-	+ + +	+ + +
* AT3G57670	NTT	AT2G42830	SHP2	+ + +	-	+ + +	+ + +

* Reported in Marsch-Martínez, N. *et al.* (2014) *Plant J*, **80**, 69-81.

Table S2. ARACNe-based coexpression network of *NTT* and *STK*.

Coexpression network: genes connected to *NO TRANSMITTING TRACT* (*NTT*)

AGI ID	*GENE ALIAS*	*BRIEF DESCRIPTION*	*SOURCE*
AT3G30350	RGF4	uncharacterized protein	[Source:EMBL;Acc:AEE77635.1]
AT5G38480	GRF3	14-3-3-like protein GF14 psi	[Source:EMBL;Acc:AED94323.1]
AT3G63200	PLP9	PATATIN-like protein 9	[Source:EMBL;Acc:AEE80447.1]
AT3G54820	PIP2;5	putative aquaporin PIP2-5	[Source:EMBL;Acc:AEE79295.1]
AT4G09600	GASA3	gibberellin-regulated protein 3	[Source:EMBL;Acc:AEE82770.1]
AT3G10090		40S ribosomal protein S28-1	[Source:EMBL;Acc:AEE74858.1]
AT5G42060		DEK, chromatin associated protein	[Source:EMBL;Acc:AED94761.1]
AT5G19760		Mitochondrial substrate carrier family protein	[Source:EMBL;Acc:AED92746.1]
AT1G72760		protein kinase-like protein	[Source:EMBL;Acc:AEE35369.1]
AT4G23310	CRK23	putative cysteine-rich receptor-like protein kinase 23	[Source:EMBL;Acc:AEE84737.1]
AT5G03370		acylphosphatase	[Source:EMBL;Acc:AED90593.1]
AT3G61080		protein kinase-like protein	[Source:EMBL;Acc:AEE80151.1]
AT1G76910		uncharacterized protein	[Source:EMBL;Acc:AEE35902.1]
AT3G26650	GAPA	glyceraldehyde-3-phosphate dehydrogenase A	[Source:EMBL;Acc:AEE77191.1]
AT2G21450	CHR34	chromatin remodeling 34	[Source:EMBL;Acc:AEC07179.1]
AT3G01660		S-adenosylmethionine-dependent methyltransferase domain-containing protein	[Source:EMBL;Acc:AEE73700.1]
AT4G05370		BCS1 AAA-type ATPase	[Source:EMBL;Acc:AEE82510.1]
AT3G46710		putative disease resistance RPP13-like protein 2	[Source:EMBL;Acc:AEE78196.1]
AT4G22890	PGR5-LIKE_A	Transmembrane protein present in thylakoids	[Source:EMBL;Acc:AEE84674.1]
AT3G08590	iPGAM2	2,3-biphosphoglycerate-independent phosphoglycerate mutase 2	[Source:EMBL;Acc:AEE74651.1]

Coexpression network: genes connected to *SEEDSTICK* (*STK*) (page 1)

AGI ID	*GENE ALIAS*	*BRIEF DESCRIPTION*	*SOURCE*
AT2G42830	SHP2	agamous-like MADS-box protein AGL5	[Source:EMBL;Acc:AEC10174.1]
AT5G18000	VDD	VERDANDI protein	[Source:EMBL;Acc:AED92494.1]
AT1G61720	BAN	anthocyanidin reductase	[Source:EMBL;Acc:AEE33879.1]
AT2G40670	ARR16 (RR16)	two-component response regulator ARR16	[Source:EMBL;Acc:AEC09862.1]
AT5G22980	scpl47	carboxypeptidase	[Source:EMBL;Acc:AED93104.1]
AT1G04040		HAD superfamily, subfamily IIIB acid phosphatase	[Source:EMBL;Acc:AEE27649.1]
AT1G72260	THI2.1	thionin 2.1	[Source:EMBL;Acc:AEE35295.1]
AT1G77610		EamA-like transporter	[Source:EMBL;Acc:AEE36000.1]
AT2G15930		uncharacterized protein	[Source:EMBL;Acc:AEC06449.1]
AT1G13130		Cellulase (glycosyl hydrolase family 5) protein	[Source:EMBL;Acc:AEE28973.1]
AT4G26590	ATOPT5 (OPT5)	oligopeptide transporter 5	[Source:EMBL;Acc:AEE85224.1]
AT5G24420	PGL5	6-phosphogluconolactonase 5	[Source:EMBL;Acc:AED93309.1]
AT3G20450		B-cell receptor-associated protein 31-like protein	[Source:EMBL;Acc:AEE76381.1]
AT4G33220	PME44	pectinesterase 44	[Source:EMBL;Acc:AEE86192.1]
AT1G10070	BCAT-2	branched-chain-amino-acid aminotransferase 2	[Source:EMBL;Acc:AEE28539.1]
AT5G58660		oxidoreductase, 2OG-Fe(II) oxygenase family protein	[Source:EMBL;Acc:AED97082.1]
AT2G32790		ubiquitin-conjugating enzyme E2 D/E	[Source:EMBL;Acc:AEC08742.1]
AT3G58280		phospholipase-like protein (PEARLI 4) with TRAF-like domain	[Source:EMBL;Acc:AEE79763.1]
AT1G07090	LSH6	uncharacterized protein	[Source:EMBL;Acc:AEE28076.1]
AT1G64830		aspartyl protease-like protein	[Source:EMBL;Acc:AEE34295.1]
AT2G31390		fructokinase	[Source:EMBL;Acc:AEC08541.1]
AT3G11240	ATE2	arginine-tRNA protein transferase 2	[Source:EMBL;Acc:AEE75019.1]
AT5G65205		Rossmann-fold NAD(P)-binding domain-containing protein	[Source:EMBL;Acc:AED98017.1]
AT5G37420		uncharacterized protein	[Source:EMBL;Acc:AED94186.1]
AT3G04540		defensin-like protein 44	[Source:EMBL;Acc:AEE74094.1]
AT2G44460	BGLU28	beta glucosidase 28	[Source:EMBL;Acc:AEC10422.1]

Coexpression network: genes connected to *SEEDSTICK* (page 2)

AGI ID	ALIAS	BRIEF DESCRIPTION	SOURCE
AT5G01790		uncharacterized protein	[Source:EMBL;Acc:AED90392.1]
AT1G29760		Putative adipose-regulatory protein (Seipin)	[Source:EMBL;Acc:AEE31126.1]
AT4G12960	GILT	Gamma interferon responsive lysosomal thiol (GILT) reductase family protein	[Source:EMBL;Acc:AEE83207.1]
AT4G14080	MEE48	putative glucan endo-1,3-beta-glucosidase A6	[Source:EMBL;Acc:AEE83368.1]
AT3G19870		uncharacterized protein	[Source:EMBL;Acc:AEE76302.1]
AT1G33990	ATMES14	methyl esterase 14	[Source:EMBL;Acc:AEE31655.1]
AT1G03680	ATHM1 (THM1)	thioredoxin M1	[Source:EMBL;Acc:AEE27596.1]
AT5G56510	APUM12 (PUM12)	pumilio 12	[Source:EMBL;Acc:AED96775.1]
AT4G15040		Subtilisin-like serine endopeptidase family protein	[Source:EMBL;Acc:AEE83544.1]
AT3G20520	SVL3	protein SEUSS-like 3	[Source:EMBL;Acc:AEE76390.1]
AT3G57960		Emsy N Terminus (ENT) domain-containing protein	[Source:EMBL;Acc:AEE79724.1]
AT1G71970		uncharacterized protein	[Source:EMBL;Acc:AEE35259.1]
AT2G40330	PYL6	abscisic acid receptor PYL6	[Source:EMBL;Acc:AEC09815.1]
AT5G51810	GA20OX2	gibberellin 20 oxidase 2	[Source:EMBL;Acc:AED96129.1]
AT4G29285	LCR24	defensin-like protein 163	[Source:EMBL;Acc:AEE85613.1]
AT5G44440		FAD-binding and BBE domain-containing protein	[Source:EMBL;Acc:AED95109.1]
AT5G11360		Interleukin-1 receptor-associated kinase 4 protein	[Source:EMBL;Acc:AED91665.1]
AT3G14530		geranylgeranyl diphosphate synthase 9	[Source:EMBL;Acc:AEE75535.1]
AT5G53190	SWEET3	Nodulin MtN3 family protein	[Source:EMBL;Acc:AED96320.1]
AT2G34520	RPS14	small subunit ribosomal protein S14	[Source:EMBL;Acc:AEC08984.1]
ATC00730	PETD	photosynthetic electron transfer D	[Source:TAIR;Acc:ATCG00730]
AT3G46880		uncharacterized protein	[Source:EMBL;Acc:AEE78214.1]
AT3G24510		defensin-like protein 259	[Source:EMBL;Acc:AEE76910.1]
AT5G40260	SWEET8	protein RUPTURED POLLEN GRAIN 1	[Source:EMBL;Acc:AED94527.1]
AT5G26720		uncharacterized protein	[Source:EMBL;Acc:AED93572.1]

Coexpression network: genes connected to *SEEDSTICK* (page 3)

AGI ID	ALIAS	*BRIEF DESCRIPTION*	SOURCE
AT1G76470		Rossmann-fold NAD(P)-binding domain-containing protein	[Source:EMBL;Acc:AEE35846.1]
AT3G15900		uncharacterized protein	[Source:EMBL;Acc:AEE75744.1]
AT1G75880		GDSL esterase/lipase EXL1	[Source:EMBL;Acc:AEE35769.1]
AT4G10120	ATSPS4F	sucrose-phosphate synthase	[Source:EMBL;Acc:AEE82845.1]
AT1G63180	UGE3	UDP-glucose 4-epimerase	[Source:EMBL;Acc:AEE34065.1]
AT4G21630		Subtilase family protein	[Source:EMBL;Acc:AEE84483.1]
AT1G67890		PAS domain-containing protein tyrosine kinase	[Source:EMBL;Acc:AEE34716.1]
AT3G51420	SSL4	strictosidine synthase-like 4 protein	[Source:EMBL;Acc:AEE78790.1]
AT5G51480	SKS2	Monocopper oxidase-like protein SKS2	[Source:EMBL;Acc:AED96089.1]
AT1G02900	ATRALF1	rapid alkalinization factor 1	[Source:EMBL;Acc:AEE27494.1]
AT4G04460		phytepsin	[Source:EMBL;Acc:AEE82391.1]
AT1G57750	MAH1	cytochrome P450, family 96, subfamily A, polypeptide 15	[Source:EMBL;Acc:AEE33459.1]
AT3G01590		glucose-6-phosphate 1-epimerase	[Source:EMBL;Acc:AEE73693.1]
AT2G35760		uncharacterized protein	[Source:EMBL;Acc:AEC09157.1]
AT1G04645		self-incompatibility protein S1-like protein	[Source:EMBL;Acc:AEE27728.1]
AT2G40540	TRK2 (KT2)	potassium transporter 2	[Source:EMBL;Acc:AEC09846.1]
AT5G06610		uncharacterized protein	[Source:EMBL;Acc:AED91042.1]
AT5G64900	PROPEP1	elicitor peptide 1	[Source:EMBL;Acc:AED97966.1]
AT1G64670	BDG1	alpha/beta-hydrolase domain-containing protein	[Source:EMBL;Acc:AEE34272.1]
AT4G39000	GH9B17	endoglucanase 23	[Source:EMBL;Acc:AEE87006.1]
AT1G22015	DD46	putative beta-1,3-galactosyltransferase 5	[Source:EMBL;Acc:AEE30185.1]

Coexpression network core

AGI ID	GENE ALIAS	BRIEF DESCRIPTION	SOURCE
AT1G06080	ADS1	delta-9 acyl-lipid desaturase 1	[Source:EMBL;Acc:AEE27937.1]
AT1G28710		nucleotide-diphospho-sugar transferase domain-containing protein	[Source:EMBL;Acc:AEE31018.1]
AT3G26140		Cellulase (glycosyl hydrolase family 5) protein	[Source:EMBL;Acc:AEE77125.1]
AT5G60140	REM11	AP2/B3 domain-containing transcription factor	[Source:EMBL;Acc:AED97284.1]
AT3G46770	REM13	AP2/B3 domain-containing transcription factor	[Source:EMBL;Acc:AEE78203.1]
AT1G25330	HAF/CES	Transcription factor bHLH75	[Source:EMBL;Acc:AEE30607.1]
AT3G21090	ABCG15	ABC transporter G family member 15	[Source:EMBL;Acc:AAM13053.1]

Table S3. Primer list.

GENE ALIAS	GENE ID	EXPERIMENT	PRIMER NAME	SEQUENCE	FRAGMENT LENGHT (bp)
Glycosyl Hydrolase	AT3G26140	ChIP-qPCR	RT 1982 (FW carg3)	CGTGTTTGATTGAATACACCACCCT	172
			RT 1983 (REV carg3)	AACAAATCCTATGTTACTCAATCATAGCTT	
			RT 2631 (FW NTT-binding site)	AGAGCTAAGACGCATGTTTTGC	136
			RT 2632 (FW NTT-binding site)	ACACGCCAGCTTCACTCTTT	
		qRT-PCR	SdF1027	GTCCGATCACGACACGTAAA	198
			SdF1028	GTCGATTCCAAACTCGCTAAGA	
		In situ hybridization	SdF632 (At3g26140_probe_FW)	CACCCTTAGATCCAACCAAGGTC	193
			SdF633 (At3g26140_probe_REV)	GAGGCTGAGATGGTCTCCCC	
ABCG15	AT3G21090	ChIP-qPCR	RT 2070 (FW cargs 10-11)	CTTGTGGCTTGTCACTTGTGG	106
			RT 2071 (REV cargs 10-11)	ATCTTTGACCTTTGCACCACT	
			RT 2627 (FW NTT-binding site)	GACTTGCTTCAATTTTAGTGGCT	159
			RT 2628 (REV NTT-binding site)	TCGTCGGACAAAAACTCTAAACTC	
		qRT-PCR	SdF1029	AGATGAGCCGTGGAGCGTAT	100
			SdF1030	CCGTTTAGCCTTTGGAGCAA	
ADS1	AT1G06080	ChIP-qPCR	RT 2072 (FW cargs 3-4)	AGGATGAGGTATCGATGGTTGC	124
			RT 2073 (REV cargs 3-4)	TGTATGTGGTGGACCAAGCA	
			RT 2633 (FW NTT-binding site)	CCGTTAGGTTTTGGTCACAGTC	163
			RT 2634 (REV NTT-binding site)	TTTACGGGTGGGTCCTCCAT	
		qRT-PCR	SdF1023	TGTCCATTTCCTCTGTCTCTTG	269
			SdF1024	TAGGACTATGTGGGTCCCTATC	
Nucleotide-diphospho-sugar transferase	AT1G28710	ChIP-qPCR	RT 2130 (FW cargs 4-7)	TGGTGTTACATCCAAATCCGGT	156
			RT 2131 (REV cargs 4-7)	CGCAAAGAGAAGAGCAACGG	
			RT 2629 (FW NTT-binding site)	AATCGAACTGGGTCATCGACTT	134
			RT 2630 (REV NTT-binding site)	TCGGAATGCCCCTTTGACTT	
		qRT-PCR	SdF1033	CCGCGGCTACAATCTTACTT	210
			SdF1034	AGCCTCATGTCGTACCATTTC	
ACTIN2		qRT-PCR	SdF1161	AATCACAGCACTTGCACC	100
			SdF1162	ATTCCTGGACCTGCCTC	
ACTIN7	AT5G09810	ChIP-qPCR	RT_045 (FW act7)	CGTTTCGCTTTCCTTAGTGTTAGCT	132
			RT_046 (REV act7)	AGCGAACGGATCTAGAGACTCACCTTG	
NTT	AT3G57670	*NTT::GUS* line	S314	ATAATCGATCCGTGGAGCCAATATAGGTCGAAC	1216
			S318	TCTCCATGGTGAAGAGAGAGAGAGAGGAAGAGAAAGG	

Manuscript 2, SUBMITTED

MADS-box and bHLH transcription factors coordinate transmitting tract development in *Arabidopsis thaliana*

AUTHORS:

Di Marzo Maurizio[1§], Roig-Villanova Irma[1,2§], Zanchetti Eva[1], Caselli Francesca[1], Gregis Veronica[1], Bardetti Paola[1,3], Matteo Chiara[1], Guazzotti Andrea[1], Elisabetta Caporali[1], Mendes Marta A.[1], Colombo Lucia[1] and Kater Martin M.[1*]

ADDRESSES:

[1]Dipartimento di Bioscienze, Università degli Studi di Milano, Via Celoria 26, 20133 Milan, Italy.
[2]Current address: Institut de Recerca i Tecnologia Agroalimentàries, (IRTA) at Center for Research in Agricultural Genomics, CRAG (CSIC-IRTA-UAB-UB), Campus UAB, Cerdanyola del Vallès, Barcelona, Spain.
[3]Current address: Center for Genomics & Systems Biology. Department of Biology New York University 12 Waverly Place, 3rd floor, New York, NY 1003.

E-mail ADDRESSES:

Maurizio Di Marzo: maurizio.dimarzo@unimi.it
Roig-Villanova Irma: irma.roig@irta.cat
Zanchetti Eva: eva.zanchetti@live.com
Bardetti Paola: pb141@nyu.edu
Matteo Chiara: matteo.chiara@unimi.it
Francesca Caselli: francesca.caselli@unimi.it
Veronica Gregis: veronica.gregis@unimi.it
Andrea Guazzotti: andrea.guazzotti@unimi.it
Elisabetta Caporali: elisabetta.caporali@unimi.it
Mendes Marta A: marta.miranda@unimi.it
Colombo Lucia: lucia.colombo@unimi.it
Kater Martin M.: martin.kater@unimi.it

*Corresponding author: Kater Martin M. : martin.kater@unimi.it; (+39)0250315050
§Both authors contributed equally to the work.

RUNNING TITLE

MADS-box and bHLH regulate transmitting tract development

HIGHLIGHT

The MADS-domain transcription factor STK acts together with CES to regulate transmitting tract development in *Arabidopsis thaliana*.

ABSTRACT

The MADS-domain transcription factor *SEEDSTICK* (*STK*) controls several aspects of plant reproduction. *STK* is co-expressed with *CESTA* (*CES*), a basic Helix-Loop-Helix (bHLH) transcription factor-encoding gene. *CES* was reported to control redundantly with the brassinosteroid positive signaling factors BRASSINOSTEROID ENHANCED EXPRESSION1 (BEE1) and BEE3 the development of the transmitting tract. Combining the *stk ces-2* mutants led to a reduction in ovule fertilization due to a defect in carpel fusion which, caused the formation of holes at the center of the septum where the transmitting tract differentiates. Combining the *stk* mutant with the *bee1 bee3 ces-2* triple mutant showed a clear enhancement of the number of unfertilized ovules and septum defects. The transcriptome profile of this quadruple mutant revealed a small subset of deregulated genes which are mainly involved in cell death, extracellular matrix and cell wall development. Our data evidence a regulatory gene network controlling transmitting tract development regulated directly or indirectly by a STK-CES containing complex and reveal new insights in the regulation of transmitting tract development by bHLH and MADS-domain transcription factors.

KEY WORDS

bHLH, cell death, cell wall, extracellular matrix, MADS-box, transmitting tract

ABBREVIATIONS

BRASSINOSTEROID ENHANCED EXPRESSION (BEE), basic Helix-Loop-Helix (bHLH), carpel margin meristem (CMM), CESTA (CES), Extracellular matrix (ECM), programmed cell death (PCD), SEEDSTICK (STK).

INTRODUCTION

The plant life cycle in Angiosperms is characterized by the alternation of diploid sporophyte and haploid gametophyte generations. The sporophyte produces spores, which then develop into gametophytes. The gametophytes produce either the male or the female gametes. Sexual reproduction requires the delivery of sperm nuclei, via the pollen tube, to the embryo sac, where fertilization occurs, and the new diploid sporophyte is formed.

The growing of the pollen tube through the female reproductive organ tissues in Angiosperms is a crucial step in plant sexual reproduction. In *Arabidopsis thaliana*, the floral female organ, the pistil or gynoecium, results from the fusion of two carpels. The apical part of the pistil is formed by the stigma and the stigma papillae, which are needed to attach the pollen. The stigma is connected by the style to the ovary, in which lodge the ovules. The septum divides the ovary into two chambers. At the centre of the septum, as in the style, the transmitting tract tissue develops. Pollen tubes must travel through several distinct tissues before reaching ovules, including the stigma, the style transmitting tract and the septum transmitting tract (Lord and Russell, 2002; Roeder and Yanofsky, 2006).

The transmitting tract differentiates from the carpel margin meristem (CMM), a meristematic tissue that develops as two internal crests that, fuse when they reach each other in the middle of the young pistil at developmental stage 9. The transmitting tract is fully developed at stage 12 of pistil development (Bowman et al., 1999; Roeder and Yanofsky, 2006; Reyes-Olalde et al., 2013). The cells composing the transmitting tract secrete an extracellular matrix (ECM), a complex mixture of polysaccharides, glycoproteins, and glycolipids that accompany the growing pollen tubes (Lennon et al., 1998).

A complex genetic network controls the development of the transmitting tract. The zinc-finger transcription factor, NO TRANSMITTING TRACT (NTT) has pivotal roles during transmitting tract development. In the *ntt* mutant, the programmed cell death (PCD) of the cells composing the transmitting tract during fertilization, which is also influenced by the ECM composing cell wall, is severely compromised (Crawford et al., 2007). The changes in PCD and ECM in the *ntt* mutant cause a partial failure in pollen tube growth, with a high percentage of non fertilized ovules from the middle to the bottom part of the siliques (Crawford et al., 2007). NTT acts upstream of three genes that are *CESTA* (*CES*), which is also named *HALF FILLED* (*HAF*), a bHLH-encoding transcription factor that acts redundantly with two phylogenetically related genes *BRASSINOSTEROID ENHANCED EXPRESSION1* (*BEE1*) and

BEE3 in the control of the style and transmitting tract development (Crawford and Yanofsky, 2011; Poppenberger et al., 2011). The triple mutant *ces bee1 bee3* shows similar defects in transmitting tract development as Crawford and collaborators previously found in the *ntt* mutant (Crawford and Yanofsky, 2011). Furthermore, ectopic expression of *CES* (*HAF*), increases the diameter of the transmitting tract allowing more pollen tubes to pass through it simultaneously (Crawford and Yanofsky, 2011).

Recently, NTT was found to interact with the MADS-domain transcription factor SEEDSTICK (STK) to control transmitting tract development (Herrera-Ubaldo et al., 2019). STK was previously identified for its role in ovule development and acts redundantly with other two MADS-box transcription factors SHATTERPROOF1 (SHP1) and SHP2 (Pinyopich et al., 2003).

NTT and *STK* have a similar expression pattern in the medial domain of the pistil (Herrera-Ubaldo et al., 2019). In the *ntt stk* double mutant the number of cells composing the CMM is similar in respect to wild type (Herrera-Ubaldo et al., 2019). However, in the *ntt stk* mutant siliques, there is a partial failure in septum fusion, and it appears to have holes. The fact that the cell number composing the CMM hasn't changed suggest that the abnormal fusion is not related to early stages of development but rather to epidermal defects (Herrera-Ubaldo et al., 2019). The partial failure of pollen tube growth in the *ntt stk* mutant is also caused by the absence of degeneration and collapse of the cells composing the septum and consequently the transmitting tract (Herrera-Ubaldo et al., 2019).

Recently, Mendes et al., (2016) performed co-expression analysis to identify new regulators of molecular pathways in which *STK* is involved. These experiments resulted in the identification of *CES*.

Here we report a genetic and molecular analysis, which revealed interactions between the AGAMOUS family members *STK*, *SHP1* and *SHP2*, the bHLH gene *CES*, and the closely related genes *BEE1* and *BEE3* in the control of transmitting tract development. We further performed a transcriptome analysis of the *bee1 bee3 stk ces-2* quadruple mutant uncovering new downstream players, involved in transmitting tract development.

MATERIALS AND METHODS

Plant material and growth conditions

All plants used in this study were in the Columbia (Col-0) ecotype. For all analyses, *Arabidopsis thaliana* seeds were incubated for 2 days at 4°C after sowing. Plants were grown

at 22°C under long day conditions (LD). The *ces-2* mutant was obtained from NASC (SAIL_674_A01 lines). The *stk*, *shp1* and *shp2* mutants were provided by M. Yanosky (Pinyopich et al., 2003), the *bee1 bee2 bee3* triple and *bee1 bee2 bee3 ces-2* quadruple mutant by J. Chory and J. Martinez, respectively (Cifuentes-Esquivel et al., 2013). The other mutant combinations analysed were obtained by crossing. The *pCES::GUS* line was provided by Prof. B. Poppenberger (Poppenberger et al., 2011).

Mutant genotyping

Genotyping of the mutants was done by PCR analysis. All the primers used in this study are listed in Table S9.

***In situ* hybridization analysis**

Arabidopsis flowers and siliques were fixed and embedded in paraffin as previously described in Dreni *et al.*, 2011. Tissue sections (8 µm) were hybridized with a *CES* specific antisense RNA probe and observed with a Zeiss Axiophot D1 microscope. Images were captured on an Axiocam MRc5 camera (Zeiss) using the Axiovision program (version 4.1).

Gus-staining analysis

GUS staining of *pCES::GUS* was performed as described in Balanzà *et al.*, 2016.

Silique analysis

The percentage of unfertilized ovules per fruit was determined by opening at least 20 mature siliques for each genotype, counting the number of unfertilized ovules and the total number of developed seeds per silique under a stereomicroscope. The statistical significance of the differences in unfertilized ovules was analysed using an Anova test followed by the Tukey HSD test (** = $p<0.01$). All the experiments were repeated four times.

Scanning Electronic Microscope (SEM) pictures

Biological samples were collected and fixed overnight at 4°C in FAE solution (10 mL formaldehyde 37%, 50 mL absolute ethanol, 5 mL glacial acetic acid, 35 mL deionized water). Fixed tissues were washed with water and post-fixed with aqueous 2% osmium tetroxide for 2 hours at room temperature. Tissues were rinsed several times in deionized water and dehydrated in a graded series of ethanol for 15 min per rinse. This step was followed by critical

point drying with liquid CO_2 and sputter-coating with gold in a Nanotech sputter coater. Specimens were analyzed using a LEO 1430 Scanning Electron Microscope.

Pollen tube guidance analysis

Experiments of pollen tube guidance were performed as previously described by Mendes *et al.*, 2016 and images were captured on an Axiocam MRc5 camera (Zeiss) using the Axiovision program (version 4.1).

Bimolecular fluorescence complementation assay (BiFC)

Coding Sequences (CDS) of *CES* and *STK* were amplified by PCR with the primers indicated in Table S9 and first cloned into pDONOR207 (Life Technologies) and subsequently into the pYFPN43 and pYFPC43 vectors (http://www.ibmcp.upv.es/FerrandoLabVectors.php). BiFC experiments were conducted as previously described in Balanzà *et al.*, 2016. Essentially, the abaxial surfaces of tobacco leaves were observed 2-5 days after agroinfiltration and the interactions were monitored using a Leica TCS the confocal microscope.

Yeast Two-Hybrid Assays

The two-hybrid assays were performed at 22°C in the yeast strain AH109 (Clontech), using the cotransformation technique (Egea-Cortines et al., 1999).

The coding sequences of *CESTA*, *STK* and *BEE1* were cloned in the Gateway vector GAL4 system (pGADT7 and pGBKT7; Clontech) passing through pDONOR207 (Life Technologies). Yeast two-hybrid interaction assays were performed on selective yeast synthetic dropout medium lacking Leu, Trp, Adenine, and His supplemented with different concentrations of 3-aminotriazole (1, 2.5, 5, 10 and 15 mM of 3-AT).

RNA extraction and qRT-PCR analysis

For the qRT-PCR experiment of *ces-2* (knockout validation) total RNA was extracted from whole inflorescences using the LiCl method as previously described (Verwoerd *et al.*, 1989). First-strand cDNA was synthesized using an IMProm-II ™ Reverse Transcription System (Promega). Enrichments fold were detected using a SYBER Green assay (Bio-Rad, http://www.bio-rad.com). The qRT-PCR assay was performed in triplicate using a Bio-Rad iCycler iQ optical system (software version 3.0a).

RNA sequencing

Total RNA was extracted from three biological replicates (1 gr) from both wild-type and *bee1 bee3 stk ces-2* mutant inflorescences till stage 12, using the Macherey Nagel 'Nucleospin RNA Plant' according to the manufacturer's instructions. RNA concentrations and integrity were determined using Qubit Fluorometer and the Qubit™ RNA XR Assay Kit (ThermoFisher Scientific).

Sequencing libraries were prepared using the NEBNext Ultra II Directional RNA library Prep Kit for Illumina (NEB) according to the manufacture's instruction and sequenced on the HiSeq Illumina platform.

Reads were mapped on the reference *Arabidopsis thaliana* genome (TAIR, version 10) using the bowtie2 program (Langmead Ben and Steven, 2012). Estimation of gene expression levels was performed using RSEM (Li and Dewey, 2011). Identification of differentially expressed genes was performed by the quasi-likelihood F-test as implemented by edgeR (Robinson et al., 2009). A False Discovery Rate (FDR) cut-off value of 0.05 was applied for the identification of significantly differentially expressed genes.

To validate the data obtained from the RNAseq experiment, we extracted total RNA from wild type and *bee1 bee3 stk ces-2* mutant inflorescences till stage 12, using the Macherey Nagel 'Nucleospin RNA Plant' according to the manufacturer's instructions. The cDNA and qRT-PCR were performed as described in the previous paragraph "RNA extraction and qRT-PCR analysis".

Accession numbers of the genes

The GenBank/EMBL accession numbers for the genes shown in this study are the following: *BEE1*, At1g18400; *BEE2*, At4g36540; *BEE3*, At1g73830; *CES*, At1g25330; *SHP1*, At3g58780; *SHP2*, At2g42830; *STK*, At4g09960. The accession number of the genes identified in the transcriptomic analysis are indicated in the corresponding tables.

RESULTS

SEEDSTICK and *CESTA* are co-expressed

In order to identify new targets, partners and/or regulators of *STK*, a bioinformatics analysis was previously performed in the laboratory to discover genes co-expressed with *STK* (Mendes et al., 2016). This kind of analysis assumes that correlation between the patterns of expression of genes in a large range of different experimental conditions could indicate a

functional relationship (Aoki et al., 2007). *CES* (At1g25330) rated among the top twenty genes having an expression correlation with *STK* of p(LIN) 0.759 and p(LOG) 0.505 (Mendes et al., 2016).

Previously, it had been reported that *CES* is expressed in carpels (Crawford and Yanofsky, 2011; Poppenberger et al., 2011). Since *STK* is expressed during female reproductive organ development (Herrera-Ubaldo et al., 2019; Pinyopich et al., 2003), we investigated in more detail the expression profile of *CES* during pistil, ovule and seed development by RNA *in situ* hybridization and by the analysis of the *pCES::GUS* reporter gene construct (Fig. 1). The RNA in situ analysis experiments showed that *CES* was expressed in ovules during early stages of development until mature ovule formation and its transcripts were also present in the transmitting tract before fertilization (Fig. 1 A-C). In mature ovules a high expression was detected in the funiculus (Fig. 1C). After fertilization and during embryo development *CES* mRNA was present at high levels in the early globular stage, and at heart and torpedo stages mRNA levels were lower (Fig.1 D-F). Analysis of the *pCES::GUS* plants confirmed the in situ data (Fig. 1 G-I) and these experiments showed that *STK* and *CES* partially overlap in their expression patterns during ovule and transmitting tract development (Crawford and Yanofsky, 2011; Herrera-Ubaldo et al., 2019; Pinyopich et al., 2003; Poppenberger et al., 2011).

Arabidopsis plants with *stk, shp, ces* and *bee* mutant combinations are partially sterile

To further analyse the role of CES, we characterized a CES loss-of-function allele that we obtained from the SAIL collection (Alonso and Stepanova, 2003). This allele, that we called *ces-2*, has a T-DNA insertion in the second exon, differently from *ces-1*, a previously published T-DNA insertion allele that is located in the last exon (Poppenberger et al., 2011). The qRT-PCR analysis performed to check *CES* expression in the *ces-2* mutant indicated that this mutant is also a null allele (Fig. S1). Analysis of *ces-2* homozygous plants did not reveal any general phenotype at the level of the entire plant, which was consistent with previous reports for the *ces* (*haf*) mutant alleles (Crawford and Yanofsky, 2011; Poppenberger et al., 2011). We crossed the *ces-2* mutant with *stk* to obtain the *stk ces-2* double mutant. The double mutant was indistinguishable from wild type plants apart from a large number of unfertilized ovules at the lower part of the siliques. In wild type plants on average 1.0% of the ovules in a silique remained unfertilized. In the *stk* mutant we observed on average 6.2% unfertilized ovules, and in the *ces-2* single mutant 11.6% (**$p<0.01$ in respect to wild type; Fig. 2 and Table S1). In the *stk ces-2* double mutant this phenotype was further increased to 28.1% of unfertilized ovules (Fig. 2 and Table S1). As in the single mutant *ces-2*, also in the double mutant *stk ces-*

2 the unfertilized ovules were located always at the lower part of the siliques (Fig. 2 and Table S1).

Since SHP1 and SHP2 are closely related to STK and have shown to control ovule identity redundantly with it (Pinyopich et al., 2003), we investigated whether they also play a role together with CES in the control of ovule fertilization. Therefore, the *shp1 shp2* double mutant was crossed with the *ces-2* mutant to obtain the *shp1 shp2 ces-2* triple mutant. The *shp1 shp2* double mutant showed on average 7.0% unfertilized ovules (Fig. 2 and Table S1). The *shp1 shp2 ces-2* triple mutant showed a clear increase to 16.2%, also in this case the unfertilized ovules were localized at the lower part of the siliques (**$p<0.01$ in respect to wild type and *shp1 shp2*; Fig. 2 and Table S1). Unfortunately we could not analyze the *stk shp1 shp2* triple mutant, because the triple mutant does not develop normal ovules (Pinyopich et al., 2003). These results suggest that the MADS-domain transcription factor STK, SHP1 and SHP2 have a role together with CES in the control of ovule fertilization.

The contribution of the *BEE* genes to this process was also investigated (Fig. 3 and Table S2). *CES* is phylogenetically related to *BEE1* and *BEE3*, which have been described as redundant with *BEE2* (Friedrichsen et al., 2002). Moreover, it has been shown that CES together with BEE1 and BEE3 redundantly control the development of the transmitting tract in the pistil (Crawford and Yanofsky, 2011; Poppenberger et al., 2011). The single mutants *bee1* and *bee3* and the multiple mutant combinations *bee1 bee3* and *bee1 bee2 bee3* did not show any obvious phenotype (Fig. 3 and Table S2). To investigate redundancy between *BEE* genes and *STK*, we obtained the *bee1 bee2 bee3 stk* quadruple mutant, that presented 9.2% of unfertilized ovules, with **$p<0.01$ when compared to wild type and the triple mutant *bee1 bee2 bee3*, which again were preferentially positioned at the lower part of the pistil (Fig. 3 and Table S2). This percentage is lower than the *bee1 bee2 bee3 ces-2* quadruple mutant, which presented in average 28.7% of unfertilized ovules (Fig. 3 and Table S2). Despite the weaker phenotype, our results demonstrated that STK and BEEs also have a role together in ovule fertilization. To investigate if combining the *ces-2* mutant could further enhance the unfertilized ovule phenotype, we generated the *bee1 bee3 stk ces-2* quadruple and the *bee1 bee2 bee3 stk ces-2* quintuple mutants. The results of this analysis showed that *bee1 bee3 stk ces-2* had on average 46.6% unfertilized ovules, and a similar result was obtained in the *bee1 bee2 bee3 stk ces-2* (44.0%) (Fig. 3 and Table S2), showing that the addition of the *bee2* allele did not further enhance the phenotype. The unfertilized ovules in these cases are localized from the middle to the bottom part of the siliques. Altogether, these results indicated that the MADS-domain

transcription factors function not only together with CES, but also with the BEEs in the control of the fertilization of all the ovules within the Arabidopsis fruit.

STK and CES regulate transmitting tract development

To better understand the defect that caused the presence of a high percentage of unfertilized ovules at the lower part of the siliques in the different mutant combinations, we performed reciprocal crosses between wild type and *stk ces-2* or *shp1 shp2 ces-2* mutant plants, to analyse if the female, male or both parts were defective. The outcome of the reciprocal crosses shown in Fig. S2, indicated that the unfertilized-ovules phenotype was only present when the mutant genotypes were used as mothers, indicates that the defects resides only in the female reproductive organ.

To further investigate the defect present in the female reproductive organs, which caused the high number of unfertilized ovules at the lower part of the siliques in the multiple mutant combinations, we analyzed the septum morphology by Scanning Electronic Microscope (SEM), at stage 17 of fruit development, when the siliques reached their maximum elongation (Roeder and Yanofsky, 2006).

The *stk* and *ces-2* single mutants presented a septum similar to wild type, while the double mutant *stk ces-2* disclosed a defect in septum morphology (Fig. 4A). The double mutant was characterized by a partial failure of septum fusion in the central portion of the septum in conjunction with the medium portion of the ovary (Fig. 4A). The quadruple mutant combinations *bee1 bee2 bee3 stk* and *bee1 bee2 bee3 ces-2* did not display defects in septum morphology when compared to wild type (Fig. 4A). However, the damage of the septum appears stronger in the quadruple mutant *bee1 bee3 stk ces-2* and in the quintuple mutant *bee1 bee2 bee3 stk ces-2* where a hole in the central portion of the septum was seen in conjunction with the medium region of the ovary (Fig. 4A).

The septum morphological analysis at stage 17 suggests a transmitting tract defect caused by a failure of the carpel fusion that happen from stage 9 to 12 (Roeder and Yanofsky, 2006). At these stages fusion occurs within the two crests of the CMM leading to septum and transmitting tract formation (Bowman et al., 1999; Roeder and Yanofsky, 2006; Reyes-Olalde et al., 2013). To confirm that the defects found in the septum and transmitting tract formation, described for *stk ces-2*, *bee1 bee3 stk ces-2* and *bee1 bee2 bee3 stk ces-2* caused a defective growth of the pollen tubes through the ovary transmitting tract, pistils were hand pollinated with wild type pollen 36 hours after an aniline blue staining was performed (Fig. 4B). In the wild-type-hand-pollinated control pistils all the pollen tubes reached the bottom part of the ovary. However,

pollen tube growth was compromised in the three mutant combinations. In the *stk ces-2* double mutant the pollen tubes did not grow further than the middle region of ovary length (Fig. 4B). A stronger phenotype was observed in *bee1 bee3 stk ces-2* quadruple and in the *bee1 bee2 bee3 stk ces-2* quintuple mutants, where the pollen tubes stopped growing at the upper part of the ovary (Fig. 4B).

The differences in septum morphology and in pollen tube growth in the double mutant *stk ces-2*, in the quadruple mutant *bee1 bee3 stk ces-2* and in the quintuple mutant *bee1 bee2 bee3 stk ces-2* compared to wild type, clearly indicate that the carpels fusion that permits the correct development of the septum and consequently of the transmitting tract, was partially disturbed in these mutants and the cause that the ovules at the lower part of the siliques remained unfertilized.

SEEDSTICK and CESTA interact in yeast and *planta*

The experiments described above showed a genetic interaction between *STK* and *CES.* To investigate if there is also a physical interaction between these proteins, Bimolecular Fluorescence Complementation (BiFC) was performed. As a positive control, cells were co-transformed with CES (YC-CES) and (YN-CES), as CES was shown to homodimerise in yeast (Poppenberger et al., 2011) (Fig. 5A). Reconstitution of YFP fluorescence in the nuclei of co-transformed cells confirmed that CES is able to interact with STK *in vivo* (Fig. 5A), supporting our idea that CES and STK form a complex that controls transmitting tract formation. The interaction between STK and CES was also confirmed by Y2H experiments (Fig. 5B). As positive control in these experiments we used the previously published interaction between BEE1 and CES (Poppenberger et al., 2011) (Fig. 5B). Furthermore, we saw that STK and BEE1 are not able to interact. All the interactions are described in Table S3.

Transcriptome analysis of the *bee1 bee3 stk ces-2* quadruple mutant reveals target genes involved in transmitting tract development

To obtain a snapshot of the regulatory network controlled by STK, CES and BEE proteins, in the development of the septum/transmitting tract, transcriptional profiles of the quadruple mutant *bee1 bee3 stk ces-2*, which displayed the most severe phenotype, were studied by deep RNA sequencing. RNA was extracted from the quadruple mutant and wild type inflorescences until stage 12 of pistil development, before fertilization since the transmitting tract is fully developed at this stage of pistil development (Roeder and Yanofsky, 2006).

For the identification of significantly differentially expressed genes, a False Discovery Rate (FDR) cut-off value of 0.05 was applied and a total of 202 differentially genes were founded. Of these 31 were up-regulated in the mutant (Table S5) while 171 down-regulated (Table S6). Remarkably functional enrichment analyses (Table S7 and Table S8) revealed that gene ontology categories such as programmed cell death (PCD), extracellular matrix (ECM) and cell wall biosynthesis components, were enriched for the up regulated genes, while the down regulated genes were involved in the carbohydrate biosynthesis process.

Interestingly, among the downregulated genes, three genes were previously described as direct targets of STK (Herrera-Ubaldo *et al.*, 2019) : *AT3G26140*, *AT1G28710* and *AT1G06080*. The *AT3G26140* gene which encodes a glycosyl hydrolase (GH5_11) is expressed in CMM during pistil development (Aspeborg et al., 2012; Herrera-Ubaldo et al., 2019). The GH5 enzymes are all mannan endo-beta-1,4-mannosidases which are known to be involved in cell wall remodeling processes (Aspeborg et al., 2012; Herrera-Ubaldo et al., 2019; Lombard et al., 2014). *AT1G28710* encodes for a nucleotide diphospho-sugar transferase protein which is involving in the biosynthesis of polysaccharides, that are fundamental components of the ECM (Herrera-Ubaldo and de Folter, 2018; Lennon et al., 1998; Tung et al., 2005). *AT1G06080* (*DELTA 9 DESATURASE1* (*ADS1*)), encodes for a fatty acid desaturase which is involved in lipid biosynthesis, expressed in flowers (Fukuchi-Mizutani et al., 1998; Heilmann et al., 2004; Yao et al., 2003) (Table 1). Down-regulation of these three genes was also confirmed by qRT-PCR (Fig. S3).

Several different genes involved in the regulation of cell death were downregulated in the quadruple mutant respect to wild type (Table 1). One of the most important is *GRIM REAPER* (*GRI*, *AT1G53130*) that encodes for a small protein with an extracellular localization that is able to positively regulate cell death (Wrzaczek et al., 2009; Wrzaczek et al., 2015) (Table 1). Moreover, we observe that *ACCELERATED CELL DEATH 6* (*ACD6*, *AT4G14400*) another positive regulator of cell death is also down-regulated (Rate et al., 2007) (Table 1).

Additionally, we notice the downregulation of three genes encoding for the Arabinogalactan proteins (AGPs) *ARABINOGALACTAN PROTEIN 5* (*AGP5*, *AT1G35230*), *AGP7* (*AT5G65390*) and *AGP14* (*AT5G56540*). AGPs are structurally complex plasma membrane and cell wall proteoglycans that are implicated in diverse developmental processes, including plant sexual reproduction (Coimbra et al., 2007; Coimbra et al., 2009; Lennon et al., 1998). Importantly, these protein are able to regulate cell death in Arabidopsis cell culture (Gao and Showalter, 1999; Guan and Nothnagel, 2004).

Several genes involved in cell wall biosynthesis processes are mis-regulated in the quadruple mutant, these include *BETA-XYLOSIDASE 3* (*BXL3*, *AT5G09730*), which encodes for an enzyme involved in arabinan and xylan catabolic process (Minic et al., 2006), and *PECTIN METHYLESTERASE 58* (*PME58*, *AT5G49180*), encoding for a pectin methylesterases contributes to cell wall modification (Turbant et al., 2016) (Table 1), which were both down-regulated. Among the up-regulated genes, there are three genes of the GDSL family of serine esterases/lipases, *AT1G75890*, *AT4G28780* and *AT4G16230* (Table 1). These genes are involved in numerous aspect of plant development, but in particular the acetylxylan esterase activity of these enzyme could contribute in the degradation of cell walls in association with xylanases, cellulases, and mannanases (Akoh et al., 2004).

Moreover, several genes involved in the auxin signaling pathway showed altered profiles of expression. These include genes encoding for Aux/IAAs proteins, *INDOLE-3-ACETIC ACID INDUCIBLE 1* (*IAA1*) (*AT4G14560*), *IAA2* (*AT3G23030*), *IAA14* (*AT4G14550*) and *IAA17* (*AT1G04250*) which were all down regulated (Table 1). The Aux/IAA proteins are the early auxin response proteins and participate in auxin signalling through interacting, as repressors, with AUXIN RESPONSE FACTOR proteins (Lavy and Estelle, 2016). In addition, the *SMALL AUXIN UPREGULATED RNA 9* (*SAUR9*) and *SAUR12* were also downregulated. The SAURs are small transcripts induced by auxin, that are localized in elongated tissues (Knauss et al., 2003; McClure and Guilfoyle, 1987). *SAUR9* and *SAUR12* are part of the *SAUR10*-clade (van Mourik et al., 2017).

Intriguingly we also detect a significant downregulation of *ATWSCP* (*AT1G72290*) which encodes for a Kunitz-type protease inhibitor, member of a small family of proteins, that are water-soluble chlorophyll protein and *LIPID TRANSFER PROTEIN 2* (*LTP2, AT2G38530*) (Table 1). *ATWSCP* is expressed in the septum and transmitting tract during its development, and after fertilization the protein is located in the medial domain of the silique where is able to regulate cell death and pollen tube growth (Bektas et al., 2012; Boex-Fontvieille et al., 2015). The *LTP2* gene encodes for a lipid transfer protein necessary for the movement of hydrophobic wax components through the hydrophilic cell wall matrix to reach the cuticle (Kunst and Samuels, 2003). LTP2 mediates cell wall loosening in vitro (Nieuwland et al., 2005).

DISCUSSION

In Arabidopsis, the gynoecium is formed by the fusion of two carpels, which fuse vertically at their margins and give rise to the carpel margin meristem. From this meristem the

transmitting tract develops, an essential tissue to facilitate the growing pollen tubes to reach the ovules and fertilize them.

Genetic redundancy between MADS-domain and bHLH transcription factors in transmitting tract development

The MADS-domain transcription factor STK has been described as a master regulator of ovule development (Pinyopich et al., 2003) and its expression is confined to female reproductive tissues (Herrera-Ubaldo et al., 2019; Pinyopich et al., 2003).

Recently, a role for STK in relation with NTT was shown during the development of transmitting tract (Herrera-Ubaldo et al., 2019). Here we reveal that STK may also act in the downstream pathway of NTT in a protein complex with CES. Our genetic analysis evidence the role and redundancies between the MADS-box genes *STK*, *SHP1* and *SHP2*, the bHLH transcription factor gene *CES* and *BEE1* and *BEE3* in the development of the transmitting tract in *Arabidopsis thaliana*. The *CES* gene was selected based on high correlation of its expression pattern with *STK* (Mendes et al., 2016) but also because this gene was shown to play a role in transmitting tract development (Crawford and Yanofsky, 2011; Poppenberger et al., 2011). *CES*, *BEE1* and *BEE3* were shown to be expressed with distinct but overlapping patterns within the reproductive tract (Crawford and Yanofsky, 2011; Poppenberger et al., 2011). In the *ces* (*haf*) *bee1 bee3* triple mutant ECM and PCD fail to occur within this tissue (Crawford and Yanofsky, 2011).

The *stk* mutant did not present any type of reproductive defect (no statistical differences when the number of unfertilized ovules was compared with the wild type), while the single mutant *ces-2* is characterized by a small but significative percentage of unfertilized ovules (Fig. 2). However, the *stk ces-2* double mutant had 28.1% of unfertilized ovules, which were almost exclusively found at the basal part of the silique (Fig. 2). This phenotype suggests, similar to the *ces bee1 bee3* triple mutant (Poppenberger et al., 2011), a defect in transmitting tract development.

Interestingly, we also observed a genetic interaction between *STK* and *BEE1* and *BEE3* in transmitting tract development since the *bee1 bee2 bee3 stk* quadruple mutant showed 9.21% unfertilized ovules at the lower part of the silique, while *stk* had only 6.2% and the triple mutant *bee1 bee2 bee3* displayed 1.8% of unfertilized ovules (Fig. 3). In the light of the fact that this phenotype was weaker than that observed for *stk ces-2* (Fig. 2), we suggest that CES plays a more predominant role in transmitting tract formation together with STK. To understand a possible role of *SHP1* and *SHP2* in the formation of the transmitting tract, the triple mutant

shp1 shp2 ces-2 was obtained. This triple mutant showed 16.2% of unfertilized ovules which is also a milder phenotype when compared to *stk ces-2* (Fig. 2). This suggests that STK is important for transmitting tract development, although is not able to cover for 100% *SHP*s function since the *shp1 shp2 ces-2* triple mutant presents a considerable percentage of unfertilized ovules.

The different degree of unfertilized ovule phenotypes obtained in the different mutant combinations points to redundancy between MADS-box, bHLH, and the BEEs transcription factor encoding genes in a dosage-dependent manner. The unfertilized ovules phenotype was only observed when different mutant alleles were combined and was more pronounced in the quadruple and quintuple mutants, suggesting an additive effect. Such a dosage dependent effect was already described for other MADS-box genes, like *FLOWERING LOCUS C* (*FLC*) that acts, in a dosage-dependent manner, as a potent repressor of the floral transition (Bastow et al., 2004; Michaels and Amasino, 2007; Sheldon et al., 2007).

Y2H and BIFC experiments showed that STK is able to interact with CES, but not with BEE1 (Fig. 5 and Table S3). This result suggests that CES might bridge the interaction between MADS and BEE proteins to form a hypothetical multimeric complex that controls correct transmitting tract formation. Cooperative action of MADS-domain and bHLH transcription factors has been previously described in mice. Molkentin and collaborators (1995) showed that MEF2 factors, a family of MADS-domain proteins expressed in muscle cells and other cell types, acted as coregulators of myogenic bHLH proteins to activate muscle genes (Molkentin et al., 1995). Moreover, the authors show that these two types of transcription factors physically interact, and that either factor can interact with the other when one is bound to DNA (Molkentin et al., 1995). Interestingly, the authors present this as a general mechanism for the regulation of transcription in specific cell types (Molkentin et al., 1995). This might also be a mechanism for the combinatorial control of MADS-domain (with STK as a main player) and bHLH (CES as principal component) transcription factors for the formation of the transmitting tract tissue in Arabidopsis.

STK and CES play a role in carpels fusion

When we discovered, by backcrossing, that the male part was not compromised in the *stk ces-2* and *shp1 shp2 ces-2* multiple mutants (Fig. S2), we decided to perform a detailed analysis of the septum morphology of the mutants displaying the most stronger phenotype related to the percentage of unfertilized ovules. As we described in the Fig. 4, when *STK* was mutated together with *CES* the fruits showed a septum fusion defect in the lower middle part in concomitance with the medial region of the ovary. This defect, was found in the double

mutant *stk ces-2*, in the quadruple mutant *bee1 bee3 stk ces-2* and in the quintuple mutant *bee1 bee2 bee3 stk ces-2*, and was previously described in the *ntt stk* double mutant, where in concomitance with the middle portion of the ovary, there is a failure in organ fusion with a septum that has a hole (Herrera-Ubaldo et al., 2019).

These phenotypes could be explained by mis-regulation of the genes involved in cuticle formation. The cuticle is a lipidic alteration of the cell wall (Yeats and Rose, 2013). The alteration in cuticle biosynthesis, deposition and wax component transports could cause organ fusion defects in plants, but in particular in flowers and carpels (Nawrath, 2006; Panikashvili et al., 2010; Sieber et al., 2007). Intriguingly transcriptional profiles of the quadruple mutant suggest a strong down-regulation of *LTP2* (Table 1), a gene involved in lipid transport and/or wax transport to form the cuticle (Kunst and Samuels, 2003). Notably, the *LTP5* gene which belongs to the same gene family as *LTP2*, and which did not show significantly altered expression in the quadruple mutant according to our analysis, is expressed in the transmitting tract and has previously involved been shown to be involved in pollen tube guidance (Chae et al., 2009; Kunst and Samuels, 2003). We believe that also *LTP2* might be involved in the correct fertilization of the ovules influencing not just the pollen tube growth but also the correct fusion of the two carpels that permits to form the septum and transmitting tract. Moreover, in the *bee1 bee3 stk ces-2* quadruple mutant we detected the overexpression of three genes encoding for GDSL esterase/lipase involved in lipid catabolism (Table 1). The overexpression of a GDSL named, *CUTICLE DESTRUCTING FACTOR 1* (*CDEF1*), causes abnormal organ fusion in leaves, stems and flowers (Takahashi et al., 2010). This gene codes for a protein which is considered a cutinase (Takahashi et al., 2010). It is possible that like for the *CDEF1* overexpression, the excess of cutinase in the quadruple mutant respect to wild type caused abnormal organ fusion.

STK and CES influence programmed cell death in transmitting tract

Cell death and tissue degeneration are required for pollen tube growth in the transmitting tract of Arabidopsis (Crawford et al., 2007). The phenotype described for combined *ces* and *bee* mutants showed that they fail to form the ECM and to accomplish PCD within the transmitting tract (Crawford and Yanofsky, 2011). Interestingly, STK has already been shown to control PCD in transmitting tract with NTT (Herrera-Ubaldo et al., 2019) but also in the receptive synergid cell through regulation of its direct target genes, *VERDANDI*

(VDD) and *VALKYRIA (VAL)*, two Reproductive Meristem (REM) transcription factors (Matias-Hernandez et. al 2010; Mendes et al., 2016).

As we show in the Table 1, in the quadruple mutant *bee1 bee3 stk ces-2* several genes involved in cell death are downregulated. One of the most interestingly is *ATWSCP*. This gene encodes for a Kunitz-type protease inhibitor localized preferentially in the transmitting tract and septum, which is involved in ECM and PCD but also in the exit of pollen tubes from the septum to reach the ovules during the fertilization phase (Bektas et al., 2012; Boex-Fontvieille et al., 2015). Also, *ACD6* is downregulated (Table 1), this gene encodes for a protein that promotes cell death in Arabidopsis (Rate et al., 2007). Furthermore, three Arabinogalactan genes (*AGPs*) resulted downregulated in the quadruple mutant (Table 1). The AGPs have been associated with ECM composition of the transmitting tract in different plant species (Gane et al., 1995; Hoggart and Clarke, 1984; Webb and Williams, 1988) and they have been shown to play a role in the regulation of PCD during pollen tube growth (Coimbra et al., 2009).

Does auxin-brassinosteroid crosstalk influence transmitting tract development?

It was recently suggested that the auxin pathway plays an important role in the specification and formation of the tissues along the pistil axis (Larsson et al., 2013a; Robert et al., 2015). However, the role of auxin signaling in transmitting tract development is still not fully understood. ARF6 and ARF8 regulate *CES* expression in the medial domain of the pistil during transmitting tract development (Crawford and Yanofsky, 2011). The double mutant *arf6 arf8* displayed reduced alcian blue staining, that detects acidic polysaccharides, the major components of the ECM (Crawford and Yanofsky, 2011). According to our RNAseq data four *Aux*/*IAA*s and two *SAUR*s genes were downregulated in the quadruple mutant in respect to wild type (Table 1). Aux/IAA proteins and SAURs might be activated in presence of brassinosteroid since evidences of a crosstalk between auxin and brassinosteroid have already been described (Nakamura et al., 2006). Moreover, *SAUR9* expression is induced by a combination of auxin and brassinosteroid (van Mourik et al., 2017). Probably a STK-CES-BEE1-BEE3 complex is able to connect the auxin-brassinosteroid crosstalk in transmitting tract tissue, however the precise role is of this crosstalk in the regulation of transmitting tract development remains unclear.

In summary, the data presented here suggest that a MADS-box-bHLH protein complex mastered by the physical interaction of STK-CES, plays a role in the regulation of different genes involved in the PCD, ECM and cell wall biosynthesis pathways and by that controlling

correct carpel fusion and transmitting tract development to guarantee efficient ovule fertilization (Fig.6).

COMPETING INTERESTS

The authors declare no competing or financial interests.

AUTHORS CONTRIBUTION

MDM and I.R-V designed, performed and analysed experiments and wrote the manuscript. E.Z, P.B, A.G, F.C, E.C, V.G. performed experiments. M.C. performed bio-informatics analyses. M.A.M performed aniline blue staining, analysed all the results and contributed writing the manuscript. L.C. and M.K. designed experiments, research strategies and contributed to the writing of the manuscript.

ACKNOWLEDGEMENTS

We thank Drs J.Chory and B. Poppenberger for seed sharing, Drs J. Martínez for seed sharing and assistance in the genotyping of the *bee* mutants. We are grateful to I. Latorre for help with *in situ* hybridisations and general laboratory assistance. MDM and L.C were funded by the SEXSEED project-Horizon2020-MSCA RISE 2016 (690946). I.R.V was funded by an EMBO Post-doctoral fellowship and by Fondo per gli Investimenti della Ricerca di Base-Futuro in Ricerca, E.Z. was funded by EVOCODE. MAM was funded by SEXSEED and Foundation for Science and technology (FCT), Portugal (SFRH/BPD/99936).

DATA AVAILABILITY

The data that support the findings of this study are openly available in the Gene Expression Omnibus (GEO) database GSE135559

https://www.ncbi.nlm.nih.gov/geo/query/acc.cgi?&acc=GSE135559, link for the dataset;

yzwzegoiznspvof, token.

BIBLIOGRAPHY

Akoh, C. C., Lee, G. C., Liaw, Y. C., Huang, T. H. and Shaw, J. F. (2004). GDSL family of serine esterases/lipases. *Prog. Lipid Res.* **43**, 534–552.

Alabadí, D., Blázquez, M. A., Carbonell, J., Ferrándiz, C. and Pérez-Amador, M. A. (2009). Instructive roles for hormones in plant development. *Int. J. Dev. Biol.* **53**, 1597–1608.

Alonso-Blanco, C., Blankestijn-de Vries, H., Hanhart, C. J. and Koornneef, M. (1999). Natural allelic variation at seed size loci in relation to other life history traits of Arabidopsis thaliana. *Proc. Natl. Acad. Sci.* **96**, 4710–4717.

Alonso, J. M. and Stepanova, A. N. (2003). T-DNA Mutagenesis in Arabidopsis BT - Plant Functional Genomics. In *Plant Molecular Biology* (ed. Grotewold, E.), pp. 177–187. Totowa, NJ: Humana Press.

Alvarez-buylla, E. R., Benítez, M., Corvera-poiré, A., Cador, C., Folter, S. De, Buen, A. G. De, Garay-arroyo, A., García-ponce, B., Jaimes-miranda, F., Rigoberto, V., et al. (2010). Flower Development. 1–57.

Alvarez, J. and Smyth, D. R. (1999). CRABS CLAW and SPATULA, two Arabidopsis genes that control carpel development in parallel with AGAMOUS. *Development* **126**, 2377–2386.

Alvarez, J. and Smyth, D. R. (2002a). CRABS CLAW and SPATULA genes regulate growth and pattern formation during gynoecium development in Arabidopsis thaliana. *Int. J. Plant Sci.* **163**, 17–41.

Alvarez, J. and Smyth, D. R. (2002b). CRABS CLAW and SPATULA Genes Regulate Growth and Pattern Formation during Gynoecium Development in Arabidopsis thaliana. *Int. J. Plant Sci.* **163**, 17–41.

Angenent, G. C. and Colombo, L. (1996). Molecular control of ovule development. *Trends Plant Sci.* **1**, 228–232.

Aoki, K., Ogata, Y. and Shibata, D. (2007). Approaches for extracting practical information from gene co-expression networks in plant biology. *Plant Cell Physiol.* **48**, 381–390.

Aspeborg, H., Coutinho, P. M., Wang, Y., Brumer, H. and Henrissat, B. (2012). Evolution, substrate specificity and subfamily classification of glycoside hydrolase family 5 (GH5). *BMC Evol. Biol.* **12**, 186.

Azhakanandam, S., Nole-Wilson, S., Bao, F. and Franks, R. G. (2008). SEUSS and AINTEGUMENTA mediate patterning and ovule initiation during gynoecium medial domain development. *Plant Physiol.* **146**, 1165–1181.

Bae, E., Bingman, C. A., Bitto, E., Aceti, D. J. and Phillips Jr., G. N. (2008). Crystal structure of Arabidopsis thaliana cytokinin dehydrogenase. *Proteins Struct. Funct. Bioinforma.* **70**, 303–306.

Balanzá, V., Navarrete, M., Trigueros, M. and Ferrándiz, C. (2006). Patterning the female side of Arabidopsis: the importance of hormones. *J. Exp. Bot.* **57**, 3457–69.

Balanzà, V., Roig-Villanova, I., Di Marzo, M., Masiero, S. and Colombo, L. (2016). Seed abscission and fruit dehiscence required for seed dispersal rely on similar genetic networks. *Development* **143**, 3372–3381.

Bartrina, I., Otto, E., Strnad, M., Werner, T. and Schmülling, T. (2011). Cytokinin Regulates the Activity of Reproductive Meristems, Flower Organ Size, Ovule Formation, and Thus Seed Yield in *Arabidopsis thaliana*. *Plant Cell* **23**, 69–80.

Bastow, R., Mylne, J. S., Lister, C., Lippman, Z., Martienssen, R. A. and Dean, C. (2004). Vernalization requires epigenetic silencing of FLC by histone methylation. *Nature* **427**, 164–167.

Bektas, I., Fellenberg, C. and Paulsen, H. (2012). Water-soluble chlorophyll protein (WSCP) of Arabidopsis is expressed in the gynoecium and developing silique. *Planta* **236**, 251–259.

Bencivenga, S., Colombo, L. and Masiero, S. (2011). Cross talk between the sporophyte and the megagametophyte during ovule development. *Sex. Plant Reprod.* **24**, 113–121.

Bencivenga, S., Simonini, S., Benková, E. and Colombo, L. (2012). The transcription factors BEL1 and SPL are required for cytokinin and auxin signaling during ovule development in Arabidopsis. *Plant Cell* **24**, 2886–2897.

Benková, E., Michniewicz, M., Sauer, M., Teichmann, T., Seifertová, D., Jürgens, G. and Friml, J. (2003). Local, efflux-dependent auxin gradients as a common module for plant organ formation. *Cell* **115**, 591–602.

Bennett, S. R. M., Alvarez, J., Bossinger, G. and Smyth, D. R. (1995). Morphogenesis in pinoid mutants of Arabidopsis thaliana. *Plant J.* **8**, 505–520.

Boex-Fontvieille, E., Rustgi, S., von Wettstein, D., Reinbothe, S. and Reinbothe, C. (2015). Water-soluble chlorophyll protein is involved in herbivore resistance activation during greening of Arabidopsis thaliana. *J. Exp. Bot.* **66**, 6119–6135.

Bowman, J. L., Smyth, D. R. and Meyerowitz, E. M. (1991). Genetic interactions among floral homeotic genes of Arabidopsis. *Development* **112**, 1–20.

Bowman, J. L., Baum, S. F., Eshed, Y., Putterill, J. and Alvarez, J. (1999a). Molecular Genetics of Gynoecium Development in Arabidopsis. In (ed. Pedersen, R. A.) and

Schatten, G. P.), pp. 155–205. Academic Press.

Bowman, J. L., Baum, S. F., Eshed, Y., Putterill, J. and Alvarez, J. (1999b). Molecular genetics of gynoecium development in Arabidopsis. *Curr. Top. Dev. Biol.* **45**, 155–205.

Bowman, J. L., Smyth, D. R. and Meyerowitz, E. M. (2007). Genes Directing Flower Development in Arabidopsis. *Plant Cell* **1**, 37.

Braatz, J., Harloff, H. J., Mascher, M., Stein, N., Himmelbach, A. and Jung, C. (2017). CRISPR-Cas9 targeted mutagenesis leads to simultaneous modification of different homoeologous gene copies in polyploid oilseed rape (Brassica napus). *Plant Physiol.* **174**, 935–942.

Braselton, J. P., Wilkinson, M. J. and Clulow, S. A. (1996). Feulgen Staining of Intact Plant Tissues for Confocal Microscopy. *Biotech. Histochem.* **71**, 84–87.

Broadhvest, J., Baker, S. C. and Gasser, C. S. (2000). SHORT INTEGUMENTS 2 promotes growth during Arabidopsis reproductive development. *Genetics* **155**, 899–907.

Carabelli, M., M., P., G., S., A., C., M., S., G., M., I., R., Carabelli, M., Possenti, M., Sessa, G., et al. (2007). Canopy shade causes a rapid and transient arrest in leaf development through auxin-induced cytokinin oxidase activity. *Genes Dev.* **21**, 1863–1868.

Carbonell-Bejerano, P., Urbez, C., Granell, A., Carbonell, J. and Perez-Amador, M. A. (2011). Ethylene is involved in pistil fate by modulating the onset of ovule senescence and the GA-mediated fruit set in Arabidopsis. *BMC Plant Biol.* **11**, 84.

Chae, K., Kieslich, C. A., Morikis, D., Kim, S.-C. and Lord, E. M. (2009). A Gain-of-Function Mutation of Arabidopsis Lipid Transfer Protein 5 Disturbs Pollen Tube Tip Growth and Fertilization . *Plant Cell* **21**, 3902–3914.

Cheng, Y., Dai, X. and Zhao, Y. (2006). Auxin biosynthesis by the YUCCA flavin monooxygenases controls the formation of floral organs and vascular tissues in Arabidopsis. *Genes Dev* **20**, 1790–1799.

Cifuentes-Esquivel, N., Bou-Torrent, J., Galstyan, A., Gallemí, M., Sessa, G., Salla Martret, M., Roig-Villanova, I., Ruberti, I. and Martínez-García, J. F. (2013). The bHLH proteins BEE and BIM positively modulate the shade avoidance syndrome in Arabidopsis seedlings. *Plant J.* **75**, 989–1002.

Clough, S. J. and Bent, A. F. (1998). Floral dip: A simplified method for Agrobacterium-mediated transformation of Arabidopsis thaliana. *Plant J.* **16**, 735–743.

Coimbra, S., Almeida, J., Junqueira, V., Costa, M. L. and Pereira, L. G. (2007). Arabinogalactan proteins as molecular markers in Arabidopsis thaliana sexual

reproduction. *J. Exp. Bot.* **58**, 4027–4035.

Coimbra, S., Costa, M., Jones, B., Mendes, M. A. and Pereira, L. G. (2009). Pollen grain development is compromised in Arabidopsis agp6 agp11 null mutants. *J. Exp. Bot.* **60**, 3133–3142.

Colombo, L., Battaglia, R. and Kater, M. M. (2008). Arabidopsis ovule development and its evolutionary conservation. *Trends Plant Sci.* **13**, 444–50.

Crawford, B. C. W. and Yanofsky, M. F. (2008). The Formation and Function of the Female Reproductive Tract in Flowering Plants. *Curr. Biol.* **18**, 972–978.

Crawford, B. C. W. and Yanofsky, M. F. (2011). HALF FILLED promotes reproductive tract development and fertilization efficiency in Arabidopsis thaliana. *Development* **138**, 2999–3009.

Crawford, B. C. W., Ditta, G. and Yanofsky, M. F. (2007). The NTT Gene Is Required for Transmitting-Tract Development in Carpels of Arabidopsis thaliana. *Curr. Biol.* **17**, 1101–1108.

Cucinotta, M., Colombo, L. and Roig-villanova, I. (2014). Ovule development , a new model for lateral organ formation. **5**, 1–12.

Cucinotta, M., Manrique, S., Guazzotti, A., Quadrelli, N. E., Mendes, M. A., Benkova, E. and Colombo, L. (2016). Cytokinin response factors integrate auxin and cytokinin pathways for female reproductive organ development. *Development* **143**, 4419–4424.

Cucinotta, M., Manrique, S., Cuesta, C., Benkova, E., Novak, O. and Colombo, L. (2018). CUP-SHAPED COTYLEDON1 (CUC1) and CUC2 regulate cytokinin homeostasis to determine ovule number in Arabidopsis. *J. Exp. Bot.* **69**, 5169–5176.

Davies, P. J. (2004). *Plant Hormones: biosynthesis, signal, transduction, action!* Kluwer Academic Publishers. Dordrecht, The Netherlands.

de Folter, S. and Angenent, G. C. (2006). trans meets cis in MADS science. *Trends Plant Sci.* **11**, 224–231.

De Folter, S., Urbanus, S. L., Van Zuijlen, L. G. C., Kaufmann, K. and Angenent, G. C. (2007). Tagging of MADS domain proteins for chromatin immunoprecipitation. *BMC Plant Biol.* **7**, 1–11.

Ding, J., Chen, B., Xia, X., Mao, W., Shi, K., Zhou, Y. and Yu, J. (2013). Cytokinin-Induced Parthenocarpic Fruit Development in Tomato Is Partly Dependent on Enhanced Gibberellin and Auxin Biosynthesis. *PLoS One* **8**, 1–11.

Dinneny, J. R., Weigel, D. and Yanofsky, M. F. (2005). A genetic framework for fruit patterning in Arabidopsis thaliana. *Development* **132**, 4687–4696.

Doench, J. G., Hartenian, E., Graham, D. B., Tothova, Z., Hegde, M., Smith, I., Sullender, M., Ebert, B. L., Xavier, R. J. and Root, D. E. (2014). Rational design of highly active sgRNAs for CRISPR-Cas9-mediated gene inactivation. *Nat. Biotechnol.* **32**, 1262–1267.

Dorcey, E., Urbez, C., Blázquez, M. A., Carbonell, J. and Perez-Amador, M. A. (2009). Fertilization-dependent auxin response in ovules triggers fruit development through the modulation of gibberellin metabolism in Arabidopsis. *Plant J.* **58**, 318–332.

Dreni, L., Pilatone, A., Yun, D., Erreni, S., Pajoro, A., Caporali, E., Zhang, D. and Kater, M. M. (2011). Functional Analysis of All AGAMOUS Subfamily Members in Rice Reveals Their Roles in Reproductive Organ Identity Determination and Meristem Determinacy. *Plant Cell* **23**, 2850–2863.

Drews, G. N. and Koltunow, A. M. . (2011). The Female Gametophyte. *Arab. B.* **9**, e0155.

Duszynska, D., McKeown, P. C., Juenger, T. E., Pietraszewska-Bogiel, A., Geelen, D. and Spillane, C. (2013). Gamete fertility and ovule number variation in selfed reciprocal F1 hybrid triploid plants are heritable and display epigenetic parent-of-origin effects. *New Phytol.* **198**, 71–81.

Egea-Cortines, M., Saedler, H. and Sommer, H. (1999). Ternary complex formation between the MADS-box proteins SQUAMOSA, DEFICIENS and GLOBOSA is involved in the control of floral architecture in Antirrhinum majus. *EMBO J.* **18**, 5370–5379.

Elliott, R. C., Betzner, A. S., Huttner, E., Oakes, M. P., Tucker, W. Q. J., Gerentes, D., Perez, P. and Smyth, D. R. (1996). AINTEGUMENTA, an APETALA2-like gene of arabidopsis with pleiotropic roles in ovule development and floral organ growth. *Plant Cell* **8**, 155–168.

Endress, P. K. (2011). Angiosperm ovules: diversity, development, evolution. *Ann. Bot.* **107**, 1465–89.

Endress, P. K. and Igersheim, A. (2000). Gynoecium Structure and Evolution in Basal Angiosperms. *Int. J. Plant Sci.* **161**, S211–S213.

Ezquer, I., Mizzotti, C., Nguema-Ona, E., Gotté, M., Beauzamy, L., Viana, V. E., Dubrulle, N., Costa de Oliveira, A., Caporali, E., Koroney, A.-S., et al. (2016). The Developmental Regulator SEEDSTICK Controls Structural and Mechanical Properties of the Arabidopsis Seed Coat. *Plant Cell* **28**, 2478–2492.

Fauser, F., Schiml, S. and Puchta, H. (2014). Both CRISPR/Cas-based nucleases and nickases can be used efficiently for genome engineering in Arabidopsis thaliana. *Plant J.*

79, 348–359.

Favaro, R., Pinyopich, A., Battaglia, R., Kooiker, M., Borghi, L., Ditta, G., Yanofsky, M. F., Kater, M. M. and Colombo, L. (2003). MADS-box protein complexes control carpel and ovule development in Arabidopsis. *Plant Cell* **15**, 2603–2611.

Ferrándiz, C., Pelaez, S. and Yanofsky, M. F. (1999). Control of Carpel and Fruit Development. *Annu. Rev. Biochem* 321–354.

Ferrándiz, C., Gu, Q., Martienssen, R. and Yanofsky, M. F. (2000a). Redundant regulation of meristem identity and plant architecture by FRUITFULL, APETALA1 and CAULIFLOWER. *Development* **127**, 725–34.

Ferrándiz, C., Liljegren, S. J. and Yanofsky, M. F. (2000b). Negative regulation of the SHATTERPROOF genes by FRUITFULL during Arabidopsis fruit development. *Science (80-.).* **289**, 436–438.

Flanagan, C. A., Hu, Y. and Ma, H. (1996). Specific expression of the AGL1 MADS-box gene suggests regulatory functions in Arabidopsis gynoecium and ovule development. *Plant J.* **10**, 343–353.

Frébort, I., Kowalska, M., Hluska, T., Frébortová, J. and Galuszka, P. (2011). Evolution of cytokinin biosynthesis and degradation. *J. Exp. Bot.* **62**, 2431–2452.

Friedrichsen, D. M., Nemhauser, J., Muramitsu, T., Maloof, J. N., Alonso, J., Ecker, J. R., Furuya, M. and Chory, J. (2002). Three redundant brassinosteroid early response genes encode putative bHLH transcription factors required for normal growth. *Genetics* **162**, 1445–1456.

Friml, J., Yang, X., Michniewicz, M., Weijers, D., Quint, A., Tietz, O., Benjamins, R., Ouwerkerk, P. B. F., Ljung, K., Sandberg, G., et al. (2004). A PINOID-Dependent Binary Switch in Apical-Basal PIN Polar Targeting Directs Auxin Efflux. *Sci.* **306**, 862–865.

Fukuchi-Mizutani, M., Tasaka, Y., Tanaka, Y., Ashikari, T., Kusumi, T. and Murata, N. (1998). Characterization of Δ9 acyl-lipid desaturase homologues from Arabidopsis thaliana. *Plant Cell Physiol.* **39**, 247–253.

Galbiati, F., Sinha Roy, D., Simonini, S., Cucinotta, M., Ceccato, L., Cuesta, C., Simaskova, M., Benková, E., Kamiuchi, Y., Aida, M., et al. (2013). An integrative model of the control of ovule primordia formation. *Plant J.* **76**, 446–55.

Galuszka, P., Popelková, H., Werner, T., Frébortová, J., Pospíšilová, H., Mik, V., Köllmer, I., Schmülling, T. and Frébort, I. (2007). Biochemical characterization of cytokinin oxidases/dehydrogenases from Arabidopsis thaliana expressed in Nicotiana

tabacum L. *J. Plant Growth Regul.* **26**, 255–267.

Gane, A. M., Clarke, A. E. and Bacic, A. (1995). Localisation and expression of arabinogalactan-proteins in the ovaries of Nicotiana alata Link and Otto. *Sex. Plant Reprod.* **8**, 278–282.

Gao, M. and Showalter, A. M. (1999). Yariv reagent treatment induces programmed cell death in Arabidopsis cell cultures and implicates arabinogalactan protein involvement. *Plant J.* **19**, 321–331.

Gasser, C. S. and Skinner, D. J. (2019). Development and evolution of the unique ovules of flowering plants.pp. 373–399.

Gasser, C. S., Broadhvest, J. and Hauser, B. A. (1998). GENETIC ANALYSIS OF OVULE DEVELOPMENT. *Annu. Rev. Plant Physiol. Plant Mol. Biol.* **49**, 1–24.

Girin, T., Paicu, T., Stephenson, P., Fuentes, S., Körner, E., O'Brien, M., Sorefan, K., Wood, T. A., Balanzá, V., Ferrándiz, C., et al. (2011). INDEHISCENT and SPATULA interact to specify carpel and valve margin tissue and thus promote seed dispersal in Arabidopsis. *Plant Cell* **23**, 3641–3653.

Gomez, M. D., Urbez, C., Perez-Amador, M. a and Carbonell, J. (2011). Characterization of constricted fruit (ctf) mutant uncovers a role for AtMYB117/LOF1 in ovule and fruit development in Arabidopsis thaliana. *PLoS One* **6**, e18760.

Gomez, M. D., Barro-Trastoy, D., Escoms, E., Saura-Sańchez, M., Sańchez, I., Briones-Moreno, A., Vera-Sirera, F., Carrera, E., Ripoll, J. J., Yanofsky, M. F., et al. (2018). Gibberellins negatively modulate ovule number in plants. *Dev.* **145**, dev163865.

Gómez, M. D., Fuster-Almunia, C., Ocaña-Cuesta, J., Alonso, J. M. and Pérez-Amador, M. A. (2019). RGL2 controls flower development, ovule number and fertility in Arabidopsis. *Plant Sci.* **281**, 82–92.

Gonçalves, B., Hasson, A., Belcram, K., Cortizo, M., Morin, H., Nikovics, K., Vialette-Guiraud, A., Takeda, S., Aida, M., Laufs, P., et al. (2015). A conserved role for CUP-SHAPED COTYLEDON genes during ovule development. *Plant J.* **83**, 732–742.

Govaerts, R. (2001). How many species of seed plants are there? *Taxon* **50**, 1085–1090.

Gremski, K., Ditta, G. and Yanofsky, M. F. (2007). The HECATE genes regulate female reproductive tract development in Arabidopsis thaliana. *Development* **134**, 3593–3601.

Grini, P. E., Thorstensen, T., Alm, V., Vizcay-Barrena, G., Windju, S. S., Jørstad, T. S., Wilson, Z. A. and Aalen, R. B. (2009). The ASH1 HOMOLOG 2 (ASHH2) histone H3 methyltransferase is required for ovule and anther development in Arabidopsis. *PLoS One* **4**,.

Gross, T., Broholm, S. and Becker, A. (2018). CRABS CLAW acts as a bifunctional transcription factor in flower development. *Front. Plant Sci.* **9**, 1–13.

Grossniklaus, U. and Schneitz, K. (1998). The molecular and genetic basis of ovule and megagametophyte development. *Semin. Cell Dev. Biol.* **9**, 227–238.

Groszmann, M., Paicu, T., Alvarez, J. P., Swain, S. M. and Smyth, D. R. (2011). SPATULA and ALCATRAZ, are partially redundant, functionally diverging bHLH genes required for Arabidopsis gynoecium and fruit development. *Plant J.* **68**, 816–829.

Gu, Q., Ferrándiz, C., Yanofsky, M. F. and Martienssen, R. (1998). The FRUITFULL MADS-box gene mediates cell differentiation during Arabidopsis fruit development. *Development* **125**, 1509–1517.

Guan, Y. and Nothnagel, E. A. (2004). Binding of Arabinogalactan Proteins by Yariv Phenylglycoside Triggers Wound-Like Responses in Arabidopsis Cell Cultures. *Plant Physiol.* **135**, 1346–1366.

Hedden, P. and Sponsel, V. (2015). A Century of Gibberellin Research. *J. Plant Growth Regul.* **34**, 740–760.

Heilmann, I., Pidkowich, M. S., Girke, T. and Shanklin, J. (2004). Switching desaturase enzyme specificity by alternate subcellular targeting. *Proc. Natl. Acad. Sci.* **101**, 10266–10271.

Heisler, M. G. B., Atkinson, A., Bylstra, Y. H., Walsh, R. and Smyth, D. R. (2001). SPATULA, a gene that controls development of carpel margin tissues in Arabidopsis, encodes a bHLH protein. *Development* **128**, 1089–98.

Herrera-Ubaldo, H. and de Folter, S. (2018). Exploring Cell Wall Composition and Modifications During the Development of the Gynoecium Medial Domain in Arabidopsis. *Front. Plant Sci.* **9**, 1–11.

Herrera-Ubaldo, H., Lozano-Sotomayor, P., Ezquer, I., Di Marzo, M., Chávez Montes, R. A., Gómez-Felipe, A., Pablo-Villa, J., Diaz-Ramirez, D., Ballester, P., Ferrándiz, C., et al. (2019). New roles of NO TRANSMITTING TRACT and SEEDSTICK during medial domain development in Arabidopsis fruits . *Development* **146**, dev172395.

Heyl, A. and Schmülling, T. (2003). Cytokinin signal perception and transduction. *Curr. Opin. Plant Biol.* **6**, 480–488.

Higuchi, M., Pischke, M. S., Mähönen, A. P., Miyawaki, K., Hashimoto, Y., Seki, M., Kobayashi, M., Shinozaki, K., Kato, T., Tabata, S., et al. (2004). In planta functions of the Arabidopsis cytokinin receptor family. *Proc. Natl. Acad. Sci. U. S. A.* **101**, 8821–8826.

Hill, T. A., Broadhvest, J., Kuzoff, R. K. and Gasser, C. S. (2006). Arabidopsis SHORT INTEGUMENTS 2 Is a Mitochondrial DAR GTPase. *Genetics* **174**, 707–718.

Hoggart, R. M. and Clarke, A. E. (1984). Arabinogalactans are common components of angiosperm styles. *Phytochemistry* **23**, 1571–1573.

Hu, Xie and Chua (2003). The Arabidopsis Auxin-Inducible Gene ARGOS Controls Lateral Organ Size. *Plant Cell* **15**, 1951–1961.

Huang, H. Y., Jiang, W. B., Hu, Y. W., Wu, P., Zhu, J. Y., Liang, W. Q., Wang, Z. Y. and Lin, W. H. (2013). BR signal influences arabidopsis ovule and seed number through regulating related genes expression by BZR1. *Mol. Plant* **6**, 456–469.

Iglesias, F. M. and Cerdán, P. D. (2016). Maintaining Epigenetic Inheritance During DNA Replication in Plants. *Front. Plant Sci.* **7**,.

Ishida, T., Aida, M., Takada, S. and Tasaka, M. (2000a). Involvement of CUP-SHAPED COTYLEDON genes in gynoecium and ovule development in Arabidopsis thaliana. *Plant Cell Physiol.* **41**, 60–67.

Ishida, T., Aida, M., Takada, S. and Tasaka, M. (2000b). Involvement of CUP-SHAPED COTYLEDON genes in gynoecium and ovule development in Arabidopsis thaliana. *Plant Cell Physiol.* **41**, 60–7.

Ishida, T., Fukuda, H., Nagawa, S., Ueda, N., Sakakibara, H., Sugimoto, K., Kuroha, T., Kojima, M. and Tokunaga, H. (2009). Functional Analyses of LONELY GUY Cytokinin-Activating Enzymes Reveal the Importance of the Direct Activation Pathway in Arabidopsis. *Plant Cell* **21**, 3152–3169.

Jofuku, K. D., Omidyar, P. K., Gee, Z. and Okamuro, J. K. (2005). Control of seed mass and seed yield by the floral homeotic gene APETALA2. *Proc. Natl. Acad. Sci.* **102**, 3117–3122.

Kant, S., Burch, D., Badenhorst, P., Palanisamy, R., Mason, J. and Spangenberg, G. (2015). Regulated Expression of a cytokinin biosynthesis gene IPT delays leaf senescence and improves yield under rainfed and irrigated conditions in canola (Brassica napus L.). *PLoS One* **10**, 1–18.

Klucher, K. M., Chow, H., Reiser, L. and Fischer, R. L. (1996). The AINTEGUMENTA gene of Arabidopsis required for ovule and female gametophyte development is related to the floral homeotic gene APETALA2. *Plant Cell* **8**, 137–153.

Knauss, S., Rohrmeier, T. and Lehle, L. (2003). The auxin-induced maize gene ZmSAUR2 encodes a short-lived nuclear protein expressed in elongating tissues. *J. Biol. Chem.* **278**, 23936–23943.

Köllmer, I., Novák, O., Strnad, M., Schmülling, T. and Werner, T. (2014). Overexpression of the cytosolic cytokinin oxidase/dehydrogenase (CKX7) from Arabidopsis causes specific changes in root growth and xylem differentiation. *Plant J.* **78**, 359–371.

Kowalska, M., Galuszka, P., Frébortová, J., Šebela, M., Béres, T., Hluska, T., Šmehilová, M., Bilyeu, K. D. and Frébort, I. (2010). Vacuolar and cytosolic cytokinin dehydrogenases of Arabidopsis thaliana: Heterologous expression, purification and properties. *Phytochemistry* **71**, 1970–1978.

Krizek, B. A. (2009). AINTEGUMENTA and AINTEGUMENTA-LIKE6 act redundantly to regulate arabidopsis floral growth and patterning. *Plant Physiol.* **150**, 1916–1929.

Kunst, L. and Samuels, A. L. (2003). Biosynthesis and secretion of plant cuticular wax. *Prog. Lipid Res.* **42**, 51–80.

Langmead Ben and Steven, S. (2012). Fast gapped-read alignment with Bowtie 2. *Nat. Methods* **9**, 357–359.

Larsson, E., Franks, R. G. and Sundberg, E. (2013a). Auxin and the arabidopsis thaliana gynoecium. *J. Exp. Bot.* **64**, 2619–2627.

Larsson, E., Franks, R. G. and Sundberg, E. (2013b). Auxin and the Arabidopsis thaliana gynoecium. *J. Exp. Bot.* **64**, 2619–27.

Laufs, P., Peaucelle, A., Morin, H. and Traas, J. (2004). MicroRNA regulation of the CUC genes is required for boundary size control in Arabidopsis meristems. *Development* **131**, 4311–22.

Lavy, M. and Estelle, M. (2016). Mechanisms of auxin signaling. *Development* **143**, 3226–3229.

Lennon, K. A., Stéphane, R., Peter, H. K. and Lord, E. M. (1998). The structure of the transmitting tissue of Arabidopsis thaliana (L.) and the path of pollen tube growth. *Sex. Plant Reprod.* 49–59.

Li, B. and Dewey, C. N. (2011). RSEM: Accurate transcript quantification from RNA-seq data with or without a reference genome. *BMC, Bionformatics* **12**, 41–74.

Liljegren, S. J., Ditta, G. S., Eshed, Y., Savidge, B., Bowman, J. L. and Yanofsky, M. F. (2000). SHATTERPROOF MADS-box genes control seed dispersal in Arabidopsis. *Nature* **404**, 766–770.

Liljegren, S. J., Roeder, A. H. K., Kempin, S. a., Gremski, K., Østergaard, L., Guimil, S., Reyes, D. K. and Yanofsky, M. F. (2004). Control of fruit patterning in Arabidopsis by INDEHISCENT. *Cell* **116**, 843–853.

Liu, Z., Franks, R. G. and Klink, V. P. (2000). Regulation of gynoecium marginal tissue formation by LEUNIG and AINTEGUMENTA. *Plant Cell* **12**, 1879–1891.

Liu, H., Ding, Y., Zhou, Y., Jin, W., Xie, K. and Chen, L. L. (2017). CRISPR-P 2.0: An Improved CRISPR-Cas9 Tool for Genome Editing in Plants. *Mol. Plant* **10**, 530–532.

Liu, P., Zhang, C., Ma, J. Q., Zhang, L. Y., Yang, B., Tang, X. Y., Huang, L., Zhou, X. T., Lu, K. and Li, J. N. (2018). Genome-wide identification and expression profiling of cytokinin oxidase/dehydrogenase (CKX) genes reveal likely roles in pod development and stress responses in oilseed rape (brassica napus L.). *Genes (Basel).* **9**, 168.

Lombard, V., Golaconda Ramulu, H., Drula, E., Coutinho, P. M. and Henrissat, B. (2014). The carbohydrate-active enzymes database (CAZy) in 2013. *Nucleic Acids Res.* **42**, 490–495.

Lord, E. M. and Russell, S. D. (2002). The Mechanisms of Pollination and Fertilization in Plants. *Annu. Rev. Cell Dev. Biol.* **18**, 81–105.

Mallory, A. C., Reinhart, B. J., Jones-Rhoades, M. W., Tang, G., Zamore, P. D., Barton, M. K. and Bartel, D. P. (2004). MicroRNA control of PHABULOSA in leaf development: importance of pairing to the microRNA 5′ region. *EMBO J.* **23**, 3356–3364.

Mantegazza, O., Gregis, V., Mendes, M. A., Morandini, P., Alves-Ferreira, M., Patreze, C. M., Nardeli, S. M., Kater, M. M. and Colombo, L. (2014). Analysis of the arabidopsis REM gene family predicts functions during flower development. *Ann. Bot.* **114**, 1507–1515.

Marhavý, P., Bielach, A., Abas, L., Abuzeineh, A., Duclercq, J., Tanaka, H., Pařezová, M., Petrášek, J., Friml, J., Kleine-Vehn, J., et al. (2011). Cytokinin Modulates Endocytic Trafficking of PIN1 Auxin Efflux Carrier to Control Plant Organogenesis. *Dev. Cell* **21**, 796–804.

Marsch-Martínez, N. and de Folter, S. (2016). Hormonal control of the development of the gynoecium. *Curr. Opin. Plant Biol.* **29**, 104–114.

Marsch-Martínez, N., Ramos-Cruz, D., Irepan Reyes-Olalde, J., Lozano-Sotomayor, P., Zúñiga-Mayo, V. M. and De Folter, S. (2012). The role of cytokinin during Arabidopsis gynoecia and fruit morphogenesis and patterning. *Plant J.* **72**, 222–234.

Masiero, S., Palme, K., Roig-Villanova, I., Sinha Roy, D., Colombo, L., Ditengou, F. A., Bencivenga, S., Simon, R. and Ceccato, L. (2013). Maternal Control of PIN1 Is Required for Female Gametophyte Development in Arabidopsis. *PLoS One* **8**, e66148.

Matias-Hernandez, L., Battaglia, R., Galbiati, F., Rubes, M., Eichenberger, C.,

Grossniklaus, U., Kater, M. M. and Colombo, L. (2010). *VERDANDI* Is a Direct Target of the MADS Domain Ovule Identity Complex and Affects Embryo Sac Differentiation in *Arabidopsis*. *Plant Cell* **22**, 1702–1715.

McClure, B. A. and Guilfoyle, T. (1987). Characterization of a class of small auxin-inducible soybean polyadenylated RNAs. *Plant Mol. Biol.* **9**, 611–623.

Mendes, M. A., Guerra, R. F., Castelnovo, B., Silva-Velazquez, Y., Morandini, P., Manrique, S., Baumann, N., Groß-Hardt, R., Dickinson, H. and Colombo, L. (2016). Live and let die: a REM complex promotes fertilization through synergid cell death in *Arabidopsis*. *Development* **143**, 2780–2790.

Michaels, S. D. and Amasino, R. M. (2007). FLOWERING LOCUS C Encodes a Novel MADS Domain Protein That Acts as a Repressor of Flowering. *Plant Cell* **11**, 949.

Minic, Z., Do, C. T., Rihouey, C., Morin, H., Lerouge, P. and Jouanin, L. (2006). Purification, functional characterization, cloning, and identification of mutants of a seed-specific arabinan hydrolase in Arabidopsis. *J. Exp. Bot.* **57**, 2339–2351.

Mizukami, Y. and Fischer, R. L. (2000). Plant organ size control: AINTEGUMENTA regulates growth and cell numbers during organogenesis. *Proc. Natl. Acad. Sci. U. S. A.* **97**, 942–947.

Mizzotti, C., Mendes, M. A., Caporali, E., Schnittger, A., Kater, M. M., Battaglia, R. and Colombo, L. (2012). The MADS box genes SEEDSTICK and ARABIDOPSIS Bsister play a maternal role in fertilization and seed development. *Plant J.* **70**, 409–420.

Mizzotti, C., Ezquer, I., Paolo, D., Rueda-Romero, P., Guerra, R. F., Battaglia, R., Rogachev, I., Aharoni, A., Kater, M. M., Caporali, E., et al. (2014). SEEDSTICK is a Master Regulator of Development and Metabolism in the Arabidopsis Seed Coat. *PLoS Genet.* **10**, e1004856.

Mizzotti, C., Rotasperti, L., Moretto, M., Tadini, L., Resentini, F., Galliani, B. M., Galbiati, M., Engelen, K., Pesaresi, P. and Masiero, S. (2018). Time-course transcriptome analysis of arabidopsis siliques discloses genes essential for fruit development and maturation. *Plant Physiol.* **178**, 1249–1268.

Mok, D. W. S. and Mok, M. C. (2001). CYTOKININ METABOLISM AND ACTION. *Annu. Rev. Plant Physiol. Plant Mol. Bio* **52**, 89–118.

Molkentin, J. D., Black, B. L., Martin, J. F. and Olson, E. N. (1995). Cooperative activation of muscle gene expression by MEF2 and myogenic bHLH proteins. *Cell* **83**, 1125–1136.

Moubayidin, L. and Østergaard, L. (2014). Dynamic control of auxin distribution imposes

a bilateral-to-radial symmetry switch during gynoecium development. *Curr. Biol.* **24**, 2743–2748.

Nahar, M. A. U., Ishida, T., Smyth, D. R., Tasaka, M. and Aida, M. (2012). Interactions of CUP-SHAPED COTYLEDON and SPATULA genes control carpel margin development in arabidopsis thaliana. *Plant Cell Physiol.* **53**, 1134–1143.

Nakamura, A., Nakajima, N., Goda, H., Shimada, Y., Hayashi, K. I., Nozaki, H., Asami, T., Yoshida, S. and Fujioka, S. (2006). Arabidopsis Aux/IAA genes are involved in brassinosteroid-mediated growth responses in a manner dependent on organ type. *Plant J.* **45**, 193–205.

Nawrath, C. (2006). Unraveling the complex network of cuticular structure and function. *Curr. Opin. Plant Biol.* **9**, 281–287.

Nemhauser, J. L., Feldman, L. J. and Zambryski, P. C. (2000). Auxin and ETTIN in Arabidopsis gynoecium morphogenesis. *Development* **127**, 3877–3888.

Nieuwland, J., Feron, R., Huisman, B. A. H., Fasolino, A., Hilbers, C. W., Derksen, J. and Mariani, C. (2005). Lipid Transfer Proteins Enhance Cell Wall Extension in Tobacco. *Plant Cell* **17**, 2009–2019.

Nole-Wilson, S., Rueschhoff, E. E., Bhatti, H. and Franks, R. G. (2010a). Synergistic disruptions in seuss cyp85A2 double mutants reveal a role for brassinolide synthesis during gynoecium and ovule development. *BMC Plant Biol.* **10**, 198.

Nole-Wilson, S., Azhakanandam, S. and Franks, R. G. (2010b). Polar auxin transport together with aintegumenta and revoluta coordinate early Arabidopsis gynoecium development. *Dev. Biol.* **346**, 181–95.

Nomura, T., Kushiro, T., Yokota, T., Kamiya, Y., Bishop, G. J. and Yamaguchi, S. (2005). The last reaction producing brassinolide is catalyzed by cytochrome P-450s, CYP85A3 in tomato and CYP85A2 in Arabidopsis. *J. Biol. Chem.* **280**, 17873–17879.

Novák, O., Hauserová, E., Amakorová, P., Doležal, K. and Strnad, M. (2008). Cytokinin profiling in plant tissues using ultra-performance liquid chromatography-electrospray tandem mass spectrometry. *Phytochemistry* **69**, 2214–2224.

Ohto, M. aki, Floyd, S. K., Fischer, R. L., Goldberg, R. B. and Harada, J. J. (2009). Effects of APETALA2 on embryo, endosperm, and seed coat development determine seed size in Arabidopsis. *Sex. Plant Reprod.* **22**, 277–289.

Okada, K., Ueda, J., Komaki, M. K., Bell, C. J. and Shimura, Y. (1991). Requirement of the Auxin Polar Transport System in Early Stages of Arabidopsis Floral Bud Formation. *Plant Cell Online* **3**, 677–684.

Pagnussat, G. C. (2005). Genetic and molecular identification of genes required for female gametophyte development and function in Arabidopsis. *Development* **132**, 603–614.

Panikashvili, D., Shi, J. X., Bocobza, S., Franke, R. B., Schreiber, L. and Aharoni, A. (2010). The arabidopsis DSO/ABCG11 transporter affects cutin metabolism in reproductive organs and suberin in roots. *Mol. Plant* **3**, 563–575.

Pinto, S. C., Mendes, M. A., Coimbra, S. and Tucker, M. R. (2019). Revisiting the Female Germline and Its Expanding Toolbox. *Trends Plant Sci.* **24**, 455–467.

Pinyopich, A., Ditta, G. S., Savidge, B., Liljegren, S. J., Baumann, E., Wisman, E. and Yanofsky, M. F. (2003). Assessing the redundancy of MADS-box genes during carpel and ovule development. *Nature* **424**, 85–8.

Poppenberger, B., Rozhon, W., Khan, M., Husar, S., Adam, G., Luschnig, C., Fujioka, S. and Sieberer, T. (2011). CESTA, a positive regulator of brassinosteroid biosynthesis. *EMBO J.* **30**, 1149–1161.

Rate, D. N., Cuenca, J. V., Bowman, G. R., Guttman, D. S. and Greenberg, J. T. (2007). The Gain-of-Function Arabidopsis acd6 Mutant Reveals Novel Regulation and Function of the Salicylic Acid Signaling Pathway in Controlling Cell Death, Defenses, and Cell Growth. *Plant Cell* **11**, 1695.

Reiser, L. and Fischer, R. L. (1993). The Ovule and the Embryo Sac. *Plant Cell* **5**, 1291–1301.

Reyes-Olalde, J. I. and de Folter, S. (2019). Control of stem cell activity in the carpel margin meristem (CMM) in Arabidopsis. *Plant Reprod.* **32**, 123–136.

Reyes-Olalde, J. I., Zuñiga-Mayo, V. M., Chávez Montes, R. A., Marsch-Martínez, N. and de Folter, S. (2013). Inside the gynoecium: At the carpel margin. *Trends Plant Sci.* **18**, 644–655.

Reyes-Olalde, J. I., Marsch-Martínez, N. and de Folter, S. (2015). Imaging early stages of the female reproductive structure of arabidopsis by confocal laser scanning microscopy. *Dev. Dyn.* **244**, 1286–1290.

Reyes-Olalde, J. I., Montes, A. C., Lozano-sotomayor, P., Herrera-ubaldo, H., Ezquer, I., Ballester, P., Jose, J., Paolo, D., Heyl, A., Colombo, L., et al. (2017). *The bHLH transcription factor SPATULA enables cytokinin signaling , and both activate auxin biosynthesis and transport genes at the medial domain of the gynoecium*.

Ripoll, J. J., Roeder, A. H. K., Ditta, G. S. and Yanofsky, M. F. (2011). A novel role for the floral homeotic gene APETALA2 during Arabidopsis fruit development. *Development* **138**, 5167–5176.

Ripoll, J. J., Bailey, L. J., Mai, Q.-A., Wu, S. L., Hon, C. T., Chapman, E. J., Ditta, G. S., Estelle, M. and Yanofsky, M. F. (2015). microRNA regulation of fruit growth. *Nat. Plants* **1**, 15036.

Rizza, A. and Jones, A. M. (2019). The makings of a gradient: spatiotemporal distribution of gibberellins in plant development. *Curr. Opin. Plant Biol.* **47**, 9–15.

Robert, H. S., Crhak Khaitova, L., Mroue, S. and Benková, E. (2015). The importance of localized auxin production for morphogenesis of reproductive organs and embryos in Arabidopsis. *J. Exp. Bot.* **66**, 5029–5042.

Robinson, M. D., McCarthy, D. J. and Smyth, G. K. (2009). edgeR: A Bioconductor package for differential expression analysis of digital gene expression data. *Bioinformatics* **26**, 139–140.

Roeder, A. H. K. and Yanofsky, M. F. (2006). *Fruit Development in Arabidopsis*.

Roeder, A. H. K., Ferrándiz, C. and Yanofsky, M. F. (2003). The Role of the REPLUMLESS Homeodomain Protein in Patterning the Arabidopsis Fruit. *Curr. Biol.* **13**, 1630–1635.

Romanov, G. A., Lomin, S. N. and Schmülling, T. (2006). Biochemical characteristics and ligand-binding properties of Arabidopsis cytokinin receptor AHK3 compared to CRE1/AHK4 as revealed by a direct binding assay. *J. Exp. Bot.* **57**, 4051–4058.

Ruzicka, K., Simásková, M., Duclercq, J., Petrásek, J., Zazímalová, E., Simon, S., Friml, J., Van Montagu, M. C. E. and Benková, E. (2009). Cytokinin regulates root meristem activity via modulation of the polar auxin transport. *Proc. Natl. Acad. Sci. U. S. A.* **106**, 4284–4289.

Sakakibara, H. (2006). CYTOKININS: Activity, Biosynthesis, and Translocation. *Annu. Rev. Plant Biol.* **57**, 431–449.

Sarojam Rajani and Venkatesan Sundaresan (2001). The Arabidopsis myc / bHLH gene ALCATRAZ enables cell separation in fruit dehiscence Sarojam Rajani * † and Venkatesan Sundaresan * ‡. *Curr. Biol.* **1**, 1914–1922.

Savidge, B., Rounsley, S. D. and Yanofsky, M. F. (1995). Temporal Relationship between the Transcription of Two Arabidopsis MADS Box Genes and the Floral Organ Identity Genes. *Plant Cell* **7**, 721.

Schaller, G. E., Bishopp, A. and Kieber, J. J. (2015). The Yin-Yang of Hormones: Cytokinin and Auxin Interactions in Plant Development. *Plant Cell Online* **27**, 44–63.

Schindelin, J., Arganda-Carreras, I., Frise, E., Kaynig, V., Longair, M., Pietzsch, T., Preibisch, S., Rueden, C., Saalfeld, S., Schmid, B., et al. (2012). Fiji: An open-source

platform for biological-image analysis. *Nat. Methods* **9**, 676–682.

Schlereth, A., Moller, B., Liu, W., Kientz, M., Flipse, J., Rademacher, E. H., Schmid, M., Jurgens, G. and Weijers, D. (2010). MONOPTEROS controls embryonic root initiation by regulating a mobile transcription factor. *Nature* **464**, 913–916.

Schmülling, T., Werner, T., Riefler, M., Krupková, E., Bartrina, I. and Manns (2003). Structure and function of cytokinin oxidase/dehydrogenase genes of maize, rice, Arabidopsis and other species. *J. Plant Res.* 241–252.

Schneitz, K., Hulskamp, M. and Pruitt, R. E. (1995). Wild-type ovule development in Arabidopsis thaliana: a light microscope study of cleared whole-mount tissue. *Plant J.* **7**, 731–749.

Schneitz, K., Baker, S. C., Gasser, C. S. and Redweik, A. (1998). Pattern formation and growth during floral organogenesis: HUELLENLOS and AINTEGUMENTA are required for the formation of the proximal region of the ovule primordium in Arabidopsis thaliana. *Development* **125**, 2555–63.

Schuster, C., Gaillochet, C. and Lohmann, J. U. (2015). Arabidopsis HECATE genes function in phytohormone control during gynoecium development. *Dev.* **142**, 3343–3350.

Sessions, A., Nemhauser, J. L., McColl, A., Roe, J. L., Feldmann, K. A. and Zambryski, P. C. (1997). ETTIN patterns the Arabidopsis floral meristem and reproductive organs. *Development* **124**, 4481–4491.

Shah, S., Karunarathna, N. L., Jung, C. and Emrani, N. (2018). An APETALA1 ortholog affects plant architecture and seed yield component in oilseed rape (Brassica napus L.). *BMC Plant Biol.* **18**, 1–12.

Sheldon, C. C., Burn, J. E., Perez, P. P., Metzger, J., Edwards, J. A., Peacock, W. J. and Dennis, E. S. (2007). The FLF MADS Box Gene: A Repressor of Flowering in Arabidopsis Regulated by Vernalization and Methylation. *Plant Cell* **11**, 445.

Shi, D.-Q. and Yang, W.-C. (2011). Ovule development in Arabidopsis: progress and challenge. *Curr. Opin. Plant Biol.* **14**, 74–80.

Shirley, N. J., Aubert, M. K., Wilkinson, L. G., Bird, D. C., Lora, J., Yang, X. and Tucker, M. R. (2019). Translating auxin responses into ovules, seeds and yield: Insight from Arabidopsis and the cereals. *J. Integr. Plant Biol.* **61**, 310–336.

Sieber, P., Schorderet, M., Ryser, U., Buchala, A., Kolattukudy, P., Metraux, J.-P. and Nawrath, C. (2007). Transgenic Arabidopsis Plants Expressing a Fungal Cutinase Show Alterations in the Structure and Properties of the Cuticle and Postgenital Organ Fusions.

Plant Cell **12**, 721.

Šimášková, M., O'Brien, J. A., Khan, M., Van Noorden, G., Ötvös, K., Vieten, A., De Clercq, I., Van Haperen, J. M. A., Cuesta, C., Hoyerová, K., et al. (2015). Cytokinin response factors regulate PIN-FORMED auxin transporters. *Nat. Commun.* **6**, 8717.

Skinner, D. J., Baker, S. C., Meister, R. J., Broadhvest, J., Schneitz, K. and Gasser, C. S. (2001). The Arabidopsis HUELLENLOS gene, which is essential for normal ovule development, encodes a mitochondrial ribosomal protein. *Plant Cell* **13**, 2719–30.

Skinner, D. J., Hill, T. A. and Gasser, C. S. (2004). Regulation of Ovule Development. **16**, 32–46.

Smyth, D. R., Bowman, J. L. and Meyerowitz, E. M. (1990). Early flower development in Arabidopsis. *Plant Cell* **2**, 755–767.

Snowdon, Rod, Lühs, Wilfried, Friedt, W. (2007). Genome Mapping and Molecular Breeding in Plants - Oilseeds. **6**, 54–56.

Sohlberg, J. J., Myrenås, M., Kuusk, S., Lagercrantz, U., Kowalczyk, M., Sandberg, G. and Sundberg, E. (2006). STY1 regulates auxin homeostasis and affects apical-basal patterning of the Arabidopsis gynoecium. *Plant J.* **47**, 112–23.

Song, J., Jiang, L. and Jameson, P. E. (2015). Expression patterns of Brassica napus genes implicate IPT, CKX, sucrose transporter, cell wall invertase, and amino acid permease gene family members in leaf, flower, silique, and seed development. *J. Exp. Bot.* **66**, 5067–5082.

Spíchal, L. (2012). Cytokinins - recent news and views of evolutionally old molecules. *Funct. Plant Biol.* **39**, 267.

Stinchcombe, J. R., Weinig, C., Ungerer, M., Olsen, K. M., Mays, C., Halldorsdottir, S. S., Purugganan, M. D. and Schmitt, J. (2004). A latitudinal cline in flowering time in Arabidopsis thaliana modulated by the flowering time gene FRIGIDA. *Proc. Natl. Acad. Sci. U. S. A.* **101**, 4712–7.

Stolz, A., Riefler, M., Lomin, S. N., Achazi, K., Romanov, G. A. and Schmülling, T. (2011). The specificity of cytokinin signalling in Arabidopsis thaliana is mediated by differing ligand affinities and expression profiles of the receptors. *Plant J.* **67**, 157–168.

Street, I. H., Mathews, D. E., Yamburkenko, M. V., Sorooshzadeh, A., John, R. T., Swarup, R., Bennett, M. J., Kieber, J. J. and Schaller, G. E. (2016). Cytokinin acts through the auxin influx carrier AUX1 to regulate cell elongation in the root. *Development* **143**, 3982–3993.

Sun, Y., Fan, X.-Y., Cao, D.-M., Tang, W., He, K., Zhu, J.-Y., He, J.-X., Bai, M.-Y., Zhu,

S., Oh, E., et al. (2010). Integration of Brassinosteroid Signal Transduction with the Transcription Network for Plant Growth Regulation in Arabidopsis. *Dev. Cell* **19**, 765–777.

Svačinová, J., Novák, O., Plačková, L., Lenobel, R., Holík, J., Strnad, M. and Doležal, K. (2012). A new approach for cytokinin isolation from Arabidopsis tissues using miniaturized purification: pipette tip solid-phase extraction. *Plant Methods* **8**, 1–14.

Takahashi, K., Shimada, T., Kondo, M., Tamai, A., Mori, M., Nishimura, M. and Hara-Nishimura, I. (2010). Ectopic expression of an esterase, which is a candidate for the unidentified plant cutinase, causes cuticular defects in arabidopsis thaliana. *Plant Cell Physiol.* **51**, 123–131.

Tan, M., Li, G., Qi, S., Liu, X., Chen, X., Ma, J., Zhang, D. and Han, M. (2018). Identification and expression analysis of the IPT and CKX gene families during axillary bud outgrowth in apple (Malus domestica Borkh.). *Gene* **651**, 106–117.

Theo C.Verwoerd, Ben M.M.Dekker and Andre Hoekema (1989). A small scale procedure for the rapid isolation of plant RNAs. *Nucleic Acid Res.* **17**, 2362.

Tung, C.-W., Dwyer, K. G., Nasrallah, M. E. and Nasrallah, J. B. (2005). Genome-Wide Identification of Genes Expressed in Arabidopsis Pistils Specifically along the Path of Pollen Tube Growth. *Plant Physiol.* **138**, 977–989.

Turbant, A., Fournet, F., Lequart, M., Zabijak, L., Pageau, K., Bouton, S. and Van Wuytswinkel, O. (2016). PME58 plays a role in pectin distribution during seed coat mucilage extrusion through homogalacturonan modification. *J. Exp. Bot.* **67**, 2177–2190.

van Mourik, H., van Dijk, A. D. J., Stortenbeker, N., Angenent, G. C. and Bemer, M. (2017). Divergent regulation of Arabidopsis SAUR genes: A focus on the SAUR10-clade. *BMC Plant Biol.* **17**, 1–14.

Vanstraelen, M. and Benková, E. (2012). Hormonal interactions in the regulation of plant development. *Annu. Rev. Cell Dev. Biol.* **28**, 463–87.

Vivian-Smith, A. and Koltunow, A. M. (1999). Genetic analysis of growth-regulator-induced parthenocarpy in Arabidopsis. *Plant Physiol.* **121**, 437–51.

Vivian-Smith, A., Luo, M., Chaudhury, A. and Koltunow, A. (2001). Fruit development is actively restricted in the absence of fertilization in Arabidopsis. *Development* **128**, 2321–31.

Webb, M. C. and Williams, E. G. (1988). The Pollen Tube Pathway in the Pistil of Lycopersicon peruvianum. *Ann. Bot.* **61**, 415–423.

Werner, T. and Schmülling, T. (2009). Cytokinin action in plant development. *Curr. Opin. Plant Biol.* **12**, 527–538.

Werner, T., Motyka, V., Laucou, V., Smets, R., Van Onckelen, H. and Schmülling, T. (2003). Cytokinin-Deficient Transgenic Arabidopsis Plants Show Multiple Developmental Alterations Indicating Opposite Functions of Cytokinins in the Regulation of Shoot and Root Meristem Activity. *Plant Cell Online* **15**, 2532–2550.

Wetzstein, H. Y., Yi, W., Porter, J. A. and Ravid, N. (2013). Flower Position and Size Impact Ovule Number per Flower, Fruitset, and Fruit Size in Pomegranate. *J. Am. Soc. Hortic. Sci.* **138**, 159–166.

Willis, K.J. Royal Botanic Gardens, K. (2017). State of the World's Plants 2017. Report.

Wrzaczek, M., Brosche, M., Kollist, H. and Kangasjarvi, J. (2009). Arabidopsis GRI is involved in the regulation of cell death induced by extracellular ROS. *Proc. Natl. Acad. Sci.* **106**, 5412–5417.

Wrzaczek, M., Vainonen, J. P., Stael, S., Tsiatsiani, L., Help-Rinta-Rahko, H., Gauthier, A., Kaufholdt, D., Bollhoner, B., Lamminmaki, A., Staes, A., et al. (2015). GRIM REAPER peptide binds to receptor kinase PRK5 to trigger cell death in Arabidopsis. *EMBO J.* **34**, 55–66.

Wurschum, T., Groß-hardt, R. and Laux, T. (2006). APETALA2 Regulates the Stem Cell Niche in the Arabidopsis Shoot Meristem, Supplemental Date2.pdf. **18**, 295–307.

Wynn, A. N., Seaman, A. A., Jones, A. L. and Franks, R. G. (2014). Novel functional roles for PERIANTHIA and SEUSS during floral organ identity specification, floral meristem termination, and gynoecial development. *Front. Plant Sci.* **5**,.

Xu, L., Zhao, Z., Dong, A., Soubigou-Taconnat, L., Renou, J.-P., Steinmetz, A. and Shen, W.-H. (2008). Di- and Tri- but Not Monomethylation on Histone H3 Lysine 36 Marks Active Transcription of Genes Involved in Flowering Time Regulation and Other Processes in Arabidopsis thaliana. *Mol. Cell. Biol.* **28**, 1348–1360.

Yang, Y., Wang, Y., Zhan, J., Shi, J., Wang, X., Liu, G. and Wang, H. (2017). Genetic and Cytological Analyses of the Natural Variation of file:///Users/mauriziodimarzo/Downloads/2007_Bookmatter_Oilseeds.pdfSeed Number per Pod in Rapeseed (Brassica napus L.). *Front. Plant Sci.* **8**, 1890.

Yant, L., Mathieu, J., Dinh, T. T., Ott, F., Lanz, C., Wollmann, H., Chen, X. and Schmid, M. (2010). Orchestration of the Floral Transition and Floral Development in Arabidopsis by the Bifunctional Transcription Factor APETALA2. *Plant Cell Online* **22**, 2156–2170.

Yao, K., Bacchetto, R. G., Lockhart, K. M., Friesen, L. J., Potts, D. A., Covello, P. S. and Taylor, D. C. (2003). Expression of the Arabidopsis ADS1 gene in Brassica juncea results in a decreased level of total saturated fatty acids. *Plant Biotechnol. J.* **1**, 221–229.

Yeats, T. H. and Rose, J. K. C. (2013). The Formation and Function of Plant Cuticles. *Plant Physiol.* **163**, 5–20.

Yuan, J. and Kessler, S. A. (2019). A genome-wide association study reveals a novel regulator of ovule number and fertility in Arabidopsis thaliana. *PLOS Genet.* **15**, e1007934.

Zuñiga-Mayo, V. M., Baños-Bayardo, C. R., Díaz-Ramírez, D., Marsch-Martínez, N. and De Folter, S. (2018). Conserved and novel responses to cytokinin treatments during flower and fruit development in Brassica napus and Arabidopsis thaliana. *Sci. Rep.* **8**, 1–10.

Zúñiga-Mayo, V. M., Gómez-Felipe, A., Herrera-Ubaldo, H. and De Folter, S. (2019). Gynoecium development: Networks in Arabidopsis and beyond. *J. Exp. Bot.* **70**, 1447–1460.

Zurcher, E., Tavor-Deslex, D., Lituiev, D., Enkerli, K., Tarr, P. T. and Muller, B. (2013). A Robust and Sensitive Synthetic Sensor to Monitor the Transcriptional Output of the Cytokinin Signaling Network in Planta. *Plant Physiol.* **161**, 1066–1075.

FIGURES and TABLES Manuscript 2

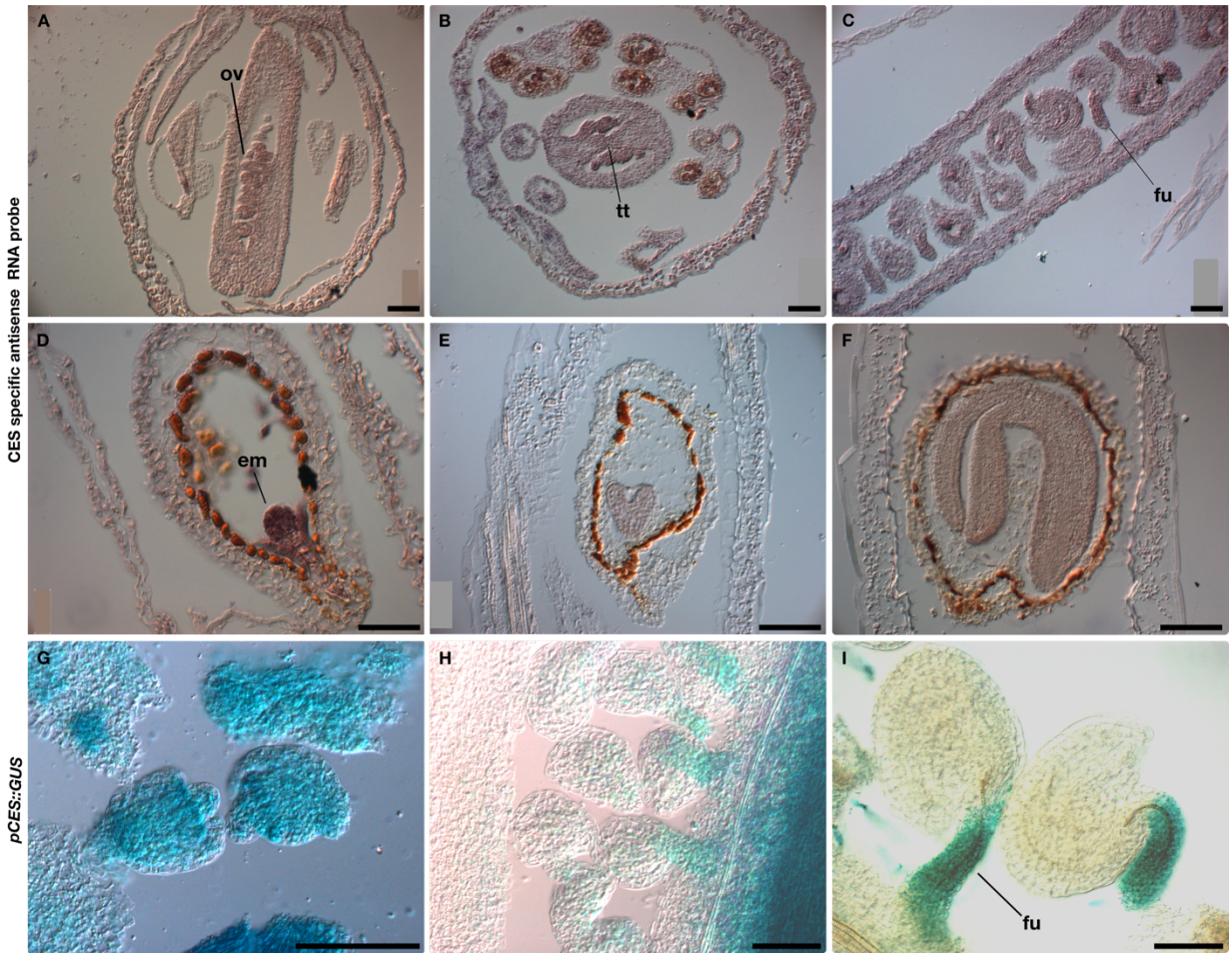

Fig. 1: Analysis of *CES* expression. *In situ* hybridization (A-F) and GUS activity of the *pCES::GUS* marker line (G-I) showed *CES* expression in ovules (A-C and G-I), transmitting tract (B), and in the embryos of the developing seeds (D-F). Em: embryo, fu: funiculus, ov: ovule, tt: transmitting tract. Scale bars: 50µm.

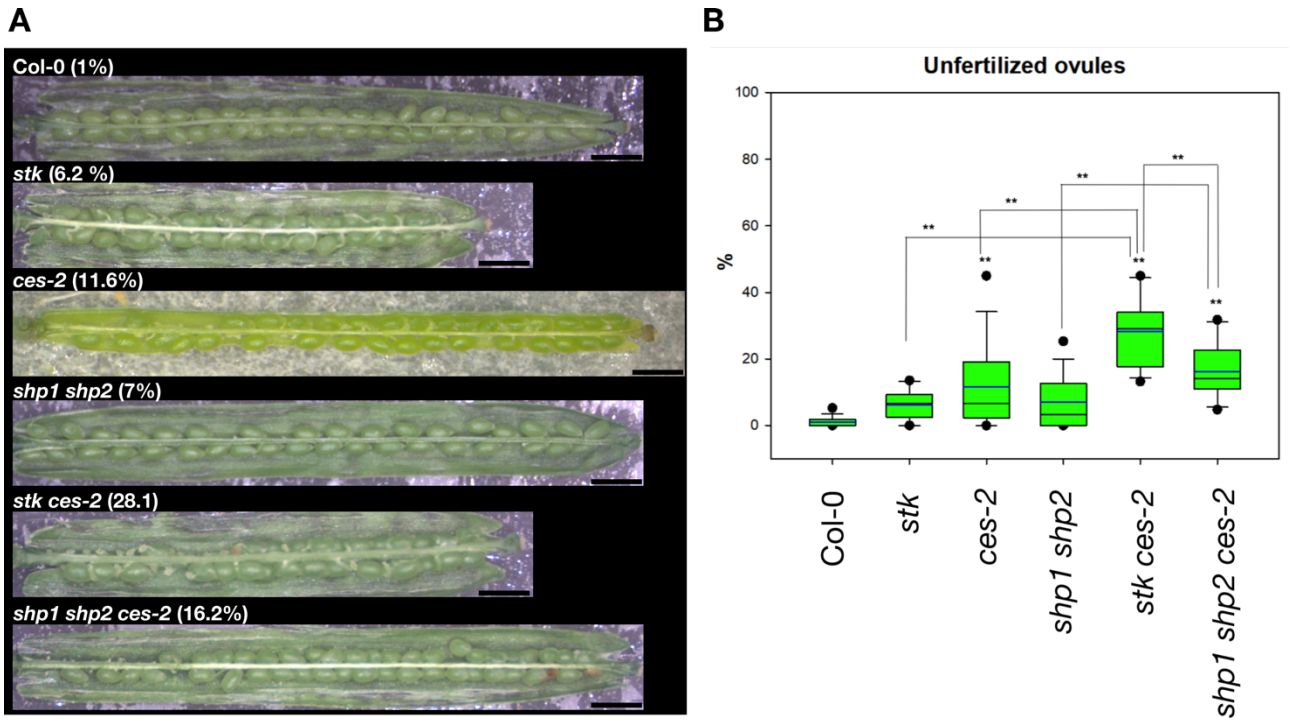

Fig. 2: Unfertilized ovules analysis in multiple mutant combination of *stk*, *ces-2* and *shp1 shp2*; (A) Stereomicroscope images of opened siliques of the *stk and ces-2* single mutants, the *stk ces-2* and the *shp1 shp2* double mutants, the *shp1 shp2 ces-2* triple mutant and the wild type Col-0; Scale bars: 1 mm. (B) Box plots of all the mutants analysed in comparison to wild type Col-0. Statistical analysis was performed using Anova followed by Tukey HSD test (** $p<0.01$).

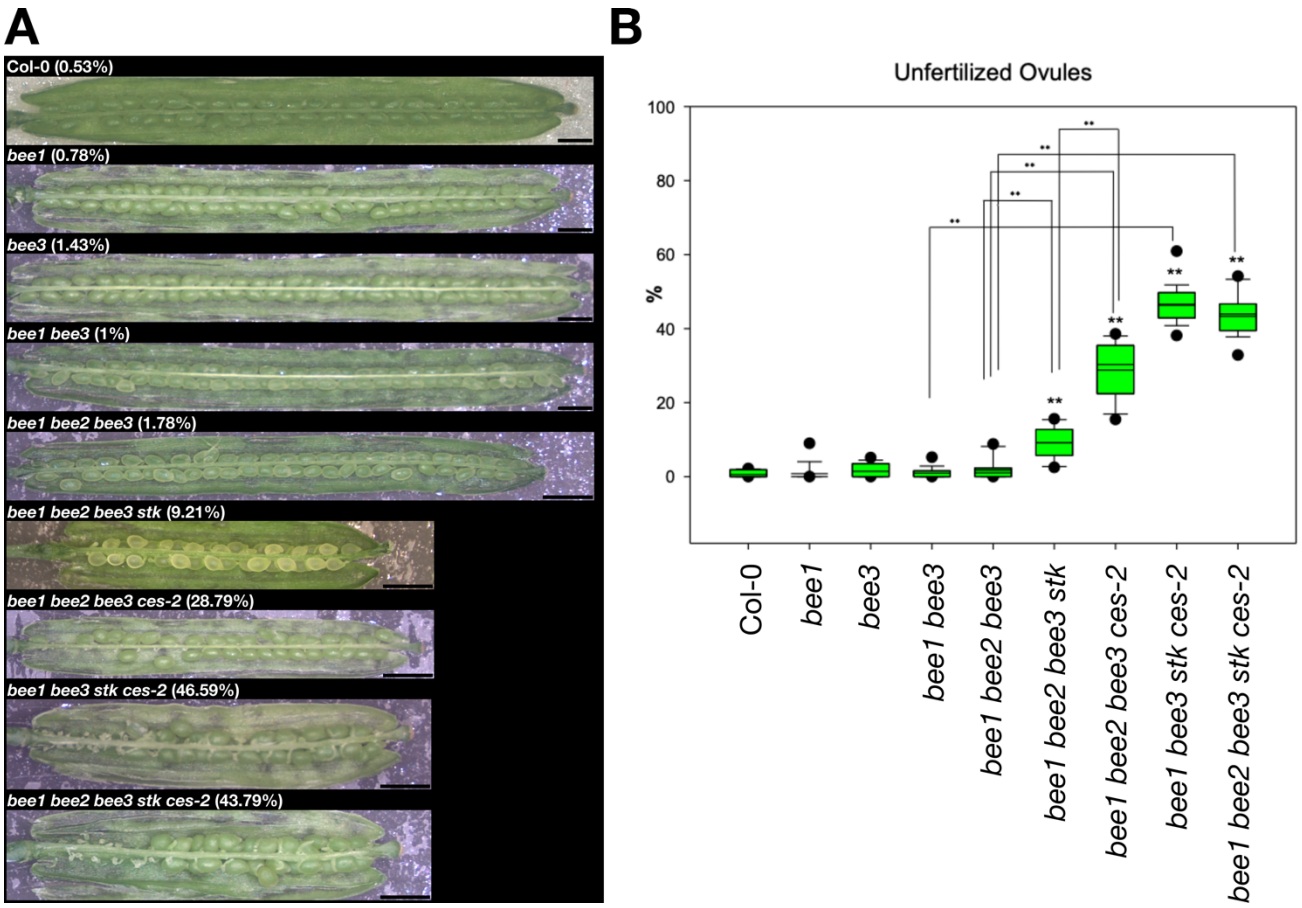

Fig. 3: Unfertilized ovules analysis in multiple mutant combination of *bee1*, *bee2*, *bee3*, *stk* and *ces-2*. (A) Stereomicroscope images of opened siliques of the *bee1* and *bee3* single, the *bee1 bee3* double mutant, the *bee1 bee2 bee3* triple mutant , the *bee1 bee2 bee3 stk,* the *bee1 bee2 bee3 ces-2* and *bee1 bee3 stk ces-2* quadruple mutants, the *bee1 bee2 bee3 stk ces-2* quintuple mutants and the wild type Col-0; Scale bars: 1 mm. (B) Box plots of all the mutants analysed in comparison to wild type Col-0. Statistical analysis was performed using Anova followed by Tukey HSD test (** $p<0.01$).

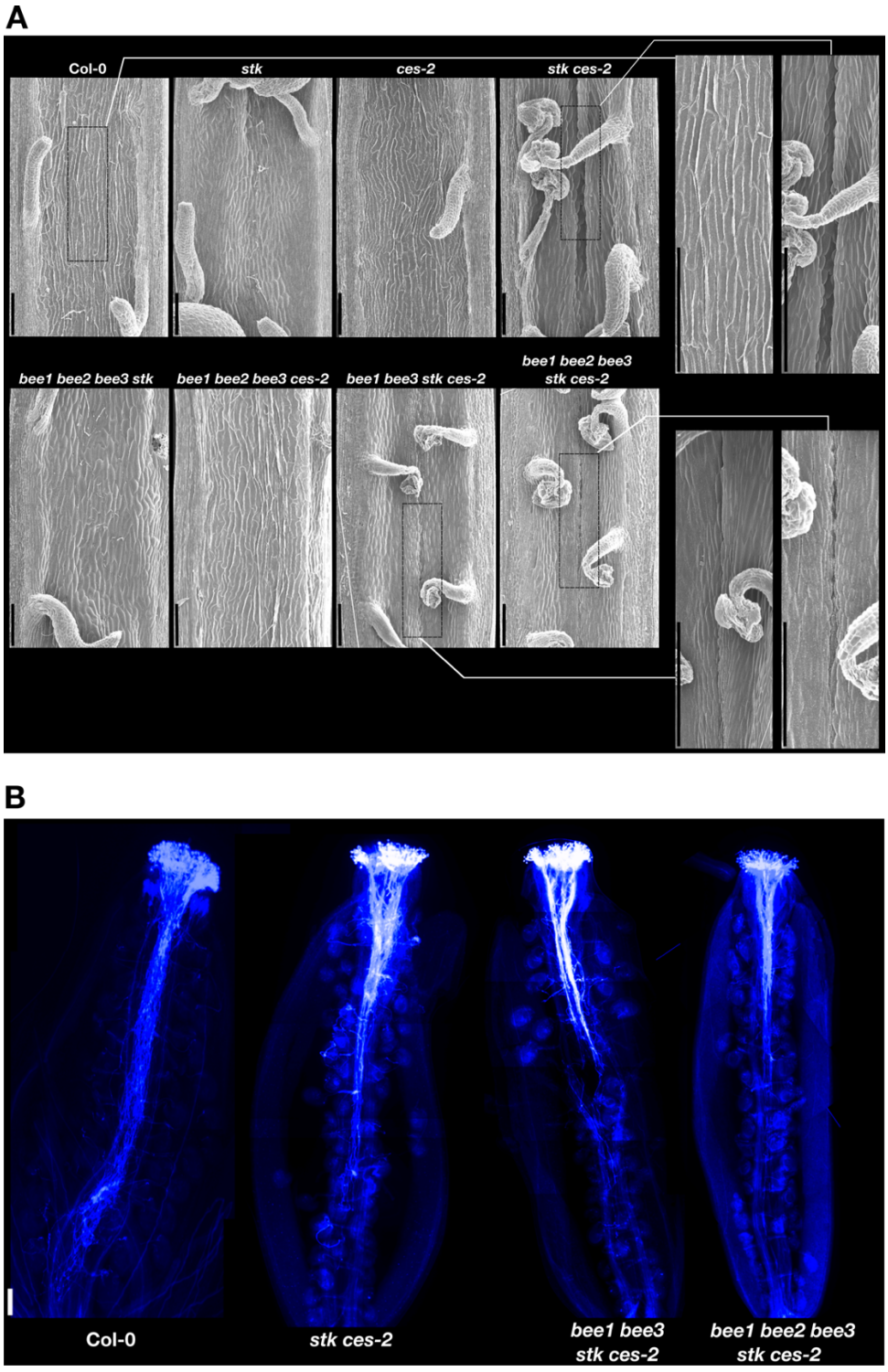

Fig. 4: **Septum analysis and pollen tube growth**. (A) Scanning electric microscope pictures of the septum of opened siliques of *stk*, *ces-2*, *stk ces-2*, *bee1 bee2 bee3 stk*, *bee1 bee2 bee3 ces-2*, *bee1 bee3 stk ces-2* and *bee1 bee2 bee3 stk ces-2* and wild type Col-0; Scale bars: 100µm. (B) Aniline blue staining of *stk ces-2, bee1 bee3 stk ces-2* and *bee1 bee2 bee3 stk ces-2* and wild type Col-0; Scale bar: 50µm

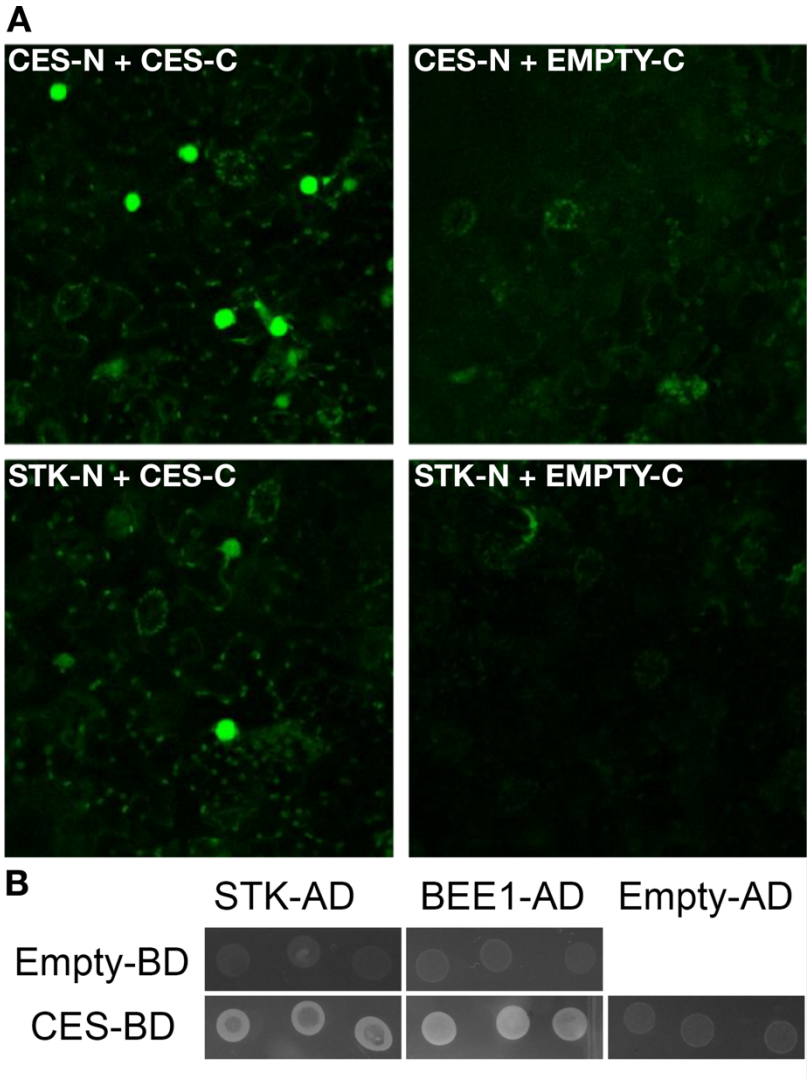

Fig. 5: STK, CES and BEE1 interaction assays of in yeast and *in planta*.

(A) BiFC assays showing the interaction of STK with CES. STK-N or CES-N: STK or CES fusion with the N-terminal part of the split YFP; STK-C or CES-C: STK or CES fusion with the C-terminal part of the split YFP. CES-N CES-C interaction was used as positive control. STK-N EMPTY-C and CES-N EMPTY-C were used as negative control.(B) Yeast two-hybrid assays testing interactions between STK-AD, BEE1-AD and CES-BD; interactions were considered positive when growth on -W-L-H +15 mM of 3-AT selective media was observed. The experiments were performed at 22°C. The CES-BEE1 interaction was chosen as a positive control (Poppenberger et al., 2011), the growth of transformants carrying empty AD or BD vectors were used as negative controls of the experiments.

Gene code	Gene Name	Fold Change	FDR	Gene function
AT4G14400	*ACD6*	-4.0117	2.33E-05	Cell death
AT1G06080	*ADS1*	-1.0338	2.17E-05	Cell wall and ECM biosynthesis
AT1G35230	*AGP5*	-2.1455	0.0145	Cell death and ECM biosynthesis
AT5G65390	*AGP7*	-1.3013	0.0024	Cell death and ECM biosynthesis
AT5G56540	*AGP14*	-0.7840	0.0473	Cell death and ECM biosynthesis
AT1G72290	*ATWSCP*	-6.5142	1.42E-07	Cell death and pollen tube growth
AT5G09730	*BXL3*	-2.0805	1.71E-06	Cell wall
AT1G75890	GDSL family of serine esterases/lipases	0.8845	0.0038	Cell wall and lipid metabolic process
AT4G28780	GDSL family of serine esterases/lipases	0.6227	0.0393	Cell wall and lipid metabolic process
AT4G16230	GDSL family of serine esterases/lipases	1.0662	0.0127	Cell wall and lipid metabolic process
AT3G26140	Glycosyl hydrolase family 5	-2.7099	3.13E-06	Cell wall and ECM biosynthesis
AT1G53130	*GRI*	-7.9981	4.16E-09	Cell death
AT4G14560	*IAA1*	-0.7727	0.0387	AUX signalling
AT3G23030	*IAA2*	-0.6711	0.0393	AUX signalling

AT4G14550	*IAA14*	-0.9381	0.0265	AUX signalling
AT1G04250	*IAA17*	-1.2215	0.0037	AUX signalling
AT2G38530	*LTP2*	-0.8702	0.0257	Lipid transport, cell death, cuticle biosynthesis
AT1G28710	nucleotide diphospho-sugar transferase protein	-1.2338	0.00008	Cell wall and ECM biosynthesis
AT5G49180	*PME58*	-0.6750	0.0459	Cell wall
AT4G36110	*SAUR9*	-1.2233	0.0447	Auxin response
AT2G21220	*SAUR12*	-0.7960	0.0239	Auxin response

Table 1: RNAseq data of candidate genes regulated by STK-CES-BEE1-BEE3 protein complex and involved in transmitting tract development.

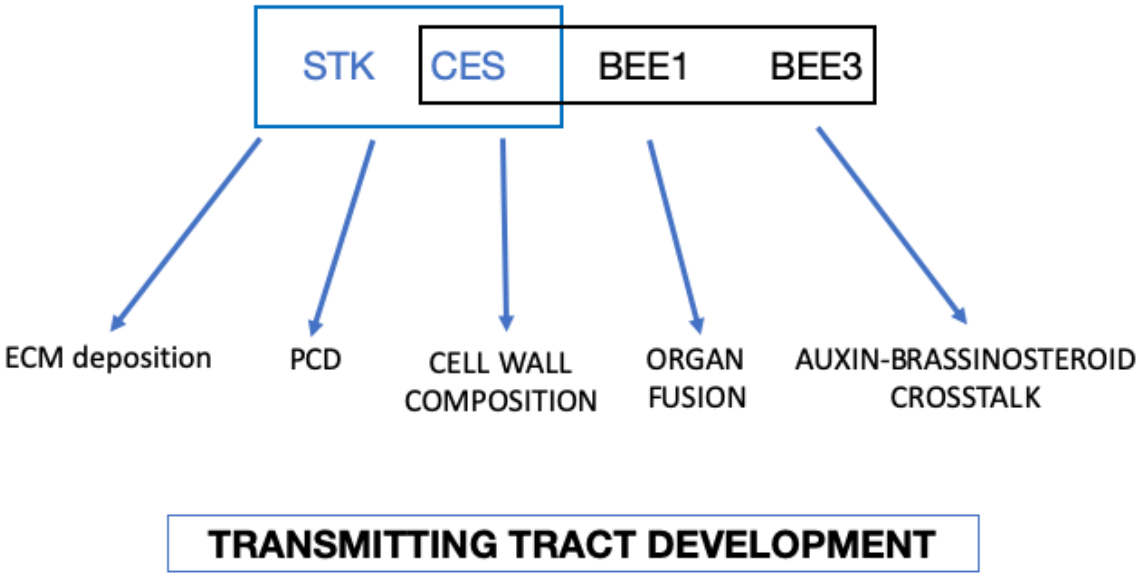

Fig. 6: Proposed model of transmitting tract development.

SUPPLEMENTARY FIGURES AND TABLES MANUSCRIPT 2

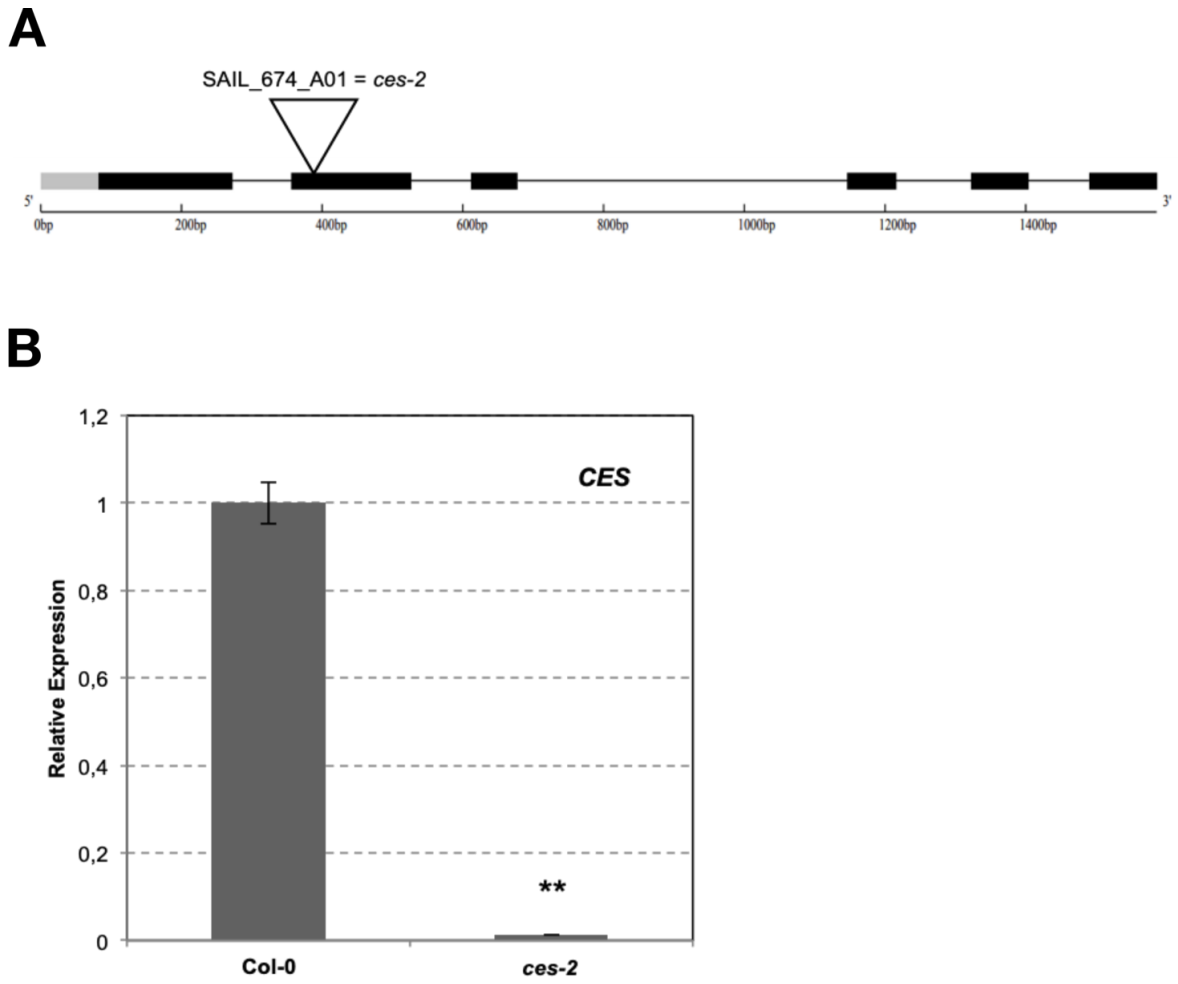

Figure S1: (A) Schematic representation of *CES* (At1g25330) genomic sequence and the T-DNA insertion corresponding to *ces-2.* The exons (black boxes) and the 5' UTR region (grey box) are shown. (B) Transcript abundance of *CES* in wt (Col-0) and *ces-2* plants, normalized to *ACTIN8*. Values are the mean ± s.e. of three independent qRT-PCR biological replicates. Asterisks indicate significant differences (**p<0.01) between the mutant and wild-type genotypes analysed through Student's *t*-test.

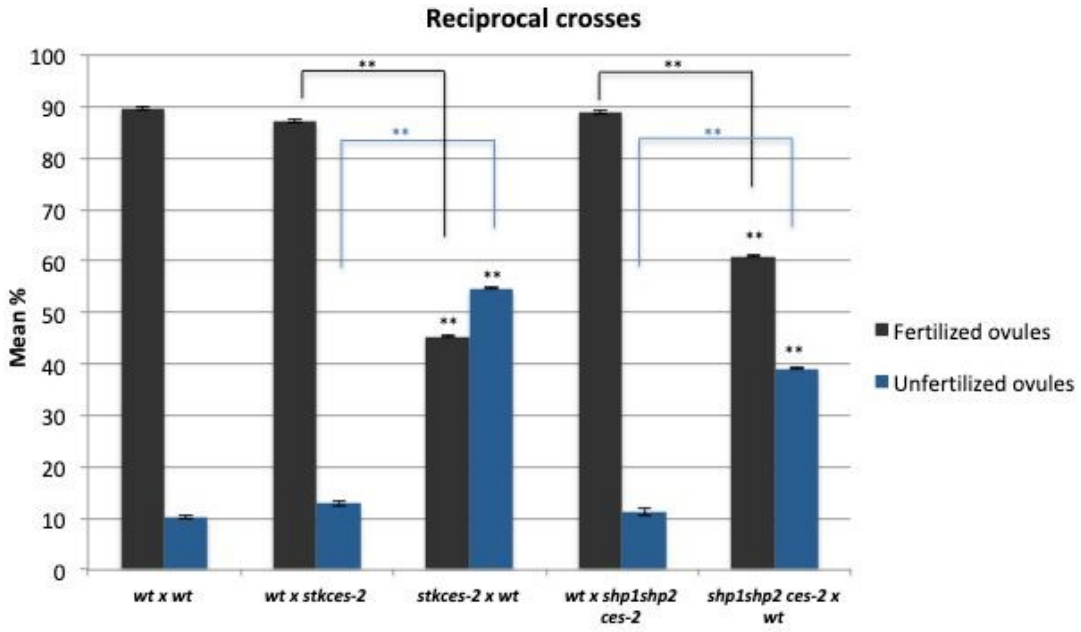

Figure S2: Analysis of reciprocal crosses between wild type and different mutant combinations. On the x-axis: female x male genotypes. Statistical analysis was performed using Anova followed by Tukey HSD tests (** $p<0.01$).

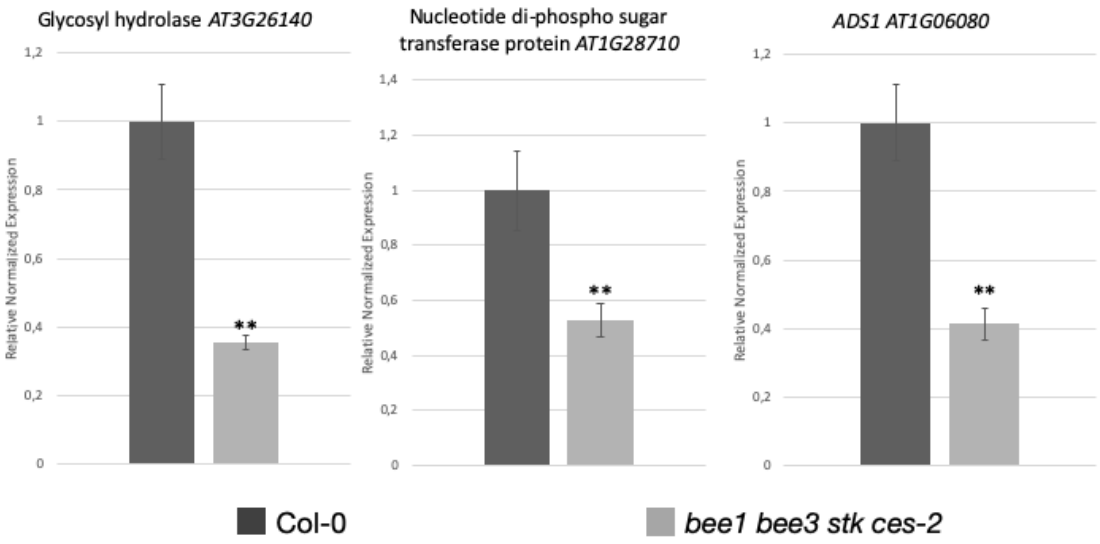

Figure S3: qRT-PCR to validate RNA sequencing data.

The genes selected to validate are: *AT3G26140*; *AT1G28710* and *AT1G06080*. Normalized with *ACTIN* and *UBIQUITIN*.Asterisks indicate significant differences (**p<0.01) between the mutant and wild-type genotypes analysed through Student's *t*-test.

Genotype	Col-0	*stk*	*ces-2*	*shp1 shp2*	*stk ces-2*	*shp1 shp2 ces-2*
Average	1.0	6.2	11.6	7.0	28.1	16.2
Median	0	6.5	8.5	3.3	29.1	14.1
Max	5.4	13.5	47.4	25.6	45.0	31.7
Min	0	0	0	0	13.2	4.8

Table S1: Unfertilized ovules data of the *stk and ces-2* single mutants*, the stk ces-2* double and the *shp1shp2 ces-2* triple mutant.

Genotype	Col-0	*bee1*	*bee3*	*bee1 bee3*	*bee1 bee2 bee3*	*bee1 bee2 bee3 stk*	*bee1 bee2 bee3 ces-2*	*bee1 bee3 stk ces-2*	*bee1 bee2 bee3 stk ces-2*
Average	0.5	0.7	1.4	1.0	1.7	9.2	28.7	46.5	43.7
Median	0	0	0	0	1	9.2	30.2	46.3	43.3
Max	2.2	9.3	5.1	5.3	8.8	15.6	38.6	61.4	54.2
Min	0	0	0	0	0	2.5	15.3	38	32.6

Table S2: Unfertilized ovules data of the *bee1 and bee3* single mutants*,* the *bee1 bee3* double mutant*,* the *bee1 bee2 bee3* triple mutant*,* the *bee1 bee2 bee3 stk*, *bee1 bee2 bee3 ces-2*, *bee1 bee3 stk ces-2* quadruple mutants and the *bee1 bee2 bee3 stk ces-2* quintuple mutant.

AD	BD	-H-L-W			-H-L-W 5mMtriAT			-H-L-W 10mMtriAT			-H-L-W 15mMtriAT			-L-W-A		
		Replicates			Replicates			Replicates			Replicates			Replicates		
		1	2	3	1	2	3	1	2	3	1	2	3	1	2	3
STK	empty	++	++	++	-	-	-	-	-	-	-	-	-	-	-	-
empty	STK	+	+	+	-	-	-	-	-	-	-	-	-	-	-	-
CESTA	empty	+	+	+	-	-	-	-	-	-	-	-	-	-	-	-
empty	CESTA	++	++	++	+	+	+	+/-	+/-	+/-	-	-	-	++	++	++
BEE1	empty	+	+	+	-	-	-	-	-	-	-	-	-	-	-	-
empty	BEE1	+	+	+	-	-	-	-	-	-	-	-	-	-	-	-
STK	**CESTA**	++	++	++	++	++	++	++	++	++	++	++	++	++	++	++
CESTA	STK	+	+	+	-	-	-	-	-	-	-	-	-	-	-	-
STK	BEE1	+	+	+	-	-	-	-	-	-	-	-	-	-	-	-
BEE1	STK	+	+	+	-	-	-	-	-	-	-	-	-	-	-	-
CESA	BEE1	++	++	++	++	++	++	+	+	+	-	-	-	++	++	++
BEE1	CESTA	++	++	++	++	++	++	++	++	++	++	++	++	++	++	++

Table S3: The yeast 2-hybrid assays have been tested on media lacking Histidine and supplemented with different concentration of 3-AT. For each interaction, three independent transformant colonies were tested. pGADT7 and pGBKT7 vectors were employed. ++ = strong growth/interaction; + = intermediate growth/interaction; +/- = weak growth/interaction; - = no growth/interaction.

Sample	Pairs of Reads	% mapped on reference transcriptome	% mapped on reference genome
Col-0 (1st replicate)	30170637	69.98%	83.41%
Col-0 (2nd replicate)	24797986	63.97%	81.23%
Col-0 (3rd replicate)	26560305	66.26%	82.53%
***bee1 bee3 stk ces-2* (1st replicate)**	31604396	67.13%	82.56%
***bee1 bee3 stk ces-2* (2nd replicate)**	25725335	67.69%	81.53%
***bee1 bee3 stk ces-2* (3rd replicate)**	28137608	68.29%	83.56%

Table S4: Number of reads obtained from each Col-0 (wt) and *bee1 bee3 stk ces-2* quadruple mutant replicate; % mapped on reference transcriptome; % mapped on reference genome.

TAIR Gene id	Col-0	*bee1 bee3 stk ces-2*	logFC	PValue	FDR	Gene Symbol and brief description
AT5G26970	0.04	0.89	4.43	0.00	0.04	unknown protein
AT3G60170	0.11	0.93	3.07	0.00	0.03	copia-like retrotransposon family
AT5G65080	2.33	13.27	2.49	0.00	0.00	MADS AFFECTING FLOWERING 5 (MAF5)
AT3G26460	0.46	2.23	2.27	0.00	0.00	Polyketide cyclase/dehydrase and lipid transport superfamily protein
AT2G05914	0.72	2.99	2.04	0.00	0.00	unknown protein
AT3G19710	0.62	2.25	1.84	0.00	0.04	branched-chain aminotransferase4 (BCAT4)
AT1G62560	2.26	6.79	1.57	0.00	0.00	flavin-monooxygenase glucosinolate S-oxygenase 3 (FMO GS-OX3)
AT5G35935	8.12	23.24	1.52	0.00	0.05	copia-like retrotransposon family
AT5G43500	19.87	49.74	1.33	0.00	0.00	actin-related protein 9 (ARP9)
AT4G12030	1.62	3.94	1.28	0.00	0.04	bile acid transporter 5 (BAT5)
AT5G14200	2.99	7.23	1.26	0.00	0.01	isopropylmalate dehydrogenase 1
AT4G13770	10.30	24.85	1.26	0.00	0.03	cytochrome P450
AT4G08115	1.74	4.16	1.26	0.00	0.04	gypsy-like retrotransposon family
AT5G52390	23.30	52.92	1.18	0.00	0.01	PAR1 protein
AT5G23010	2.72	6.15	1.16	0.00	0.04	methylthioalkylmalate synthase 1 (MAM1)
AT3G49270	6.10	13.00	1.09	0.00	0.01	molecular_function unknown
AT4G16230	2.19	4.59	1.07	0.00	0.01	GDSL-like Lipase/Acylhydrolase superfamily protein
AT4G23600	60.31	123.75	1.03	0.00	0.03	CORONATINE INDUCED 1 (CORI3)
AT4G15210	276.54	544.47	0.98	0.00	0.01	ARABIDOPSIS THALIANA BETA-AMYLASE (ATBETA-AMY)
AT1G75890	5.91	10.96	0.88	0.00	0.00	GDSL-like Lipase/Acylhydrolase superfamily protein
AT1G62540	39.98	69.16	0.79	0.00	0.05	flavin-monooxygenase glucosinolate S-oxygenase 2 (FMO GS-OX2)
AT1G48750	186.47	321.36	0.78	0.00	0.01	Bifunctional inhibitor/lipid-transfer protein/seed storage 2S albumin superfamily protein
AT2G32430	55.42	92.39	0.74	0.00	0.04	Galactosyltransferase family protein
AT1G74930	66.60	107.40	0.69	0.00	0.04	ORA47
AT4G19430	76.20	123.02	0.69	0.00	0.02	unknown protein
AT1G60190	27.48	44.08	0.68	0.00	0.00	ARM repeat superfamily protein
AT4G28780	21.20	32.74	0.62	0.00	0.04	GDSL-like Lipase/Acylhydrolase superfamily protein
AT4G30650	69.15	106.47	0.62	0.00	0.02	Low temperature and salt responsive protein family
AT3G54600	13.57	20.37	0.58	0.00	0.03	Class I glutamine amidotransferase-like superfamily protein
AT3G54820	50.69	73.23	0.53	0.00	0.03	plasma membrane intrinsic protein 2
AT4G39940	18.44	26.45	0.52	0.00	0.04	APS-kinase 2 (AKN2)

Table S5: RNAseq, genes up-regulated in the quadruple mutant *bee1 bee3 stk ces-2* compared to wild type. Column 1: Gene id according to the TAIR10 annotation of the *A. thaliana* genome; Column 2: Average expression in the wild type background. Values are expressed in log Counts Per Million

(CPM); Column 3: Average expression in the *bee1 bee3 stk ces-2* mutant. Values are expressed in log Counts Per Million (CPM); Column 4: Log Fold change of expression between mutant and wild type plants; Column 5: p-value for differential expression; Column 6: Benjamini Hochberg adjusted P-value for differential expression. A Significance cut-off of 0.05 is applied; Column 7: Brief description of the gene according to TAIR10 (if available).

TAIR Gene id	Col-0	*bee1 bee3 stk ces-2*	logFC	PValue	FDR	Gene Symbol and brief description
AT2G32890	4.62	0.00	-9.43	0.00	0.00	RALF-like 17 (RALFL17)
AT4G13266	3.50	0.00	-9.04	0.00	0.00	unknown protein
AT4G18540	1.84	0.00	-8.11	0.00	0.00	unknown protein
AT1G53130	23.38	0.09	-8.00	0.00	0.00	GRIM REAPER (GRI)
AT3G12000	55.84	0.21	-7.95	0.00	0.00	S-locus related protein SLR1, putative (S1)
AT5G19880	7.97	0.03	-7.62	0.00	0.00	Peroxidase superfamily protein
AT1G53480	40.96	0.24	-7.42	0.00	0.00	MTO 1 RESPONDING DOWN 1 (MRD1)
AT1G23720	0.67	0.00	-6.68	0.00	0.01	Proline-rich extensin-like family protein
AT1G72290	74.93	0.82	-6.51	0.00	0.00	Kunitz family trypsin and protease inhibitor protein
AT3G03670	4.17	0.07	-5.81	0.00	0.00	Peroxidase superfamily protein
AT2G41800	7.43	0.16	-5.40	0.00	0.00	Protein of unknown function, DUF642
AT5G20330	11.39	0.34	-5.05	0.00	0.00	beta-1,3-glucanase 4 (BETAG4)
AT2G15080	0.71	0.02	-4.87	0.00	0.03	receptor like protein 19 (RLP19)
AT1G73830	4.32	0.15	-4.77	0.00	0.00	BR enhanced expression 3 (BEE3)
AT3G14520	8.69	0.34	-4.66	0.00	0.00	Terpenoid cyclases/Protein prenyltransferases superfamily protein
AT2G43795	0.96	0.04	-4.57	0.00	0.00	unknown protein
AT4G11290	17.90	0.83	-4.44	0.00	0.00	Peroxidase superfamily protein
AT2G01422	35.28	1.66	-4.39	0.00	0.00	unknown protein
AT1G25330	36.95	1.79	-4.36	0.00	0.00	basic helix-loop-helix (bHLH) DNA-binding superfamily protein
AT1G61560	10.74	0.57	-4.24	0.00	0.00	MILDEW RESISTANCE LOCUS O 6 (MLO6)
AT2G43610	31.11	1.73	-4.18	0.00	0.00	Chitinase family protein
AT5G22980	16.89	0.90	-4.18	0.00	0.00	serine carboxypeptidase-like 47 (scpl47)
AT3G22250	1.01	0.05	-4.13	0.00	0.03	UDP-Glycosyltransferase superfamily protein
AT2G40680	2.44	0.13	-4.12	0.00	0.00	similar to unknown protein [Arabidopsis thaliana] (TAIR:AT5G52065.1)
AT2G46960	0.92	0.05	-4.01	0.00	0.00	cytochrome P450, family 709, subfamily B, polypeptide 1 (CYP709B1)
AT4G14400	3.11	0.18	-4.01	0.00	0.00	ACCELERATED CELL DEATH 6 (ACD6)
AT5G36110	3.08	0.19	-4.00	0.00	0.00	cytochrome P450, family 716, subfamily A, polypeptide 1 (CYP716A1)
AT4G34250	5.98	0.39	-3.92	0.00	0.00	3-ketoacyl-CoA synthase 16 (KCS16)
AT4G00910	1.99	0.15	-3.65	0.00	0.00	Aluminium activated malate transporter family protein
AT3G61035	2.74	0.23	-3.50	0.00	0.00	Cytochrome P450 superfamily protein

AT4G26420	0.80	0.07	-3.45	0.00	0.01	GAMT1
AT1G36060	3.06	0.30	-3.31	0.00	0.00	Integrase-type DNA-binding superfamily protein
AT1G30795	29.33	3.04	-3.27	0.00	0.00	Glycine-rich protein family
AT3G02940	1.69	0.16	-3.26	0.00	0.00	myb domain protein 107 (MYB107)
AT3G22231	2.53	0.27	-3.23	0.00	0.00	PATHOGEN AND CIRCADIAN CONTROLLED 1 (PCC1)
AT3G59850	3.91	0.44	-3.13	0.00	0.00	Pectin lyase-like superfamily protein
AT5G57550	1.83	0.20	-3.12	0.00	0.01	xyloglucan endotransglucosylase/hydrolase 25 (XTH25)
AT5G58782	7.82	0.92	-3.07	0.00	0.00	Undecaprenyl pyrophosphate synthetase family protein
AT5G20260	2.16	0.25	-3.07	0.00	0.00	Exostosin family protein
AT1G67105	6.83	0.82	-3.06	0.00	0.00	unknown protein
AT5G41040	3.66	0.48	-2.91	0.00	0.01	HXXXD-type acyl-transferase family protein
AT5G24110	1.58	0.22	-2.89	0.00	0.04	WRKY DNA-binding protein 30 (WRKY30)
AT4G33600	3.54	0.49	-2.84	0.00	0.00	unknown protein
AT3G04210	15.05	2.14	-2.78	0.00	0.02	Disease resistance protein (TIR-NBS class)
AT4G33610	0.70	0.10	-2.72	0.00	0.02	glycine-rich protein
AT3G26140	31.18	4.77	-2.71	0.00	0.00	Cellulase (glycosyl hydrolase family 5) protein
AT3G50470	1.59	0.23	-2.68	0.00	0.04	homolog of RPW8 3 (HR3)
AT3G59030	1.34	0.22	-2.58	0.00	0.00	TRANSPARENT TESTA 12 (TT12)
AT2G17000	5.18	0.89	-2.51	0.00	0.00	Mechanosensitive ion channel family protein
AT5G35390	7.94	1.40	-2.49	0.00	0.00	Leucine-rich repeat protein kinase family protein
AT4G23370	0.66	0.12	-2.40	0.00	0.04	unknown protein
AT3G26210	3.50	0.70	-2.34	0.00	0.02	cytochrome P450, family 71, subfamily B, polypeptide 23 (CYP71B23)
AT4G09960	51.42	10.22	-2.33	0.00	0.00	SEEDSTICK (STK)
AT3G57260	1.31	0.24	-2.30	0.00	0.02	beta-1,3-glucanase 2 (BGL2)
AT3G30720	21.45	4.39	-2.27	0.00	0.00	QUA-QUINE STARCH (QQS)
AT5G44580	1.80	0.38	-2.24	0.00	0.00	unknown protein
AT2G02010	9.48	2.02	-2.22	0.00	0.00	glutamate decarboxylase 4 (GAD4)
AT1G53490	14.51	3.16	-2.20	0.00	0.00	RING/U-box superfamily protein
AT1G35230	1.37	0.29	-2.15	0.00	0.01	arabinogalactan protein 5 (AGP5)
AT5G09730	172.56	40.81	-2.08	0.00	0.00	beta-xylosidase 3 (BXL3)
AT3G24225	1.45	0.34	-2.07	0.00	0.01	CLAVATA3/ESR-RELATED 19 (CLE19)
AT2G15650	8.26	1.99	-2.06	0.00	0.00	copia-like retrotransposon family, has a 5.0e-227 P-value blast match to gb|AAO73527.1| gag-pol polyprotein (Glycine max) (SIRE1) (Ty1_Copia-family)
AT1G44970	124.88	30.16	-2.05	0.00	0.00	Peroxidase superfamily protein

AT1G08930	29.18	7.05	-2.03	0.00	0.03	EARLY RESPONSE TO DEHYDRATION 6 (ERD6)
AT3G62150	5.84	1.44	-1.98	0.00	0.03	P-glycoprotein 21 (PGP21)
AT1G18400	11.08	2.79	-1.98	0.00	0.00	BR enhanced expression 1 (BEE1)
AT4G23130	1.20	0.29	-1.96	0.00	0.04	cysteine-rich RLK (RECEPTOR-like protein kinase) 5 (CRK5)
AT4G11890	2.40	0.61	-1.96	0.00	0.03	Protein kinase superfamily protein
AT1G05450	9.36	2.46	-1.92	0.00	0.00	Bifunctional inhibitor/lipid-transfer protein/seed storage 2S albumin superfamily protein
AT1G72416	6.35	1.66	-1.91	0.00	0.04	Chaperone DnaJ-domain superfamily protein
AT4G19970	4.12	1.11	-1.89	0.00	0.00	CONTAINS InterPro DOMAIN/s: Nucleotide-diphospho-sugar transferase, predicted (InterPro:IPR005069)
AT3G50480	16.23	4.37	-1.87	0.00	0.01	homolog of RPW8 4 (HR4)
AT3G10560	4.80	1.32	-1.87	0.00	0.00	UNFERTILIZED EMBRYO SAC 9 (UNE9)
AT1G65790	2.33	0.62	-1.86	0.00	0.05	receptor kinase 1 (RK1)
AT2G47130	2.29	0.63	-1.85	0.00	0.01	NAD(P)-binding Rossmann-fold superfamily protein
AT2G46440	6.32	1.74	-1.83	0.00	0.01	cyclic nucleotide-gated channels (CNGC11)
AT4G37400	2.21	0.62	-1.81	0.00	0.01	cytochrome P450, family 81, subfamily F, polypeptide 3 (CYP81F3)
AT1G21130	6.91	2.02	-1.77	0.00	0.00	O-methyltransferase family protein
AT5G54060	1.44	0.43	-1.76	0.00	0.04	UDP-glucose:flavonoid 3-o-glucosyltransferase (UF3GT)
AT4G38550	35.15	10.36	-1.75	0.00	0.04	Arabidopsis phospholipase-like protein (PEARLI 4) family
AT5G38900	1.47	0.44	-1.72	0.00	0.01	Thioredoxin superfamily protein
AT5G11360	4.68	1.44	-1.68	0.00	0.02	Interleukin-1 receptor-associated kinase 4 protein
AT2G05540	57.76	18.17	-1.66	0.00	0.05	Glycine-rich protein family
AT4G21870	22.64	7.12	-1.66	0.00	0.00	HSP20-like chaperones superfamily protein
AT5G44130	8.02	2.52	-1.65	0.00	0.02	FASCICLIN-like arabinogalactan protein 13 precursor (FLA13)
AT1G76930	2.75	0.86	-1.65	0.00	0.02	extensin 4 (EXT4)
AT1G75040	5.83	1.84	-1.64	0.00	0.00	pathogenesis-related gene 5 (PR5)
AT2G33020	1.59	0.50	-1.63	0.00	0.02	receptor like protein 24 (RLP24)
AT4G36430	1.58	0.51	-1.62	0.00	0.01	Peroxidase superfamily protein
AT1G65490	10.48	3.45	-1.58	0.00	0.05	unknown protein
AT4G12890	16.84	5.78	-1.55	0.00	0.00	Gamma interferon responsive lysosomal thiol (GILT) reductase family protein
AT1G58889	6.30	2.19	-1.51	0.00	0.02	copia-like retrotransposon family, has a 0. P-value blast match to dbj|BAA78425.1| polyprotein (Arabidopsis

						thaliana) (AtRE1) (Ty1_Copia-element)
AT3G23120	8.86	3.12	-1.49	0.00	0.01	receptor like protein 38 (RLP38)
AT3G45940	8.15	2.90	-1.49	0.00	0.00	Glycosyl hydrolases family 31 protein
AT1G21250	32.47	11.81	-1.45	0.00	0.00	cell wall-associated kinase (WAK1)
AT2G45180	61.98	22.61	-1.45	0.00	0.02	Bifunctional inhibitor/lipid-transfer protein/seed storage 2S albumin superfamily protein
AT1G71690	3.96	1.47	-1.44	0.00	0.03	Protein of unknown function (DUF579)
AT1G51805	41.05	15.21	-1.42	0.00	0.04	Leucine-rich repeat protein kinase family protein
AT4G23170	5.00	1.91	-1.37	0.00	0.01	EP1
AT1G70680	9.24	3.60	-1.36	0.00	0.01	Caleosin-related family protein
AT5G44020	34.98	13.50	-1.36	0.00	0.04	HAD superfamily, subfamily IIIB acid phosphatase
AT5G50200	4.17	1.59	-1.36	0.00	0.04	WOUND-RESPONSIVE 3 (WR3)
AT2G25510	15.94	6.32	-1.32	0.00	0.02	unknown protein
AT2G40750	6.20	2.48	-1.31	0.00	0.01	WRKY DNA-binding protein 54 (WRKY54)
AT5G65390	4.95	2.00	-1.30	0.00	0.00	arabinogalactan protein 7 (AGP7)
AT3G56410	5.35	2.14	-1.30	0.00	0.04	Protein of unknown function (DUF3133)
AT4G22690	86.77	35.26	-1.30	0.00	0.04	cytochrome P450, family 706, subfamily A, polypeptide 1 (CYP706A1)
AT2G41090	33.06	13.45	-1.29	0.00	0.00	Calcium-binding EF-hand family protein
AT5G46590	4.50	1.83	-1.29	0.00	0.01	NAC domain containing protein 96 (NAC096)
AT2G18300	2.82	1.17	-1.25	0.00	0.04	basic helix-loop-helix (bHLH) DNA-binding superfamily protein
AT5G42230	18.10	7.62	-1.25	0.00	0.00	serine carboxypeptidase-like 41 (scpl41)
AT1G28710	51.85	22.04	-1.23	0.00	0.00	Nucleotide-diphospho-sugar transferase family protein
AT4G36110	5.39	2.29	-1.22	0.00	0.04	SAUR-like auxin-responsive protein family
AT1G04250	20.41	8.77	-1.22	0.00	0.00	AUXIN RESISTANT 3 (AXR3)
AT5G23510	4.67	1.98	-1.21	0.00	0.01	unknown protein
AT1G65190	5.45	2.41	-1.18	0.00	0.01	Protein kinase superfamily protein
AT1G32860	10.40	4.75	-1.13	0.00	0.00	Glycosyl hydrolase superfamily protein
AT1G18020	19.80	9.35	-1.08	0.00	0.04	FMN-linked oxidoreductases superfamily protein
AT5G38970	4.58	2.17	-1.06	0.00	0.04	brassinosteroid-6-oxidase 1 (BR6OX1)
AT1G06080	34.94	17.05	-1.03	0.00	0.00	delta 9 desaturase 1 (ADS1)
AT5G40780	14.17	6.95	-1.03	0.00	0.00	lysine histidine transporter 1
AT4G23010	28.88	14.27	-1.02	0.00	0.00	UDP-galactose transporter 2 (UTR2)

AT1G13110	4.48	2.22	-1.00	0.00	0.04	cytochrome P450, family 71 subfamily B, polypeptide 7 (CYP71B7)
AT4G36770	8.55	4.29	-1.00	0.00	0.01	UDP-Glycosyltransferase superfamily protein
AT1G35710	14.78	7.38	-1.00	0.00	0.01	Protein kinase family protein with leucine-rich repeat domain
AT2G19800	53.28	26.69	-1.00	0.00	0.04	myo-inositol oxygenase 2 (MIOX2)
AT3G51920	12.74	6.40	-0.98	0.00	0.03	calmodulin 9 (CAM9)
AT2G23200	15.59	7.89	-0.98	0.00	0.03	Protein kinase superfamily protein
AT5G51810	15.29	7.77	-0.98	0.00	0.01	gibberellin 20 oxidase 2 (GA20OX2)
AT4G14550	5.98	3.10	-0.94	0.00	0.03	indole-3-acetic acid inducible 14 (IAA14)
AT1G78780	11.42	5.96	-0.94	0.00	0.02	pathogenesis-related family protein
AT1G52290	11.61	6.08	-0.92	0.00	0.04	Protein kinase superfamily protein
AT5G24910	8.95	4.78	-0.90	0.00	0.02	cytochrome P450, family 714, subfamily A, polypeptide 1 (CYP714A1)
AT1G22740	7.71	4.13	-0.90	0.00	0.04	RAB GTPase homolog G3B (RABG3B)
AT5G60140	21.16	11.53	-0.88	0.00	0.01	AP2/B3-like transcriptional factor family protein
AT2G38530	92.36	50.55	-0.87	0.00	0.03	lipid transfer protein 2 (LTP2)
AT4G19460	9.41	5.21	-0.86	0.00	0.02	UDP-Glycosyltransferase superfamily protein
AT3G22240	19.93	11.12	-0.84	0.00	0.03	unknown protein
AT2G44080	13.66	7.76	-0.81	0.00	0.04	ARGOS-like (ARL)
AT1G06520	43.43	24.89	-0.80	0.00	0.05	glycerol-3-phosphate acyltransferase 1 (GPAT1)
AT2G21220	14.04	8.07	-0.80	0.00	0.02	SAUR-like auxin-responsive protein family
AT1G69730	13.68	7.93	-0.79	0.00	0.02	Wall-associated kinase family protein
AT5G56540	21.87	12.73	-0.78	0.00	0.05	arabinogalactan protein 14 (AGP14)
AT1G63260	15.91	9.23	-0.78	0.00	0.03	tetraspanin10 (TET10)
AT4G14560	17.88	10.46	-0.77	0.00	0.04	indole-3-acetic acid inducible (IAA1)
AT4G28490	32.10	18.90	-0.76	0.00	0.04	HAESA (HAE)
AT4G24040	29.43	17.31	-0.76	0.00	0.05	trehalase 1 (TRE1)
AT1G65480	29.65	17.52	-0.76	0.00	0.01	FLOWERING LOCUS T (FT)
AT3G12170	10.33	6.17	-0.75	0.00	0.04	Chaperone DnaJ-domain superfamily protein
AT2G13790	43.56	25.99	-0.74	0.00	0.03	somatic embryogenesis receptor-like kinase 4 (SERK4)
AT4G38860	8.32	4.98	-0.74	0.00	0.05	SAUR-like auxin-responsive protein family
AT4G30270	167.83	103.21	-0.70	0.00	0.02	xyloglucan endotransglucosylase/hydrolase 24 (XTH24)
AT5G14920	82.01	50.49	-0.70	0.00	0.05	Gibberellin-regulated family protein

AT1G03400	11.79	7.34	-0.68	0.00	0.03	2-oxoglutarate (2OG) and Fe(II)-dependent oxygenase superfamily protein
AT1G26540	23.65	14.74	-0.68	0.00	0.04	Agenet domain-containing protein
AT5G49180	35.05	21.97	-0.68	0.00	0.05	Plant invertase/pectin methylesterase inhibitor superfamily
AT1G34750	14.24	8.92	-0.67	0.00	0.02	Protein phosphatase 2C family protein
AT3G23030	49.78	31.20	-0.67	0.00	0.04	indole-3-acetic acid inducible 2 (IAA2)
AT5G21150	164.79	104.25	-0.66	0.00	0.00	ARGONAUTE 9 (AGO9)
AT5G61010	17.69	11.22	-0.66	0.00	0.03	exocyst subunit exo70 family protein E2 (EXO70E2)
AT5G59810	28.38	18.08	-0.65	0.00	0.05	SBT5.4
AT5G24530	31.32	20.06	-0.64	0.00	0.03	DOWNY MILDEW RESISTANT 6 (DMR6)
AT4G15450	43.04	27.75	-0.63	0.00	0.00	Senescence/dehydration-associated protein-related
AT1G58602	34.90	22.52	-0.63	0.00	0.05	LRR and NB-ARC domains-containing disease resistance protein
AT1G76520	22.31	14.62	-0.61	0.00	0.04	Auxin efflux carrier family protein
AT1G05490	55.61	36.68	-0.60	0.00	0.02	chromatin remodeling 31 (chr31)
AT3G51430	20.36	13.71	-0.57	0.00	0.04	YELLOW-LEAF-SPECIFIC GENE 2 (YLS2)
AT5G07580	35.63	24.01	-0.57	0.00	0.05	Integrase-type DNA-binding superfamily protein
AT5G18860	26.80	18.18	-0.56	0.00	0.02	inosine-uridine preferring nucleoside hydrolase family protein
AT3G47250	21.82	14.86	-0.55	0.00	0.03	Plant protein of unknown function (DUF247)
AT1G58180	31.22	21.48	-0.54	0.00	0.05	beta carbonic anhydrase 6 (BCA6)

Table S6: RNAseq, genes down-regulated in the quadruple mutant *bee1 bee3 stk ces-2* compared to wild type. Column 1: Gene id according to the TAIR10 annotation of the *A. thaliana* genome; Column 2: Average expression in the wild type background. Values are expressed in log Counts Per Million (CPM); Column 3: Average expression in the *bee1 bee3 stk ces-2* mutant. Values are expressed in log Counts Per Million (CPM); Column 4: Log Fold change of expression between mutant and wild type plants; Column 5: p-value for differential expression; Column 6: Benjamini Hochberg adjusted P-value for differential expression. A Significance cut-off of 0.05 is applied; Column 7: Brief description of the gene according to TAIR10 (if available).

GO_acc	term_type	Term	pvalue	FDR
GO:0050896	P	response to stimulus	2.40E-08	9.20E-06
GO:0010033	P	response to organic substance	2.70E-07	5.10E-05
GO:0042221	P	response to chemical stimulus	2.30E-06	0.00029
GO:0019825	F	oxygen binding	1.80E-06	0.00036
GO:0020037	F	heme binding	4.90E-06	0.00048
GO:0051704	P	multi-organism process	6.20E-06	0.0006
GO:0051707	P	response to other organism	1.10E-05	0.00083
GO:0016798	F	hydrolase activity, acting on glycosyl bonds	1.70E-05	0.0011
GO:0009607	P	response to biotic stimulus	2.00E-05	0.0013
GO:0046906	F	tetrapyrrole binding	3.00E-05	0.0015
GO:0009719	P	response to endogenous stimulus	5.10E-05	0.0028
GO:0005506	F	iron ion binding	7.50E-05	0.003
GO:0003824	F	catalytic activity	0.00011	0.0036
GO:0009725	P	response to hormone stimulus	7.90E-05	0.0038
GO:0005488	F	binding	0.00016	0.0045
GO:0004553	F	hydrolase activity, hydrolyzing O-glycosyl compounds	0.00021	0.0047
GO:0016684	F	oxidoreductase activity, acting on peroxide as acceptor	0.00024	0.0047
GO:0004601	F	peroxidase activity	0.00024	0.0047
GO:0016209	F	antioxidant activity	0.0005	0.009
GO:0009751	P	response to salicylic acid stimulus	0.00024	0.01
GO:0016740	F	transferase activity	0.00066	0.011
GO:0030312	C	external encapsulating structure	0.00037	0.015
GO:0005618	C	cell wall	0.00035	0.015
GO:0009505	C	plant-type cell wall	0.00081	0.022
GO:0016301	F	kinase activity	0.0016	0.024
GO:0009055	F	electron carrier activity	0.0017	0.024
GO:0016491	F	oxidoreductase activity	0.0036	0.048
GO:0008219	P	cell death	0.0015	0.05
GO:0016265	P	death	0.0015	0.05

Table S7: Gene Ontology analysis of the genes up-regulated in the quadruple mutant *bee1 bee3 stk ces-2* in comparison with wild type. Column 1: Gene Ontology (GO) term unique identifier; Column 2: Gene Ontology term functional category: P= biological process; F= molecular function; C= cellular component; Column 3: Gene ontology term official name; Column 4: p-value for the enrichment of the GO term in the gene set; Column 5: Benjamin Hochberg adjusted p-value, a significance cut-off of 0.05 is applied.

GO_acc	term_type	Term	pvalue	FDR
GO:0019758	P	glycosinolate biosynthetic process	2.20E-14	8.10E-13
GO:0019761	P	glucosinolate biosynthetic process	2.20E-14	8.10E-13
GO:0016144	P	S-glycoside biosynthetic process	2.20E-14	8.10E-13
GO:0019757	P	glycosinolate metabolic process	3.20E-13	5.80E-12
GO:0019760	P	glucosinolate metabolic process	3.20E-13	5.80E-12
GO:0016143	P	S-glycoside metabolic process	3.20E-13	5.80E-12
GO:0016138	P	glycoside biosynthetic process	1.60E-12	2.50E-11
GO:0016137	P	glycoside metabolic process	9.80E-12	1.30E-10
GO:0044272	P	sulfur compound biosynthetic process	1.90E-11	2.30E-10
GO:0044262	P	cellular carbohydrate metabolic process	1.50E-10	1.60E-09
GO:0034637	P	cellular carbohydrate biosynthetic process	3.50E-10	3.50E-09
GO:0006790	P	sulfur metabolic process	1.50E-09	1.40E-08
GO:0016051	P	carbohydrate biosynthetic process	7.00E-09	6.00E-08
GO:0005975	P	carbohydrate metabolic process	7.50E-08	5.90E-07
GO:0019748	P	secondary metabolic process	3.10E-07	2.30E-06
GO:0050896	P	response to stimulus	0.00079	0.0054
GO:0044238	P	primary metabolic process	0.0012	0.008
GO:0009058	P	biosynthetic process	0.0015	0.0094
GO:0009719	P	response to endogenous stimulus	0.0029	0.016
GO:0008152	P	metabolic process	0.003	0.016
GO:0044249	P	cellular biosynthetic process	0.0038	0.02
GO:0010033	P	response to organic substance	0.0076	0.036
GO:0044237	P	cellular metabolic process	0.0075	0.036
GO:0006950	P	response to stress	0.019	0.086
GO:0042221	P	response to chemical stimulus	0.042	0.18
GO:0009987	P	cellular process	0.047	0.2
GO:0044260	P	cellular macromolecule metabolic process	0.57	1
GO:0043170	P	macromolecule metabolic process	0.67	1
GO:0003824	F	catalytic activity	0.0077	0.027
GO:0016740	F	transferase activity	0.0097	0.027
GO:0005488	F	binding	0.93	1
GO:0012505	C	endomembrane system	0.00018	0.0074
GO:0005623	C	cell	0.0021	0.029
GO:0044464	C	cell part	0.0021	0.029
GO:0043229	C	intracellular organelle	0.34	1
GO:0043227	C	membrane-bounded organelle	0.26	1
GO:0043226	C	organelle	0.34	1
GO:0009536	C	plastid	0.14	1
GO:0016020	C	membrane	0.17	1
GO:0005737	C	cytoplasm	0.45	1
GO:0043231	C	intracellular membrane-bounded organelle	0.26	1
GO:0044444	C	cytoplasmic part	0.36	1
GO:0044424	C	intracellular part	0.23	1
GO:0005622	C	intracellular	0.27	1

Table S8: Gene Ontology analysis of the genes down-regulated in the quadruple mutant *bee1 bee3 stk ces-2* in comparison with wild type; Column 1: Gene Ontology (GO) term unique

identifier; Column 2: Gene Ontology term functional category: P= biological process; F= molecular function; C= cellular component; Column 3: Gene ontology term official name; Column 4: p-value for the enrichment of the GO term in the gene set; Column 5: Benjamin Hochberg adjusted p-value, a significance cut-off of 0.05 is applied.

Name	Sequence	Function
Atp_0204	GCTTGTTCTGATAGCACCAACACTAGCA	STK and *stk* genotyping
Atp_0561	GGAACTCAAAGAGTCTCCCATCAG	STK and *stk* genotyping
Atp_2785	GGCACGGTTTGAGCCATATAAC	*ces-2* genotyping
Atp_2786	GCATCACTGCCATTCCCATTGC	*ces-2* genotyping
Atp_2812	TAGCATCTGAATTTCATAACCAATCTCGATACAC	*ces-2* genotyping (with Atp_2785)
Atp_0206	GATGCACTCGAAATCAGCCAATTTTAGAC	*shp1* genotyping (with Atp_207)
Atp_0207	GTGACGGAAGGAGGGTTGACG	*shp1* genotyping
Atp_0208	GTCTACTGATGAGTTGTCACTAGG	*shp1* genotyping
Atp_0645	GTTCTTGGTAAAAACATACTTGCC	*shp2* genotyping
Atp_0646	CCCTTCTTTTTTTGGGATATTATTG	*shp2* genotyping
Atp_0647	AGCGGATAACAATTTCACACAGGA	*shp2* genotyping (with Atp_646)
Atp_4361	CCCGGAAACTCTCCAGACAGTAGTAACAA	*bee1* genotyping
Atp_4362	CCTTATAACATCCGGGCACCATATCTTGCA	*bee1* genotyping
Atp_3744	GGCAATCAGCTGTTGCCCGTCTCACTGGTG	*bee1* genotyping (with Atp_4362)
Atp_4363	GCAGAGGATGAAACAGAGCCAAGCATGAA	*bee2* genotyping
Atp_4364	GGAGGACCTGTGAAGTAAGCCTGAAACTAG	*bee2* genotyping
Atp_3744	GGCAATCAGCTGTTGCCCGTCTCACTGGTG	*bee2* genotyping (with Atp_4364)
Atp_4365	CTCTACCTCTTCTGCTCAAGTTTCCATAAA	*bee3* genotyping
Atp_4366	AATCATAGCAAACATCACCAGTCTTACGAG	*bee3* genotyping
Atp_3744	GGCAATCAGCTGTTGCCCGTCTCACTGGTG	*bee3* genotyping (with Atp_4366)
Atp_3957	CCAGGATGCTACAAGGCAAT	*CES* qRT-PCR in *ces-2*
Atp_3958	ATCCGTTGGCTCAATATCCA	*CES* qRT-PCR in *ces-2*
RT_147	CTGTTCACGGAACCCAATTC	*UBIQUITIN* housekeeping
RT_148	GGAAAAAGGTCTGACCGACA	*UBIQUITIN* housekeeping
RT_861	CTCAGG TATTGCAGACCGTATGAG	*ACTIN* housekeeping
RT_862	CTGGACCTGCTTCATCATACTCTG	*ACTIN* housekeeping
RT_2870	GTCCGATCACGACACGTAAA	qRT-PCR *AT3G26140*

RT_2871	GTCGATTCCAAACTCGCTAAGA	qRT-PCR *AT3G26140*
RT_2872	TGTCCATTTCCTCTGTCTCTTG	qRT-PCR *AT1G06080*
RT_2873	TAGGACTATGTGGGTCCCTATC	qRT-PCR *AT1G06080*
RT_2874	CCGCGGCTACAATCTTACTT	qRT-PCR *AT1G28710*
RT_2875	AGCCTCATGTCGTACCATTTC	qRT-PCR *AT1G28710*

Table S.9: Primers used for transmitting tract project

Article

Cell Reports

SEEDSTICK Controls *Arabidopsis* Fruit Size by Regulating Cytokinin Levels and *FRUITFULL*

Graphical Abstract

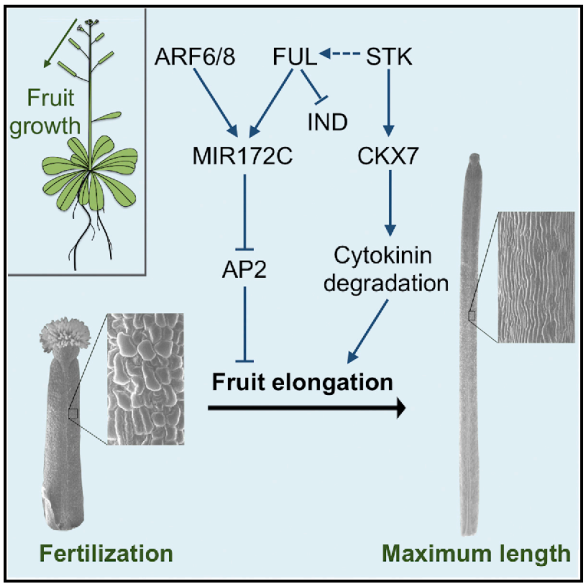

Authors

Maurizio Di Marzo, Humberto Herrera-Ubaldo, Elisabetta Caporali, ..., Marta A. Mendes, Stefan de Folter, Lucia Colombo

Correspondence

lucia.colombo@unimi.it

In Brief

Di Marzo et al. establish that defects in *Arabidopsis* fruit size are accompanied by alterations in the metabolism of the plant hormone cytokinin, which is critical for cell elongation. SEEDSTICK influences fruit elongation by directly regulating cytokinin degradation via CKX7 and indirectly modulating the expression of the MADS-box gene *FRUITFULL*.

Highlights

- Modulation of the cytokinin pathway is critical for determining fruit size
- Cytokinins play opposing roles in pistil/fruit growth before and after fertilization
- SEEDSTICK integrates cytokinin and molecular pathways to regulate fruit size

Di Marzo et al., 2020, Cell Reports *30*, 2846–2857
February 25, 2020
https://doi.org/10.1016/j.celrep.2020.01.101

CellPress

OPEN ACCESS
CellPress

Cell Reports
Article

SEEDSTICK Controls *Arabidopsis* Fruit Size by Regulating Cytokinin Levels and *FRUITFULL*

Maurizio Di Marzo,[1] Humberto Herrera-Ubaldo,[2] Elisabetta Caporali,[1] Ondřej Novák,[3] Miroslav Strnad,[3] Vicente Balanzà,[1,4] Ignacio Ezquer,[1] Marta A. Mendes,[1] Stefan de Folter,[2] and Lucia Colombo[1,5,*]

[1]Dipartimento di BioScienze, Università degli Studi di Milano, Milan, Milan 20133, Italy
[2]Unidad de Genómica Avanzada (LANGEBIO), Centro de Investigación y de Estudios Avanzados del Instituto Politécnico Nacional (CINVESTAV-IPN), Irapuato, Guanajuato 36824, México
[3]Laboratory of Growth Regulators, Faculty of Science of Palacký University & Institute of Experimental Botany of the Czech Academy of Sciences, Olomouc, Olomouc 78371, Czech Republic
[4]Instituto de Biologia Molecular y Celular de Plantas, Consejo Superior de Investigacione Cientificas, Universidad Politecnica de Valencia, Valencia, Valencia 46022, Spain
[5]Lead Contact
*Correspondence: lucia.colombo@unimi.it
https://doi.org/10.1016/j.celrep.2020.01.101

SUMMARY

Upon fertilization, the ovary increases in size and undergoes a complex developmental process to become a fruit. We show that cytokinins (CKs), which are required to determine ovary size before fertilization, have to be degraded to facilitate fruit growth. The expression of *CKX7*, which encodes a cytosolic CK-degrading enzyme, is directly positively regulated post-fertilization by the MADS-box transcription factor STK. Similar to *stk*, two *ckx7* mutants possess shorter fruits than wild type. Quantification of CKs reveals that *stk* and *ckx7* mutants have high CK levels, which negatively control cell expansion during fruit development, compromising fruit growth. Overexpression of *CKX7* partially complements the *stk* fruit phenotype, confirming a role for CK degradation in fruit development. Finally, we show that STK is required for the expression of *FUL*, which is essential for valve elongation. Overall, we provide insights into the link between CKs and molecular pathways that control fruit growth.

INTRODUCTION

Fruit, whose main function is to protect and disperse its seeds, has contributed to the evolutionary success of angiosperms. The dry and dehiscent fruit of *Arabidopsis* is a silique formed by two lateral valves and separated from the central replum by the valve margin tissue. The differentiation and development of the fruit from the ovary is triggered by the double-fertilization process (stage 13), and the fruit reaches its maximum length at stage 17-B (Ferrándiz et al., 1999; Roeder and Yanofsky, 2006). Double fertilization causes a local increase in auxin concentration, which results in the activation of gibberellin (GA) biosynthesis. The synchronized action of the two hormones controls the differentiation of the ovary into a fruit (Alabadí et al., 2009). AUXIN RESPONSE FACTOR (ARF) 6 and ARF8 interact with the MADS-box transcription factor FRUITFULL (FUL) to recruit microRNA 172c (miR172c), which is required to inhibit the repressor of fruit elongation, *APETALA 2* (*AP2*) (José Ripoll et al., 2015). FUL also represses the expression of *INDEHISCENT* (*IND*), which encodes a basic-helix-loop-helix (bHLH) transcription factor that negatively regulates fruit growth (Liljegren et al., 2004).

Cytokinins (CKs) have been implicated in regulating placenta length/size and determining ovule number (Cucinotta et al., 2016). Indeed, higher-order *crf* (*cytokinin response factor*) mutants possess fewer ovules and smaller placentas, which suggests they have defects in cell proliferation and/or expansion (Cucinotta et al., 2016).

CKs are also involved in valve margin differentiation (Marsch-Martínez et al., 2012). The *IND* fruit phenotype of *shp1 shp2* double mutants, which results from defects in valve margin differentiation (Liljegren et al., 2000), can be rescued by exogenous CK treatment (Marsch-Martínez et al., 2012). The CYTOKININ OXIDASE/DEHYDROGENASE (CKX) proteins catalyze the irreversible inactivation of CKs, transforming them to adenine and a corresponding side chain-derived aldehyde (Mok and Mok, 2001; Spíchal, 2012). The CKX enzymes differ in their subcellular localization, chemical characteristics, and substrate specificity (Galuszka et al., 2007; Werner et al., 2003). Reduced CK degradation in the *ckx3 ckx5* double mutant causes an increase in pistil length and a consequent increase in seed yield (Bartrina et al., 2011). The *CKX7* gene is one of the seven members of the CKX family (Mok and Mok, 2001). It encodes a unique CKX protein that localizes to the cytosolic compartment of the cell, where it degrades a specific CK pool (Köllmer et al., 2014). The CKX7 protein has the lowest similarity to other *Arabidopsis* CKX members but is more similar to CKX-like proteins of bacteria and green algae (Schmülling et al., 2003). It has been reported that CKX7 is required for appropriate root growth and xylem differentiation (Köllmer et al., 2014).

In this manuscript, we report the function of CKX7 and CKs in fruit elongation and the role of the MADS-box transcription factor SEEDSTICK (STK) as a central integrator of the CK hormonal pathway and the molecular network controlling fruit size.

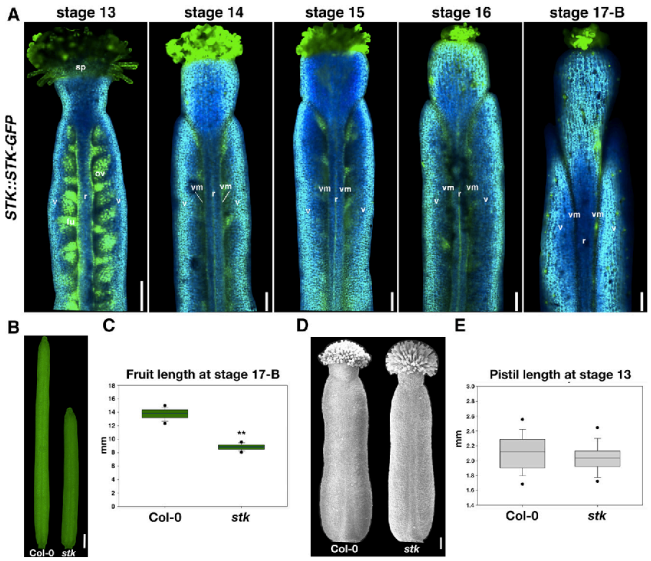

Figure 1. STK Protein Localization and Morphological Characterization of *stk* Fruit and Pistils

(A) Confocal images of *STK::STK-GFP* (Col-0) in pistils (stage 13) and during fruit elongation stages (stages 14 to 17-B). r, replum; sp, stigma papillae; v, valve; vm, valve margin. Scale bars, 100 μm.

(B) Stereomicroscope images of *stk* and Col-0 siliques at stage 17-B. Scale bar, 1 mm.

(C) Boxplot representing *stk* and Col-0 silique length at stage 17-B. Boxes indicate the first quartile (Q1), the mean, and the third quartile (Q3); the black dots represent maximum and minimum values. The length of the fruits was evaluated by measuring 20 siliques for each genotype for three biological replicates. Statistical analysis was performed using Student's t test (**$p < 0.01$).

(D) SEM imaging of *stk* and Col-0 pistils at stage 13. Scale bar, 100 μm.

(E) Boxplot representing *stk* and Col-0 pistil length at stage 13. Boxes indicate the first quartile (Q1), the mean, and the third quartile (Q3); the black dots represent maximum and minimum values. The length of the pistils was evaluated by measuring 20 pistils for each genotype in two biological replicates.

RESULTS

STK Is Required for Fruit Elongation

Recently, the presence of *STK* transcripts has been demonstrated in siliques at different developmental stages (Mizzotti et al., 2018). To better characterize the localization of the STK protein, we analyzed the *STK::STK-GFP* (Mizzotti et al., 2014) marker line in pistils during anthesis (stage 13) and in siliques from stage 14 to stage 17-B. During fertilization (stage 13), the STK-GFP protein was localized to stigma papillae, the funiculus, ovules, and the replum (Figure 1A). During fruit growth, the protein was localized within the medial domain of the fruit, in the vascular bundle of the replum, and in the valve margin from stage 14 to stage 16 (Figure 1A). At stage 17-B, no GFP signal was observed in the replum, whereas it was still detected in the valve margin (Figure 1A).

The *stk* mutant is characterized by shorter fruits than wild type (Pinyopich et al., 2003; Herrera-Ubaldo et al., 2019). At stage 17-B, when siliques reach their maximum size and length (Ferrándiz et al., 1999; Roeder and Yanofsky, 2006), the *stk* mutant is characterized by shorter fruits than those of wild type (*stk*: mean = 8.84 mm, n = 60; Col-0: mean = 13.82 mm, n = 60) (Figures 1B and 1C). However, the length of *stk* pistils (Figures 1D and 1E) at anthesis did not differ significantly from that of wild-type pistils (*stk*: mean = 2.03 mm, n = 40; Col-0: mean = 2.11, n = 40). These data show that STK positively regulates fruit elongation following fertilization.

CK Signaling Is Altered in *stk* during Fruit Elongation

CKs positively regulate pistil development, and a deficiency in CK production, perception, or response causes a decrease in pistil size (Cucinotta et al., 2016, 2018; Reyes-Olalde et al., 2017). By contrast, an increase in the amount of CKs and consequently CK response causes an increase in pistil size (Bartrina et al., 2011). However, the role of CKs in determining silique length has not previously been described. Therefore, we studied CK signaling in *stk* pistils and fruits with respect to the wild type, using the *TCSn::GFP* marker that is activated in response to CKs (Zürcher et al., 2013). The GFP signal was localized to the medial domain, the replum, and the style and stigma of wild-type pistils before fertilization at stage 12 (Figure 2A). A similar pattern of GFP expression was detected in *stk* (Figure 2G). At stage 13, there was a clear increase in GFP signal in the replum and style of *stk* with respect to wild type (Figures 2B and 2H). During fruit elongation, CK signaling decreased in the medial domain of wild-type fruit. In particular, a weak GFP signal was still detected in the replum at stage 14 (Figure 2C), whereas from stage 15 onward, no GFP was visible (Figures 2D–2F). By contrast, *TCSn* was still active in the *stk* replum and style at stage 14 (Figure 2I), in the replum at stage 15 (Figure 2J), and in the valve margin at stage 16 (Figure 2K), whereas no GFP was detected at stage 17-B (Figure 2L). In conclusion, wild-type CK signaling decreased after fertilization, concomitant with the onset of fruit elongation, whereas in *stk*, CK signaling remained detectable until at least stage 16.

STK Directly Regulates *CKX7* Expression

To understand the basis for the increased CK signaling in *stk* mutant fruit with respect to wild type (Figure 2), we hypothesized that a difference might exist in the activity of the genes involved in CK metabolism. We particularly focused on CK

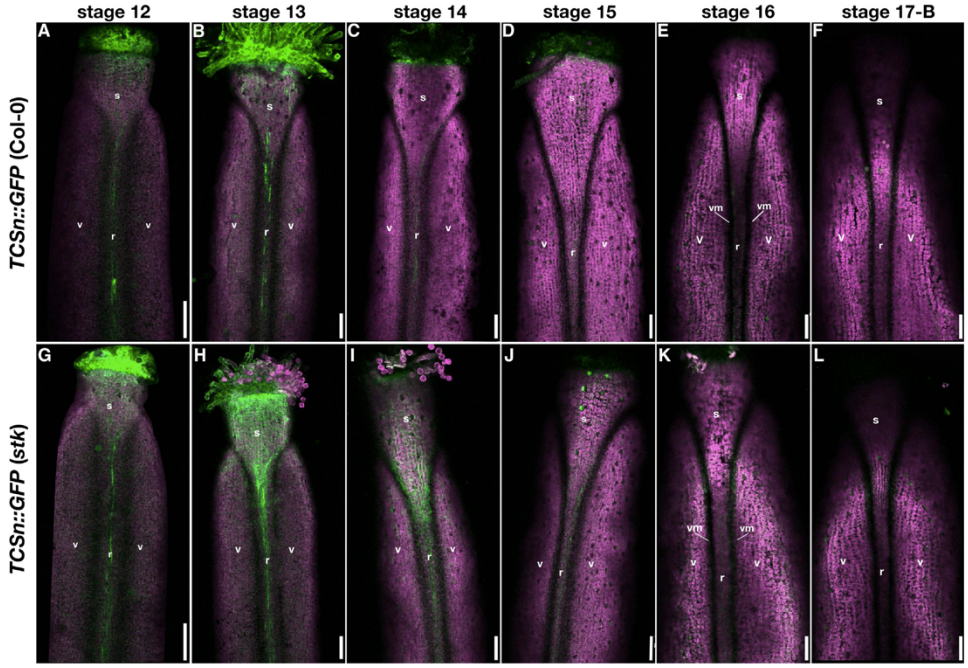

Figure 2. Comparative *In Vivo* CK Signaling in Pistils and Fruits of *stk* and Col-0, Revealed by Confocal Imaging Using the *TCSn::GFP* Marker

(A–F) *TCSn::GFP* expression in Col-0. Stage 12 pistil before fertilization (A), stage 13 pistil during fertilization (B), stage 14 of fruit development (C), stage 15 of fruit development (D), stage 16 of fruit development (E), and stage 17-B of fruit development (F).

(G–L) *TCSn::GFP* expression in *stk*. Stage 12 pistil (G), stage 13 (H), stage 1 (I) 4, stage 15 (J), stage 16 (K), and stage 17-B (L). r, replum; s, style; v, valve; vm, valve margin. Scale bars, 100 μm.

degradation, which is catalyzed by the CKX enzymes that regulate the amount of CKs in cells (Mok and Mok, 2001; Spíchal, 2012). We performed qPCR to quantify expression of the *CKX* genes in wild-type and *stk* mutant pistils/siliques at stages 13–14, 15–16, 17-A, and 17-B of fruit growth. We analyzed the transcript levels of *CKX1*, *CKX3*, and *CKX5*, whose roles in pistil/silique development have been previously described (Bartrina et al., 2011; Werner et al., 2003), as well as that of *CKX6*, whose promoter is active in the funiculus (Werner et al., 2003), and *CKX7*, which is expressed in fruits of different species, including *Arabidopsis thaliana*, *Brassica napus*, and *Malus domestica* (Liu et al., 2018; Mizzotti et al., 2018; Tan et al., 2018). The comparative analysis of *CKX* expression revealed that only *CKX7* expression was lower in *stk* than in wild type at stages 13–14, 15–16, 17-A, and 17-B (Figure 3A). We analyzed *CKX7* promoter activity in *stk* at the same stages used for expression analysis, using the *pCKX7::GUS* construct. The *CKX7* promoter was active in the vascular tissues of the pistil and fruit (Figure 3B; see also Figure S1). In wild type, the **β-glucuronidase** (GUS) signal was present in the lateral vascular bundles of the valves and in the vascular bundle of the replum following fertilization and during fruit elongation (up to stage 17-B) (Figure 3B). However, no *CKX7* promoter activity was observed in *stk* at all stages analyzed (Figure 3B). These results suggest that STK might control CK degradation by transcriptionally regulating *CKX7*. To determine whether STK directly regulates *CKX7*, we performed a chromatin immunoprecipitation (ChIP) assay using anti-GFP antibodies and chromatin from *stk* siliques up to stage 16, from plants expressing *STK::STK-GFP* (Mizzotti et al., 2014). We analyzed the *CKX7* promoter sequence for the presence of MADS-domain CArG-box binding sites (Egea-Cortines et al., 1999; de Folter and Angenent, 2006). Among the eight putative CArG boxes we identified in the *CKX7* promoter and tested for direct binding by STK, the ChIP assay revealed significant enrichment of binding to the regions spanning CArG-box 4 and CArG-box 5 in the *CKX7* promoter in *STK::STK-GFP* compared with the wild-type control (Figure 3C). Therefore, STK can directly bind the *CKX7* promoter, and the increased level of CK signaling observed in *stk* medial fruit tissues during fruit elongation might result from a local downregulation of *CKX7*, which is responsible for cytosolic CK degradation in cells in these tissues.

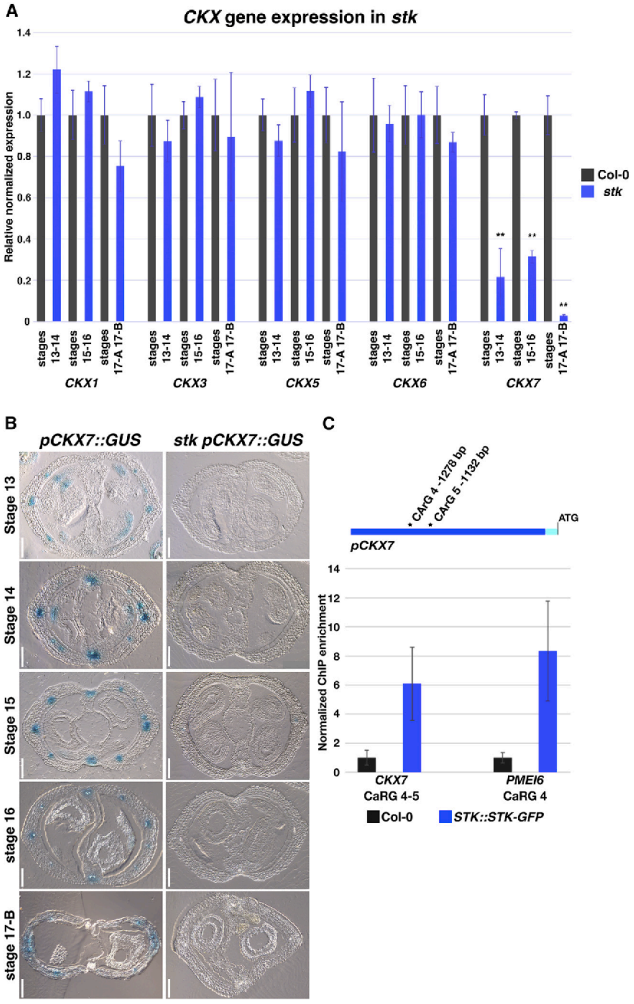

Figure 3. STK Directly Regulates *CKX7* Expression

(A) Expression of *CKX1*, *CKX3*, *CKX5*, *CKX6*, and *CKX7* in *stk* and Col-0 at stages 13–14, 15–16, 17-A, and 17-B. Statistical analysis was performed using Student's t test (**$p < 0.01$) and gene expression was normalized to that of *ACTIN* and *UBIQUITIN*. Histograms show a representative experiment in which error bars represent the SD for three technical replicates. Three qPCR (biological replicates) were performed and generated similar results.

(B) Cross-sections showing expression of *pCKX7::GUS* from stage 13 to stage 17-B in *stk* and Col-0. Scale bars, 100 μm. At the right bottom corner of the stk pCKX7::GUS (stage 14) image the scale bar automatically generated by the microscope has been covered to show uniform scale bars in this panel.

(C) Representation of the *CKX7* promoter showing the position of the CArG boxes. Representative ChIP experiment between *STK::STK-GFP* and Col-0. Error bars represent the SD for three technical replicates. The fold enrichment was calculated against data for Col-0. *PECTIN METHYLESTERASE INHIBITOR 6* (*PMEI6*) CArG 4 was used as a positive, and data were normalized with *ACTIN2/7*.

The CK Cytosolic Pool Regulates Cell Elongation during Fruit Development

To evaluate the role of *CKX7* during fruit elongation, we investigated the phenotype of two independent *ckx7* mutants and a *35S::CKX7* overexpression line. The first *ckx7* mutant allele contained a transfer DNA (T-DNA) insertion in the second intron (*ckx7* SAIL_515_A07). We generated a second mutant allele using CRISPR/Cas9 technology. The second mutant allele (named *ckx7 T*) carried a T insertion within the first exon at position 254 from the ATG start (Figure S2A). This insertion causes a frameshift in the FAD binding domain and the formation of a premature stop codon after 129 aa, creating a truncated protein with no enzymatic activity (Bae et al., 2008). The pistils of stage 13 *ckx7*, *ckx7 T*, and *35S::CKX7* plants were the same length as wild-type pistils (Figures S3A and S3B). At stage 17-B, the fruits of *ckx7* and *ckx7 T* plants were shorter (*ckx7* = 10.87 mm, n = 60; *ckx7 T* = 12.45 mm, n = 60) than those of wild type (Col-0 = 13.54 mm, n = 60) but were longer than those of *stk* (Figures 4A and 4B, see also Figures 1B and 1C). Conversely, the overexpression line *35S::CKX7* produced longer fruits (*35S::CKX7* = 15.13 mm, n = 60) than wild-type plants (Figures 4A and 4B). Altogether, the data suggest a positive role for *CKX7* in promoting fruit elongation following fertilization.

To clarify the potential role of CKs in cell proliferation and/or elongation during fruit maturation, we analyzed in detail the shape and morphology of the valve cells in *stk*, *ckx7*, and *ckx7 T* and the overexpression line *35S::CKX7* at stage 17-B (Figures 4C–4H). We analyzed valve cells, because it has been demonstrated that increased fruit size results from the elongation of epidermal cells (Vivian-Smith et al., 2001). We used Feulgen staining, adapted for siliques, to analyze cell morphology (Braselton et al., 1996). The total number of valve cells in *stk*, *ckx7*, and *ckx7 T* mutants and in the *35S::CKX7* overexpression line was similar to that of wild type, whereas cell length differed among the various genotypes (Figures 4C–4H). Specifically, mean cell length in *stk* valves (Figure 4D) was lower

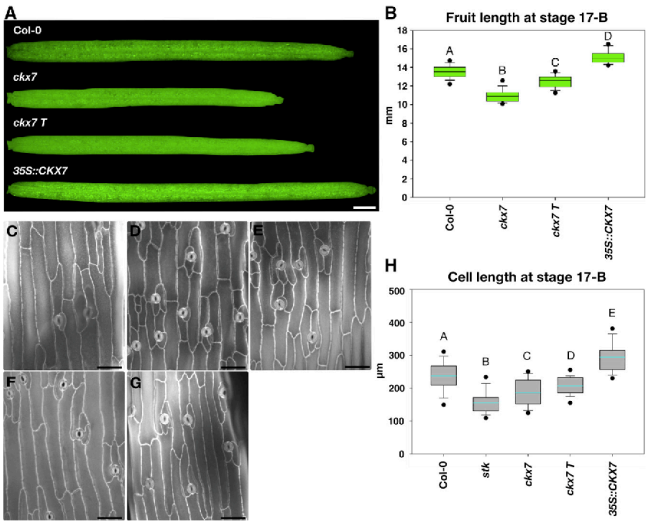

Figure 4. CK Degradation Is Essential for Correct Fruit Elongation

(A) Stereomicroscope images of *ckx7*, *ckx7 T*, *35S::CKX7*, and Col-0 siliques at stage 17-B. Scale bar, 1 mm.

(B) Boxplot representing the fruit length for the genotypes in (A). Boxes indicate the first quartile (Q1), the mean, and the third quartile (Q3); the black dots represent maximum and minimum values. The length of the fruits was evaluated by measuring 20 siliques for each genotype for three biological replicates.

(C–G) Confocal images of valve fruit cells: (C) Col-0, (D) *stk*, (E) *ckx7*, (F) *ckx7 T*, and (G) *35S::CKX7*. Scale bars, 50 µm.

(H) Boxplot representing cell length in the mutants and the overexpression line. Boxes indicate the first quartile (Q1), the mean, and the third quartile (Q3); the black dots represent maximum and minimum values. Cell length was evaluated by measuring 30 cells for each genotype for three biological replicates.

Statistical analyses were performed using ANOVA followed by Tukey's HSD test. Different letters indicate statistically significant differences ($p < 0.01$).

than in wild type (Figure 4C) (*stk* = 155.11 µm, Col-0 = 237.33 µm, Figure 4H). A similar decrease in cell length was observed for the two *ckx7* mutant alleles (Figures 4E and 4F) (*ckx7* = 185.38 µm, *ckx7 T* = 206.82 µm, Figure 4H), whereas valve cells in *35S::CKX7* plants (Figure 4G) were longer than cells in wild type (*35S::CKX7* = 281.26 µm, Figure 4H).

In conclusion, the valve cells of *stk*, *ckx7*, and *ckx7 T* mutants, from which the absence of CKX7 causes an increase in the pool of cytosolic CKs, were shorter than in wild type; conversely, those in the *35S::CKX7* line were longer. These data suggest that the cytosolic CK pool plays an important role in the regulation of cell elongation and consequently in the regulation of fruit growth.

The Quantity of *cis*-Zeatin (cZ) and *trans*-Zeatin (tZ) CKs in *stk*, *ckx7*, and *ckx7 T* Is Affected during Fruit Growth

To evaluate whether the increased and more persistent activity of the *TCSn* marker in *stk* (Figure 2) resulted from an increase in CK concentration in developing siliques, we performed a metabolic analysis in which we quantified CKs. In particular, we quantified CKs at early stages of fruit growth (from stage 13 to stage 16) and at late stages of fruit elongation (stages 17-A and 17-B) in *stk* and in the two single mutants *ckx7* and *ckx7 T*. As described earlier, these three single mutants possess shorter fruits than wild type (Figures 1B and 1C, see also Figures 4A and 4B). We focused on active CK forms. However, data for inactive CK forms are presented in Tables 1 and S1.

The active isoprenoid CKs are cZ, tZ, isopentenyladenine (*IP*), and dihydrozeatin (*DHZ*) (Mok and Mok, 2001; Sakakibara, 2006; Spíchal, 2012). These active bases derive from the direct precursor riboside (R) and riboside monophosphate (RMP) forms (cZR and cZRMP, tZR and tZRMP, *IP*R and *IP*RMP, and *DHZ*R and *DHZ*RMP) (Mok and Mok, 2001; Sakakibara, 2006; Spíchal, 2012). These precursors can be considered active because the CK receptors, which mediate cellular CK response, display sensitivity to these forms (Romanov et al., 2006; Stolz et al., 2011).

At early stages of fruit development, cZ-type active bases and precursors increased in all mutants with respect to wild type (Table 1). Notably, the *stk*, *ckx7*, and *ckx7 T* mutants contained more active cZ than wild type (Table 1). Moreover, *stk* and *ckx7 T* contained a higher amount of cZR (Table 1). At same stages of silique development, the three single mutants *stk*, *ckx7*, and *ckx7 T* showed a general decrease in active tZ (Table 1). In particular, the *stk*, *ckx7*, and *ckx7 T* mutants possessed a low amount of tZR, and a small concentration of tZRMP was measured only in *stk* and *ckx7 T* (Table 1).

More cZ-type CKs were present in *ckx7* at late stages. Only the *ckx7* mutant had a higher concentration of the cZ base (Table 1). However, the concentration of cZR was higher in the two single *ckx7* mutants than in wild type, and the level of cZRMP in *stk* was lower than in wild type (Table 1). At same developmental stage, *stk* contained more tZ-type CKs than wild type (Table 1), and *stk* and *ckx7 T* contained more tZR than wild type at same stages (Table 1). One tZ precursor had a different concentration in the two single *ckx7* mutants. A lower quantity of tZRMP was measured in *ckx7* than in wild type, whereas *stk* and *ckx7 T* possessed the same concentration of this precursor as wild type (Table 1).

The concentration of active *IP* in the mutants did not differ from that in wild type at early and late stages of fruit elongation (Table S1). Only the concentration of the precursor *IP*R was lower in *stk* and *ckx7 T* during early stages of fruit elongation, whereas at late stages, *IP*RMP was present at a higher level in *ckx7 T* than in wild type (Table S1). A decrease in the quantity of the *DHZ* precursors

Table 1. Profile of cZ and tZ CKs in *ckx7*, *ckx7 T*, *stk*, and Col-0

Genotype Stage 13 to 16	Total *cZ* Types	*cZ*	*cZR*	*cZRMP*	*cZOG*	*cZROG*	*cZ7G*	*cZ9G*
Col-0	28.52 ± 3.63	0.40 ± 0.05	3.48 ± 0.21	16.67 ± 3.11	0.31 ± 0.04	2.20 ± 0.18	5.32 ± 0.67	0.14 ± 0.03
ckx7	41.32 ± 3.69**	0.92 ± 0.10***	4.39 ± 0.64	16.62 ± 2.32	0.54 ± 0.07**	2.72 ± 0.39	16.01 ± 1.49***	0.48 ± 0.07***
ckx7 T	43.33 ± 1.68***	0.79 ± 0.08***	4.57 ± 0.68*	20.61 ± 1.34	0.59 ± 0.10**	2.67 ± 0.18*	13.71 ± 0.69***	0.39 ± 0.05***
stk	31.58 ± 04.02	0.54 ± 0.09**	4.54 ± 0.63*	19.74 ± 3.65	0.30 ± 0.02	1.90 ± 0.10*	4.49 ± 0.24	0.08 ± 0.02*
Genotype Stages 13 to 16	Total *tZ* Types	*tZ*	*tZR*	*tZRMP*	*tZOG*	*tZROG*	*tZ7G*	*tZ9G*
Col-0	34.72 ± 3.19	0.45 ± 0.10	10.18 ± 1.15	14.08 ± 1.72	0.98 ± 0.03	0.89 ± 0.06	6.15 ± 0.52	2.00 ± 0.32
ckx7	28.84 ± 2.95	0.44 ± 0.08	7.31 ± 1.15*	10.87 ± 1.64	0.76 ± 0.10**	0.75 ± 0.06*	6.32 ± 0.44	2.39 ± 0.22
ckx7 T	23.89 ± 2.06**	0.33 ± 0.07	6.17 ± 0.96**	7.45 ± 0.73***	0.72 ± 0.06***	0.69 ± 0.13	6.12 ± 0.29	2.41 ± 0.51
stk	27.19 ± 0.92**	0.43 ± 0.07	7.63 ± 1.07*	10.18 ± 1.27*	0.85 ± 0.06*	0.67 ± 0.08**	5.60 ± 0.37	1.83 ± 0.10
Genotype Stages 17-A and 17-B	Total *cZ* Types	*cZ*	*cZR*	*cZRMP*	*cZOG*	*cZROG*	*cZ7G*	*cZ9G*
Col-0	28.36 ± 2.67	0.63 ± 0.10	1.75 ± 0.29	20.49 ± 2.10	0.22 ± 0.02	0.91 ± 0.13	4.18 ± 0.45	0.18 ± 0.02
ckx7	37.20 ± 3.85*	0.91 ± 0.10*	3.38 ± 0.87*	21.37 ± 2.36	0.43 ± 0.07**	1.40 ± 0.14**	9.34 ± 1.06***	0.39 ± 0.05***
ckx7 T	29.52 ± 3.00	0.69 ± 0.03	2.55 ± 0.45*	18.74 ± 2.43	0.30 ± 0.04*	1.19 ± 0.14*	5.38 ± 0.29**	0.23 ± 0.02*
stk	20.71 ± 1.87**	0.52 ± 0.11	1.75 ± 0.33	13.76 ± 1.97**	0.18 ± 0.04	1.06 ± 0.18	3.08 ± 0.19**	0.15 ± 0.01
Genotype Stages 17-A and 17-B	Total *tZ* Types	*tZ*	*tZR*	*tZRMP*	*tZOG*	*tZROG*	*tZ7G*	*tZ9G*
Col-0	43.45 ± 5.55	0.99 ± 0.18	10.59 ± 2.55	24.03 ± 1.72	2.47 ± 0.49	1.73 ± 0.12	2.45 ± 0.13	1.18 ± 0.14
ckx7	19.56 ± 1.54***	0.92 ± 0.20	6.63 ± 1.44	4.07 ± 0.82***	2.12 ± 0.18	1.59 ± 0.09	2.71 ± 0.03*	1.53 ± 0.08*
ckx7 T	53.27 ± 5.95	1.17 ± 0.11	18.94 ± 2.43**	26.04 ± 3.33	1.96 ± 0.21	1.49 ± 0.16	2.48 ± 0.23	1.18 ± 0.21
stk	57.70 ± 3.62**	1.10 ± 0.09	17.27 ± 2.06*	29.16 ± 3.35	3.14 ± 0.28	2.26 ± 0.49	3.23 ± 0.19**	1.54 ± 0.18

The data are in picomoles per gram of fresh weight; means ± SD (n = 4). Total *cis*-Zeatin (total *cZ* types): *cis*-Zeatin (*cZ*), *cis*-Zeatin riboside (*cZR*), *cis*-Zeatin riboside-5′-monophosphate (*cZRMP*), *cis*-Zeatin-O-glucoside (*cZOG*), *cis*-Zeatin riboside-O-glucoside (*cZROG*), *cis*-Zeatin-7-glucosides (*cZ7G*), and *cis*-Zeatin-9-glucoside (*cZ9G*) from stage 13 to stage 16 of fruit development in *ckx7*, *ckx7 T*, *stk*, and Col-0. Total *trans*-Zeatin (total *tZ* types): *trans*-Zeatin (*tZ*), *trans*-Zeatin riboside (*tZR*), *trans*-Zeatin riboside-5′-monophosphate (*tZRMP*), *trans*-Zeatin-O-glucoside (*tZOG*), *trans*-Zeatin riboside-O-glucoside (*tZROG*), *trans*-Zeatin-7-glucosides (*tZ7G*), and *trans*-Zeatin-9-glucoside (*tZ9G*) from stage 13 to stage 16 of fruit development in *ckx7*, *ckx7 T*, *stk*, and Col-0. Total *cZ* types: *cZ*, *cZR*, *cZRMP*, *cZOG*, *cZROG*, *cZ7G*, and *cZ9G* at stages 17-A and 17-B of fruit development in *ckx7*, *ckx7 T*, *stk*, and Col-0. Total *tZ* types: *tZ*, *tZR*, *tZRMP*, *tZOG*, *tZROG*, *tZ7G*, and *tZ9G* at stages 17-A and 17-B of fruit development in *ckx7*, *ckx7 T*, *stk*, and Col-0. Statistical analysis was performed using Student's t test (*$p < 0.05$, **$p < 0.01$, ***$p < 0.001$).

DHZR and *DHZ*RMP was observed in the three mutants during early and late stages of fruit growth (Table S1).

In conclusion, similarities were observed in the concentration of active CKs among the three mutants compared with the wild type, which highlights the influence of CKs in determining final fruit size.

STK and *CKX7* Function in the Same Pathway to Regulate Fruit Elongation

Because *CKX7* might function in the same pathway as *STK* to control fruit elongation, we crossed the two single T-DNA mutants *stk* and *ckx7* to create the double *stk ckx7* mutant and measured the length of its fruits. *stk ckx7* possessed shorter siliques than wild type and *ckx7*, but these were not significantly different in length from *stk* siliques (Figures S4A and S4B). To investigate the potential role of CK degradation in the *stk* mutant phenotype, we attempted to complement the *stk* phenotype with the *35S::CKX7* construct. The rationale was that if *stk* is defective in CK degradation because of *CKX7* downregulation, leading to a higher level of CKs in elongating *stk* fruits, *CKX7* overexpression in *stk* might induce the degradation of CKs in fruit tissues and complement the *stk* phenotype. We obtained five independent transformed plants (*stk 35S::CKX7*), and all displayed partial rescue of the *stk* fruit-length phenotype (Figures S4C and S4D). The double-mutant phenotype confirms that STK acts upstream of *CKX7*; however, because *stk* is epistatic to *ckx7* and the overexpression of *CKX7* only partially rescued the *stk* phenotype, *STK* probably regulates fruit elongation via a CK-dependent pathway and a CK-independent pathway (explored later in more detail).

Finally, to corroborate the hypothesis that CKs negatively influence fruit elongation, we exogenously applied 6-benzylaminopurine (BAP) to *stk* and wild-type siliques at stage 13 for 5 days, analyzed the length of the resulting siliques at stage 17-B, and compared it with that of mock-treated control siliques (Figures S4E and S4F). Exogenous BAP treatment resulted in a reduction in fruit length in wild-type siliques when compared with the mock control and a further reduction in the length in *stk* with respect to the mock (Figures S4E and S4F). This confirms that the final fruit length is regulated by CKs.

FUL Is Downregulated in *stk*

To explain the partial rescue of the *stk* short silique phenotype in the transgenic mutant *35S::CKX7*, we investigated alternative pathways required for fruit growth that might be regulated by STK. It has been shown that ARF6 and ARF8 cofunction with FUL to directly activate *MIR172C* expression in the promotion of valve elongation, because miR172c negatively regulates *AP2*, which is a repressor of fruit elongation (José Ripoll et al., 2015). In wild type, the g*FUL:GFP* fusion protein was localized to the valves and the replum upon fertilization at stage 13. However, from stage 14 onward, FUL-GFP expression was reduced (Figures 5A–5E). In *stk*, FUL-GFP expression was lower than in wild type starting from stage 13 and was absent at stages 15 and 16, whereas at stage 17-B, a weak GFP signal was detected in the medial domain of the fruit (Figures 5F–5J). We also confirmed by qPCR that *FUL* is downregulated in *stk* at different fruit developmental stages with respect to wild type (Figure 5K). To study the genetic interaction between the two MADS-box transcription factors STK and FUL, we analyzed the fruit length of the double *stk ful* mutant at stage 17-B (Figures 5L and 5M). *stk ful* displayed shorter fruits than wild type (*stk ful* = 3.79 mm, n = 60; Col-0 = 14.18 mm, n = 60) and both *stk* and *ful* single mutants (*stk* = 8.89 mm, n = 60; *ful* = 4.61 mm, n = 60) (Figures 5L and 5M). The additive phenotype of the double mutant suggests that both MADS-box proteins regulate fruit elongation via two distinct parallel pathways.

Therefore, we compared *MIR172C* and *AP2* expression in *stk* fruits by qPCR with that in wild type. As expected, *MIR172C* expression was lower, whereas *AP2* expression was higher in *stk* with respect to wild type (Figures 5N and 5O). FUL is also necessary to confine *IND* activity within the valve margin (Liljegren et al., 2004). Ectopic lignification caused by increased *IND* expression in the valves of *ful* causes a failure of valve elongation (Liljegren et al., 2004). To confirm that the downregulation of *FUL* in *stk* also affects FUL targets, we analyzed *IND* expression in *stk* fruits at different developmental stages by qPCR and found it to be increased in *stk* compared with wild type (Figure 5P). These data suggest that STK modulates *FUL* expression, which is required to downregulate *AP2* (via miR172c) and *IND*, thereby promoting silique elongation in *Arabidopsis*.

DISCUSSION

STK Is Fundamentally Required for Fruit Growth

The siliques of the *stk* mutant were shorter siliques than those in wild type (Figures 1B and 1C), despite the normal seed set (Mizzotti et al., 2012), demonstrating the importance of this MADS-domain transcription factor in fruit elongation. Activity of the *STK* promoter was observed in the medial domain of the pistils up to stage 13 (Herrera-Ubaldo et al., 2019). We detected STK-GFP protein from fertilization up to stage 16 in the replum and in the valve margin up to stage 17-B, when siliques reach their final size (Figure 1A). It has been reported that genes that are expressed exclusively in the medial domain of the silique can influence the final fruit length. The expression of *REPLUMLESS* (*RPL*) and *NO TRANSMITTING TRACT* (*NTT*) is confined to the medial domain of the fruit, and mutation of either gene results in siliques that are shorter than wild-type siliques (Crawford et al., 2007; Dinneny et al., 2005; Herrera-Ubaldo et al., 2019; Roeder et al., 2003), highlighting the importance of the replum and the ability of genes expressed in this tissue to influence fruit growth.

The Regulatory Interaction of CKs, *STK*, and *CKX7* Is Crucial for Fruit Growth

CKs are centrally important in controlling the cell cycle and cell expansion during the development of roots and pistils (Bartrina et al., 2011; Cucinotta et al., 2016; Street et al., 2016). Different approaches can be used to increase the levels of CKs in plants and thus to study their importance in plant development. One method is to increase the activity of the ISOPENTENYL TRANSFERASE (IPT) enzymes, which synthesize CKs (Sakakibara, 2006), or to inhibit CK degradation by CKX enzymes, which is the approach that we adopted here.

The expression of the synthetic marker line *TCSn::GFP* revealed an increase in CK signaling during the initial stages of fruit growth in *stk* (Figure 2). To better characterize the basis of this increase in CK signaling, we analyzed the expression of various members of the *CKX* family that encode enzymes involved in CK

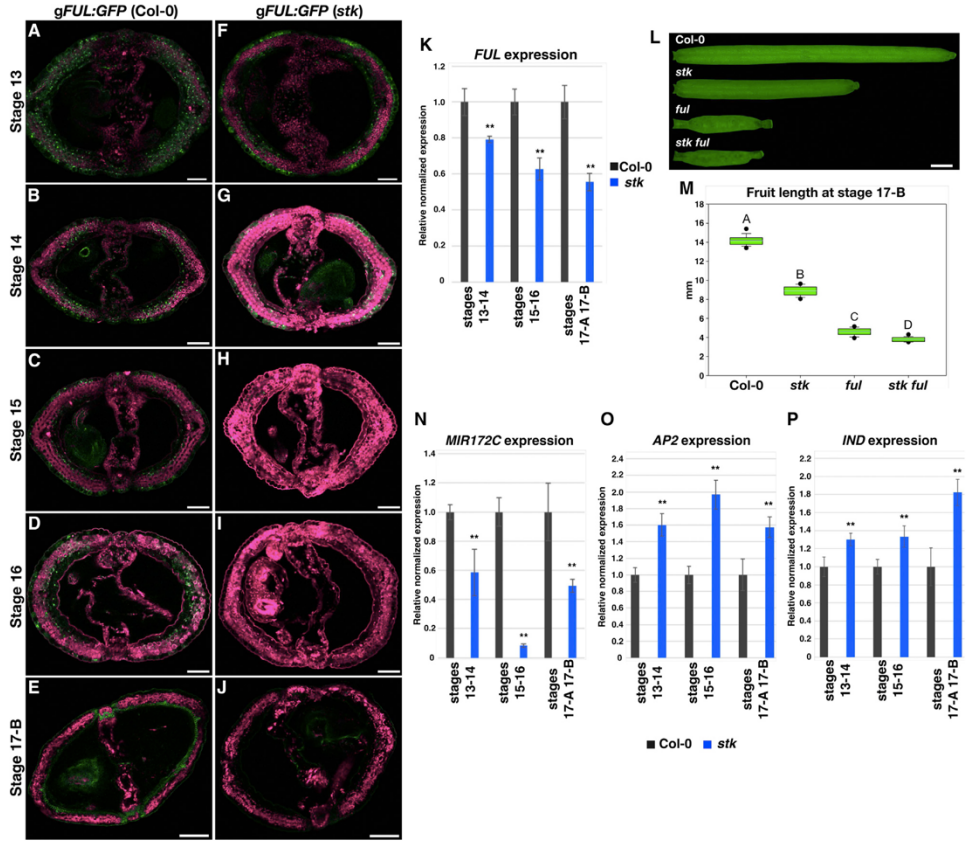

Figure 5. The Role of *STK* in Valve Elongation Pathways

Expression of g*FUL:GFP* in *stk* and Col-0 from stage 13 to stage 17-B.

(A–E) g*FUL:GFP* in Col-0. (A) stage 13 pistil during fertilization, (B) stage 14 of fruit development, (C) stage 15 of fruit development, (D) stage 16 of fruit development, (E) stage 17-B of fruit development. Scale bars, 50 μm.

(F–J) g*FUL:GFP* in *stk*. (F) stage 13 pistil during fertilization, (G) stage 14 of fruit development, (H) stage 15 of fruit development, (I) stage 16 of fruit development, (J) stage 17-B of fruit development. Scale bars, 50 μm.

(K) qPCR to analyze *FUL* expression in *stk* and Col-0 siliques at stages 13–14, 15–16, 17-A, and 17-B. Statistical analysis was performed using Student's t test (**$p < 0.01$). Expression was normalized with *ACTIN* and *UBIQUITIN*. Histograms show a representative experiment in which error bars represent the SD of three technical replicates. Three qPCR (biological replicates) were performed and generated similar results.

(L) Stereomicroscope images of *stk*, *ful*, *stk ful* siliques, and Col-0 at stage 17-B. Scale bar, 1 mm.

(M) Boxplot representing fruit length values of the genotypes described in (L). Boxes indicate the first quartile (Q1), the mean, and the third quartile (Q3); the black dots represent maximum and minimum values. The length of the fruits was evaluated by measuring 20 siliques for each genotype for three biological replicates. Statistical analysis was performed using ANOVA followed by Tukey's HSD test, where different letters indicate statistically significant differences ($p < 0.01$).

(N–P) Expression of (N) *MIR172C*, (O) *AP2*, and (P) *IND* in *stk* and Col-0 siliques at stages 13–14, 15–16, 17-A, and 17-B. Statistical analyses were performed using Student's t test (**$p < 0.01$). Expression data are normalized to expression of *ACTIN* and *UBIQUITIN*. Histograms show a representative experiment in which error bars represent the SD for three technical replicates. Three qPCR (biological replicates) were performed and generated similar results.

degradation (Mok and Mok, 2001; Figure 3A). We found that only *CKX7* was differentially expressed in *stk* and wild type at different fruit developmental stages (Figure 3A). The expressions of *STK* and *CKX7* overlap in the medial domain of the fruit. However, *CKX7* promoter activity was detected not only in the medial domain of the fruit, similar to STK protein (Figure 1A), but also

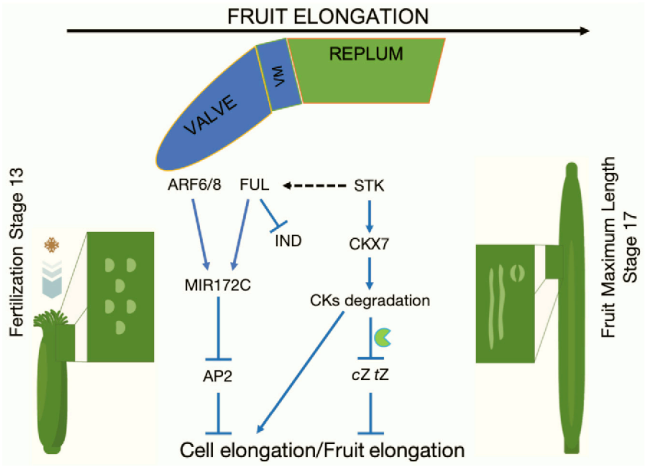

Figure 6. Genetic Model for the Regulation of Fruit Elongation in *Arabidopsis thaliana*

Based on genetic, molecular, and hormonal data presented in this study, we propose a model whereby fruit elongation is regulated by STK, which positively regulates *CKX7* activity in the replum. CKX7 degrades *c*Z and *t*Z CK in fruit cells, leading to an inhibition of cell/fruit elongation. Moreover, STK indirectly regulates *FUL*, which plays a crucial role in the valve elongation pathways. VM, valve margin.

in the lateral vascular bundle of the valves (Figure 3B), in which STK is not expressed. Finally, we demonstrate here that STK is a direct positive regulator of *CKX7* (Figure 3C).

CKX7 Defines Fruit Final Size

We show that the absence of CKX7 activity and the consequent reduction in CK degradation in two *ckx7* mutant alleles caused a dramatic reduction in fruit elongation compared with wild type (Figures 4A and 4B). Conversely, ectopic CK degradation resulting from *CKX7* overexpression in *35S::CKX7* plants resulted in increased fruit length (Figures 4A and 4B). A role for CKX proteins in fruit elongation has been recently suggested based on expression analysis in other closely related species. In particular, an orthologous gene in *Brassica napus*, *BnCKX7-1*, is preferentially expressed in leaves and siliques (Liu et al., 2018; Song et al., 2015). Expression analysis of different *BnCKX* genes from vegetative to reproductive phases revealed that the ortholog of *AtCKX7* is more highly expressed in a *B. napus* cultivar with longer siliques than in one characterized by shorter siliques (Liu et al., 2018). In addition to the results here for *Arabidopsis*, the role of CK in fruit growth appears to be conserved, at least among the Brassicaceae.

Moreover, similar to in the Brassicaceae (Zuñiga-Mayo et al., 2018), exogenous CK treatment in *Arabidopsis* reduces the length of wild-type siliques (Figures S4E and S4F). Treating *stk* with BAP after fertilization causes a further reduction in fruit length (Figures S4E and S4F). The exogenous BAP treatments demonstrate the negative impact of excess CKs on fruit elongation in all Brassicaceae species.

The *stk* and *ckx7* Mutants Have a Higher Amount of CKs during Fruit Growth

The genetic network that regulates CK homeostasis is extremely complex. Therefore, to confirm that the fruit length phenotype described for *stk* and *ckx7* mutants results from an increase in the quantity of CKs, we metabolically profiled the CKs present in fruit mutants with respect to wild type (Tables 1 and S1). At early stages of fruit growth (stages 13 to 16) the endogenous levels of *c*Z bases and the precursors *c*Z and *c*ZR were higher in the mutant than in wild type (Table 1). The amount of *c*Z remained high in the *ckx7* mutant alleles at late stages 17-A and 17-B (Table 1), whereas the concentration of a precursor of the active form (cZRMP) was lower in *stk* than in wild type (Table 1). The lower *CKX7* catalytic activity in *stk* fruits at early stages and the absence of enzymatic activity in the *ckx7* mutant alleles at early and late stages caused an increase in *c*Z forms. This conclusion is consistent with the observation that *c*Z-type CKs are significantly reduced when *CKX7* is overexpressed in seedlings (Köllmer et al., 2014).

By contrast, we detected a general reduction in the concentration of *t*Z bases and their precursor in the mutants compared with wild type at early stages of fruit elongation (Table 1). However, at late stages, *stk* contained a higher amount of *t*Z-type CKs (Table 1), in particular, an increased concentration of *t*ZR, similar to *ckx7 T*. The *t*Z-type CKs are considered a lower-affinity substrate for the CKX7 enzyme (Galuszka et al., 2007; Köllmer et al., 2014; Kowalska et al., 2010). However, at late stages of fruit elongation, we detected a large increase in the amount of *t*Z types not only in *stk* and *ckx7* but also in *ckx7 T* (Table 1). These data suggest that the CKX7 enzyme might have different substrate affinities toward *t*Z at different developmental stages. At late developmental stages, the substrate affinity for CKX7 might be the same as that for *c*Z and *t*Z. In conclusion, the three mutants contained similar concentrations of *c*Z and *t*Z during different stages of fruit development with respect to wild type.

The concentration of active *IP* CKs in the mutants analyzed was relatively similar to that in wild type, whereas the amount of degradation products increased in the *ckx7* mutants throughout fruit growth (Table S1). The data are consistent with those in the literature, because CKX7 has a high affinity for *IP*-type CKs (Galuszka et al., 2007; Köllmer et al., 2014; Kowalska et al., 2010), but further experiments are required to explain the changes in concentration of *IP* CKs in *stk*. During late stages of fruit growth, *stk* contained fewer *IP* degradation products (Table S1).

Finally, the concentration of *DHZ*, a reduced form of *tZ* (Mok and Mok, 2001; Sakakibara, 2006; Spíchal, 2012), was lower in the mutants than in wild type at early and late developmental stages, especially the riboside precursors (*DHZ*R and *DHZ*RMP) (Table S1). These CKs are not degraded by CKXs (Spíchal, 2012). Potentially, the increasing amount of *tZ*, especially at late stages of fruit development, might reduce the concentration of *DHZ* in the mutants compared with the wild type, because this type of CK is a metabolic derivative form of *tZ*.

The Cytosolic CK Pool Must Be Degraded to Promote Cell Elongation in Fruit

In roots, CKs inhibit cell elongation in the primary root by activating typeB ARABIDOPSIS RESPONSE REGULATORs (RESPONSE REGULATORs (ARRs), which in turn, activate the auxin influx carrier AUX1 to modulate auxin transport (Street et al., 2016). The data here suggest that the cytosolic CK pool can potentially repress cell elongation in fruit, similar to in roots. In particular, the cytosolic CK pool, which preferentially consists of *cZ* and *tZ*, might be involved in this repression activity. Notably, CKs have an opposite role in fruit to that in pistils. The importance of CKs in the control of placenta size and number of ovules before fertilization has been demonstrated, and a reduction in the CK transcriptional response in the *crf2 crf3 crf6* triple mutant during pistil development causes a reduction in pistil size and a diminution in total ovule number (Cucinotta et al., 2016). Furthermore, CK signaling mutants show a reduction in pistil size and ovule number (Reyes-Olalde et al., 2017). The positive role of CKs in pistil elongation is confirmed by the *ckx3 ckx5* double mutant, which has longer pistils than wild type because of an increase in CK levels caused by a lack of CKX proteins, with a consequent upregulation of the CK transcriptional response (Bartrina et al., 2011). Before fertilization, CKs promote pistil cell division and elongation and regulate the number of ovule primordia. To facilitate pistil elongation, cell proliferation has to exceed cell differentiation. This is positively regulated by CKs before fertilization and negatively regulated after fertilization.

The Genetic Network Controlled by STK Regulates *FUL* Activity in Fruits

The partial complementation of the *stk* fruit length phenotype by the overexpression of *CKX7* (Figures S4C and S4D) confirms that these two genes act in the same pathway, with STK upstream of CKX7. However, the rescue was only partial, which suggests that STK might act in a pathway independent of that in which *CKX7* expression contributes to the correct degradation of the cytosolic CK pool to appropriately regulate fruit elongation post-fertilization. *FUL* is the most important regulator of valve epidermal cell elongation (Gu et al., 1998). The expression of FUL protein in valves, as monitored via the GFP fusion marker line *gFUL:GFP* (Figures 5A–5J), was lower in *stk* than in wild type. The same result was obtained when we analyzed the transcript levels of *FUL* in *stk* via qPCR (Figure 5K). However, because STK protein is not expressed in valves (Figure 1A), the regulation of *FUL* by STK here is indirect. Similar to in *stk*, *ful* shows increased CK signaling compared with wild type, as monitored by *TCSn::GFP* (Marsch-Martínez et al., 2012). However, increased *TCSn::GFP* expression in *stk* was observed in the replum (Figure 2), which spatially overlapped *STK* expression (Figure 1A), whereas the increased GFP signal in *ful* was present in the valves (Marsch-Martínez et al., 2012) and spatially overlapped *FUL* expression (Figures 5A–5E). The additive phenotype of the double *stk ful* mutant (Figures 5L and 5M) suggests that both MADS-box transcription factors regulate fruit elongation via parallel pathways. The decrease in FUL protein expression in *stk* subsequently downregulates *MIR172* gene expression (Figure 5N), which is essential to promote valve elongation by inhibiting AP2 (José Ripoll et al., 2015), the expression of which is upregulated in *stk* (Figure 5O). Finally, *IND* expression was upregulated in *stk* (Figure 5P). It is known that *IND* expression in *ful* mutant valves causes ectopic lignification and is considered responsible for the lack of cell elongation in *ful* mutant valve cells (Liljegren et al., 2004). These data suggest that STK might influence pathways independent of the *STK-CKX7* pathway described earlier, such as the FUL-MIR172-AP2 and FUL-IND pathways that control valve elongation.

A central unanswered question in plant developmental biology is the identification of hormone-sensing mechanisms and signal transduction pathways that connect regulatory pathways with the activation of developmental programs. Transcriptional networks and hormonal pathways are highly interconnected, and the identification of branchpoints will help to clarify the components that determine the dynamic growth of specific tissues during differentiation. Taking into account the data presented here, we propose a major role for STK in the integration of two pathways, whereby CKs in general and *cZ* and *tZ* levels in particular critically control fruit size (Figure 6).

STAR★METHODS

Detailed methods are provided in the online version of this paper and include the following:

- KEY RESOURCES TABLE
- LEAD CONTACT AND MATERIALS AVAILABILITY
- EXPERIMENTAL MODEL AND SUBJECT DETAILS
  - Plant material and growth conditions
- METHODS DETAILS
  - Binary vector construction and *Arabidopsis* transformation
  - CRISPR Cas9 genome editing to generate ckx7 T
  - Pistil and silique length analysis
  - Scanning electronic microscopy
  - Confocal analysis
  - GUS Assay
  - Expression analysis
  - ChIP assay
  - Hormone treatment
  - Quantification of endogenous cytokinins
  - Feulgen staining for siliques
- QUANTIFICATION AND STATISTICAL ANALYSIS
- DATA AND CODE AVAILABILITY

SUPPLEMENTAL INFORMATION

Supplemental Information can be found online at https://doi.org/10.1016/j.celrep.2020.01.101.

OPEN ACCESS
CellPress

ACKNOWLEDGMENTS

We thank J. Irepan Reyes-Olalde for helpful suggestions on the confocal imaging of *TCSn::GFP* and g*FUL:GFP*. We also thank Charlotte Morgado, Paulo Roberto Llerena Leon, and Domenico Loperfido for help with phenotypic analysis. Part of this work was carried out at NOLIMITS, the advanced imaging facility of the Università degli Studi di Milano. Some experiments were performed in the frame of the H2020-MSCA RISE project (ExpoSeed GA-691109). I.E. acknowledges the Università degli Studi di Milano (Linea 2-DBS), and M.A.M. acknowledges the Foundation for Science and Technology Portugal (FCT-SFRH/BPD/99936/2014). The work was also supported by the Czech Science Foundation (project 18-07563S). Work in the S.d.F. laboratory was also financed by Mexican National Council of Science and Technology (CONACyT) grants CB-2012-177739 and FC-2015-2/1061.

AUTHOR CONTRIBUTIONS

M.D.M. performed most experiments and wrote the manuscript. H.H.-U. performed the GUS assays. E.C. performed scanning electron microscopy (SEM) imaging. O.N. and M.S. performed CK metabolic analysis. V.B. and I.E. helped with the main experiments and writing the manuscript. M.A.M. and S.d.F. designed the experimental strategy and helped to write the manuscript. All authors analyzed the data. L.C. designed the research and wrote the manuscript.

DECLARATION OF INTERESTS

The authors declare no competing interests.

Received: July 1, 2019
Revised: September 13, 2019
Accepted: January 29, 2020
Published: February 25, 2020

REFERENCES

Alabadí, D., Blázquez, M.A., Carbonell, J., Ferrándiz, C., and Pérez-Amador, M.A. (2009). Instructive roles for hormones in plant development. Int. J. Dev. Biol. *53*, 1597–1608.

Bae, E., Bingman, C.A., Bitto, E., Aceti, D.J., and Phillips, G.N., Jr. (2008). Crystal structure of *Arabidopsis thaliana* cytokinin dehydrogenase. Proteins *70*, 303–306.

Bartrina, I., Otto, E., Strnad, M., Werner, T., and Schmülling, T. (2011). Cytokinin regulates the activity of reproductive meristems, flower organ size, ovule formation, and thus seed yield in *Arabidopsis thaliana*. Plant Cell *23*, 69–80.

Braselton, J.P., Wilkinson, M.J., and Clulow, S.A. (1996). Feulgen staining of intact plant tissues for confocal microscopy. Biotech. Histochem. *71*, 84–87.

Clough, S.J., and Bent, A.F. (1998). Floral dip: A simplified method for Agrobacterium-mediated transformation of Arabidopsis thaliana. Plant J. *16*, 735–743.

Crawford, B.C.W., Ditta, G., and Yanofsky, M.F. (2007). The NTT gene is required for transmitting-tract development in carpels of *Arabidopsis thaliana*. Curr. Biol. *17*, 1101–1108.

Cucinotta, M., Manrique, S., Guazzotti, A., Quadrelli, N.E., Mendes, M.A., Benkova, E., and Colombo, L. (2016). Cytokinin response factors integrate auxin and cytokinin pathways for female reproductive organ development. Development *143*, 4419–4424.

Cucinotta, M., Manrique, S., Cuesta, C., Benkova, E., Novak, O., and Colombo, L. (2018). CUP-SHAPED COTYLEDON1 (CUC1) and CUC2 regulate cytokinin homeostasis to determine ovule number in *Arabidopsis*. J. Exp. Bot. *69*, 5169–5176.

de Folter, S., and Angenent, G.C. (2006). trans meets cis in MADS science. Trends Plant Sci. *11*, 224–231.

de Folter, S., Urbanus, S.L., van Zuijlen, L.G.C., Kaufmann, K., and Angenent, G.C. (2007). Tagging of MADS domain proteins for chromatin immunoprecipitation. BMC Plant Biol. *7*, 47.

Dinneny, J.R., Weigel, D., and Yanofsky, M.F. (2005). A genetic framework for fruit patterning in *Arabidopsis thaliana*. Development *132*, 4687–4696.

Egea-Cortines, M., Saedler, H., and Sommer, H. (1999). Ternary complex formation between the MADS-box proteins SQUAMOSA, DEFICIENS and GLOBOSA is involved in the control of floral architecture in Antirrhinum majus. EMBO J. *18*, 5370–5379.

Ezquer, I., Mizzotti, C., Nguema-Ona, E., Gotté, M., Beauzamy, L., Viana, V.E., Dubrulle, N., Costa de Oliveira, A., Caporali, E., Koroney, A.S., et al. (2016). The Developmental Regulator SEEDSTICK Controls Structural and Mechanical Properties of the *Arabidopsis* Seed Coat. Plant Cell *28*, 2478–2492.

Fauser, F., Schiml, S., and Puchta, H. (2014). Both CRISPR/Cas-based nucleases and nickases can be used efficiently for genome engineering in *Arabidopsis thaliana*. Plant J. *79*, 348–359.

Ferrándiz, C., Pelaz, S., and Yanofsky, M.F. (1999). Control of carpel and fruit development in *Arabidopsis*. Annu. Rev. Biochem. *68*, 321–354.

Ferrándiz, C., Gu, Q., Martienssen, R., and Yanofsky, M.F. (2000). Redundant regulation of meristem identity and plant architecture by FRUITFULL, APETALA1 and CAULIFLOWER. Development *127*, 725–734.

Galuszka, P., Popelková, H., Werner, T., Frébortová, J., Pospíšilová, H., Mik, V., Köllmer, I., Schmülling, T., and Frébort, I. (2007). Biochemical characterization of cytokinin oxidases/dehydrogenases from *Arabidopsis thaliana* expressed in *Nicotiana tabacum* L. J. Plant Growth Regul. *26*, 255–267.

Gu, Q., Ferrándiz, C., Yanofsky, M.F., and Martienssen, R. (1998). The FRUITFULL MADS-box gene mediates cell differentiation during *Arabidopsis* fruit development. Development *125*, 1509–1517.

Herrera-Ubaldo, H., Lozano-Sotomayor, P., Ezquer, I., Di Marzo, M., Chávez Montes, R.A., Gómez-Felipe, A., Pablo-Villa, J., Diaz-Ramirez, D., Ballester, P., Ferrándiz, C., et al. (2019). New roles of NO TRANSMITTING TRACT and SEEDSTICK during medial domain development in *Arabidopsis* fruits. Development *146*, dev172395.

José Ripoll, J., Bailey, L.J., Mai, Q.A., Wu, S.L., Hon, C.T., Chapman, E.J., Ditta, G.S., Estelle, M., and Yanofsky, M.F. (2015). microRNA regulation of fruit growth. Nat. Plants *1*, 15036.

Köllmer, I., Novák, O., Strnad, M., Schmülling, T., and Werner, T. (2014). Overexpression of the cytosolic cytokinin oxidase/dehydrogenase (CKX7) from *Arabidopsis* causes specific changes in root growth and xylem differentiation. Plant J. *78*, 359–371.

Kowalska, M., Galuszka, P., Frébortová, J., Šebela, M., Béres, T., Hluska, T., Šmehilová, M., Bilyeu, K.D., and Frébort, I. (2010). Vacuolar and cytosolic cytokinin dehydrogenases of *Arabidopsis thaliana*: heterologous expression, purification and properties. Phytochemistry *71*, 1970–1978.

Liljegren, S.J., Ditta, G.S., Eshed, Y., Savidge, B., Bowman, J.L., and Yanofsky, M.F. (2000). SHATTERPROOF MADS-box genes control seed dispersal in *Arabidopsis*. Nature *404*, 766–770.

Liljegren, S.J., Roeder, A.H.K., Kempin, S.A., Gremski, K., Østergaard, L., Guimil, S., Reyes, D.K., and Yanofsky, M.F. (2004). Control of fruit patterning in *Arabidopsis* by INDEHISCENT. Cell *116*, 843–853.

Liu, H., Ding, Y., Zhou, Y., Jin, W., Xie, K., and Chen, L.L. (2017). CRISPR-P 2.0: An Improved CRISPR-Cas9 Tool for Genome Editing in Plants. Mol. Plant *10*, 530–532.

Liu, P., Zhang, C., Ma, J.Q., Zhang, L.Y., Yang, B., Tang, X.Y., Huang, L., Zhou, X.T., Lu, K., and Li, J.N. (2018). Genome-wide identification and expression profiling of cytokinin oxidase/dehydrogenase (CKX) genes reveal likely roles in pod development and stress responses in oilseed rape (*Brassica napus* L.). Genes (Basel) *9*, 168.

Marsch-Martínez, N., Ramos-Cruz, D., Irepan Reyes-Olalde, J., Lozano-Sotomayor, P., Zúñiga-Mayo, V.M., and de Folter, S. (2012). The role of cytokinin during *Arabidopsis gynoecia* and fruit morphogenesis and patterning. Plant J. *72*, 222–234.

Matias-Hernandez, L., Battaglia, R., Galbiati, F., Rubes, M., Eichenberger, C., Grossniklaus, U., Kater, M.M., and Colombo, L. (2010). *VERDANDI* is a direct target of the MADS domain ovule identity complex and affects embryo sac differentiation in *Arabidopsis*. Plant Cell *22*, 1702–1715.

Mendes, M.A., Guerra, R.F., Castelnovo, B., Silva-Velazquez, Y., Morandini, P., Manrique, S., Baumann, N., Groß-Hardt, R., Dickinson, H., and Colombo, L. (2016). Live and let die: a REM complex promotes fertilization through synergid cell death in *Arabidopsis*. Development *143*, 2780–2790.

Mizzotti, C., Mendes, M.A., Caporali, E., Schnittger, A., Kater, M.M., Battaglia, R., and Colombo, L. (2012). The MADS box genes SEEDSTICK and ARABIDOPSIS Bsister play a maternal role in fertilization and seed development. Plant J. *70*, 409–420.

Mizzotti, C., Ezquer, I., Paolo, D., Rueda-Romero, P., Guerra, R.F., Battaglia, R., Rogachev, I., Aharoni, A., Kater, M.M., Caporali, E., and Colombo, L. (2014). SEEDSTICK is a master regulator of development and metabolism in the *Arabidopsis* seed coat. PLoS Genet. *10*, e1004856.

Mizzotti, C., Rotasperti, L., Moretto, M., Tadini, L., Resentini, F., Galliani, B.M., Galbiati, M., Engelen, K., Pesaresi, P., and Masiero, S. (2018). Time-course transcriptome analysis of *Arabidopsis* siliques discloses genes essential for fruit development and maturation. Plant Physiol. *178*, 1249–1268.

Mok, D.W.S., and Mok, M.C. (2001). CYTOKININ METABOLISM AND ACTION. Annu. Rev. Plant Physiol. Plant Mol. Biol. *52*, 89–118.

Novák, O., Hauserová, E., Amakorová, P., Doležal, K., and Strnad, M. (2008). Cytokinin profiling in plant tissues using ultra-performance liquid chromatography-electrospray tandem mass spectrometry. Phytochemistry *69*, 2214–2224.

Pinyopich, A., Ditta, G.S., Savidge, B., Liljegren, S.J., Baumann, E., Wisman, E., and Yanofsky, M.F. (2003). Assessing the redundancy of MADS-box genes during carpel and ovule development. Nature *424*, 85–88.

Reyes-Olalde, J.I., Marsch-Martínez, N., and de Folter, S. (2015). Imaging early stages of the female reproductive structure of *Arabidopsis* by confocal laser scanning microscopy. Dev. Dyn. *244*, 1286–1290.

Reyes-Olalde, J.I., Zúñiga-Mayo, V.M., Serwatowska, J., Chavez Montes, R.A., Lozano-Sotomayor, P., Herrera-Ubaldo, H., Gonzalez-Aguilera, K.L., Ballester, P., Ripoll, J.J., Ezquer, I., et al. (2017). The bHLH transcription factor SPATULA enables cytokinin signaling, and both activate auxin biosynthesis and transport genes at the medial domain of the gynoecium. PLoS Genet *13*, e1006726.

Roeder, A.H., and Yanofsky, M.F. (2006). Fruit Development in Arabidopsis. Arabidopsis Book *4*, e0075.

Roeder, A.H.K., Ferrándiz, C., and Yanofsky, M.F. (2003). The role of the REPLUMLESS homeodomain protein in patterning the *Arabidopsis* fruit. Curr. Biol. *13*, 1630–1635.

Romanov, G.A., Lomin, S.N., and Schmülling, T. (2006). Biochemical characteristics and ligand-binding properties of *Arabidopsis* cytokinin receptor AHK3 compared to CRE1/AHK4 as revealed by a direct binding assay. J. Exp. Bot. *57*, 4051–4058.

Sakakibara, H. (2006). Cytokinins: activity, biosynthesis, and translocation. Annu. Rev. Plant Biol. *57*, 431–449.

Schindelin, J., Arganda-Carreras, I., Frise, E., Kaynig, V., Longair, M., Pietzsch, T., Preibisch, S., Rueden, C., Saalfeld, S., Schmid, B., et al. (2012). Fiji: an open-source platform for biological-image analysis. Nat. Methods *9*, 676–682.

Schmülling, T., Werner, T., Riefler, M., Krupková, E., and Bartrina y Manns, I. (2003). Structure and function of cytokinin oxidase/dehydrogenase genes of maize, rice, *Arabidopsis* and other species. J. Plant Res. *116*, 241–252.

Song, J., Jiang, L., and Jameson, P.E. (2015). Expression patterns of *Brassica napus* genes implicate IPT, CKX, sucrose transporter, cell wall invertase, and amino acid permease gene family members in leaf, flower, silique, and seed development. J. Exp. Bot. *66*, 5067–5082.

Spíchal, L. (2012). Cytokinins—recent news and views of evolutionally old molecules. Funct. Plant Biol. *39*, 267.

Stolz, A., Riefler, M., Lomin, S.N., Achazi, K., Romanov, G.A., and Schmülling, T. (2011). The specificity of cytokinin signalling in *Arabidopsis thaliana* is mediated by differing ligand affinities and expression profiles of the receptors. Plant J. *67*, 157–168.

Street, I.H., Mathews, D.E., Yamburkenko, M.V., Sorooshzadeh, A., John, R.T., Swarup, R., Bennett, M.J., Kieber, J.J., and Schaller, G.E. (2016). Cytokinin acts through the auxin influx carrier AUX1 to regulate cell elongation in the root. Development *143*, 3982–3993.

Svačinová, J., Novák, O., Plačková, L., Lenobel, R., Holík, J., Strnad, M., and Doležal, K. (2012). A new approach for cytokinin isolation from *Arabidopsis* tissues using miniaturized purification: pipette tip solid-phase extraction. Plant Methods *8*, 17.

Tan, M., Li, G., Qi, S., Liu, X., Chen, X., Ma, J., Zhang, D., and Han, M. (2018). Identification and expression analysis of the IPT and CKX gene families during axillary bud outgrowth in apple (Malus domestica Borkh.). Gene *651*, 106–117.

Verwoerd, T.C., Dekker, B.M., and Hoekema, A. (1989). A small-scale procedure for the rapid isolation of plant RNAs. Nucleic Acids Res. *17*, 2362.

Vivian-Smith, A., Luo, M., Chaudhury, A., and Koltunow, A. (2001). Fruit development is actively restricted in the absence of fertilization in *Arabidopsis*. Development *128*, 2321–2331.

Werner, T., Motyka, V., Laucou, V., Smets, R., Van Onckelen, H., and Schmülling, T. (2003). Cytokinin-deficient transgenic *Arabidopsis* plants show multiple developmental alterations indicating opposite functions of cytokinins in the regulation of shoot and root meristem activity. Plant Cell *15*, 2532–2550.

Zuñiga-Mayo, V.M., Baños-Bayardo, C.R., Díaz-Ramírez, D., Marsch-Martínez, N., and de Folter, S. (2018). Conserved and novel responses to cytokinin treatments during flower and fruit development in *Brassica napus* and *Arabidopsis thaliana*. Sci. Rep. *8*, 6836.

Zürcher, E., Tavor-Deslex, D., Lituiev, D., Enkerli, K., Tarr, P.T., and Müller, B. (2013). A robust and sensitive synthetic sensor to monitor the transcriptional output of the cytokinin signaling network in planta. Plant Physiol. *161*, 1066–1075.

STAR★METHODS

KEY RESOURCES TABLE

REAGENT or RESOURCE	SOURCE	IDENTIFIER
Antibodies		
anti-GFP polyclonal antibody	Clontech	CAT# 632460; RRID: AB_2314544
Chemicals, Peptides, and Recombinant Proteins		
6-benzylaminopurine (BAP)	Sigma Aldrich	CAT# B3408
Isotope-labeled internal standards	(Novák et al., 2008)	N/A
Experimental Models: Organisms/Strains		
Arabidopsis: *stk-2*	(Pinyopich et al., 2003)	N/A
Arabidopsis: *ckx7*	NASC	SAIL_515_A07
Arabidopsis: *ful-2*	(Ferrándiz et al., 2000)	N/A
Arabidopsis: *stk ckx7*	This study	N/A
Arabidopsis: *stk ful*	This study	N/A
Arabidopsis: *STK::STK-GFP*	(Mizzotti et al., 2014)	N/A
Arabidopsis: *TCSn::GFP*	(Zürcher et al., 2013)	N/A
Arabidopsis: *gFUL:GFP*	(de Folter et al., 2007)	N/A
Arabidopsis: *stk TCSn::GFP*	This study	N/A
Arabidopsis: stk *gFUL:GFP*	This study	N/A
Arabidopsis: *pCKX7::GUS*	(Mendes et al., 2016)	N/A
Arabidopsis: *stk pCKX7::GUS*	This study	N/A
Oligonucleotides		
Fw *ACTIN2/7* (ChIP experiments) CCAATCGTGAGAAAATGACTCAG	(Matias-Hernandez et al., 2010)	AtP_0329
Rev *ACTIN2/7* (ChIP experiments) CCAAACGCAGAATAGCATGTGG	(Matias-Hernandez et al., 2010)	AtP_0330
Fw *PMEI6* CARG-4 (ChIP experiments) TCTCTCTCGATCTCCATTTG	(Ezquer et al., 2016)	RT 1925
Rev *PMEI6* CARG-4 (ChIP experiments) AGAGTAAACGTGATAGGAGA	(Ezquer et al., 2016)	RT 1926
Fw p*CKX7* CARG-4 and 5 (ChIP experiments) AGACAAACGTTAAACCTAAC	This study	Atp_6961
Rev p*CKX7* CARG-4 and 5 (ChIP experiments) TGTACTGAGACATTCGTAG	This study	Atp_6962
Primers for plant genotyping, CRISPR-mediated mutagenesis, and gene expression analyses are listed in Table S2	This study	N/A
Software and Algorithms		
CRISPR-P 2.0	(Liu et al., 2017)	N/A

LEAD CONTACT AND MATERIALS AVAILABILITY

Further information and requests for resources and reagents should be directed to the Lead Contact, Lucia Colombo (lucia.colombo@unimi.it). Plant lines generated in this study will be made available on request, but we may require a completed Materials Transfer Agreement if there is potential for commercial application.

EXPERIMENTAL MODEL AND SUBJECT DETAILS

Plant material and growth conditions

Seeds of *Arabidopsis thaliana* plants were germinated on soil in long-day conditions (16 h light, 8 h dark) at 22°C. All genotypes used in this study were in Columbia-0 (Col-0) ecotype. The *stk*-2 mutant was provided by M. Yanofsky (Pinyopich et al., 2003). The T-DNA insertion mutant for *ckx7* was obtained from the Nottingham *Arabidopsis* Stock Centre (NASC) and was SAIL_515_A07 line (http://arabidopsis.info; see Figure S2B for knockout validation). The *ful*-2 mutant was provided by C. Ferrándiz (Ferrándiz et al., 2000). The *stk ckx7* (*ckx7* SAIL_515_A07 allele) and *stk ful* plants were obtained by crossing the single mutants. The *STK::STK-GFP* marker-line used in this work was described in Mizzotti et al. (2014). The transgenic line *TCSn::GFP* was provided by B. Muller (Zürcher et al., 2013). The transgenic line g*FUL:GFP* was provided by S. de Folter (de Folter et al., 2007). The *stk TCSn::GFP* and *stk* g*FUL:GFP* plants were obtained by crossing. The transgenic line *pCKX7::GUS* was provided by N. Baumann and

R. Groß-Hardt (Mendes et al., 2016). The *stk pCKX7::GUS* plants were obtained by crossing. Primers used for genotyping are listed in Table S2.

METHODS DETAILS

Binary vector construction and *Arabidopsis* transformation

For ectopic *CKX7* expression in wild-type and *stk* plants, the *CKX7* cDNA was cloned under the control of the cauliflower mosaic virus (CaMV) *35S* promoter (NOB 2252). The *CKX7* cDNA was amplified by PCR by high-fidelity Phusion DNA polymerase (Thermo Fisher Scientific) using primers Atp_4677 and Atp_4678. The PCR product was then recombined into the pDONR207 vector (BP Gateway reaction) and sequenced. The PCR product cloned into the DONR vector was then recombined into the pB2GW7 binary vector under control of the CaMV *35S* promoter (LR Gateway reaction) according to the manufacturer's instructions (Thermo Fisher Scientific). Positive colonies (NOB 2252) were selected on LB agar plates containing spectinomycin (100 mg/L) and sequenced. Binary vectors were used to transform *Agrobacterium tumefaciens* (NOB 2329) and *Arabidopsis* plants were transformed using the floral dip method (Clough and Bent, 1998). Primers used for cloning and genotyping are listed in Table S2. See Figure S2C for overexpression validation.

CRISPR Cas9 genome editing to generate ckx7 T

The cloning of the construct to generate another *ckx7* mutant allele was performed following the protocol previously described (Fauser et al., 2014). The protospacer sequence was designated with the aid of CRISPR-P 2.0 software (Liu et al., 2017). The primers used to generate the protospacer are listed in Table S2 (Atp_6702 and Atp_6703). The protospacer was cloned into the pEn-Chimera entry vector, then the gRNA was cloned into the destination vector (pDe-Cas9) using Gateway technology. Positive colonies were selected and used to transform Col-0 plants via *Agrobacterium tumefaciens* using the floral dip method (Clough and Bent, 1998). Finally, we analyzed plants with a single insertion without Cas9 in the T3, T4 and T5 generation to obtain three independent biological replicates.

Pistil and silique length analysis

Pistils at stage 13 (*stk*, *ckx7*, *ckx7 T*, *35S::CKX7*, and Col-0) and siliques at stage 17-B for each genotype (*stk*, *ckx7*, *ckx7 T*, *35S::CKX7*, *stk ckx7*, *stk* x *35S::CKX7*, *ful-2*, *stk ful-2* and Col-0) were collected and images were taken using a stereomicroscope. Pistil and fruit length measurements were obtained using Fiji software (Schindelin et al., 2012). Statistical analyses were performed using the Student t test (*$p < 0.05$, **$p < 0.0$) and ANOVA followed by the Tukey's HSD test (*$p < 0.05$, **$p < 0.01$). Each experiment was performed three times.

Scanning electronic microscopy

Biological samples were collected and fixed overnight at 4°C in FAE solution (10 mL formaldehyde 37%, 50 mL absolute ethanol, 5 mL glacial acetic acid and 35 mL deionized water). Fixed tissues were washed with water and post-fixed with aqueous 2% osmium tetroxide for 2 h at room temperature. Tissues were rinsed several times in deionised water and dehydrated in a graded series of ethanol for 15 min per rinse. This step was followed by critical point drying with liquid CO_2 and sputter-coating with gold in a Nanotech sputter coater. Specimens were analyzed using a LEO 1430 Scanning Electron Microscope.

Confocal analysis

Pistils and siliques of *STK::STK-GFP* plants were collected and mounted in water and observed with a Nikon A1 laser scanning confocal microscope. Analysis of *TCSn::GFP* and g*FUL:GFP* was performed using the protocol described by Reyes-Olalde et al. (2015) and confocal fluorescence images were captured using a confocal laser scanning inverted microscope LSM 510 META (Carl Zeiss, Germany).

GUS Assay

Staining for GUS in *stk* and Col-0 backgrounds containing *pCKX7::GUS* was performed as previously described (Herrera-Ubaldo et al., 2019).

Expression analysis

For transcript quantification, total RNA was extracted from siliques at stages 13–14, 15–16, 17-A and 17-B for expression analysis using the LiCl protocol (Verwoerd et al., 1989). For knockout and overexpression validation, RNA was extracted from stages 13 to 16 using the LiCl protocol (Verwoerd et al., 1989). The cDNA was obtained using an IMProm-II™ Reverse Transcription System (Promega). The q-PCR assay was conducted in triplicate in a Bio-Rad iCycler iQ Optical System using the iTaq Universal SYBR Green Supermix, Bio-Rad (Bio-Rad, http://www.bio-rad.com). The relative transcript enrichment of genes of interest was calculated by normalizing against two housekeeping genes (*ACTIN* and *UBIQUITIN*). Statistical differences were identified with the Student t test (**$p < 0.01$). The primers used for qPCR are listed Table S2.

ChIP assay

The *CKX7* promoter region was analyzed to identify potential CArG boxes. The ChIP experiment was performed as previously described in Ezquer et al. (2016). One gram of silique material from stages 14 to 16 was used for chromatin extraction from *STK::STK–GFP* (Mizzotti et al., 2014) and Col-0 wild-type plants. For immunoprecipitation, we used 1.5 μL anti-GFP polyclonal antibody for each sample (Clontech 632460). Enrichment of the target regions was calculated by qPCR (iTaq Universal SYBR Green Supermix, Bio-Rad) using a Bio-Rad iCycler iQ optical system. The relative enrichment of the targets obtained from *STK::STK–GFP* siliques was compared with the enrichment obtained from wild type. *ACTIN 2/7* was used for normalization as previously described (Matias-Hernandez et al., 2010). To establish the efficiency of the chromatin immunoprecipitation, we used the fourth CArG box of *PMEI6* as a positive control (Ezquer et al., 2016). Three independent ChIP experiments were performed. The primers used are listed in the Key Resources Table and Table S2.

Hormone treatment

Seeds of *stk* and Col-0 were germinated in a growth chamber, and plants were grown in soil under standard greenhouse conditions. Two weeks after bolting, Col-0 and *stk* plants were treated with a drop application on the pistil at stage 13 (anthesis) and subsequent siliques were treated for 5 days with 100 μM 6-benzylaminopurine (BAP, SigmaAldrich, https://www.sigmaaldrich.com) 0.02% Silwet L-77 (SigmaAldrich) or a mock solution (0.02% Silwet L-77 in NaOH 1M). Silique length was measured one week after the end of the treatment. Statistical analysis was performed using ANOVA followed by Tukey's HSD test (**$p < 0.01$).

Quantification of endogenous cytokinins

Quantification of CK metabolites was performed as previously described in Svačinová et al. (2012). Approximately 0.2 g silique material from stages 14 to 16 (early fruit growth stages) and 17-A and 17-B were harvested for each genotype. Samples (20 mg FW) were extracted in 1.0 mL modified Bieleski buffer (60% MeOH, 10% HCOOH and 30% H_2O) together with a cocktail of stable isotope-labeled internal standards (0.25 pmol CK bases, ribosides, *N*-glucosides, and 0.5 pmol CK *O*-glucosides and nucleotides were added per sample). The extracts were purified using multi-StageTips (containing C18/SDB-RPSS/Cation-SR layers), the eluates were then evaporated to dryness in a vacuum and stored at −20°C. Cytokinin levels were determined using ultra-high performance liquid chromatography-electrospray tandem mass spectrometry (UHPLC-MS/MS) using stable isotope-labeled internal standards as a reference. Four independent biological replicates were harvested for each genotype. Statistical analysis was performed using the Student's t test (*$p < 0.05$, **$p < 0.01$, ***$p < 0.001$).

Feulgen staining for siliques

The reagents used were as described previously (Braselton et al., 1996) with slight modifications. We used 20 different siliques of each genotype at stage 17-B to measure cell length. The samples were excited with an argon ion laser at 488 nm and emissions were detected between 515 and 600 nm. Image capture was performed using a Nikon A1 laser scanning confocal microscope. Statistical analysis consisted of ANOVA followed by the Tukey's HSD test (*$p < 0.05$, **$p < 0.01$).

QUANTIFICATION AND STATISTICAL ANALYSIS

Information about statistical tests used, sample sizes (*n*), and *p-value*s for each experiment are detailed in the relevant STAR Methods sections.

DATA AND CODE AVAILABILITY

Sequence data from this article can be found in the GenBank/EMBL data libraries under the following accession numbers: *AP2*, At4g36920; *CKX1*, At2g41510; *CKX3*, At5g56970; *CKX5* At1g75450; *CKX6*, At3g63440; *CKX7*, At5g21482; FUL, At5g60910; *IND*, At4g00120; *MIR172C* At3g11435; *STK*, At4g09960.

Cell Reports, Volume *30*

Supplemental Information

SEEDSTICK Controls *Arabidopsis* Fruit Size by Regulating Cytokinin Levels and *FRUITFULL*

Maurizio Di Marzo, Humberto Herrera-Ubaldo, Elisabetta Caporali, Ondřej Novák, Miroslav Strnad, Vicente Balanzà, Ignacio Ezquer, Marta A. Mendes, Stefan de Folter, and Lucia Colombo

SUPPLEMENTAL FIGURES AND TABLES

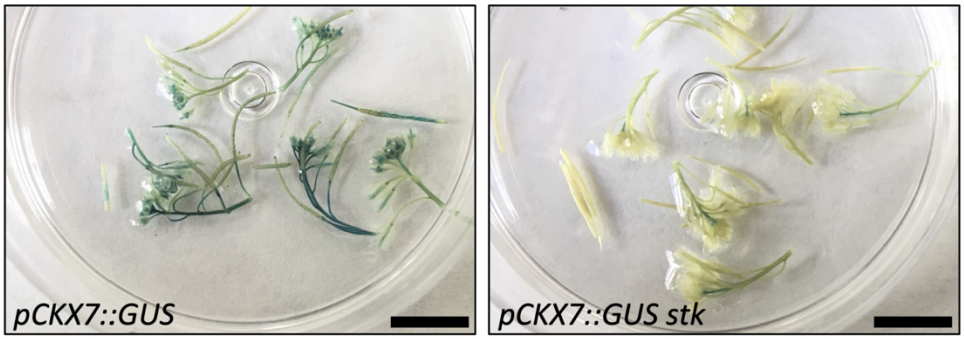

Figure S1. *pCKX7::GUS* analysis. Related to Figure 3.

Stereomicroscope images of *pCKX7::GUS* in (Col-0) and *stk* backgrounds. Scale bars = 1 cm.

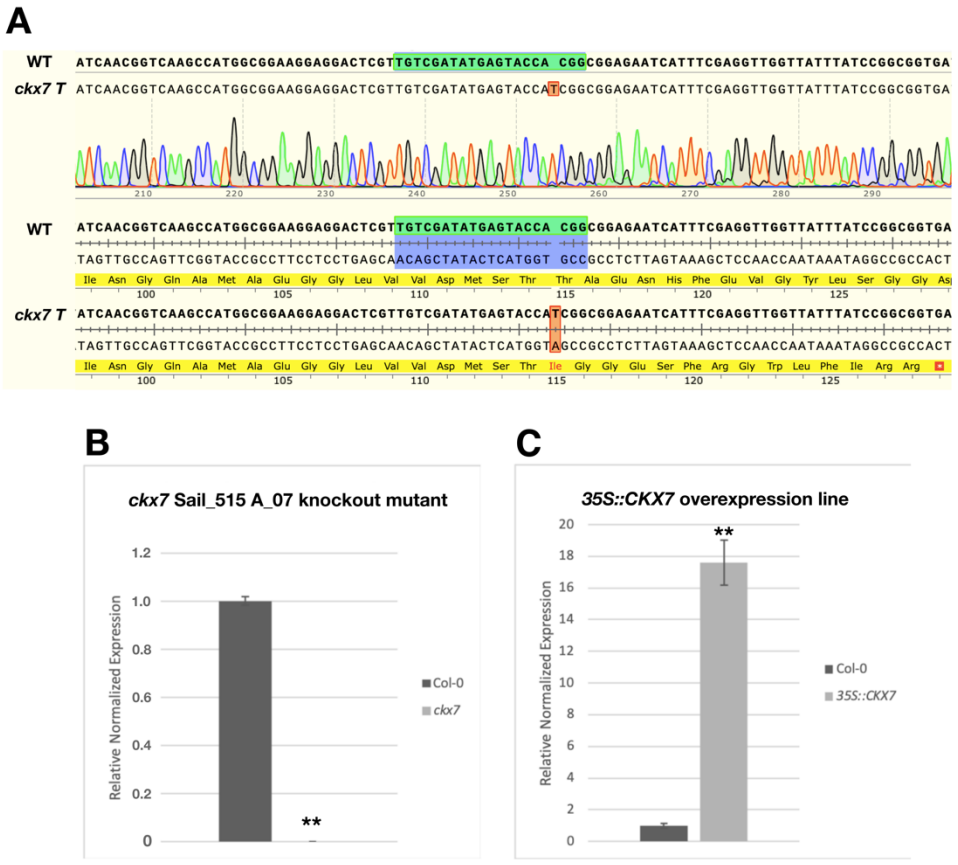

Figure S2. ***ckx7 T* CRISPR Cas9 mutant description and qPCR to validate the *ckx7* knockout mutant and *35S::CKX7* overexpression line. Related to Figure 4**.

(A) The position of the T insertion was in the first exon after nucleotide in position 254. The insertion causes a frameshift with the generation of a premature stop codon after 129 aa; (B) *ckx7* Sail_515_A_07 knockout mutant allele; (C) *35S::CKX7* line. Statistical analysis was performed using the Student's *t*-test (** $p < 0.01$). Expression data were normalised with *ACTIN* and *UBIQUITIN*. Histograms show a representative experiment in which error bars represent the SD for three technical replicates. Three qPCR (biological replicates) were performed and generated similar results.

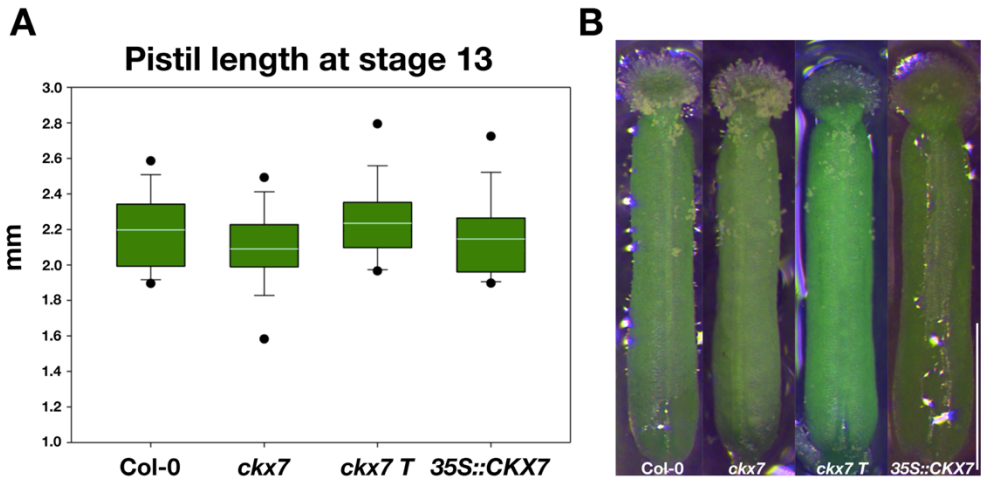

Figure S3. ***CKX7* acts after fertilization to promote fruit elongation. Related to Figure 4**.

(A) The box plot represents the pistil length of the mutants and overexpression line (Col-0 = 2.19 mm, *ckx7* = 2.09 mm, *ckx7 T* = 2.23 mm, *35S::CKX7* = 2.15 mm; n = 20); (B) Stereomicroscope images of *ckx7*, *ckx7 T*, *35S::CKX7* and Col-0 pistils at stage 13. Scale bar = 1 mm. Statistical analysis was performed using ANOVA followed by Tukey's HSD test.

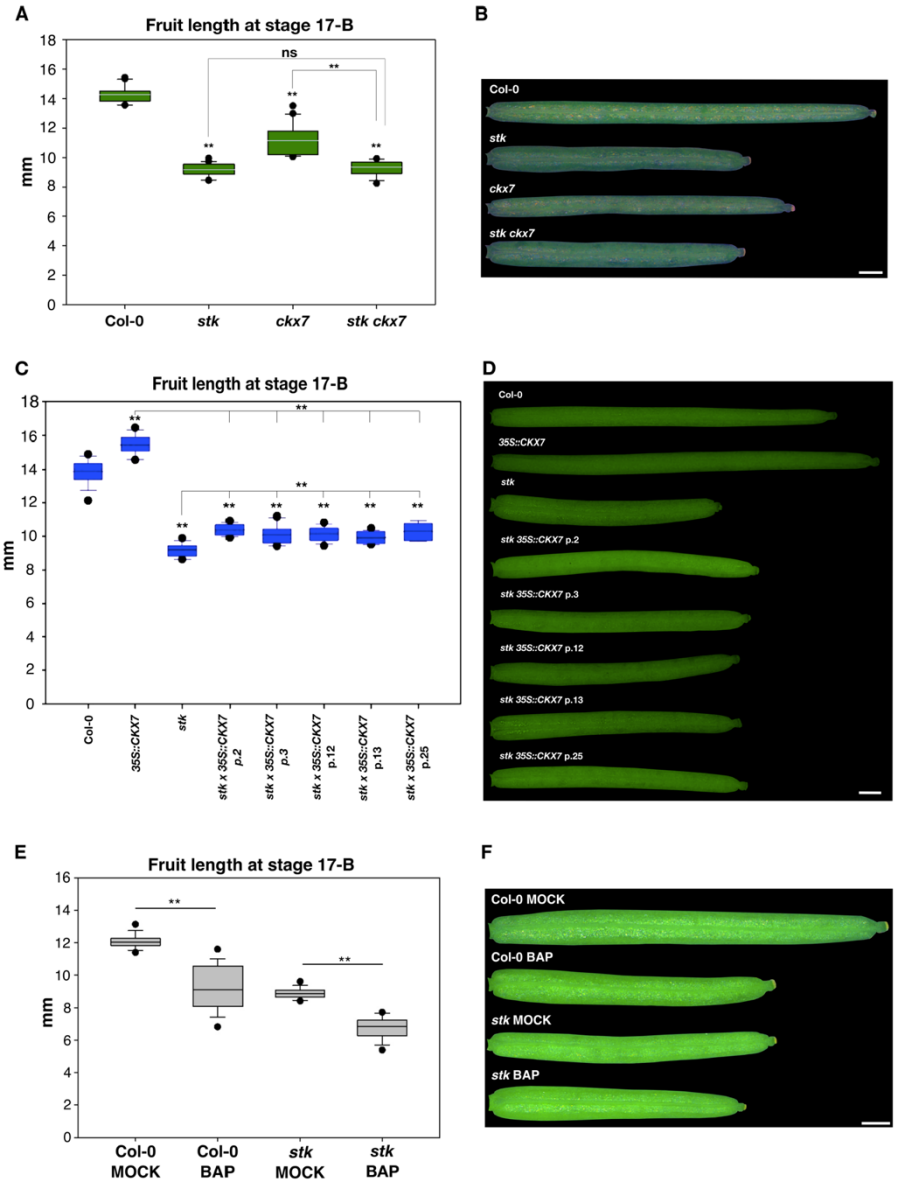

Figure S4. STK acts upstream of *CKX7* and exogenous CK treatment reduces fruit length in *stk* and Col-0. Related to Figures 1 and 4.

(A) The box plot represents fruit length at stage 17-B of *stk* (mean = 9.18 mm, *n* = 20), *ckx7* (mean = 11.14 mm, *n* = 20), *stk ckx7* (mean = 9.35 mm, *n* = 20) compared to Col-0 (mean = 14.65 mm, *n* = 20); (B) Stereomicroscope images of *stk*, *ckx7*, *stk ckx7* and Col-0 siliques at stage 17-B. Scale bar =

1 mm; (C) The box plots represents a rescue experiment of *stk x 35S::CKX7* plants (plant 2 mean = 10.40 mm; p 3 mean = 10.30 mm; p 12 mean = 10.15 mm; p 13 mean = 9.95 mm; plant 25 mean = 10.31 mm; n = 15), *stk* (mean = 9.19 mm, n = 15) and *35S::CKX7* (mean = 15.46 mm, n = 15) compared to Col-0 (mean = 13.88 mm, n=15); (D) Stereomicroscope images of *stk* x *35S::CKX7*, *35S::CKX7*, *stk* and Col-0 siliques at stage 17-B; Scale bar = 1 mm. (E) The box plots represent fruit length at stage 17-B of Col-0 (mean = 9.23 mm, n = 45) and *stk* (mean = 6.74 mm, n = 80) treated with BAP compared to the mock control (Col-0-MOCK, mean = 12.10 mm, n = 50; *stk*-MOCK, mean = 8.90 mm, n = 40); (F) Stereomicroscope pictures of treated *stk* and Col-0 siliques with BAP and MOCK control. Scale bar = 1 mm. Statistical analyses were performed using ANOVA followed by Tukey's HSD test. (**$p < 0.01$; ns: not significant).

Genotype stage 13 to16	Total *IP*-types	*IP*	*IPR*	*IPRMP*	*IP7G*	*IP9G*
Col-0	15.95 ± 1.89	0.38 ± 0.07	3.29 ± 0.15	8.99 ± 1.83	3.04 ± 0.34	0.32 ± 0.09
ckx7	24.58 ± 1.35 ***	0.56 ± 0.13	2.73 ± 0.54	7.91 ± 0.59	12.27 ± 0.60 ***	1.10 ± 0.10 ***
ckx7 T	23.36 ± 1.81 **	0.59 ± 0.08	2.76 ± 0.22 *	7.20 ± 1.77	11.79 ± 1.18 ***	1.28 ± 0.16 ***
stk	11.28 ± 0.56 **	0.28 ± 0.08	2.08 ± 0.39 **	6.10 ± 0.98	2.55 ± 0.23	0.27 ± 0.04

Genotype Stages 17-A, 17-B	Total *IP*-types	*IP*	*IPR*	*IPRMP*	*IP7G*	*IP9G*
Col-0	12.16 ± 0.58	0.54 ± 0.14	1.36 ± 0.28	4.83 ± 1.10	4.88 ± 0.64	0.54 ± 0.08
ckx7	26.27 ± 2.54 ***	0.74 ± 0.17	1.68 ± 0.38	5.13 ± 0.87	17.35 ± 1.63 ***	1.37 ± 0.16 ***
ckx7 T	18.40 ± 1.98 **	0.62 ± 0.09	2.12 ± 0.47	8.08 ± 1.44 *	6.71 ± 0.82 *	0.87 ± 0.13 *
stk	9.54 ± 0.39 ***	0.45 ± 0.09	1.27 ± 0.25	5.04 ± 0.71	2.45 ± 0.30 **	0.33 ± 0.07 *

Genotype stage 13 to16	Total *DHZ* types	*DHZ*	*DHZ*R	*DHZ*RMP	*DHZ*OG	*DHZ*ROG	*DHZ*7G	*DHZ*9G
Col-0	11.61 ± 0.22	<LOD	1.33 ± 0.19	0.63 ± 0.05	0.51 ± 0.03	0.62 ± 0.10	8.20 ± 0.23	0.31 ± 0.03
ckx7	9.33 ± 0.44 ***	<LOD	1.01 ± 0.19	0.57 ± 0.10	0.33 ± 0.03 ***	0.34 ± 0.04 **	6.81 ± 0.28 ***	0.27 ± 0.02
ckx7 T	10.25 ± 1.26	<LOD	1.10 ± 0.20	0.45 ± 0.02 **	0.39 ± 0.03 **	0.44 ± 0.09	7.58 ± 0.94	0.29 ± 0.04
stk	9.87 ± 0.75 **	<LOD	0.99 ± 0.12 *	0.48 ± 0.05 *	0.39 ± 0.03 **	0.49 ± 0.11	7.23 ± 0.53 *	0.28 ± 0.06

Genotype stage 17-A, 17-B	Total *DHZ* types	*DHZ*	*DHZ*R	*DHZ*RMP	*DHZ*OG	*DHZ*ROG	*DHZ*7G	*DHZ*9G
Col-0	5.28 ± 0.21	<LOD	0.80 ± 0.16	0.47 ± 0.05	0.56 ± 0.07	0.21 ± 0.02	3.11 ± 0.20	0.14 ± 0.02
ckx7	4.56 ± 0.33	<LOD	0.50 ± 0.10	0.16 ± 0.04	0.45 ± 0.04	0.22 ± 0.03	3.08 ± 0.38	0.15 ± 0.03

	*		*	***				
ckx7 T	5.23 ± 0.57	<LOD	0.86 ± 0.04	0.29 ± 0.05 **	0.38 ± 0.05 *	0.21 ± 0.03	3.39 ± 0.54	0.12 ± 0.02
stk	5.77 ± 0.17 *	<LOD	0.50 ± 0.05 *	0.34 ± 0.07 *	0.49 ± 0.04	0.22 ± 0.02	4.06 ± 0.25 **	0.16 ± 0.02

Genotype stage 13 to16	Total cytokinins	Total CK bases	Total CK risosides	Total CK nucleotides	Total CK O-glucosides	Total CK N-glucosides
Col-0	90.81 ± 7.25	1.23 ± 0.20	18.29 ± 1.25	40.38 ± 4.49	5.51 ± 0.25	25.40 ± 1.94
ckx7	104.07 ± 6.59	1.92 ± 0.23 **	15.44 ± 2.28	35.61 ± 3.31	5.44 ± 0.28	45.67 ± 2.49 ***
ckx7 T	101.10 ± 2.97	1.72 ± 0.09 **	14.61 ± 1.96 *	35.72 ± 2.79	5.50 ± 0.17	43.57 ± 0.38 ***
stk	79.92 ± 5.13	1.25 ± 0.10	15.24 ± 2.15	36.50 ± 3.64	4.60 ± 0.09 **	22.33 ± 1.04

Genotype stage 17-A, 17-B	Total cytokinins	Total CK bases	Total CK risosides	Total CK nucleotides	Total CK O-glucosides	Total CK N-glucosides
Col-0	89.25 ± 4.82	2.16 ± 0.28	14.49 ± 2.74	49.83 ± 3.45	6.09 ± 0.69	16.67 ± 1.24
ckx7	87.59 ± 5.32	2.56 ± 0.32	12.18 ± 2.13	30.73 ± 3.25 ***	6.21 ± 0.24	35.91 ± 2.69 ***
ckx7 T	106.43 ± 10.86 *	2.48 ± 0.22	24.47 ± 3.23 **	53.15 ± 6.85	5.54 ± 0.38	20.80 ± 1.75 *
stk	93.52 ± 4.86	2.06 ± 0.28	20.80 ± 2.59 *	48.30 ± 5.49	7.36 ± 0.90	15.00 ± 0.76

Table S1. CKs quantification in *ckx7 ckx7 T*, *stk* and Col-0. Related to Table 1.

Data are pmol/g fresh weight; means ± S.D. (n = 4), <LOD: not detected. Total isopentenyladenine cytokinins (Total *IP*-types), isopentenyladenine riboside (*IP*R), isopentenyladenine riboside-5′-monophosphate (*IP*RMP), isopentenyladenine 7-glucoside (*IP*7G), isopentenyladenine 9-glucoside (*IP*9G) from stages 13 to 16 of fruit development in *ckx7 ckx7 T*, *stk* and Col-0; Total *IP*-types, *IP*R, *IP*RMP, *IP*7G and *IP*9G at stages 17-A and 17-B of fruit development in *ckx7*, *ckx7 T* and *stk* compared to Col-0; Total dihydrozeatin (*DHZ*); dihydrozeatin riboside (*DHZ*R), dihydrozeatin riboside-5′-monophosphate (*DHZ*RMP), dihydrozeatin *O*-glucosides (*DHZ*OG); dihydrozeatin riboside-*O*-glucoside (*DHZ*ROG), dihydrozeatin 7-glucoside (*DHZ*7G), dihydrozeatin 9-glucoside

55 (*DHZ*9G) from stages 13 to 16 of fruit development in *ckx7 ckx7 T*, *stk* and Col-0; Total dihydrozeatin
56 (*DHZ*); *DHZ*R, *DHZ*RMP, *DHZ*OG, *DHZ*ROG, *DHZ*7G and *DHZ*9G at stages 17-A and 17-B of fruit
57 development in *ckx7 ckx7 T*, *stk* and Col-0; Total CK, total CK bases, total CK ribosides, total CK
58 O-Glucosides, total CK N-Glucosides from stages 13 to 16 of fruit development in *ckx7 ckx7 T*, *stk*
59 and Col-0; Total CK, total CK bases, total CK ribosides, total CK O-Glucosides, total CK N-
60 Glucosides at stages 17-A and 17-B of fruit development in *ckx7 ckx7 T*, *stk* and Col-0. Statistical
61 analysis was performed using the Student's *t*-test (*$p < 0.05$, **$p < 0.01$, *** $p < 0.001$).
62

Name	Sequence	Function
AtP_0560	CACTGTCCAAGAAATCAATGCCGC	Fw *stk-2* genotyping
AtP_0561	GGAACTCAAAGAGTCTCCCATCAG	Rev *stk-2* genotyping
AtP_1220	GCCTTTTCAGAAATGGATAAATAGCCTTGCTTCC	LB1 SAIL for *ckx7* genotyping
AtP_2340	GTCGTGCTCCACCATGTTGA	Rev on Cas9 construct
AtP_3938	GCTAGGGTTTTGCTACAGCC	Fw *ckx7* Sail 515_A07 genotyping
AtP_3939	CGTCTTGAGTGAACTCATCG	Rev *35S::CKX7* genotyping
AtP_3941	CACGGACGTCCGATCATCC	Rev *ckx7* Sail 515_A07 genotyping
AtP_4603	CTCGGATTCCATTGCCCAGCTAT	Fw on 35S:: construct to genotype *35S::CKX7*
AtP_4677	GGGGACAAGTTTGTACAAAAAAGCAGGCTcc **ATG**ATAGCTTACATAGAACCATACTTCTT	Fw *CKX7* cloning
AtP_4678	GGGGACCACTTTGTACAAGAAAGCTGGGTgg **TCA**AAGAGACCTATTGAAAATCTTTT	Rev *CKX7* cloning
Atp_6702	**ATTG**TGTCGATATGAGTACCACGG	Fw CRISPR *CKX7* Protospacer
Atp_6703	**AAAC**CCGTGGTACTCATATCGACA	Rev CRISPR *CKX7* Protospacer
Atp_6828	TCTACGGATGGTGTTTCTGAGTC	Fw *ckx7 T* CRISPR genotype and sequencing
Atp_6829	CAAGTAACGACGTCACCATTTCC	Rev *ckx7 T* CRISPR genotype and sequencing
RT 31	GAAGGACAATTAGTCCAATGCTC	Fw *FUL* gene expression, qPCR
RT 32	GTGAGATAGTTCTACTCGTTCG	Rev *FUL* gene expression, qPCR
RT 147	CTGTTCACGGAACCCAATTC	Fw ubiquitin housekeeping qPCR
RT 148	GGAAAAAGGTCTGACCGACA	Rev ubiquitin housekeeping qPCR
RT 432	GTGGAGTAGAAGCGGATATC	Fw *AP2* gene expression, qPCR
RT 433	ATTGACCCATTCGAGCTTCC	Rev *AP2* gene expression, qPCR
RT 452	CTCAGCCTCACCATCTCCTC	Fw *IND* gene expression, qPCR
RT 453	CACCTGCCGTTTCAAGAACT	Rev *IND* gene expression, qPCR
RT 609	ACCGTCCGATTGAAATCTCC	Rev *ckx7* Sail 515_A07 knockout mutant analysis, qPCR
RT 861	CTCAGGTATTGCAGACCGTATGAG	Fw *ACTIN7* housekeeping, qPCR
RT 862	CTGGACCTGCTTCA CATACTCTG	Rev *ACTIN7* housekeeping, qPCR
RT 1542	GGTTTTGCTACAGCCAGCTCC	Fw *CKX7* gene expression, qPCR
RT 1543	GGTCAGCACCGTTGACAAAC	Rev *CKX7* gene expression, qPCR
RT 2817	CAACTCAACCATTGACAAG	Fw *ckx7* Sail 515_A07 knockout mutant analysis, qPCR
RT 2836	CCGTCTTGAGTCTTGAAAAG	Fw *MIR172c* gene expression, qPCR (Ripoll et al., 2015)
RT 2837	GAAATACCTCCGATCTGTGA	Rev *MIR172c* gene expression, qPCR (Ripoll et al., 2015)

Table S2. List of the primers used in this study. Related to STAR methods.

Journal of Experimental Botany
doi:10.1093/jxb/eraa050 Advance Access Publication 18 February 2020

FLOWERING NEWSLETTER REVIEW

Gynoecium size and ovule number are interconnected traits that impact seed yield

Mara Cucinotta[1,], Maurizio Di Marzo[1], Andrea Guazzotti[1], Stefan de Folter[2], Martin M. Kater[1] and Lucia Colombo[1,*,]

[1] Dipartimento di Bioscienze, Università degli Studi di Milano, Via Celoria 26, 20133 Milan, Italy
[2] Unidad de Genómica Avanzada (UGA-Langebio), Centro de Investigación y de Estudios Avanzados del Instituto Politecnico Nacional (CINVESTAV-IPN), Km. 9.6 Libramiento Norte, Carretera Irapuato-Leon, CP 36824 Irapuato, Gto., Mexico

* Correspondence: lucia.colombo@unimi.it

Received 13 October 2019; Editorial decision 13 January 2020; Accepted 24 January 2020

Editor: Frank Wellmer, Trinity College Dublin, Ireland

Abstract

Angiosperms form the largest group of land plants and display an astonishing diversity of floral structures. The development of flowers greatly contributed to the evolutionary success of the angiosperms as they guarantee efficient reproduction with the help of either biotic or abiotic vectors. The female reproductive part of the flower is the gynoecium (also called pistil). Ovules arise from meristematic tissue within the gynoecium. Upon fertilization, these ovules develop into seeds while the gynoecium turns into a fruit. Gene regulatory networks involving transcription factors and hormonal communication regulate ovule primordium initiation, spacing on the placenta, and development. Ovule number and gynoecium size are usually correlated and several genetic factors that impact these traits have been identified. Understanding and fine-tuning the gene regulatory networks influencing ovule number and pistil length open up strategies for crop yield improvement, which is pivotal in light of a rapidly growing world population. In this review, we present an overview of the current knowledge of the genes and hormones involved in determining ovule number and gynoecium size. We propose a model for the gene regulatory network that guides the developmental processes that determine seed yield.

Keywords: Gynoecium, hormones, organ boundary, ovule number, ovule primordia, pistil, seed yield.

Introduction

Life on earth is affected by plants in varied ways. Of the estimated 400 000 extant plant species, approximately 94% are seed plants (Govaerts, 2001; Willis, 2017). This demonstrates that seed development and dispersion strategies greatly contributed to the success of this organismal group. The vast majority of seed plants are angiosperms and only a comparatively small number are gymnosperms. Both plant divisions produce ovules; however, only angiosperm species produce flowers, and as another selective advantage, each flower produces one or more gynoecia that protect and nourish the ovules. Following fertilization, the gynoecium (or pistil) generally develops into a fruit and ovules develop into seeds.

Depending on the species, the gynoecium consists of one or more carpels, which can be fused or unfused (Endress and Igersheim, 2000). The Arabidopsis gynoecium consists of two fused carpels (Smyth *et al.*, 1990; Alvarez-Buylla *et al.*, 2010). Along the margins where the carpels fuse, a meristematic tissue, termed the carpel margin meristem (CMM), is formed.

The CMM gives rise to the placenta, ovules, septum, and transmitting tract (Reyes-Olalde *et al.*, 2013; Reyes-Olalde and de Folter, 2019). Inside an ovule the female gametophyte develops, comprising three antipodal cells, a central cell, two synergids, and an egg cell (Bencivenga *et al.*, 2011; Drews and Koltunow, 2011). Therefore, ovule development is a crucial process during the plant life cycle and has been studied in many species. In recent decades, many reviews on ovule development have been written, demonstrating its importance and the degree of active research in this area (e.g. Reiser and Fischer, 1993; Angenent and Colombo, 1996; Grossniklaus and Schneitz, 1998; Gasser *et al.*, 1998; Bowman *et al.*, 1999; Skinner *et al.*, 2004; Colombo *et al.*, 2008; Shi and Yang, 2011; Endress, 2011; Cucinotta *et al.*, 2014; Gasser and Skinner, 2019; Pinto *et al.*, 2019; Shirley *et al.*, 2019).

To complement existing literature, this review focuses on recent discoveries in ovule development and gynoecium size determination. An overview is provided of the genes and hormonal communication involved in the developmental programs (Fig. 1; Table 1). Understanding the regulatory networks that determine ovule number and gynoecium size is important as they hugely impact seed yield, and fine-tuning them appears to be a particularly promising strategy for enhancing crop yields.

Placenta development and ovule primordium initiation in Arabidopsis

Periclinal cell divisions within the sub-epidermal tissue of the placenta initiate ovule primordium development at stage 9 of flower development (Roeder and Yanofsky, 2006).

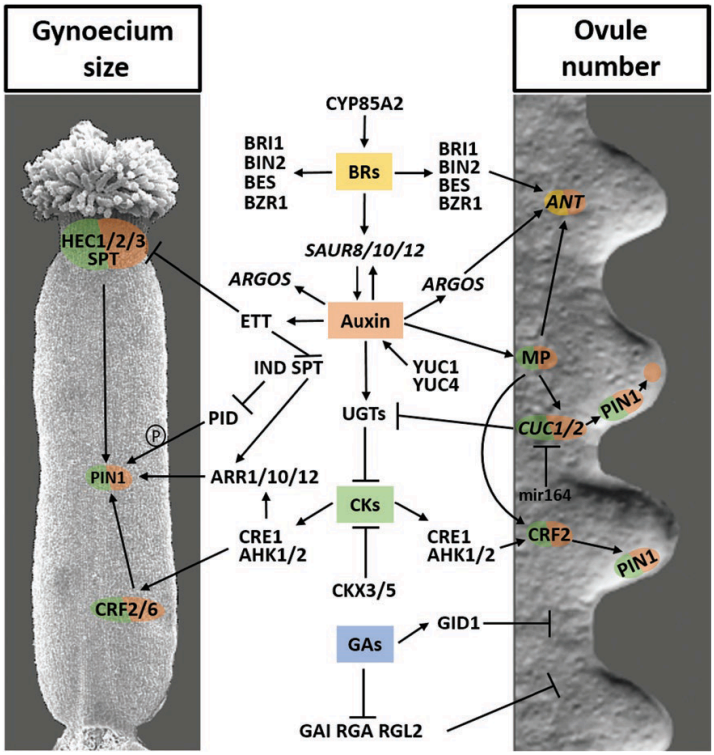

Fig. 1. Proposed model for the regulation of pistil growth and ovule primordium initiation. A gynoecium of Arabidopsis is shown on the left while the image on the right depicts ovule primordia; in the centre, the interconnected gene network that regulates the two processes is shown. Auxin, through ETT, regulates gynoecium fusion and elongation by repressing *IND*, *HEC*s, and *SPT*, which in turn modulate polarization of the auxin efflux carrier PIN1 via repressing *PID*. CK positively regulates *PIN1* expression. In particular, the CK response mediated by CRFs and ARRs is directly required for pistil elongation and indirectly affects ovule primordium initiation. *CRF2* regulation by MP further integrates the auxin–CK crosstalk. Moreover, MP directly regulates *CUC1* and *CUC2* expression. In turn, CUCs control *PIN1* expression and PIN1 protein localization, which is required for correct ovule primordium development. CUCs positively influence the CK pathway by transcriptionally repressing the CK-inactivating glycosyltransferase enzymes (UGTs). *ANT*, whose expression is controlled by auxin and BRs, is required for cell division in ovule primordia. *ANT* is also regulated by auxin via MP and ARGOS. BR signalling also positively affects pistil elongation. GA has a negative effect on ovule number, but its connection with other hormones remains to be addressed.

Table 1. Genes involved in determining gynoecium size and/or ovule number

Gene name	Family or protein type	Gynoecium size	Ovule number	Reference
ANT	AP2/EREBP transcription factor	*ant-9* ↓ *ant-4* ↓ *35S::ANT* ↑	*ant-1* ↓ *ant-3* ↓ *ant-4* ↓ *ant-9* ↓	Elliott *et al.* (1996), Liu *et al.* (2000), Azhakanandam *et al.* (2008), Krizek (2009), Wynn *et al.* (2014)
ARGOS	ARGOS protein	*35S::ARGOS* ↑		Hu *et al.* (2003)
CRC	YABBY transcription factor	*crc-1* ↓		Gross *et al.* (2018)
SPT	bHLH transcription factor	*spt-2* ↓	*spt-2* ↓	Heisler *et al.* (2001), Alvarez and Smyth (2002), Nahar *et al.* (2012)
ETT (*ARF3*)	ARF transcription factor	*ett-1* ↓ *ett-2* ↓		Sessions *et al.* (1997), Nemhauser *et al.* (2000)
HEC1, *HEC2*, *HEC3*	bHLH transcription factor	*hec1 hec2 hec3* ↓		Gremski *et al.* (2007)
ARR1, *ARR10*, *ARR12*	Type-B ARR transcription factor	*arr1 arr10 arr12* ↓	*arr1 arr10 arr12* ↓	Reyes-Olalde *et al.* (2017)
CRF2, *CRF3*, *CRF6*	ERF transcription factor	*crf2 crf3 crf6* ↓	*crf2 crf3 crf6* ↓	Cucinotta *et al.* (2016)
PIN1	PIN auxin efflux carrier	*pin1* ↓	*pin1* ↓ *pin1-5* ↓	Okada *et al.* (1991), Bencivenga *et al.* (2012), Cucinotta *et al.* (2016)
CKX3, *CKX5*	CKX cytokinin oxidase/dehydrogenase protein	*ckx3 ckx5* ↑	*ckx3 ckx5* ↑	Bartrina *et al.* (2011)
UGT85A3, *UGT73C1*	UDP-glucosyl transferase	*35S::UGT85A3* ↓ *35S::UGT73C1* ↓	*35S::UGT85A3* ↓ *35S::UGT73C1* ↓	Cucinotta *et al.* (2018)
SAUR8, *SAUR10*, *SAUR12*	SAUR-like auxin-responsive protein family	*35S::SAUR8* ↑ *35S::SAUR10* ↑ *35S::SAUR12* ↑		van Mourik *et al.* (2017)
BZR1	Brassinosteroid signalling regulatory protein	*bzr1-1D* ↑	*bzr1-1D* ↑	Huang *et al.* (2013)
BIN2	ATSK (shaggy-like kinase) family	*bin2* ↓	*bin2* ↓	Huang *et al.* (2013)
DET2	3-Oxo-5-α-steroid 4-dehydrogenase protein	*det2* ↓	*det2* ↓	Huang *et al.* (2013)
BRI1	Leucine-rich receptor-like protein kinase protein	*bri1-5* ↓	*bri1-5* ↓	Huang *et al.* (2013)
CYP85A2	Cytochrome p450 enzyme		*cyp85a2-1* ↓ *cyp85a2-2* ↓	Nole-Wilson *et al.* (2010b)
SEU	Transcriptional adaptor	*seu-1* ↓	*seu-1* ↓	Nole-Wilson *et al.* (2010b)
CTR1	RAF homologue of serine/threonine kinase	*ctr1-1* ↓		Carbonell-Bejerano *et al.* (2011)
REV	Homeobox-leucine zipper protein		*ant rev* ↓	Nole-Wilson *et al.* (2010a)
LUG	WD40/YVTN repeat-like-containing domain transcription factor		*lug-1* ↓ *lug-3* ↓	Azhakanandam *et al.* (2008)
PAN	bZIP transcription factor	*ant pan* ↓ *seu pan* ↓	*ant pan* ↓ *seu pan* ↓	Wynn *et al.* (2014)
HLL	Ribosomal protein L14p/L23e	*hll* ↓	*hll* ↓	Schneitz *et al.* (1998), Skinner *et al.* (2001)
SIN2	P-loop containing nucleoside triphosphate hydrolase superfamily protein	*sin-2* ↓	*sin-2* ↓	Broadhvest *et al.* (2000)
YUC1, *YUC4*	Flavin-binding monooxygenase protein		*yuc1 yuc4* ↓	Cheng *et al.* (2006)
AHK2, *AHK3*, *CRE1*	Histidine kinase		*cre1-12 ahk2-2 ahk3-3* ↓	Bencivenga *et al.* (2012)
CUC1, *CUC2*	NAC transcription factor		*cuc1 cuc2* ↓ *pSTK::CUC1/RNAi* *cuc2-1* ↓	Galbiati *et al.* (2013)
MIR164A	microRNA		*35S::MIR164A* ↓	Gonçalves *et al.* (2015)
GAI, *RGA*, *RGL2*	GRAS transcription factor	*gaiT6 rgaT2 rgl2-1* ↓	*gaiT6 rgaT2 rgl2-1* ↓	Gomez *et al.* (2018)
GID1A, *GID1B*	α/β-Hydrolase superfamily protein		*gid1ab* ↑	Gomez *et al.* (2018)
REM22	B3 protein transcription factor		*rem22-1* ↑	Gomez *et al.* (2018)
UNE16	Homeodomain-like superfamily protein		*une16-1* ↓	Gomez *et al.* (2018)
NERD1	GW repeat- and PHD-finger-containing protein NERD		*nerd1-2* ↓ *nerd1-4* ↓	Yuan and Kessler (2019)
ONA2	Unknown protein		*ona2* ↓	Yuan and Kessler (2019)
ASHH2	Histone-lysine *N*-methyltransferase		*ashh2* ↓	Grini *et al.* (2009)

Up- and down-pointing arrows represent how the mutant phenotype impacts either gynoecium size or ovule number.

Subsequently, three layers of primordium cells form a finger-like structure during stage 10, which then differentiates into three regions along the proximal–distal axis: the funiculus, the chalaza, and the nucellus (Schneitz *et al.*, 1995). These three regions undergo distinct but interdependent developmental processes. The nucellus is the site of megasporogenesis, where the megaspore mother cell differentiates and locates to the uppermost, central, and subepidermal position of the digit-shaped ovule primordium (reviewed in Pinto *et al.*, 2019). The chalaza is the region from which the inner and outer integuments develop, and these finally envelop and protect the embryonic sac. The funiculus remains attached to the gynoecium via the placental tissue and this connection is required for the transport of nutrients to the ovule (Fig. 1). For this reason, the placental tissue is fundamental for ovule primordia formation, and for determining their number and maintenance.

In Arabidopsis, placental tissue differentiates from the CMM, which is the central ridge of cells that fuse and give rise to the septum. Placental tissue differentiates along the length of the septum adjacent to the lateral walls (Alvarez and Smyth, 2002; Nole-Wilson *et al.*, 2010*a*; Reyes-Olalde *et al.*, 2013). Communication between transcription factors and hormones is essential to maintain the meristematic activity of the placenta, to determine the sites of ovule initiation and ovule identity, and to establish the distance between two adjacent ovules (Cucinotta *et al.*, 2014). Several genes that are important for placenta development have been described in the literature (reviewed by Cucinotta *et al.*, 2014; Reyes-Olalde and de Folter, 2019), including *AINTEGUMENTA* (*ANT*), *CUP-SHAPED COTYLEDON 1* (*CUC1*) and *CUC2*, *LEUNIG* (*LUG*), *MONOPTEROS* (*MP*), and *PERIANTHIA* (*PAN*) (Fig. 1; Table 1).

AINTEGUMENTA encodes an AP2 transcription factor (Klucher *et al.*, 1996) and positively regulates organ size via determining cell number and meristematic competence. *Ant* mutants have fewer and smaller floral organs than the wild-type. In particular, the *ant-9* mutant is characterized by unfused carpels at the tip of the pistil (Elliott *et al.*, 1996), whereas in *ant-4*, the size of floral organs is reduced (Krizek, 2009). In contrast to these mutant phenotypes, Arabidopsis plants that overexpress *ANT* possess larger floral organs than the wild-type (Mizukami and Fischer, 2000). Expression of *ANT* is controlled by *AUXIN-REGULATED GENE INVOLVED IN ORGAN SIZE* (*ARGOS*), an auxin-inducible gene (Hu *et al.*, 2003). When *ARGOS* is overexpressed, floral organs become enlarged, resulting in longer siliques than those of wild-type (Hu *et al.*, 2003). This was one of the first pieces of evidence that implicated a key role for auxin in pistil development.

ANT expression initiates in the placenta and is maintained throughout all stages of ovule development, in particular in the chalaza region and in the integuments. The reduced ovule number phenotype of the *ant* mutant is exacerbated when it is combined with other mutations that affect CMM and placenta development, such as *revoluta* (*rev*), suggesting that the activity of the *REV* gene, which encodes a class III homeodomain leucine zipper transcription factor, is also required for placenta formation (Nole-Wilson *et al.*, 2010*a*). ANT interacts with the transcriptional repressor SEUSS (SEU) and simultaneous loss of both protein activities severely affects placenta development and leads to a complete loss of ovule formation. When a weaker *ant-3* allele was combined with *seu-3*, placenta development was maintained but the number of ovules that initiated was reduced to approximately half of that observed in Col-0 wild-type plants (Azhakanandam *et al.*, 2008). Another transcriptional co-regulator involved in gynoecium patterning is LEUNIG (LUG). Strong *lug-1* and intermediate *lug-3* alleles show a failure in ridge fusion and a reduction in the amount of placental tissue, with a consequent decrease in the number of ovules formed (Liu *et al.*, 2000). The combination of *lug* and *ant* mutations results in gynoecia that are unable to develop ovules (Liu *et al.*, 2000). The loss of ovules in the *ant* and *seu* backgrounds is strongly enhanced by mutations in the *PERIANTHIA* (*PAN*) gene, which encodes a bZIP transcription factor that is expressed in the gynoecium medial ridge, placenta, and ovules, where it promotes ovule formation (Wynn *et al.*, 2014).

Similar to *ANT*, factors important for integument growth often affect ovule primordium formation. Two examples are *HUELLENLOS* (*HLL*) and *SHORT INTEGUMENTS 2* (*SIN2*). *HLL* encodes a mitochondrial ribosomal protein and its mutation is associated with smaller gynoecia and a 10% reduction in the number of ovules (Schneitz *et al.*, 1998; Skinner *et al.*, 2001). Shorter gynoecia that bear fewer ovules are also observed in the *sin2* mutant; however, more interestingly, the absence of *SIN2* function leads to an abnormal distribution of ovules along the placenta (Broadhvest *et al.*, 2000), in which the distance between ovules is greater than in the wild-type; thus, a reduction in ovule number is caused by a reduction in gynoecium size and by the reduced ability of the placental tissue to initiate ovule primordia. *SIN2* encodes a mitochondrial DAR GTPase and, similar to HLL, is hypothesized to function in mitochondrial ribosome assembly (Hill *et al.*, 2006). Notably, these two ribosomal proteins, which are targeted to the mitochondria, are necessary for ovule primordium formation, and it has been suggested that impaired mitochondrial function might cause cell-cycle arrest in the placenta and subsequently in the ovule integuments (Broadhvest *et al.* 2000).

Complex hormonal communication promotes ovule initiation and determines pistil size

Plant organogenesis requires cells to proliferate, grow, and differentiate in a coordinated way. The intercellular communication required during organ initiation is mediated by different phytohormones (Davies, 2004; Vanstraelen and Benková, 2012; Schaller *et al.*, 2015; Marsch-Martínez and de Folter, 2016). As will be discussed in this review, auxins, cytokinins (CKs), gibberellins (GAs), and brassinosteroids (BRs) all play fundamental roles in ovule primordium formation (Fig. 1).

In most auxin-related mutants, defects in gynoecium formation lead to the reduction or absence of placental tissue and the corresponding absence of ovules (reviewed in Balanzá *et al.*, 2006; Larsson *et al.*, 2013; Cucinotta *et al.*, 2014). This phenotype is common to all mutants in which auxin synthesis

or transport pathways are compromised, such as *yucca1 yucca4* (*yuc1 yuc4*) (Cheng *et al.*, 2006) and *pin1-1* (Okada *et al.*, 1991) or is similar to that following treatment with the polar auxin transport inhibitor 1-naphthyl phthalamic acid (NPA) (Nemhauser *et al.*, 2000).

Polar auxin transport is mediated by the PINFORMED1 (PIN1) efflux transporter and is required to create a zone with an auxin concentration maximum in the placenta, where the founder cells of the ovule primordia will be specified (Benková *et al.*, 2003; Ceccato *et al.*, 2013; Galbiati *et al.*, 2013). Subsequently, the orientation of PIN1 within the membrane relocalizes and redirects auxin flow, establishing a gradient with a maximum at the apices of the formed primordia. In developing organs, auxin distribution can be monitored *in vivo* by imaging a synthetic auxin-inducible promoter, *DR5*. In plants that express green fluorescent protein (GFP) from the *DR5* promoter, green fluorescence is detected at the apices of the ovule primordia, consistent with PIN1-mediated auxin flow directed to the apex (Benková *et al.*, 2003; Galbiati *et al.*, 2013). The weak *pin1-5* mutant allele can produce some flowers in which the pistils have slightly reduced valves, which on average contain only nine ovules (Bennett *et al.*, 1995; Sohlberg *et al.*, 2006; Bencivenga *et al.*, 2012).

CKs occupy a central role in the regulation of cell division and cell differentiation. They are positive regulators of ovule formation, as demonstrated by the phenotype of mutants in which CK pathways are altered. In the *ckx3 ckx5* double mutant, the degradation of CKs is compromised and the consequent increase in the levels of these hormones leads to an increased activity of the reproductive meristem (Bartrina *et al.*, 2011). Moreover, the longer than normal gynoecia of *ckx3 ckx5* double mutants contain about twice as many ovules as those of the wild-type, indicating an increase in the meristematic capacity of placental tissue (Bartrina *et al.*, 2011). By contrast, reduced ovule formation is observed in mutants in which the synthesis or perception of CKs is compromised. Plants that carry mutations in genes that encode all three CK receptors, *cytokinin response 1* (*cre1-12*), *histidine kinase 2* (*ahk2-2*), and *ahk3*, develop five ovules per pistil on average, in addition to showing pleiotropic growth defects (Higuchi *et al.*, 2004; Bencivenga *et al.*, 2012). The AHK2 and AHK3 receptors are expressed throughout ovule development, from the early stages until maturity, whereas *CRE1/AHK4* is expressed in the chalaza region and subsequently in the integuments, suggesting that AHK2 and AHK3 preferentially contribute to ovule primordium formation (Bencivenga *et al.*, 2012). The ovule and gynoecium phenotype of the *cre1-12 ahk2-2 ahk3-3* triple mutant resembles that of the weak *pin1-5* mutant allele (Bencivenga *et al.*, 2012). This similarity is due to the downregulation of *PIN1* expression in the triple mutant, suggesting that during the early stages of ovule development, CK activates *PIN1* expression. Bencivenga *et al.* (2012) showed that treating inflorescences with the synthetic CK 6-benzylaminopurine (BAP) increases *PIN1* expression in the gynoecium. Strikingly, treatment with BAP causes the formation of on average 20 additional ovule primordia in each gynoecium, which are positioned between the existing primordia formed before the treatment. This suggests that placental tissue at the boundaries between ovules maintains meristematic competence. During root development, CK affects auxin polar transport via PIN1 both at the transcriptional and post-transcriptional levels. In contrast to the situation in the gynoecium, CK negatively regulates the expression of *PIN1* in the root and controls the endorecycling of PIN1 from the membrane to direct it to vacuoles for lytic degradation (Ruzicka *et al.*, 2009; Marhavý *et al.*, 2011). In roots, CYTOKININ RESPONSE FACTORS (CRFs), especially CRF2, CRF3, and CRF6, transcriptionally regulate *PIN1* by binding to its promoter at the *cis*-regulatory *PIN CYTOKININ RESPONSE ELEMENT* (*PCRE*) (Šimášková *et al.*, 2015) and modulate its expression in response to CK. Similarly, CRFs also mediate *PIN1* expression in ovules in response to CK (Cucinotta *et al.*, 2016). Indeed, *PIN1* expression is reduced in the *crf2 crf3 crf6* (*crf2/3/6*) triple mutant and cannot be increased by CK treatment. The placenta in *crf2/3/6* is also shorter, but this is not sufficient to explain the 30% decrease in ovule number as ovule density is lower in *crf2/3/6* than in the wild-type (Cucinotta *et al.*, 2016). Because *PIN1* expression in *crf2/3/6* was unresponsive to CK application, the mutant was significantly less sensitive to CK treatment than the wild-type with regard to an increase in ovule number and pistil length. Auxin also regulates *CRF2*, which is a direct target of the auxin response factor (ARF) AUXIN RESPONSE FACTOR 5/MONOPTEROS (ARF5/MP) (Schlereth *et al.*, 2010), highlighting another convergence point between auxin and CK.

Another ARF family member that is required for appropriate apical–basal gynoecium patterning is ARF3/ETTIN (ETT). The *ett* mutant is characterized by a shorter ovary with an elongated style and gynophore (Sessions *et al.*, 1997). A similar gynoecium phenotype resulted from treatment with the auxin transport inhibitor (NPA), suggesting that ETT plays a key role in auxin signalling along the apical–basal gynoecium axis (Nemhauser *et al.*, 2000). Moreover, ETT restricts the expression domain of *SPATULA* (*SPT*), which encodes a basic helix–loop–helix (bHLH) transcription factor (Heisler *et al.*, 2001). Mutations in *SPT* causes a split-carpel phenotype in the apical part of the gynoecium, leading to a slight reduction in ovule number (Alvarez and Smyth, 1999; Nahar *et al.*, 2012). SPT dimerizes with another bHLH transcription factor, INDEHISCHENT (IND), to repress the expression of *PINOID* (Girin *et al.*, 2011), which encodes a serine/threonine kinase that regulates PIN1 polarization via phosphorylation (Friml *et al.*, 2004). The repression of *PID* by SPT and IND allows the formation of a radially symmetric auxin ring in the upper part of the gynoecium that is required for correct style and stigma development (Moubayidin and Østergaard, 2014).

Furthermore, SPT interacts with the three closely related bHLH transcription factors, HECATE1 (HEC1), HEC2, and HEC3 (Gremski *et al.*, 2007), and similar to *ett, hec-1 hec-2 hec-3* triple mutants possess an elongated style and shorter ovaries. The HEC proteins and SPT promote auxin transport in concert by activating *PIN1* and *PIN3* expression (Schuster *et al.*, 2015) and also transcriptionally activate the type-A ARABIDOPSIS RESPONSE REGULATORS (ARR-As), which are negative regulators of CK signalling (Schuster *et al.*, 2015). Via this dual

action on auxin transport and CK response, HECs and SPT regulate wild-type gynoecium fusion at the apex, and style and stigma development. Furthermore, SPT alone in the medial domain activates the type-B ARRs, especially ARR1, which are positive regulators of CK signalling. The *arr1 arr10 arr12* triple mutant possesses a shorter gynoecium and significantly fewer ovules than the wild-type (Reyes-Olalde *et al.*, 2017).

In addition to auxin localization, correct auxin signalling is also required for wild-type gynoecium development, as confirmed by a recent study on members of the Small Auxin-Upregulated RNA (SAUR) family, which were initially identified as short transcripts that were rapidly upregulated in response to auxin (McClure and Guilfoyle, 1987). When *SAUR8*, *SAUR10*, and *SAUR12* are ectopically overexpressed in Arabidopsis, the gynoecium and resulting siliques are longer than in wild-type, suggesting that auxin positively regulates gynoecium length and, probably indirectly, silique length (van Mourik *et al.*, 2017). Notably, *SAUR* gene expression increased 100-fold following combined auxin and BR treatment (van Mourik *et al.*, 2017). BRs are clearly involved in pistil growth and ovule number specification; gynoecia of the enhanced BR-signalling mutant *brassinazole-resistant 1-1D* (*bzr1-1D*) not only contained more ovules than wild-type but they were also longer. By contrast, BR-deficient mutants such as *de-etiolated 2* (*det-2*), *brassinosteroid insensitive 1* (*bri1-5*) and *brassinosteroid-insensitive 2* (*bin2-1*) developed shorter pistils with fewer ovules (Huang *et al.*, 2013).

The involvement of BRs in gynoecium and ovule development was also confirmed by Nole-Wilson *et al.* (2010*b*), who observed that a reduction in the expression of *CYP85A2*, which encodes an enzyme involved in the final step of brassinolide biosynthesis (Nomura *et al.*, 2005), enhances the *seuss* mutant phenotypic disruptions in ovules and gynoecia (Nole-Wilson *et al.*, 2010*b*).

CUP-SHAPED COTYLEDON 1 and 2 function synergistically with auxin and cytokinins

During ovule primordium formation, CK homeostasis requires two NAC-domain transcription factors, CUP-SHAPED COTYLEDON 1 (CUC1) and CUC2. These are expressed in lateral organ boundaries and function redundantly during organ boundary determination. *CUC1* and *CUC2* are expressed in the septum and placenta, and following the emergence of ovule primordia, *CUC2* expression is restricted to the borders between the ovules (Ishida *et al.*, 2000; Galbiati *et al.*, 2013; Gonçalves *et al.*, 2015). The *CUC1* and *CUC2* genes are both post-transcriptionally regulated by *miR164* microRNAs (Laufs *et al.*, 2004; Mallory *et al.*, 2004). Gynoecia of the *in vitro* regenerated *cuc1 cuc2* mutant as well as of *cuc2-1 pSTK::CUC1_RNAi* plants have reduced ovule numbers. The *cuc1 cuc2* double mutant has on average fewer than 10 ovules per pistil (Ishida *et al.*, 2000), whereas *cuc2-1 pSTK::CUC1_RNAi* plants, in which *CUC1* was specifically silenced in the placenta and ovules, showed a 20% reduction in ovule number, but gynoecium length was not affected. In pistils of these plants, ovules were more widely spaced when compared with the wild-type (Galbiati *et al.*, 2013). This result was confirmed by silencing *CUC1* and *CUC2* by overexpressing *MIR164A*, which strongly reduced ovule number, indicating a major contribution of *CUC1* and *CUC2* to ovule initiation (Gonçalves *et al.*, 2015). The analysis of PIN1–GFP expression in *cuc2-1 pSTK::CUC1_RNAi* plants revealed that CUC1 and CUC2 redundantly promote *PIN1* expression and PIN1 membrane localization in ovules. Treatment with BAP increased *PIN1* expression and complemented the reduced ovule number phenotype of *cuc2-1 pSTK::CUC1_RNAi* plants (Galbiati *et al.*, 2013). Therefore, CKs act downstream from or in parallel with CUC1 and CUC2 to induce the expression of *PIN1*. Recently, it has been demonstrated that CUC1 and CUC2 induce CK responses *in vivo* and function upstream of CK by transcriptionally repressing *UGT73C1* and *UGT85A3*, which encode two enzymes involved in CK inactivation (Cucinotta *et al.*, 2018). Consistent with this result, the concentration of inactive CK glucosides was higher in *cuc2-1 pSTK::CUC1_RNAi* inflorescences than in wild-type plants.

The expression of *CUC1* and *CUC2* is also linked with auxin signalling: their expression pattern coincides with that of the auxin response factor ARF5/MP (see above) and both genes are downregulated in pistils of the weak *mp-S319* mutant allele (Galbiati *et al.*, 2013). During the early stages of placenta development and ovule formation, ARF5/MP directly transcriptionally activates *CUC1* and *CUC2*, but also *ANT*. The observation that BAP treatment did not complement the ovule number phenotype of *ant-4* suggests that ANT functions independently of *CUC1* and *CUC2*. This is further supported by the additive effects on the reduction in ovule number observed in *ant-4 cuc2-1 pSTK:CUC1_RNAi* plants (Galbiati *et al.*, 2013). Together these data suggest that ANT promotes cell proliferation, whereas CUC1 and CUC2 regulate CK homeostasis and auxin transport. Although CUC3 shares high similarity with CUC1 and CUC2, the *cuc3* mutant was not affected in ovule initiation and number, but together with CUC2, CUC3 promotes ovule separation; this is reflected by the *cuc2 cuc3* double mutant, which produces seeds that result from the fusion of two ovules (Gonçalves *et al.*, 2015). These results suggest that specific *CUC* genes independently promote ovule initiation and ovule separation.

Lee *et al.* (2009) identified LATERAL ORGAN FUSION 1 (LOF1) to be involved in lateral organ separation and to functionally overlap with CUC2 and CUC3. The *LOF1* gene is expressed at the base of ovule primordia and its overexpression results in a wrinkled pistil with an enlarged replum, an amorphous septum and an irregular ovule distribution (Gomez *et al.*, 2011).

The role of gibberellins in ovule primordium formation

GAs are involved in key developmental processes throughout the plant life cycle, from seed germination in particular, to flowering time (reviewed in Hedden and Sponsel, 2015; Rizza and Jones, 2019), but their involvement in ovule initiation

has only recently been demonstrated. Gomez and colleagues (2018) showed that DELLA proteins, which belong to a subfamily of the plant-specific GRAS family of transcriptional regulators that repress GA signalling, positively regulate ovule number in Arabidopsis. In addition to DELLA proteins, the GA signalling core includes the GA receptor GID1. When GID1 binds bioactive GA, the GA–GID1–DELLA complex is formed and triggers the polyubiquitination and degradation of DELLA proteins. The *della* triple mutant *gaiT6 rgaT2 rgl2-1* produces fewer ovules than wild-type (Gomez *et al.*, 2018). By contrast, the gain-of-function DELLA mutant *gai-1*, which cannot be degraded upon GA sensing, produced more ovules. Consistent with this observation, the double *gid1a gid1b* mutant, which cannot perceive GA, forms more ovules than the wild-type, demonstrating a negative correlation between GAs and ovule number (Gomez *et al.*, 2018). The *GAI*, *RGA*, *RGL2*, *GID1a*, and *GID1b* genes are expressed in placental tissue and outgrowing ovules. The reduction in ovule number was more dramatic in the *gaiT6 rgaT2 rgl2-1* triple mutant than that in ovary length, resulting in a lower ovule density, whereas the dominant *gai-1* mutant has an increased ovule/placenta ratio, suggesting that GAs predominantly affect ovule initiation and not placenta elongation.

Other evidence to demonstrate that DELLA proteins promote ovule formation derives from an experiment in which the expression of the stable mutant protein *rgaΔ17* under the control of the *ANT* promoter in the placenta resulted in the formation of 20% more ovules than in control lines (Gomez *et al.*, 2018). This effect of GAs on the number of developing ovules was not correlated with auxin signalling or transport, and neither PIN1 localization nor *DR5* expression was affected by GA treatment or DELLA activity (Gomez *et al.*, 2018).

Confirmation of a positive role for *RGL2* in determining ovule number came from the analysis of transgenic lines in which RGL2-dependent GA signalling was blocked by the expression of a dominant version of RGL2 (*pRGL2:rgl2Δ17*) (Gómez *et al.*, 2019). Pistils of *pRGL2:rgl2Δ17* plants contained 10% more ovules than those of the wild-type, whereas pistil length did not differ, indicating that the main function of rgl2Δ17 is to positively promote ovule primordium formation but not placenta elongation (Gómez *et al.*, 2019). Furthermore, Gomez *et al.* (2018) identified *REPRODUCTIVE MERISTEM 22* (*REM22*) and *UNFERTLIZED EMBRYO SAC 16* (*UNE16*) via transcriptomic analysis to be DELLA targets that are positive regulators of ovule initiation. REM22 is a B3 family transcription factor that is expressed in the placenta (Mantegazza *et al.*, 2014) and increased *REM22* expression in the *rem22-1* enhancer allele significantly increases ovule number. UNE16 is a transcription factor involved in embryo sac development and the knockdown allele *une16-1* produces fewer ovules. Because *UNE16* expression is regulated by BRs (Pagnussat *et al.*, 2005; Sun *et al.*, 2010), it represents a potential nexus for crosstalk between GAs and BRs in ovule initiation. The establishment of GA as an important additional component of the ovule regulatory network has introduced an additional layer of complexity to the current model for ovule initiation and it remains to be established how GAs integrate into this model. GAs might function antagonistically to CKs and BRs, which in contrast to GAs, positively regulate pistil size and ovule number.

Finally, the *ctr1-1* constitutive ethylene-responsive mutant possesses a shorter gynoecium at anthesis compared with wild-type and a delay in the response to GA_3 treatment that induces gynoecium senescence, suggesting that ethylene affects gynoecium size, probably by interactions with GA pathways (Carbonell-Bejerano *et al.*, 2011).

In conclusion, there is ample evidence for complex interactions between different hormonal pathways that together determine ovule number and pistil size.

Ovule number: the ecotype matters

It has been known for 20 years that the number of ovules varies hugely among different Arabidopsis ecotypes (diploid accessions) (Alonso-Blanco *et al.*, 1999): for example, the Landsberg *erecta* accession produces 20% more ovules than the Cape Verde Islands (Cvi) accession. Recently, 189 Arabidopsis accessions from the Arabidopsis Biological Resource Center were analysed for differences in ovule number and they display a remarkable degree of variation, ranging from 39 to 82 ovules per pistil (Yuan and Kessler, 2019). The commonly used reference accession Col-0 lies in the middle of the range, with a mean ovule number of 63, which is strongly dependent on experimental growth conditions. Ovule number, in contrast to, for instance, flowering time, does not correlate with geographical origin (Stinchcombe *et al.*, 2004; Yuan and Kessler, 2019). By conducting a genome-wide association study on these 189 accessions, two loci associated with ovule number were identified (Yuan and Kessler, 2019): *NEW ENHANCER OF ROOT DWARFISM* (*NERD1*) and *OVULE NUMBER ASSOCIATED 2* (*ONA2*). Mutation of *NERD1* or *ONA2* leads to a significant reduction in ovule number, with a stronger phenotype in the *nerd1-2* and *nerd1-4* alleles. *ONA2* encodes a protein of unknown function and was not further analysed. In addition to a reduction in ovule number, *nerd* mutants display additional severe male and female fertility defects. *NERD1* encodes an integral membrane protein mainly localized to the Golgi. Notably, *NERD1* expression is lower in Altai-5 and Kas-2 accessions, which have low ovule numbers (Yuan and Kessler, 2019), but high *NERD1* expression in Altai-5 leads to a significant increase in ovule number. However, overexpression of NERD1 in Col-0 plants did not affect ovule number, indicating that NERD1 function in determining ovule number is background-dependent (Yuan and Kessler, 2019).

Considerable genetic variation in ovule number was also described for F_1 triploids of different Arabidopsis genotypes by Duszynska *et al.* (2013), who observed differences in ovule number between genetically identical F_1-hybrid offspring, after crossing parental genome excess lines (2m:1p with 1m:2p). These effects can only be explained by epigenetic mechanisms that affect genes controlling ovule number, for example DNA or histone methylation. The analysis of null alleles of *ASH1 HOMOLOG 2* (ASH2), which show a remarkable 80% reduction in ovule number, provided a clear example of

the involvement of histone methylation in determining ovule number (Grini *et al.*, 2009). The transcriptional state of the *ASH2* locus remains active during development via H3K36 trimethylation (Xu *et al.*, 2008). It will be highly relevant to study the effect of epigenetic modifications induced by biotic and abiotic stresses in determining ovule number. Epigenetic responses to stress are fundamental to create the plasticity required for plant survival, especially considering that plants are sessile organisms. These epigenetic changes can be temporally transmitted, even in the absence of the original stress (Iglesias and Cerdán, 2016). Furthermore, variation in ovule number in response to fluctuations in environmental conditions, such as temperature, can be used to understand the plasticity and inheritability of (epigenetic) adaptation and response to temperature stress. Variation in ovule number under stress conditions is, of course, also highly relevant from an ecological, environmental, and evolutional perspective.

Ovule number decreases with ageing

Ovule number varies throughout inflorescence development: early flowers developing on the main inflorescence (from the fifth to the twenty-fifth flower) of Arabidopsis *Ler* plants produced a relatively invariable number of ovules, whereas flowers that developed later had pistils with fewer ovules (Gomez *et al.*, 2018;Yuan and Kessler, 2019). Loss- and gain-of-function mutants of *DELLA* genes showed an increase in ovule number in early- and late-arising flowers (Gomez *et al.*, 2018). To minimize age-related variation in their genome-wide association studies,Yuan and Kessler (2019) only counted ovules in flowers 6–10 from the main inflorescence.

It has been reported for other plant species that flower position as well as size influences ovule number per flower. For example, in pomegranate, the number of ovules per flower was significantly influenced by flower size, with more ovules being produced in larger flowers (Wetzstein *et al.*, 2013).

Overall, when studying changes in ovule numbers it is important to be aware of the possible variation in the different flowers of the plant. Therefore, large numbers will have to be analysed using thorough statistical analyses, especially for genotypes that show only relatively minor changes.

A 'gold mine' for seed yield improvement within the Brassicaceae

Improving seed yield via the genetic manipulation of crops has historically been a central goal in agricultural research. The enormous body of data, which has been generated and shared by the scientific community over the past decades, represents a true 'gold mine' for translational and applied research. The determination of pistil size and ovule number may be considered one of the most straightforward traits that can be enhanced to improve overall seed yield in species characterized by multiovulate ovaries and the increasing amount of literature on this topic evidences an active and prolific research field. Although some questions concerning the networks controlling seed number and pistil size remain open, comprehensive knowledge of the phytohormone interactions involved in these pathways is already available and applicable (Cucinotta *et al.*, 2014; Zúñiga-Mayo *et al.*, 2019; Reyes-Olalde and de Folter, 2019).

Understanding these developmental processes in Arabidopsis can inform promising strategies for knowledge transfer to closely related and agronomically important crops. Rapeseed (*Brassica napus*), another Brassicaceae species, is an important breeding target, since it is a crop widely cultivated in Europe, Asia, Canada, and Australia. It is characterized by an oil-rich seed and its processing provides both rapeseed oil (used as edible vegetable oil or as biodiesel) and a by-product mostly used as cattle fodder (Snowdon *et al.*, 2007).

It has recently been demonstrated that Arabidopsis and *B. napus* share well-conserved response mechanisms to CK treatment (Zuñiga-Mayo *et al.*, 2018). Strikingly, exogenous CK application causes a reduction in silique length in *B. napus*. However, these shorter siliques contain increased ovule numbers and upon manual pollination, the plants show an increase in seed yield of 18%. Intriguingly, increases in ovule and seed number have also been observed in the offspring of the treated plants, suggesting that the mechanism has an underlying epigenetic basis (Zuñiga-Mayo *et al.*, 2018).

An increase in CK level has also been reported to beneficially affect seed yield in transgenic *B. napus* lines expressing the CK biosynthetic enzyme isopentenyltransferase (*IPT*) under the Arabidopsis promoter of the *AtMYB32* gene. An increase in seed yield of up to 23% was obtained in the transgenic lines that were analysed (Kant *et al.*, 2015).

CK homeostasis is mediated by CYTOKININ OXIDASES/DEHYDROGENASES (CKXs) during pistil and silique development in Arabidopsis. Remarkably, the expression level of *CKX* genes in *B. napus* is associated with silique length, and RNA-sequencing and qRT-PCR analyses revealed a significantly different expression level of *BnCKX5-1*, *5-2*, *6-1*, and *7-1* in two distinct cultivated varieties with long versus short siliques (Liu *et al.*, 2018). These findings open up promising strategies with which to modulate silique length in *B. napus* by manipulating *CKX* gene expression.

In addition to phytohormones, genetic knowledge from Arabidopsis can be successfully applied to *B. napus* crop improvement. Mutations in the K-box of the Arabidopsis orthologue of *APETALA1* in *B. napus* caused a significant increase in the number of seeds per plant (Shah *et al.*, 2018). These generated alleles could conceivably be introduced into a rapeseed breeding programme in field trials.

Germplasm of *B. napus* revealed substantial natural variation with respect to seed number per pod. Current rapeseed cultivars produce on average 20 seeds per pod, which is far lower than the maximum observed among the germplasm resources (Yang *et al.*, 2017). Moreover, genetic improvement promises to deliver a massive improvement in seed yield (Yang *et al.*, 2017). The gold mine of knowledge obtained from the closely related species Arabidopsis will certainly be fundamentally important in the exploitation of the encouraging genetic variation potential. Furthermore, it has recently been demonstrated that CRISPR–Cas9 technology can be efficiently applied to precisely induce targeted mutation in rapeseed (Braatz

et al., 2017), making it a powerful tool for future genetic improvement. Similarly, existing knowledge could be used to improve other Brassicaceae species, or even non-phylogenetically related species such as soybean.

Acknowledgements

The authors' work is supported by the H2020 Marie Skłodowska-Curie Actions of European Commission (H2020-MSCA-RISE-2015 EXPOSEED and MSCA-RISE-2014 PROCROP projects) also acknowledges the Mexican National Council of Science and Technology (CONACyT) grants FC-2015-2/1061 and CB2017-2018 A1-S-10126. The authors would like to thank John Chandler for editing the paper.

References

Alonso-Blanco C, Blankestijn-de Vries H, Hanhart CJ, Koornneef M. 1999. Natural allelic variation at seed size loci in relation to other life history traits of *Arabidopsis thaliana*. Proceedings of the National Academy of Sciences, USA **96**, 4710–4717.

Alvarez J, Smyth DR. 1999. *CRABS CLAW* and *SPATULA*, two *Arabidopsis* genes that control carpel development in parallel with AGAMOUS. Development **126**, 2377–2386.

Alvarez J, Smyth DR. 2002. *CRABS CLAW* and *SPATULA* genes regulate growth and pattern formation during gynoecium development in *Arabidopsis thaliana*. International Journal of Plant Sciences **163**, 17–41.

Alvarez-Buylla ER, Benítez M, Corvera-Poiré A, *et al.* 2010. Flower development. The Arabidopsis Book **8**, e0127.

Angenent GC, Colombo L. 1996. Molecular control of ovule development. Trends in Plant Science **1**, 228–232.

Azhakanandam S, Nole-Wilson S, Bao F, Franks RG. 2008. SEUSS and AINTEGUMENTA mediate patterning and ovule initiation during gynoecium medial domain development. Plant Physiology **146**, 1165–1181.

Balanzá V, Navarrete M, Trigueros M, Ferrándiz C. 2006. Patterning the female side of *Arabidopsis*: the importance of hormones. Journal of Experimental Botany **57**, 3457–3469.

Bartrina I, Otto E, Strnad M, Werner T, Schmülling T. 2011. Cytokinin regulates the activity of reproductive meristems, flower organ size, ovule formation, and thus seed yield in *Arabidopsis thaliana*. The Plant Cell **23**, 69–80.

Bencivenga S, Colombo L, Masiero S. 2011. Cross talk between the sporophyte and the megagametophyte during ovule development. Sexual Plant Reproduction **24**, 113–121.

Bencivenga S, Simonini S, Benková E, Colombo L. 2012. The transcription factors BEL1 and SPL are required for cytokinin and auxin signaling during ovule development in Arabidopsis. The Plant Cell **24**, 2886–2897.

Benková E, Michniewicz M, Sauer M, Teichmann T, Seifertová D, Jürgens G, Friml J. 2003. Local, efflux-dependent auxin gradients as a common module for plant organ formation. Cell **115**, 591–602.

Bennett SRM, Alvarez J, Bossinger G, Smyth DR. 1995. Morphogenesis in *pinoid* mutants of *Arabidopsis thaliana*. The Plant Journal **8**, 505–520.

Bowman JL, Baum SF, Eshed Y, Putterill J, Alvarez J. 1999. Molecular genetics of gynoecium development in Arabidopsis. Current Topics in Developmental Biology **45**, 155–205.

Braatz J, Harloff HJ, Mascher M, Stein N, Himmelbach A, Jung C. 2017. CRISPR-Cas9 targeted mutagenesis leads to simultaneous modification of different homoeologous gene copies in polyploid oilseed rape (*Brassica napus*). Plant Physiology **174**, 935–942.

Broadhvest J, Baker SC, Gasser CS. 2000. SHORT INTEGUMENTS 2 promotes growth during Arabidopsis reproductive development. Genetics **155**, 899–907.

Carbonell-Bejerano P, Urbez C, Granell A, Carbonell J, Perez-Amador MA. 2011. Ethylene is involved in pistil fate by modulating the onset of ovule senescence and the GA-mediated fruit set in Arabidopsis. BMC Plant Biology **11**, 84.

Ceccato L, Masiero S, Sinha Roy D, Bencivenga S, Roig-Villanova I, Ditengou FA, Palme K, Simon R, Colombo L. 2013. Maternal control of PIN1 is required for female gametophyte development in Arabidopsis. PLoS ONE **8**, e66148.

Cheng Y, Dai X, Zhao Y. 2006. Auxin biosynthesis by the YUCCA flavin monooxygenases controls the formation of floral organs and vascular tissues in Arabidopsis. Genes & Development **20**, 1790–1799.

Colombo L, Battaglia R, Kater MM. 2008. Arabidopsis ovule development and its evolutionary conservation. Trends in Plant Science **13**, 444–450.

Cucinotta M, Colombo L, Roig-Villanova I. 2014. Ovule development, a new model for lateral organ formation. Frontiers in Plant Science **5**, 117.

Cucinotta M, Manrique S, Cuesta C, Benkova E, Novak O, Colombo L. 2018. CUP-SHAPED COTYLEDON1 (CUC1) and CUC2 regulate cytokinin homeostasis to determine ovule number in Arabidopsis. Journal of Experimental Botany **69**, 5169–5176.

Cucinotta M, Manrique S, Guazzotti A, Quadrelli NE, Mendes MA, Benkova E, Colombo L. 2016. Cytokinin response factors integrate auxin and cytokinin pathways for female reproductive organ development. Development **143**, 4419–4424.

Davies PJ. 2004. Plant hormones: biosynthesis, signal, transduction, action! Dordrecht, The Netherlands: Kluwer Academic Publishers.

Drews GN, Koltunow AM. 2011. The female gametophyte. The Arabidopsis Book **9**, e0155.

Duszynska D, McKeown PC, Juenger TE, Pietraszewska-Bogiel A, Geelen D, Spillane C. 2013. Gamete fertility and ovule number variation in selfed reciprocal F1 hybrid triploid plants are heritable and display epigenetic parent-of-origin effects. New Phytologist **198**, 71–81.

Elliott RC, Betzner AS, Huttner E, Oakes MP, Tucker WQ, Gerentes D, Perez P, Smyth DR. 1996. *AINTEGUMENTA*, an *APETALA2*-like gene of Arabidopsis with pleiotropic roles in ovule development and floral organ growth. The Plant Cell **8**, 155–168.

Endress PK. 2011. Angiosperm ovules: diversity, development, evolution. Annals of Botany **107**, 1465–1489.

Endress PK, Igersheim A. 2000. Gynoecium structure and evolution in basal angiosperms. International Journal of Plant Sciences **161**, S211–S213.

Friml J, Yang X, Michniewicz M, *et al.* 2004. A PINOID-dependent binary switch in apical-basal PIN polar targeting directs auxin efflux. Science **306**, 862–865.

Galbiati F, Sinha Roy D, Simonini S, *et al.* 2013. An integrative model of the control of ovule primordia formation. The Plant Journal **76**, 446–455.

Gasser CS, Broadhvest J, Hauser BA. 1998. Genetic analysis of ovule development. Annual Review of Plant Physiology and Plant Molecular Biology **49**, 1–24.

Gasser CS, Skinner DJ. 2019. Development and evolution of the unique ovules of flowering plants. Current Topics in Developmental Biology **131**, 373–399.

Girin T, Paicu T, Stephenson P, *et al.* 2011. INDEHISCENT and SPATULA interact to specify carpel and valve margin tissue and thus promote seed dispersal in *Arabidopsis*. The Plant Cell **23**, 3641–3653.

Gomez MD, Barro-Trastoy D, Escoms E, *et al*. 2018. Gibberellins negatively modulate ovule number in plants. Development **145**, dev163865.

Gómez MD, Fuster-Almunia C, Ocaña-Cuesta J, Alonso JM, Pérez-Amador MA. 2019. RGL2 controls flower development, ovule number and fertility in Arabidopsis. Plant Science **281**, 82–92.

Gomez MD, Urbez C, Perez-Amador MA, Carbonell J. 2011. Characterization of *constricted fruit* (*ctf*) mutant uncovers a role for *AtMYB117/LOF1* in ovule and fruit development in *Arabidopsis thaliana*. PLoS ONE **6**, e18760.

Gonçalves B, Hasson A, Belcram K, *et al.* 2015. A conserved role for *CUP-SHAPED COTYLEDON* genes during ovule development. The Plant Journal **83**, 732–742.

Govaerts R. 2001. How many species of seed plants are there? Taxon **50**, 1085–1090.

Gremski K, Ditta G, Yanofsky MF. 2007. The *HECATE* genes regulate female reproductive tract development in *Arabidopsis thaliana*. Development **134**, 3593–3601.

Grini PE, Thorstensen T, Alm V, Vizcay-Barrena G, Windju SS, Jørstad TS, Wilson ZA, Aalen RB. 2009. The ASH1 HOMOLOG 2 (ASHH2) histone H3 methyltransferase is required for ovule and anther development in Arabidopsis. PLoS ONE **4**, e7817.

Gross T, Broholm S, Becker A. 2018. CRABS CLAW acts as a bifunctional transcription factor in flower development. Frontiers in Plant Science **9**, 835.

Grossniklaus U, Schneitz K. 1998. The molecular and genetic basis of ovule and megagametophyte development. Seminars in Cell & Developmental Biology **9**, 227–238.

Hedden P, Sponsel V. 2015. A century of gibberellin research. Journal of Plant Growth Regulation **34**, 740–760.

Heisler MG, Atkinson A, Bylstra YH, Walsh R, Smyth DR. 2001. *SPATULA*, a gene that controls development of carpel margin tissues in *Arabidopsis*, encodes a bHLH protein. Development **128**, 1089–1098.

Higuchi M, Pischke MS, Mähönen AP, *et al.* 2004. *In planta* functions of the *Arabidopsis* cytokinin receptor family. Proceedings of the National Academy of Sciences, USA **101**, 8821–8826.

Hill TA, Broadhvest J, Kuzoff RK, Gasser CS. 2006. Arabidopsis *SHORT INTEGUMENTS 2* is a mitochondrial DAR GTPase. Genetics **174**, 707–718.

Hu Y, Xie Q, Chua NH. 2003. The Arabidopsis auxin-inducible gene *ARGOS* controls lateral organ size. The Plant Cell **15**, 1951–1961.

Huang HY, Jiang WB, Hu YW, Wu P, Zhu JY, Liang WQ, Wang ZY, Lin WH. 2013. BR signal influences Arabidopsis ovule and seed number through regulating related genes expression by BZR1. Molecular Plant **6**, 456–469.

Iglesias FM, Cerdán PD. 2016. Maintaining epigenetic inheritance during DNA replication in plants. Frontiers in Plant Science **7**, 38.

Ishida T, Aida M, Takada S, Tasaka M. 2000. Involvement of *CUP-SHAPED COTYLEDON* genes in gynoecium and ovule development in *Arabidopsis thaliana*. Plant & Cell Physiology **41**, 60–67.

Kant S, Burch D, Badenhorst P, Palanisamy R, Mason J, Spangenberg G. 2015. Regulated expression of a cytokinin biosynthesis gene IPT delays leaf senescence and improves yield under rainfed and irrigated conditions in canola (*Brassica napus* L.). PLoS ONE **10**, e0116349.

Klucher KM, Chow H, Reiser L, Fischer RL. 1996. The *AINTEGUMENTA* gene of Arabidopsis required for ovule and female gametophyte development is related to the floral homeotic gene *APETALA2*. The Plant Cell **8**, 137–153.

Krizek B. 2009. *AINTEGUMENTA* and *AINTEGUMENTA-LIKE6* act redundantly to regulate Arabidopsis floral growth and patterning. Plant Physiology **150**, 1916–1929.

Larsson E, Franks RG, Sundberg E. 2013. Auxin and the *Arabidopsis thaliana* gynoecium. Journal of Experimental Botany **64**, 2619–2627.

Laufs P, Peaucelle A, Morin H, Traas J. 2004. MicroRNA regulation of the CUC genes is required for boundary size control in *Arabidopsis* meristems. Development **131**, 4311–4322.

Lee D-K, Geisler M, Springer PS. 2009. *LATERAL ORGAN FUSION1* and *LATERAL ORGAN FUSION2* function in lateral organ separation and axillary meristem formation in *Arabidopsis*. Development **136**, 2423–2432.

Liu P, Zhang C, Ma JQ, *et al*. 2018. Genome-wide identification and expression profiling of cytokinin oxidase/dehydrogenase (*CKX*) genes reveal likely roles in pod development and stress responses in oilseed rape (*Brassica napus* L.). Genes **9**, 168.

Liu Z, Franks RG, Klink VP. 2000. Regulation of gynoecium marginal tissue formation by LEUNIG and AINTEGUMENTA. The Plant Cell **12**, 1879–1892.

Mallory AC, Reinhart BJ, Jones-Rhoades MW, Tang G, Zamore PD, Barton MK, Bartel DP. 2004. MicroRNA control of *PHABULOSA* in leaf development: importance of pairing to the microRNA 5′ region. The EMBO Journal **23**, 3356–3364.

Mantegazza O, Gregis V, Mendes MA, Morandini P, Alves-Ferreira M, Patreze CM, Nardeli SM, Kater MM, Colombo L. 2014. Analysis of the arabidopsis *REM* gene family predicts functions during flower development. Annals of Botany **114**, 1507–1515.

Marhavý P, Bielach A, Abas L, *et al.* 2011. Cytokinin modulates endocytic trafficking of PIN1 auxin efflux carrier to control plant organogenesis. Developmental Cell **21**, 796–804.

Marsch-Martínez N, de Folter S. 2016. Hormonal control of the development of the gynoecium. Current Opinion in Plant Biology **29**, 104–114.

McClure BA, Guilfoyle T. 1987. Characterization of a class of small auxin-inducible soybean polyadenylated RNAs. Plant Molecular Biology **9**, 611–623.

Mizukami Y, Fischer RL. 2000. Plant organ size control: *AINTEGUMENTA* regulates growth and cell numbers during organogenesis. Proceedings of the National Academy of Sciences, USA **97**, 942–947.

Moubayidin L, Østergaard L. 2014. Dynamic control of auxin distribution imposes a bilateral-to-radial symmetry switch during gynoecium development. Current Biology **24**, 2743–2748.

Nahar MA, Ishida T, Smyth DR, Tasaka M, Aida M. 2012. Interactions of *CUP-SHAPED COTYLEDON* and *SPATULA* genes control carpel margin development in *Arabidopsis thaliana*. Plant & Cell Physiology **53**, 1134–1143.

Nemhauser JL, Feldman LJ, Zambryski PC. 2000. Auxin and *ETTIN* in Arabidopsis gynoecium morphogenesis. Development **127**, 3877–3888.

Nole-Wilson S, Azhakanandam S, Franks RG. 2010*a*. Polar auxin transport together with *AINTEGUMENTA* and *REVOLUTA* coordinate early Arabidopsis gynoecium development. Developmental Biology **346**, 181–195.

Nole-Wilson S, Rueschhoff EE, Bhatti H, Franks RG. 2010*b*. Synergistic disruptions in *seuss cyp85A2* double mutants reveal a role for brassinolide synthesis during gynoecium and ovule development. BMC Plant Biology **10**, 198.

Nomura T, Kushiro T, Yokota T, Kamiya Y, Bishop GJ, Yamaguchi S. 2005. The last reaction producing brassinolide is catalyzed by cytochrome P-450s, CYP85A3 in tomato and CYP85A2 in *Arabidopsis*. The Journal of Biological Chemistry **280**, 17873–17879.

Okada K, Ueda J, Komaki MK, Bell CJ, Shimura Y. 1991. Requirement of the auxin polar transport system in early stages of Arabidopsis floral bud formation. The Plant Cell **3**, 677–684.

Pagnussat GC, Yu HJ, Ngo QA, Rajani S, Mayalagu S, Johnson CS, Capron A, Xie LF, Ye D, Sundaresan V. 2005. Genetic and molecular identification of genes required for female gametophyte development and function in *Arabidopsis*. Development **132**, 603–614.

Pinto SC, Mendes MA, Coimbra S, Tucker MR. 2019. Revisiting the female germline and its expanding toolbox. Trends in Plant Science **24**, 455–467.

Reiser L, Fischer RL. 1993. The ovule and the embryo sac. The Plant Cell **5**, 1291–1301.

Reyes-Olalde JI, de Folter S. 2019. Control of stem cell activity in the carpel margin meristem (CMM) in Arabidopsis. Plant Reproduction **32**, 123–136.

Reyes-Olalde JI, Zuñiga-Mayo VM, Chávez Montes RA, Marsch-Martínez N, de Folter S. 2013. Inside the gynoecium: at the carpel margin. Trends in Plant Science **18**, 644–655.

Reyes-Olalde JI, Zúñiga-Mayo VM, Serwatowska J, *et al.* 2017. The bHLH transcription factor SPATULA enables cytokinin signaling, and both activate auxin biosynthesis and transport genes at the medial domain of the gynoecium. PLoS Genetics **13**, e1006726.

Rizza A, Jones AM. 2019. The makings of a gradient: spatiotemporal distribution of gibberellins in plant development. Current Opinion in Plant Biology **47**, 9–15.

Roeder AH, Yanofsky MF. 2006. Fruit development in *Arabidopsis*. The Arabidopsis Book **4**, e0075.

Ruzicka K, Simásková M, Duclercq J, Petrásek J, Zazímalová E, Simon S, Friml J, Van Montagu MC, Benková E. 2009. Cytokinin regulates root meristem activity via modulation of the polar auxin transport. Proceedings of the National Academy of Sciences, USA **106**, 4284–4289.

Schaller GE, Bishopp A, Kieber JJ. 2015. The yin-yang of hormones: cytokinin and auxin interactions in plant development. The Plant Cell **27**, 44–63.

Schlereth A, Möller B, Liu W, Kientz M, Flipse J, Rademacher EH, Schmid M, Jürgens G, Weijers D. 2010. MONOPTEROS controls embryonic root initiation by regulating a mobile transcription factor. Nature **464**, 913–916.

Schneitz K, Baker SC, Gasser CS, Redweik A. 1998. Pattern formation and growth during floral organogenesis: *HUELLENLOS* and *AINTEGUMENTA* are required for the formation of the proximal region of the ovule primordium in *Arabidopsis thaliana*. Development **125**, 2555–2563.

Schneitz K, Hulskamp M, Pruitt RE. 1995. Wild-type ovule development in *Arabidopsis thaliana*: a light microscope study of cleared whole-mount tissue. The Plant Journal **7**, 731–749.

Schuster C, Gaillochet C, Lohmann JU. 2015. Arabidopsis *HECATE* genes function in phytohormone control during gynoecium development. Development **142**, 3343–3350.

Sessions A, Nemhauser JL, McColl A, Roe JL, Feldmann KA, Zambryski PC. 1997. *ETTIN* patterns the *Arabidopsis* floral meristem and reproductive organs. Development **124**, 4481–4491.

Shah S, Karunarathna NL, Jung C, Emrani N. 2018. An *APETALA1* ortholog affects plant architecture and seed yield component in oilseed rape (*Brassica napus* L.). BMC Plant Biology **18**, 380.

Shi DQ, Yang WC. 2011. Ovule development in Arabidopsis: progress and challenge. Current Opinion in Plant Biology **14**, 74–80.

Shirley NJ, Aubert MK, Wilkinson LG, Bird DC, Lora J, Yang X, Tucker MR. 2019. Translating auxin responses into ovules, seeds and yield: Insight from *Arabidopsis* and the cereals. Journal of Integrative Plant Biology **61**, 310–336.

Šimášková M, O'Brien JA, Khan M, *et al.* 2015. Cytokinin response factors regulate PIN-FORMED auxin transporters. Nature Communications **6**, 8717.

Skinner DJ, Baker SC, Meister RJ, Broadhvest J, Schneitz K, Gasser CS. 2001. The Arabidopsis *HUELLENLOS* gene, which is essential for normal ovule development, encodes a mitochondrial ribosomal protein. The Plant Cell **13**, 2719–2730.

Skinner DJ, Hill TA, Gasser CS. 2004. Regulation of ovule development. The Plant cell **16 Suppl**, S32–S45.

Smyth DR, Bowman JL, Meyerowitz EM. 1990. Early flower development in *Arabidopsis*. The Plant Cell **2**, 755–767.

Snowdon RJ, Lühs W, Friedt W. 2007. Genome mapping and molecular breeding in plants. Oilseeds **6**, 54–56.

Sohlberg JJ, Myrenås M, Kuusk S, Lagercrantz U, Kowalczyk M, Sandberg G, Sundberg E. 2006. *STY1* regulates auxin homeostasis and affects apical-basal patterning of the Arabidopsis gynoecium. The Plant Journal **47**, 112–123.

Stinchcombe JR, Weinig C, Ungerer M, Olsen KM, Mays C, Halldorsdottir SS, Purugganan MD, Schmitt J. 2004. A latitudinal cline in flowering time in *Arabidopsis thaliana* modulated by the flowering time gene FRIGIDA. Proceedings of the National Academy of Sciences, USA **101**, 4712–4717.

Sun Y, Fan XY, Cao DM, *et al.* 2010. Integration of brassinosteroid signal transduction with the transcription network for plant growth regulation in *Arabidopsis*. Developmental Cell **19**, 765–777.

van Mourik H, van Dijk ADJ, Stortenbeker N, Angenent GC, Bemer M. 2017. Divergent regulation of Arabidopsis *SAUR* genes: a focus on the *SAUR10*-clade. BMC Plant Biology **17**, 245.

Vanstraelen M, Benková E. 2012. Hormonal interactions in the regulation of plant development. Annual Review of Cell and Developmental Biology **28**, 463–487.

Wetzstein HY, Yi W, Porter JA, Ravid N. 2013. Flower position and size impact ovule number per flower, fruitset, and fruit size in pomegranate. Journal of the American Society for Horticultural Science **138**, 159–166.

Willis KJ 2017. State of the world's plants 2017. Kew: Royal Botanic Gardens.

Wynn AN, Seaman AA, Jones AL, Franks RG. 2014. Novel functional roles for *PERIANTHIA* and *SEUSS* during floral organ identity specification, floral meristem termination, and gynoecial development. Frontiers in Plant Science **5**, 130.

Xu L, Zhao Z, Dong A, Soubigou-Taconnat L, Renou JP, Steinmetz A, Shen WH. 2008. Di- and tri- but not monomethylation on histone H3 lysine 36 marks active transcription of genes involved in flowering time regulation and other processes in *Arabidopsis thaliana*. Molecular and Cellular Biology **28**, 1348–1360.

Yang Y, Wang Y, Zhan J, Shi J, Wang X, Liu G, Wang H. 2017. Genetic and cytological analyses of the natural variation of seed number per pod in rapeseed (*Brassica napus* L.). Frontiers in Plant Science **8**, 1890.

Yuan J, Kessler SA. 2019. A genome-wide association study reveals a novel regulator of ovule number and fertility in *Arabidopsis thaliana*. PLoS Genetics **15**, e1007934.

Zuñiga-Mayo VM, Baños-Bayardo CR, Díaz-Ramírez D, Marsch-Martínez N, De Folter S. 2018. Conserved and novel responses to cytokinin treatments during flower and fruit development in *Brassica napus* and *Arabidopsis thaliana*. Scientific Reports **8**, 6836.

Zúñiga-Mayo VM, Gómez-Felipe A, Herrera-Ubaldo H, de Folter S. 2019. Gynoecium development: networks in Arabidopsis and beyond. Journal of Experimental Botany **70**, 1447–1460.

ACKNOWLEDGMENTS

I would like to thank my supervisor, professor Lucia Colombo, for her helpfulness and continuous help throughout my PhD.

My colleagues of the lab 1 and the entire Colombo group;

The PhD directors Professors Martin M. Kater and Marco Muzi Falconi.

I also thank the evaluation committee of my PhD composed by Prof. Bonza Maria Cristina, Prof. Jaume Martinez and Prof. Stefan de Folter, the PhD thesis committee composed by: Prof. Ruud Demmagd and Dr. Bruno Leonardo;

I would also like to thank all the collaborators, Mexico (de Folter lab.), Czech Republic (Novak-Strnad lab.) and Italy (Università Bicocca, Mantegazza lab.).

Last but not least the secretary of the PhD School Mrs. Margherita Russo.